CONTROLS ON POROSITY AND PERMEABILITY IN THE CARMEL FORMATION: IMPLICATIONS FOR CARBON SEQUESTRATION AT GORDON CREEK, UTAH

by

William Graham Payne

Submitted in Partial Fulfillment
of the Requirements for the

Masters of Science in Geology

New Mexico Institute of Mining and Technology
Department of Earth & Environmental Science
Socorro, New Mexico

August, 2011

DEDICATION

I would like to dedicate this study first to my loyal friends Annette, Nate, Ted, Christy, Colin, Holly, and Diesel for helping me keep my sanity, even from several thousand miles away. Your friendship means much more than I could ever say and I love you all. I promise to visit as often as I can.

Next, I like to thank my rugby coach and dear friend Dave Wheelock. You helped me improve my individual game, but more importantly, you helped me develop my coaching style and taught me the deeper reasons for playing and loving the game. I can't even think about my time in New Mexico without thinking about the Pygmies and your leadership. I've said it before and I'll say it again, you are one of the finest human beings I have ever had the pleasure of knowing.

"To win the game is great,
to play the game is greater,
to love the game is greatest."

My advisor, Peter Mozley, has been an inestimable help in the creation of this work. His patience and guidance in the field and lab, as well as his assistance in editing, was the most necessary element in the completion of this thesis.

Finally, I would like to thank my sister Susanna, my brother Harrison, my mom Mary-Susan, and my dad Robert. I love you with all of my heart.

ABSTRACT

High quality estimates of reservoir and seal properties for proposed CO_2 injection sites are vital for predicting how CO_2 will behave in the subsurface and quantifying the likelihood that a site will effectively sequester CO_2. This thesis focuses on characterizing the quality of the seal, and to a lesser extent, the reservoir for a proposed carbon sequestration site at the Gordon Creek field in Carbon County, Utah. At the Gordon Creek field, the reservoir for the proposed injection is the Navajo Sandstone, with the Carmel Formation acting as the primary seal. We are investigating the controls on porosity and permeability in both units, with an emphasis on determining the sealing behavior of the Carmel Formation. Because conventional core material is not yet available from the site, the approach has been to examine outcrop analogs of the reservoir and caprock lithologies. The outcrop derived observations were supplemented with thin sections obtained from drill cuttings from wells at the Gordon Creek site.

The Carmel Formation is a near-shore assemblage of limestone, siltstone, shale, sandstone, and bedded gypsum. It changes laterally across Utah, from more carbonate-dominated lithofacies in the west, to more clastic-dominated lithofacies in the east. Because of the lateral changes in lithology, it was necessary to examine outcrops of the Carmel at Mt. Carmel Junction and on the San Rafael Swell. The Mt. Carmel Junction site is thought to best represent what is at the Gordon Creek field based on electric logs

and placement relative to paleoshoreline. There, the Carmel is approximately 150 m thick, consisting of limestone, silt/shale, sandstone, and gypsum. However, the San Rafael Swell outcrop is also a reasonable analog and is particularly well exposed.

Samples collected from the two outcrop locations, as well as subsurface samples from the proposed injection site, were analyzed using a combination of petrography, stable isotope geochemistry, electron microprobe analysis, and mercury injection capillary pressure/tight rock analysis.

Pore-filling calcite and gypsum cements and compaction account for most of the porosity loss in the Carmel Formation. Porosity in the limestone beds in the Carmel is low, because they are dominantly carbonate muds. In the shales the only macroscopic porosity is fracture related. There are multiple mineralized fractures throughout the Carmel (gypsum, calcite) that could be present at depth. The fractures are mainly developed in limestone and, to a lesser extent, sandstone beds. In a few places they can be seen to extend into adjacent shale beds.

Permeability values from the Carmel range from 10^{-1}-10^{-6} mD, with capillary pressure curves indicating that various lithologies could effectively sequester the 4 million tons of CO_2 that will be injected into the Navajo at this site. Based on the petrophysical data, the Carmel could effectively sequester a maximum of 20,603 feet (breakthrough pressure) 12,504 feet (threshold pressure) of CO_2. The major sealing units within the Carmel include micritic limestones, shales, and bedded gypsum, with the Co-op Creek and Paria River Members being the most effective seals.

There is a risk associated with seismically unresolved faults or fractures that could allow CO_2 to bypass the Carmel. In addition, because some of the sealing lithologies in

the Carmel are brittle (limestones), there might be open fractures that cut through the Carmel. However, based on stable isotope analysis of the mineralized fractures, the precipitating fluid is compatible with two scenarios: 1) high temperature ~0 SMOW waters at depth, or 2) low temperature meteoric water. With the low temperature meteoric water scenario real fractures in the subsurface are likely to be open.

Keywords: carbon sequestration; CO_2 sequestration; Carmel, diagenesis; stable isotope; MICP; permeability; porosity; Gordon Creek; seal; Southwest Partnership

ACKNOWLEDGEMENTS

I would like to thank my committee members: Peter S. Mozley, Andrew Campbell, Brian McPherson, and Tom Dewers for all their assistance in preparing and editing this thesis. I would also like to thank Reid Grigg for helping me with the financial side of this project, Her-Yuan Chen for his assistance with petrophysical calculations, John L. Wilson for his help with the field permeability instrumentation, Earl Reynolds for being my field assistant, Liz Petri for helping me understand the fracture network along Interstate-70, Jason Heath for putting up with my endless questions, for sending me useful journal articles, and discussions concerning sealing capabilities, Geoffrey Rawlings at the New Mexico Bureau of Geology and Mineral Resources for his assistance in understanding the field permeameter, the New Mexico Firefighters Training Academy for technical assistance with the field permeameter, Wagner Petrographic for cutting my thin sections, and Poro-Technology for doing the MICP testing.

TABLE OF CONTENTS

LIST OF FIGURES

Page

LIST OF TABLES

Page

Chapter 1: Introduction

Significance and research approach

The Southwest Regional Partnership on Carbon Sequestration (SWP), a consortium supported by the U.S. Department of Energy and its National Energy Technology Laboratory (NETL), has selected the Gordon Creek field in Carbon County, Utah to be a Phase III injection site for CO_2 sequestration (McPherson and Grigg, 2010). The Phase III project is intended to demonstrate the feasibility of CO_2 sequestration at an industrial scale. At Gordon Creek, the Navajo Sandstone is the target injection unit, and the Carmel Formation is the primary seal (caprock).

This thesis details a preliminary study of the Carmel Formation, with emphasis on understanding controls on its potential to act as an effective caprock. In addition, portions of the Navajo Sandstone near the contact with the Carmel Formation, and the Temple Cap Formation, an intervening unit that may be present at Gordon Creek, were also characterized.

Methods include field description, petrographic analysis of outcrop and subsurface samples, stable isotope analysis of fracture filling cements, permeability/porosity/capillary pressure analysis of samples, and qualitative/quantitative analysis of sedimentary textures and elemental composition of cements using an electron microprobe. Because conventional core is not yet available for the Carmel Formation at Gordon Creek, outcrop data are the primary source of information for this study. Using outcrops as analogues of the subsurface seal provides the added benefit of obtaining data on the lateral heterogeneity of the units at a variety of scales, which is critical to assessing the likelihood of seal bypass systems, such as fracture networks (Cartwright, 2007); this

study focused on taking representative samples from outcrops instead of multiple samples from the same stratigraphic unit.

Sampling and outcrop description were done at two locations: the western side of the San Rafael Swell along Interstate-70 (hereafter referred to as I-70), and outcrops near Mount Carmel Junction, Utah (hereafter referred to as MCJ). The Carmel Formation is slightly different at each location, primarily because of variations in depositional settings, so comparing and contrasting each site was important for a better understanding of the Carmel Formation and its properties at Gordon Creek.

Determining the effectiveness of the Carmel Formation as a seal is vital to forecasting the amount of CO_2 that can be safely sequestered, as well as in understanding which lithologies will act as the principal sealing units within the formation. Because the Carmel Formation contains a variety of lithologies, the overall approach followed in this thesis is to evaluate the sealing potential (petrophysical characteristics) of each major lithofacies in order to evaluate its behavior.

For the Phase III injection at Gordon Creek, the SWP is planning to inject a large amount of CO_2 into the Navajo: 300,000 tons of CO_2 the first year, 600,000 tons the second, and 1,000,000 the third and fourth years at the Gordon Creek site (McPherson and Grigg, 2010). The CO_2 will be obtained from the Permian-age White Rim Sandstone utilizing a high-pressure pipeline with a capacity of 50 MMCFD (million cubic feet per day), with an additional pipeline used for brine disposal (McPherson and Grigg, 2010). The CO_2 will be injected at a pressure of approximately 1,400 psi in order to ensure that it remains in a supercritical state (McPherson and Grigg, 2010).

Research questions

The principal research question addressed in this study is whether or not the Carmel Formation will be an effective caprock for the sequestration of CO_2 in the underlying Navajo Sandstone. Associated questions include: 1) Has diagenesis of the Carmel Formation reduced or enhanced porosity and permeability? 2) Are the mineralized fractures present in outcrops likely to also be present at depth? 3) What are the petrophysical (porosity/permeability) characteristics of each member of the Carmel Formation?

Geologic setting of the Carmel Formation

Depositional setting

During the middle Jurassic, the Carmel-Twin Creek Seaway covered much of modern Utah; this seaway was the result of the Cordilleran syncline (Freeman, 1976). This restricted marine environment was the primary depositional setting of the Carmel Formation, and resulted in subtidal, supratidal, and intratidal deposits (Bannister et al., 1998; De Gibert and Ekdale, 1999). Prior to the middle Jurassic, large eolian sand dunes dominated the landscape, depositing the Navajo Sandstone, which is stratigraphically beneath the Carmel Formation, separated by the J-2 unconformity.

The Carmel Formation contains subtidal limestone deposits, as well as intertidal and supratidal deposits. There are two main transgressive-regressive sequences within the Carmel Formation. The Co-op Creek Member continuing up through the gypsum layer of the Paria River Member represents the first transgressive sequence, whereas the units

above the gypsum represent the second transgressive sequence (De Gilbert and Ekdale, 1999).

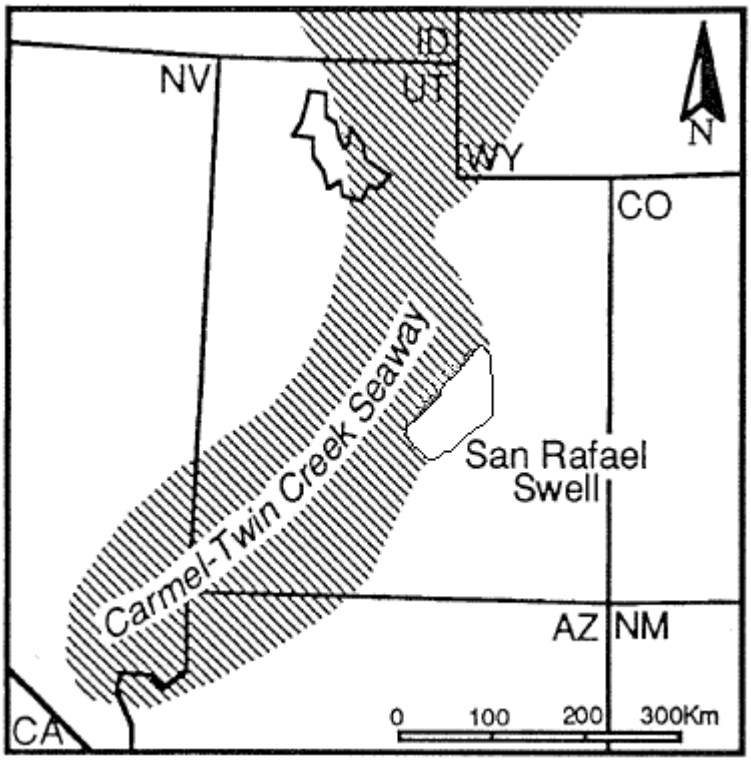

Figure 1. Carmel-Twin Creek Seaway during the Jurassic in Utah. Modified from De Gibert and Ekdale, 1999.

Stratigraphy

The Carmel Formation is a Jurassic assemblage of limestone, shale, siltstone, sandstone, and gypsum. It is separated from the underlying Navajo Sandstone by the J-2 unconformity with the Entrada Formation stratigraphically above (Peterson and Pipiringos, 1979). The Carmel Formation is the lowest unit in the San Rafael Group of central Utah. In some locations, there is a layer of reworked Navajo Sandstone called the Page Sandstone in-between the Navajo Sandstone and the Carmel Formation. The Carmel Formation is subdivided into four distinct members: the Co-op Creek, the Crystal Creek,

the Paria River, and the Windsor. For the stratigraphy at Gordon Creek, please refer to Figure 2.

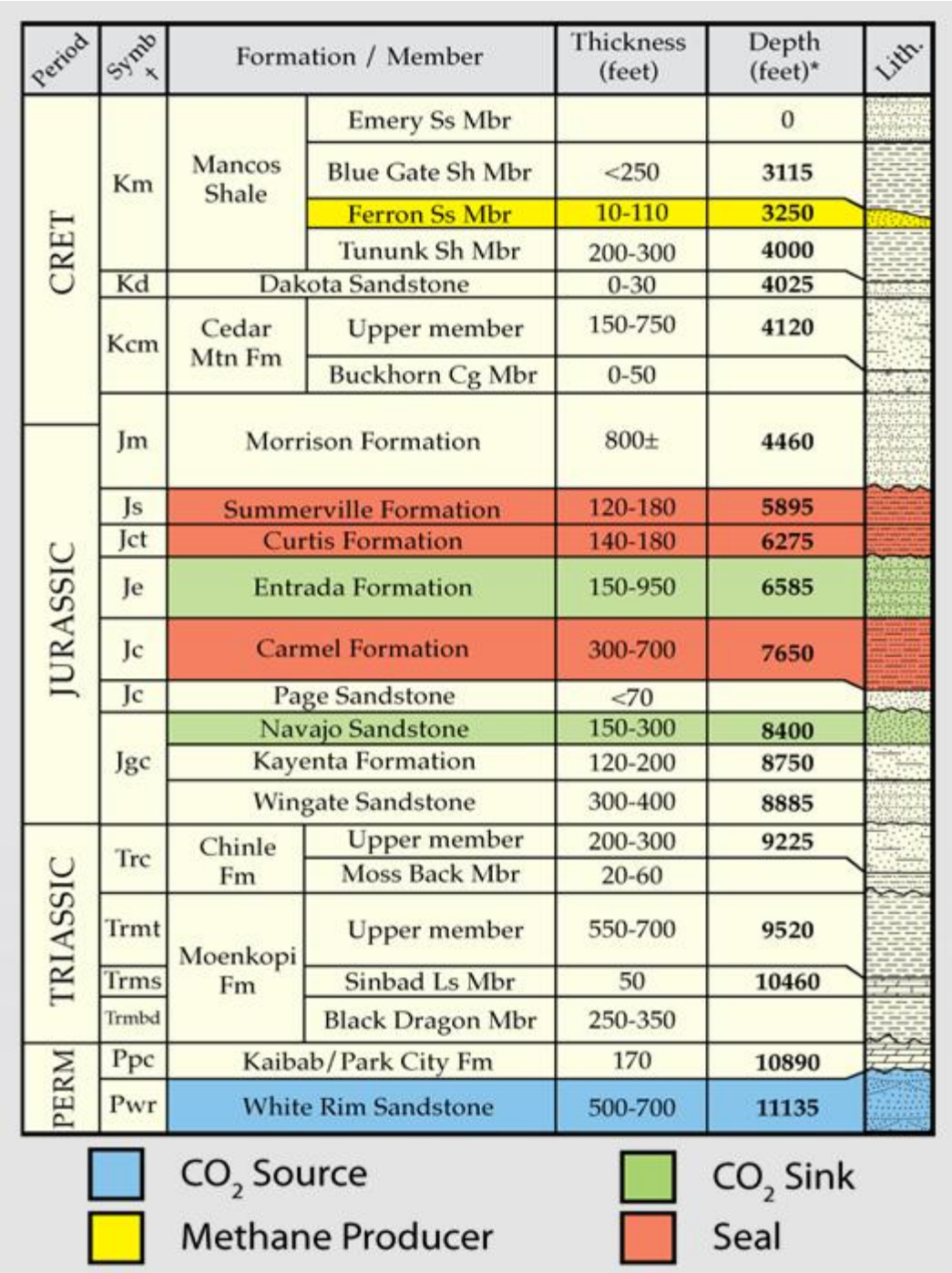

Figure 2. Stratigraphic section reflecting the subsurface at Gordon Creek. The primary injection target in the Navajo Sandstone with the Carmel Formation acting as a seal. The CO_2 source is from the White Rim Sandstone. Modified from Esser et al., 2010.

At the I-70 site, the Co-op Creek Member is 14.1 meters thick, consisting of shales and limestones, whereas at the MCJ site, it is 73 meters thick, consisting of limestone. The Crystal Creek Member at I-70 is 6.5 meters thick, consisting of limestone and shale, whereas at the MCJ site is 66 meters thick consisting of limestone. The Paria River Member at I-70 is 17.5 meters thick, consisting of gypsum and bedded limestone, whereas at the MCJ site, it is only 6 meters of gypsum, being cut off by the Sevier Fault.

Site descriptions

Subsurface at Gordon Creek

Subsurface samples were obtained from the Utah Core Research Center in Salt Lake City, Utah. Many of the wells in the area are producing oil and gas from shallower units, and only two wells had cuttings and chips from the Carmel. It was originally intended that the data obtained from these samples would be used to help better choose outcrop sites, as well as provide an accurate representation of the Carmel Formation at depth. Unfortunately, because of the low vertical resolution in sampling, these samples were not a reliable source of information.

Interstate-70

The I-70 sampling location was on the western side of the San Rafael Swell along Interstate 70, approximately 0.1 miles east of the Moore Rd. exit (38.849301° N, 110.90291° W). The underlying Navajo Sandstone through the Windsor Member of the Carmel Formation is exposed at this road cut. The Carmel Formation is 38.05 meters thick at this location (measured). The Windsor Member is not present 1.4 meters past its

contact with the underlying Paria River; The Carmel Formation is buried to the west, along with the exact contact with the overlying Entrada Formation. The I-70 site outcrop stratigraphy consists of a mixture of carbonate and clastic lithologies (thick sequences of limestone, along with shale, siltstone, gypsum, and sandstone; many of the sandstones are in fact either limy sandstones or sandy limestones).

Mount Carmel Junction

This sampling location is southwest of the town of Mount Carmel Junction, Utah (37.22724° N, 112.684818° W). At this location, there is an additional unit between the Navajo and the Carmel: the Temple Cap Formation, which consists of the Esplin Member and the White Throne Member. The Carmel Formation is exposed along a series of hills in the area, so a composite stratigraphic section was made. The Carmel is 150 meters thick at this location (measured), with the upper portion of the Paria River and Windsor Members missing because the Sevier Fault.

Figure 3. Utah State map with sampling locations (I-70 and MCJ) represented by red circles, and Gordon Creek field represented by a blue square.

Chapter 2: Methodology

Field work

The two field sites were visited to produce rough stratigraphic columns to form the basis for sampling. Based on field observations, the Carmel Formation was divided into four lithofacies. This breakdown is identical to the member breakdown of the Carmel Formation. Data were compiled into sections, and then compared to sections produced in the same areas by Douglas Sprinkle at the Utah Geological Survey (Sprinkle et al., 2010). During outcrop description work, samples were collected of each lithologic unit and their sampling height above the datum recorded (the Navajo/Carmel contact at I-70 and the Temple Cap/Carmel contact at MCJ). Calcite and gypsum veins that are present locally in the Carmel Formation were also sampled.

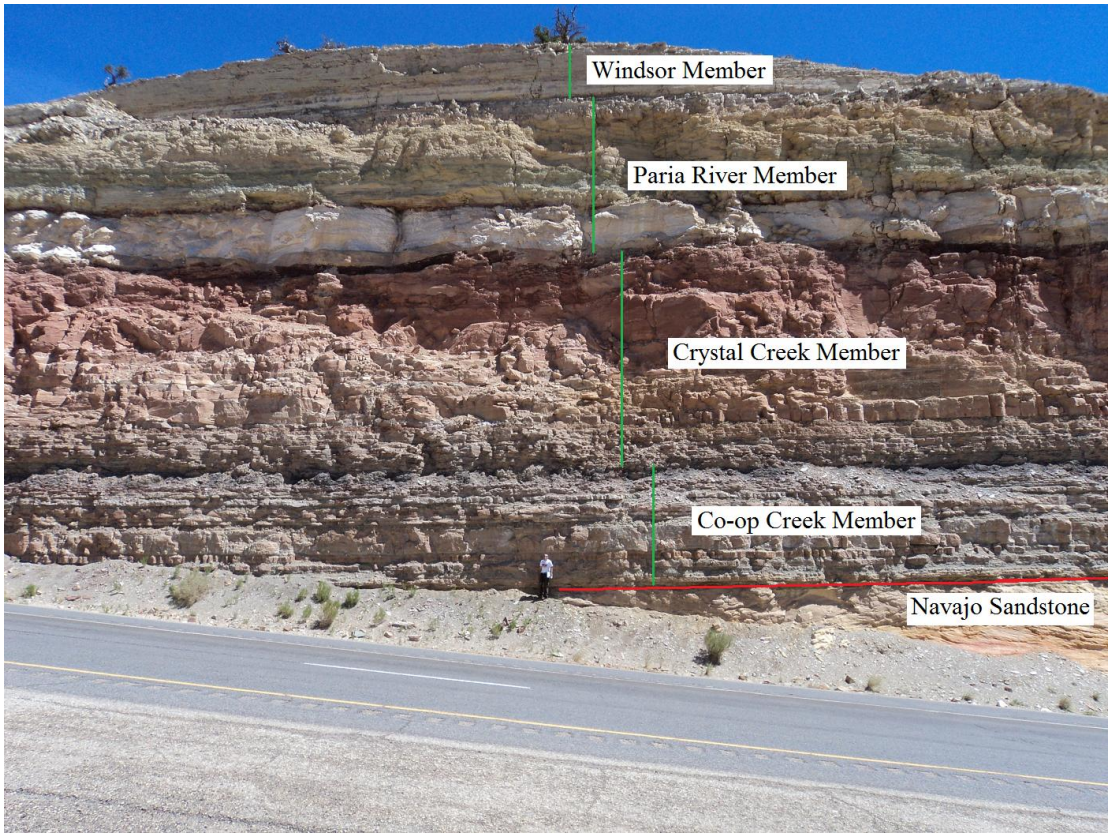

Figure 4. I-70 outcrop photo with members labeled. The red line is the contact between the underlying Navajo Sandstone and the Carmel Formation, otherwise known as the J-2 unconformity. Each member is represented by a green line representing the vertical extent of each of the four members. Handsome graduate student for scale.

Petrography

For each sample, thin sections were made to help determine porosity, paragenesis, diagenetic alterations, and rock classification. Thin sections are standard sized (24 X 36 X 0.03 mm) prepared by Wagner Petrographic, Lindon, UT. The siltstones/shales were impregnated with Rhodamine-B, whereas the limestones and gypsum were infused with blue epoxy to differentiate true porosity from that produced by plucking during thin-section preparation. For clastic samples, a standard 300 point count was performed following the Gazzi-Dickinson method (Dickinson, 1970). The percentages of minerals obtained from the count were used to classify the sample and to obtain a porosity value.

Stable isotopes

To help constrain the environment of formation of mineralized fractures that are locally present in the Carmel Formation, samples of fracture-filling calcite and gypsum were collected and analyzed for $\delta^{18}O$ and $\delta^{13}C$ for calcite, and $\delta^{34}S$ for gypsum.

Calcite samples

The calcite samples were crushed and ground into a fine powder, to ensure complete dissolution of the calcite. Calcite samples along with the standards (Solenhofen Limestone, NBS No. 18, and IAE-CO-9) for calibration were measured on a mass spectrometer. 0.25 ± 0.05 mg of the calcite samples were weighed on a calibrated scale, and placed into sample vials. The vials were then sealed with a cap and septum to prevent atmosphere from entering or exiting the vials. Helium gas was then injected into the vials for two minutes to flush out any air in the vials.

After the He_4 flooding, 10 drops of phosphoric acid (H_3PO_4) was injected into each vial to completely dissolve the calcite. The vials were then put in a sample block and heated to 45°C for 4 hours to allow the reaction of sample and acid to complete.

After the reaction had run to completion, the CO_2 gas was analyzed on a Thermo-Finnign Delta and XP in continuous flow mode. For each sample, a duplicate was run to ensure precision.

Gypsum samples

The gypsum samples were crushed and ground into an even powder. 2.0 ± 0.1 mg of gypsum sample and 4.0 ± 0.1 mg of vanadium pentoxide (V_2O_5) were put into small

tin cups, which were then wrapped and folded to seal the container. The sealed tin cups were then loaded into an elemental analyzer, set at 1020 °C. The vanadium pentoxide combined with the gypsum sample creates SO_2 gas when flashed in the elemental analyzer. After the reaction had run to completion, the CO_2 gas was analyzed on a Thermo-Finnign Delta and XP in continuous flow mode. For each sample, a duplicate was run to ensure precision.

Field/portable air permeametry

I attempted to use a mini permeameter to obtain permeability data from the various Carmel Formation lithofacies. The permeameter uses an air tank to force compressed air into the rock, reading the amount of pressure that is necessary to move air through the rock. The instrument (Figure 5) was built and designed by J. Matt Davis at the University of New Hampshire, and described in detail by Jen Wilson (Wilson, 2004).

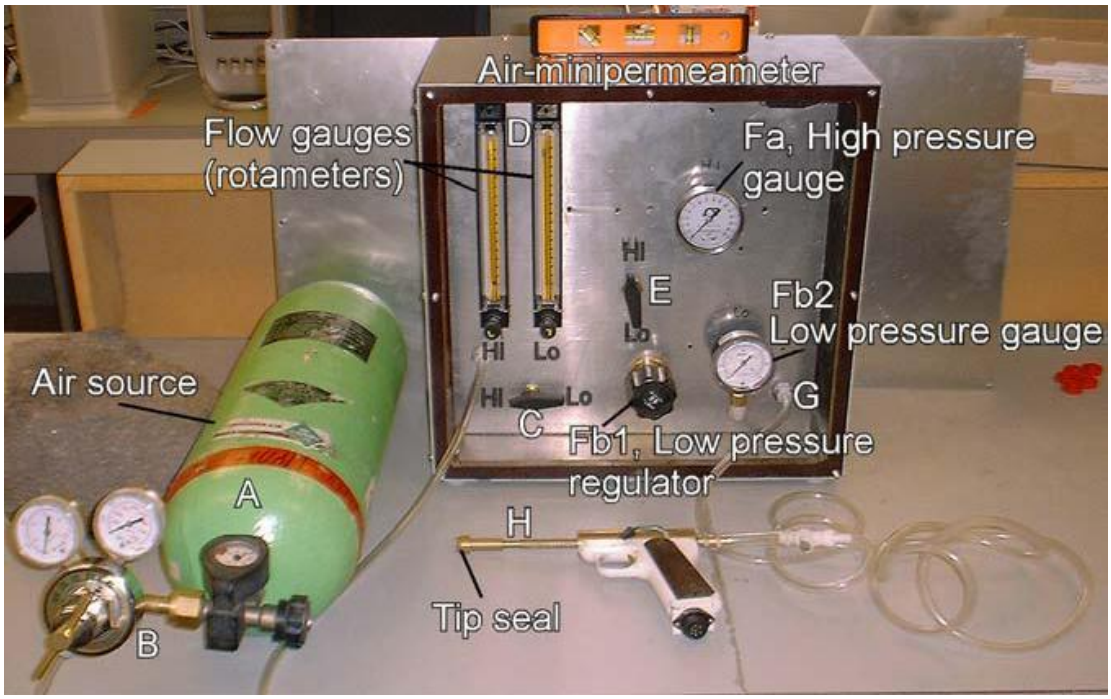

Figure 5. Diagram of portable air permeameter used in field work. From Wilson, 2004.

To begin, the instrument should to be level, and temperature and barometric pressure recorded for the permeability calculations. To ensure accurate data a clean rock surface needs to be prepared (Figure 6). This allows minimally weathered rock to be measured. A rock hammer and chisel were used to clean off the top 5 mm of rock for each grid location. Each grid site consisted of 12 sampling locations in a 4 X 3 pattern. To ensure that reproducible data is being obtained, the first site was measured 4 times, and then re-measured each time the measurement of a new sampling row begun.

Figure 6. Outcrop photo of prepared site for field permeametry. Note prepared 4X3 sampling grid and field permeametry gun. Rock hammer for scale. From Navajo Sandstone at I-70 site.

Attempts to obtain data from the various lithofacies in the Carmel were mostly unsuccessful, because the permeabilities were below the detection limit of the instrument

(the portable air permeameter cannot measure permeability on samples with a value of less then 1 mD (Wilson, 2004)). However, it was possible to obtain data from the more permeable Navajo Sandstone (see corresponding section in Results).

Lab permeametry

Mercury injection capillary pressure

For lab permeametry, samples were chosen with the assumption that similar lithologies with similar diagenetic alterations would have approximately the same permeability and porosity. Using this assumption, 13 limestone samples were tested. However, this also meant that only one sample was tested from the Crystal Creek Member because the limestones in the upper section of the Co-op Creek were nearly identical in lithology and paragenesis to those present in the above Crystal Creek Member. There were only two limestone samples tested from Paria River Member.

For these limestone samples, mercury injection capillary pressure (MICP) testing was performed by Poro-Technology. This method involves injecting mercury into a sample and measuring the pressure buildup and decay at the top and bottom of the sample.

Poro-Technology cut the samples into plugs oriented perpendicular to bedding. This ensures that the data provided would be related to vertical movement of fluids, and not along bedding planes, which could have a different permeability value. The samples were then jacketed with epoxy, and MICP analysis performed. The method provided information on capillary pressure, permeability, and porosity. The additional porosity values are a useful check on the porosity values obtained through petrography.

Tight rock analysis

For the siltstone/shale samples, all of the outcrop samples were too fractured and weathered for MICP testing, so it was suggested by J. E. Heath (2010, personal communication) to use TerraTek Inc. tight rock analysis (TRA) method of measuring permeability. TerraTek's exact methodology is proprietary, but it involves gas absorption testing after samples are crushed (to remove porosity associated with fractures).

Electron microprobe

To better understand the elemental composition and zonation of the calcite and dolomite, as well as the nature of some of the clays present in the Carmel, we decided to perform both qualitative and quantitative analysis on a number of samples.

To begin, any unpolished thin sections needed to be polished. This was accomplished by grinding the thin sections on 15 μm polishing paper for 3 minutes, 6μ polishing paper for 6 minutes, and 2μ polishing paper for 1 minute. After this polishing, the thin sections were coated with carbon.

Additional polished samples were made for some of the calcite veins. These were prepared by breaking the samples into smaller pieces that could fit into the microprobe, and then embedding them in epoxy. These were then placed in an oven set at 80°C for 24 hours to allow the epoxy to cure. These cured pieces were then ground down until the sample surface was exposed on a 163 μm grinding plate. They were then polished on a 68 μm grinding plate for 3 minutes, a 30 μm grinding plate for 3 minutes, 15 μm polishing paper for 3 minutes, 6 μm polishing paper for 3 minutes, and 2 μm polishing paper for 1 minute. After this polishing, the billets were coated with carbon.

Samples were loaded into the microprobe for analysis and analyzed using a 15 kV beam. Quantitative analysis of the chemistry of calcite and dolomite cements was performed, as well as analysis on calcite veins. These analyses were plotted on ternary diagrams.

To take secondary electron (SE) images, rock samples were physically broken into approximately 1 cm^3 pieces. These samples were then placed into metal cups with double-sided tape set in the bottom to hold the samples. These were then carbon-coated, and loaded into the electron microprobe and analyzed with a 15 kV beam.

Chapter 3: Results

Petrography, diagenesis, and petrophysical characteristics by member

For each member of the Carmel and Temple Cap Formations, a detailed petrographic analysis was performed. Each clastic thin section was classified according to Folk, and each carbonate thin section was classified using Dunham/Folk (Dunham, 1962; Folk, 1974). Each clastic thin section also had a 300-point count performed to determine mineralogical make-up, porosity percentage, and influence of diagenesis. The combined data from the 300-point count study is shown in Table 1.

Table 1. Modal composition of samples determined by 300 point clast count data by percent. Organized into detrital/framework grains, diagenetic minerals, and porosity.

	Detrital									Diagenetic					Porosity
	Q	F	VRF	SRF	FF	Cl	C	O	Q	Cl	C	G	O		
MCJ															
Sinawava															
6/10/10-1	25	2		1		63		Tr							9
6/10/10-2	23	5	Tr	2		53									17
6/10/10-3	64	Tr		1							4				31
Navajo															
6/10/10-4	56	2		Tr				Tr	3	7					31
6/10/10-5	65	2		3				0		3	10				17
6/10/10-6	67	1		1				1		1	9				20
White Throne															
6/10/10-7	67			1				Tr	1		12				18
6/10/10-8	69	1		1				Tr	1						28
Esplin															
6/10/10-9	20			2		49						25			4
6/10/10-10	63			1				2	1	6	15				12
6/10/10-11	33	Tr		1		45		1			14		5		1
Co-Op Creek															
6/10/10-14	16			Tr	2		76				1				5
Crystal Creek															
6/11/10-24	60	1	2	3		26									7
I-70															
Crystal Creek															
6/12/10-31FG	24			Tr		1	59	Tr			10	2			4

Q=Quartz, F=Feldspar, FF=Fossil Fragment, Cl=Clay, C=Carbonate, G=Gypsum, O=Other, Tr=Trace

Navajo Sandstone

Composition, texture, and structure

The Navajo Sandstone is a quartz arenite consisting of fine lower to very fine upper, moderately well-sorted sand grains (Folk, 1974). The unit has large-scale cross-bedding, indicative of an eolian depositional environment. At the MCJ site the Navajo is

cut by deformation bands and deformation band faults that intersect bedding at a high angle (Figure 9). At the MCJ site the Navajo also contains macroscopic zones of calcite cement, which form subspherical nodules (Figure 9).

Diagenesis

The principal diagenetic events in the Navajo are: precipitation of calcite cement and calcite replacement of feldspar, compaction, feldspar dissolution, and kaolinite precipitation. The characteristics of these events and their paragenetic relationships are outlined below.

Compaction, as evidenced by an abundance of long contacts, is one of the earliest diagenetic events to affect the Navajo (Figure 10). The presence of numerous long contacts in calcite cemented regions indicates that some compaction occurred prior to calcite cementation. However, the degree of compaction outside of calcite cemented areas is somewhat greater, suggesting that compaction continued subsequent to calcite cement precipitation.

Poikilotopic crystals of calcite cement are locally abundant, particularly at the MCJ site. Calcite cementation seems to have occurred prior to feldspar dissolution and kaolinite precipitation (Figure 10). Evidence for this includes: (1) its position adjacent to grain boundaries in pores filled with kaolinite, (2) the presence of grain dissolution voids and skeletal feldspars in calcite cemented zones (i.e., dissolution voids have not been filled with calcite). In addition to precipitation of pore filling calcite, the preservation of feldspar texture (twinning) indicates that feldspar grains have been pseudomorphically

replaced by calcite in places (Figure 11, 12). The timing of this replacement with respect to the other alterations is uncertain.

Evidence for grain dissolution is abundant in the Navajo, including grain-sized pores and skeletal feldspar grains. Direct evidence for the paragenetic relationship between grain dissolution and kaolinite is lacking. However, because kaolinite is mainly found in grain sized aggregates, it may have originated as a byproduct of feldspar dissolution (i.e., insoluble aluminum remains behind as a clay phase; Figure 13).

Petrophysics

Porosity values determined from the 300-point counts range from 16-31%. From field permeametry, the Navajo was determined to have a range in permeability of 0.74 to 1.020 D (740 to 1,020 mD) from two field grids (Figure 6).

Although the deformation bands were not measured, there is data available from another study of the Navajo Sandstone within the San Rafael Swell that had host rock permeability values extremely similar to those measured in this study (Solum et al., 2010). This site had permeability values ranging from 660-1100 mD with an average of 880 mD in the host rock, while the deformation bands ranged from 0.002-10.6 mD with an average of 0.13 mD. This means that the deformation bands had permeabilties 10^{-6} to 10^{-3} different than those in the host rock.

Figure 7. Upper Navajo Sandstone from the MCJ site. Note large cross-stratification and deformation band faults. Handsome graduate student for scale.

Figure 8. Contact between underlying Navajo Sandstone and Co-op Creek Member of the Carmel Formation at the I-70 site. Within the Co-op Creek thinly laminated siltstones and shales are interbedded with small layers of gypsum, and beds of intrasparite/sparatic quartz grainstone. Rock hammer for scale.

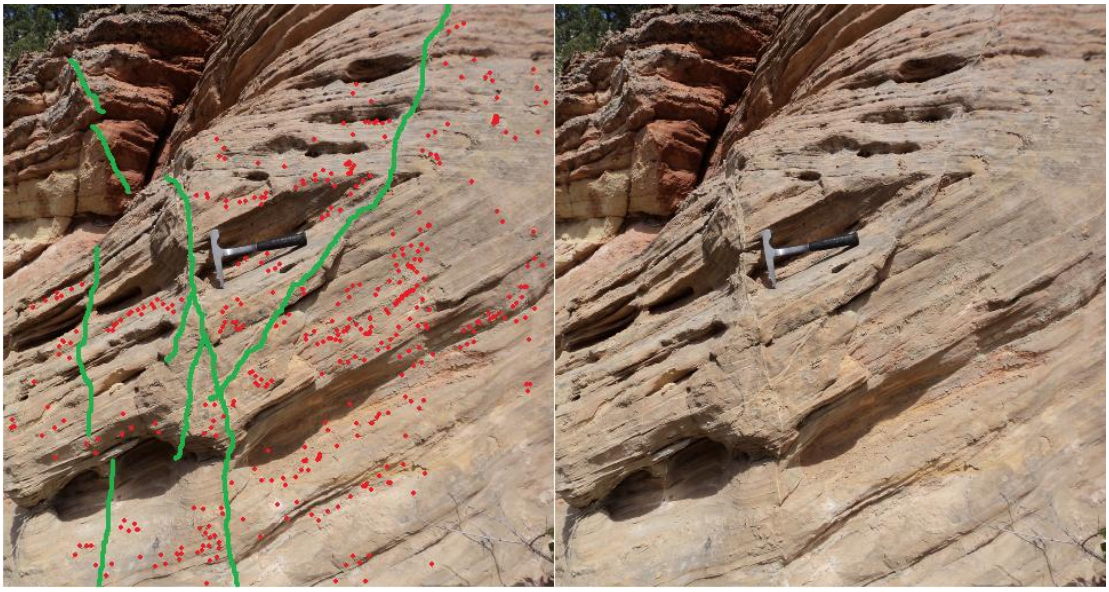

Figure 9. Upper Navajo Sandstone with deformation band faults and calcite nodules at MCJ site. Left photograph shows deformation bands highlighted in green and calcite nodules highlighted in red (not every deformation band and calcite nodule is highlighted). Unaltered photograph on right for comparison. Rock hammer for scale.

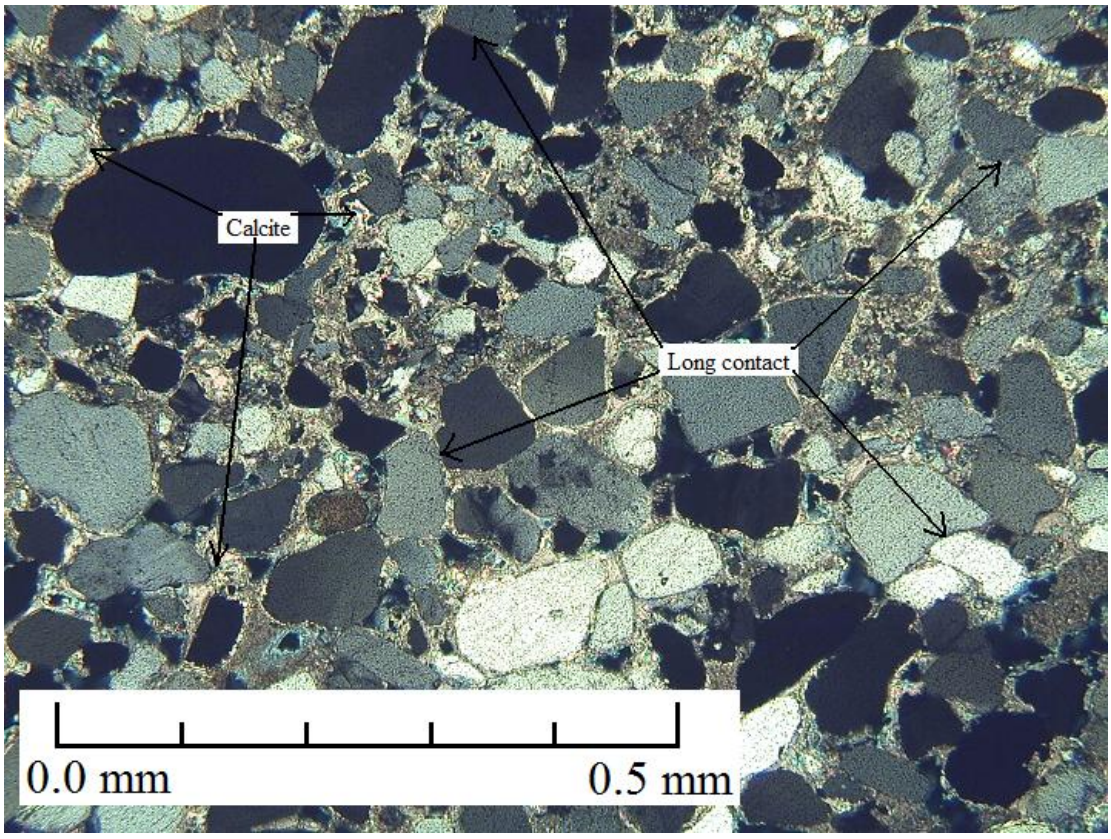

Figure 10. Photomicrograph showing compaction evidenced by abundant long contacts in the Navajo Sandstone prior to calcite cementation. Sample 6/10/10-5.

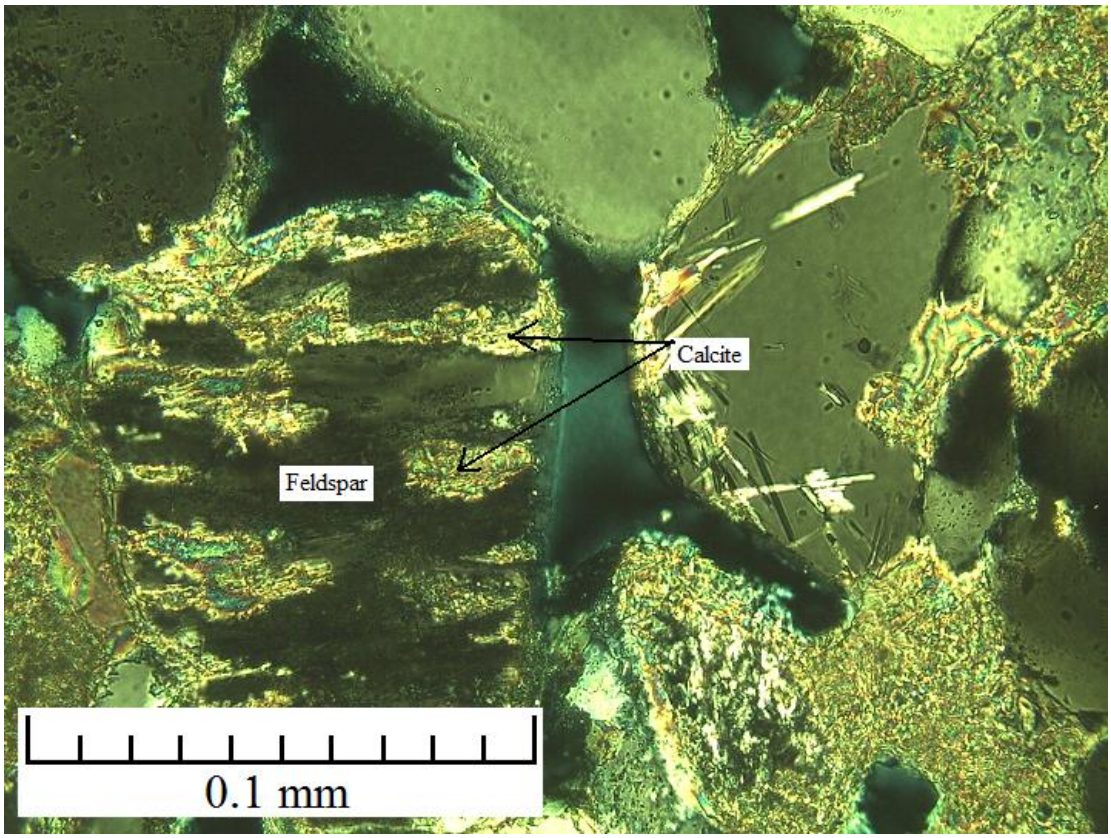

Figure 11. Photomicrograph showing partial calcite replacement of feldspars in the Navajo Sandstone. If calcite was simply precipitating out in void spaces, then the porosity between the framework grains would be cemented with calcite. Sample 6/10/10-5.

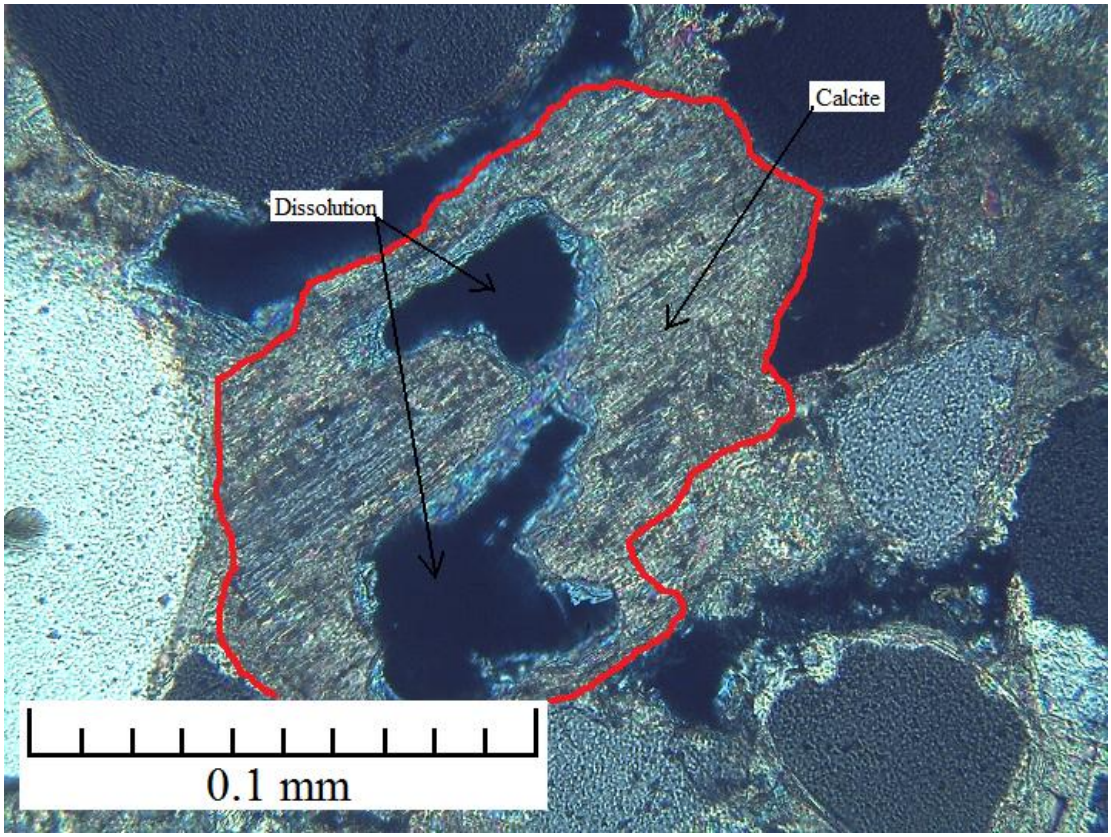

Figure 12. Photomicrograph showing partial pseudomorphic replacement of feldspar by calcite prior to feldspar dissolution in the Navajo Sandstone (feldspar grain outlined in red). Texture of feldspar grain is still evident, thus replacement of feldspar must have occurred before dissolution of feldspar. Sample 6/10/10-5.

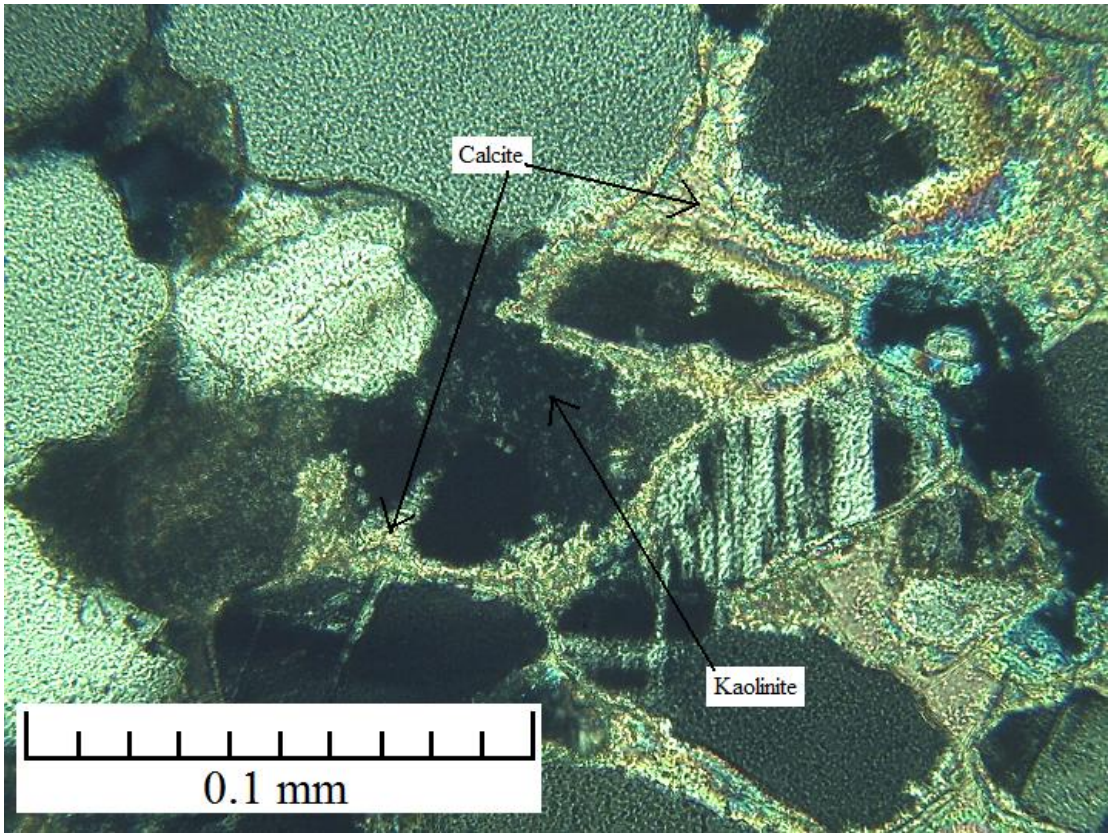

Figure 13. Photomicrograph showing kaolinite filling pore space between quartz grains. Where kaolinite touches quartz grains, there is no calcite cement in between. This suggests that the calcite precipitated after the kaolinite. Sample 6/10/10-5.

Sinawava Member of the Temple Cap Formation

Composition, texture, and structure

The Sinawava Member of the Temple Cap Formation consists of quartz arenite and siltstones. The quartz arenite sample is remarkably similar to the White Throne Member of the Temple Cap Formation (samples 6/10/10-7 and 6/10/10-8). Because the exact contact between the White Throne and the Sinawava was buried, it is possible that the sample was mistaken for being Sinawava (the red clay coloration of the Sinawava could have colored the lower White Throne); it is also possible that the transitional environment from the Sinawava to the White Throne resulted in the deposition of similar

sediments. The exact nature of the structure of the Sinawava Member is unknown because it is poorly exposed at MCJ.

Diagenesis

The principle diagenetic alterations of the Sinawava are: compaction, calcite cementation, feldspar overgrowths, and feldspar dissolution. The characteristics of these events and their paragenetic relationships are outlined below.

Compaction, as evidenced by the presence of deformed clay lamina and abundance of long contacts of framework grains, is the first diagenetic alteration (Figure 14). This must have happened prior to calcite cementation because there are numerous long contacts within the cemented areas.

Feldspar overgrowths must have occurred before feldspar dissolution because the feldspar overgrowths are not present within the dissolution voids (Figure 15). Having overgrowths survive while the grain experiences dissolution is common because the authigenic feldspar is usually more stable under near surface conditions. Due to the rarity of feldspars in the Sinawava (less than 1%), paragenetic relationships between compaction/calcite cementation and feldspar overgrowths/feldspar dissolution could not be determined.

Petrophysics

One sample from the Sinawava Member had a porosity of 8.61% and a permeability of 0.000117 mD determined by TRA. From separate three thin sections

from the Sinawava Member, porosity ranged from 9-31% (determined from 300-point count).

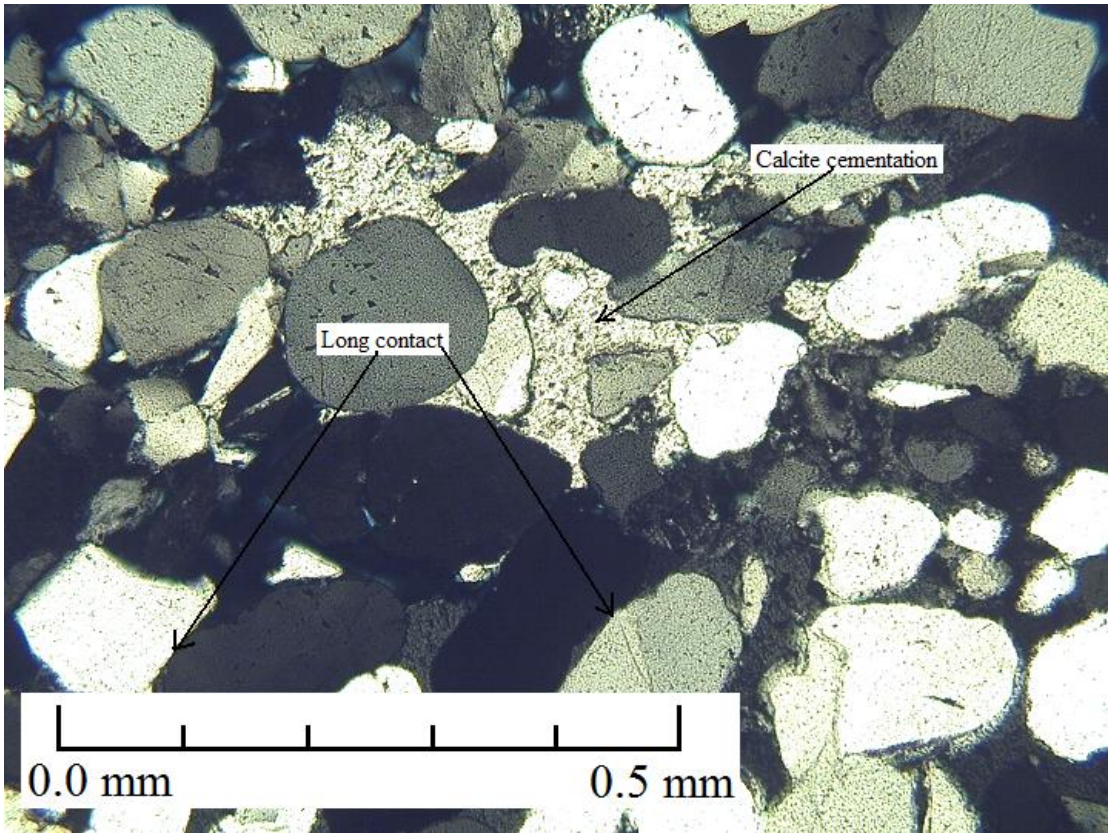

Figure 14. Photomicrograph showing compaction evidenced by numerous long contacts inside calcite cemented areas in the Sinawava Member. Calcite cementation must have occurred after compaction. Sample 6/10/10-3.

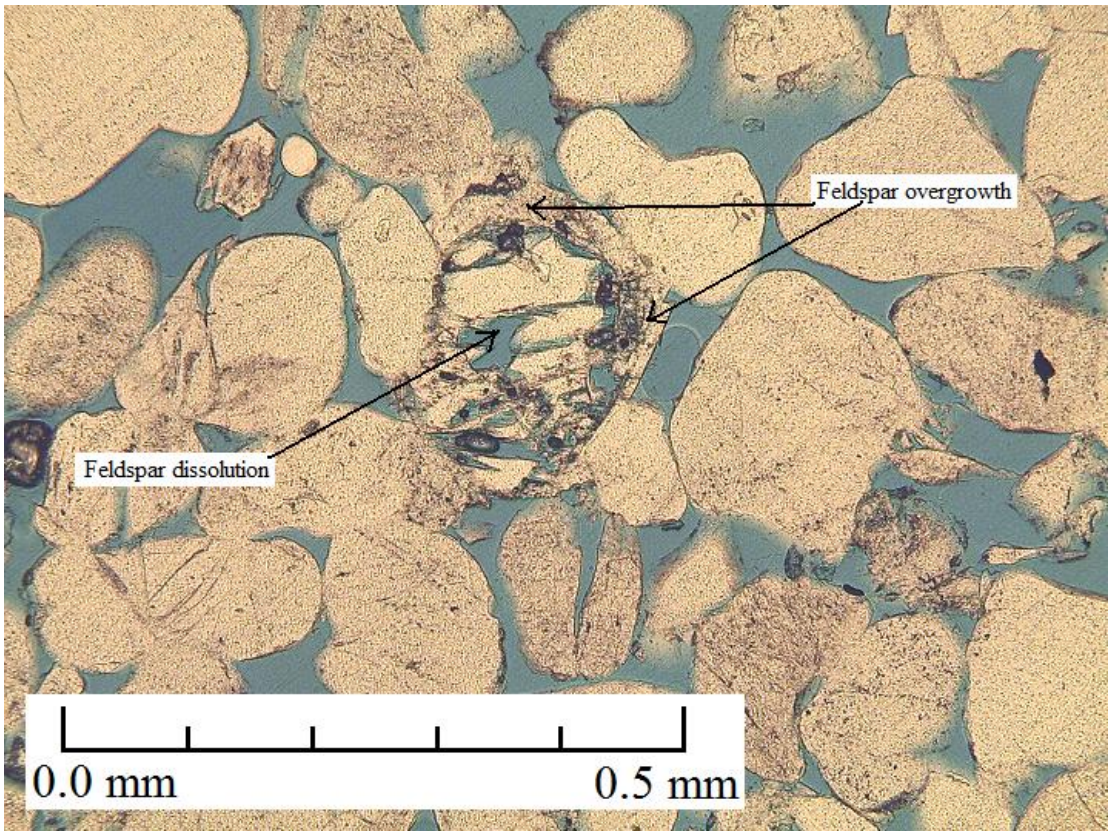

Figure 15. Photomicrograph showing feldspar overgrowth precipitation prior to feldspar dissolution in the Sinawava Member. In addition, feldspar dissolution must have occurred after compaction because the skeletal grain is not crushed. Sample 6/10/10-3.

White Throne Member of the Temple Cap Formation

Composition, texture, and structure

The White Throne is a quartz arenite (Table 1) consisting of fine-upper to medium-lower, moderately sorted, well rounded grains. The unit has high angle cross-strata, with ubiquitous deformation bands. The White Throne is noticeably more friable than the Navajo. There are no calcite cemented nodules in the White Throne.

Diagenesis

The principle diagenetic alterations in the White Throne are: compaction, calcite cementation, feldspar dissolution, and kaolinite precipitation. The characteristics of these events and their paragenetic relationships are outlined below.

Compaction, as evidenced by the presence of abundant long contacts, was the earliest diagenetic alteration. This compaction must have occurred prior to calcite cementation because there are long contacts within calcite cemented zones (Figure 16); compaction occurred before feldspar dissolution because there are skeletal feldspars that are not crushed (Figure 17).

Calcite cementation and psuedomorphic partial replacement of feldspars occurred before feldspar dissolution because there are voids present in partially replaced feldspar grains (Figure 16). If calcite cementation occurred after dissolution, then these voids would be filled in with calcite.

Feldspar dissolution likely occurred before kaolinite precipitation for two reasons: 1) insoluble aluminum from feldspar can act as source for kaolinite and, 2) kaolinite occurs in grain sized clumps (Figure 18).

Petrophysics

Porosity values determined from the 300-point counts range from 18-28% from two samples of the White Throne examined.

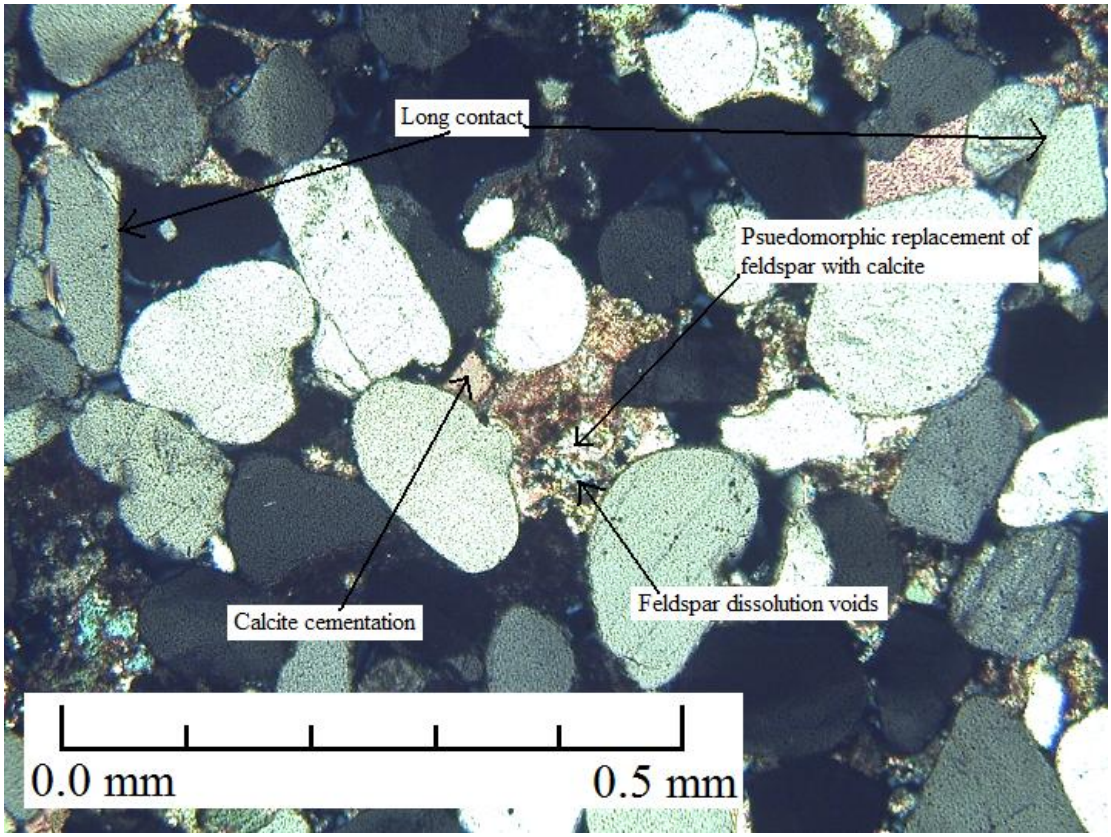

Figure 16. Photomicrograph showing compaction evidenced by numerous long contacts within calcite cemented areas, as well as psuedomorphic replacement of feldspar grains with calcite. Sample 6/10/10-7.

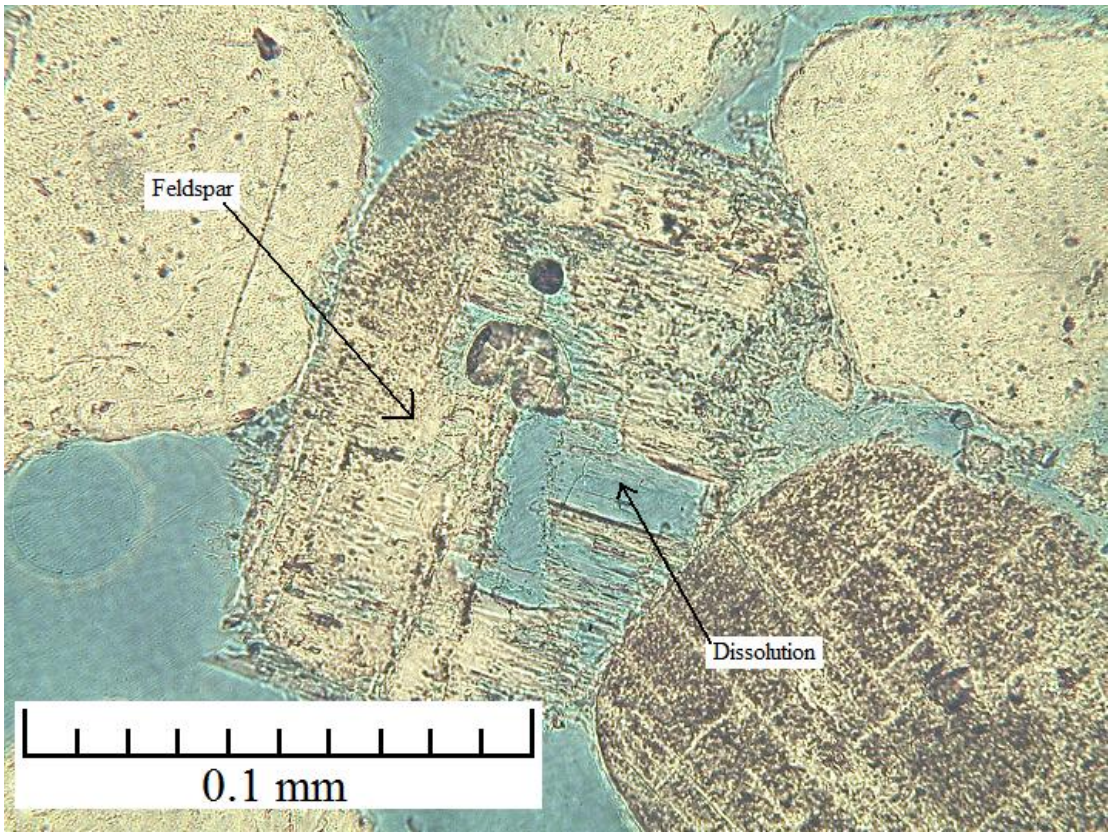

Figure 17. Photomicrograph showing skeletal feldspar in the White Throne Member. Compaction must have occurred before feldspar dissolution, or else the grain would be crushed. Sample 6/10/10-8.

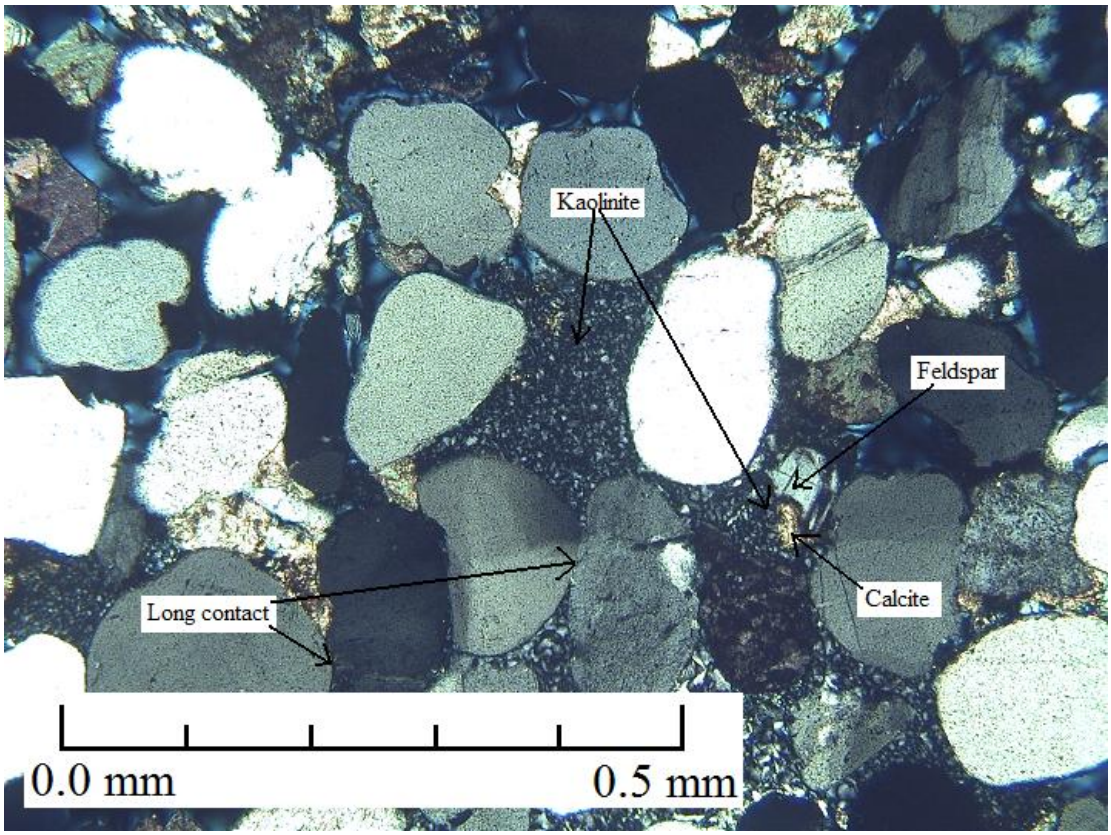

Figure 18. Photomicrograph showing kaolinite cementation. Kaolinite is also replacing feldspar grain. Sample 6/10/10-8.

Esplin Member of the Temple Cap Formation

Composition, texture, and structure

The Esplin Member consists of siltstones and quartz arenites. The contacts between the White Throne Member and the overlying Co-op Creek are buried at the Mount Carmel Junction site. The quartz arenite sample is remarkably similar to the White Throne Member of the Temple Cap Formation (samples 6/10/10-7 and 6/10/10-8). Because the exact contact between the White Throne and the Esplin was buried, it is possible that the sample was mistakenly identified as Esplin; it is also possible that the transitional environment from the White Throne to the Esplin resulted in the deposition of similar sediments.

Diagenesis

The principle diagenetic alterations in the Esplin Member are: precipitation of (chlorite?) clay rims, compaction, calcite cementation and partial replacement of feldspars, and feldspar dissolution.

Precipitation of clay rims must have occurred first for several reasons: 1) clay rims are present in between compacted grains, 2) clay rims are present in calcite cemented areas, and 3) clay rims are present on outside of skeletal feldspars but not inside (Figure 19). This clay is most likely chlorite because the clay precipitated as clay rims on the outside of grains (this texture is commonly associated with chlorite), and the clay is green under plane light.

Compaction occurred before calcite cementation because there are numerous long contacts between framework grains within calcite cemented regions (Figure 19).

Calcite cementation and partial replacement of feldspars occurred before feldspar dissolution because there are void spaces in the partially replaced feldspars and if calcite cementation occurred after dissolution, these spaces would be filled in with calcite instead of remaining empty (Figure 19).

Petrophysics

One sample from the Esplin Member had a porosity of 13.5% and a permeability of 0.000118 mD determined by TRA. From thin section 300-point counts, porosity ranged from 0.7-12%.

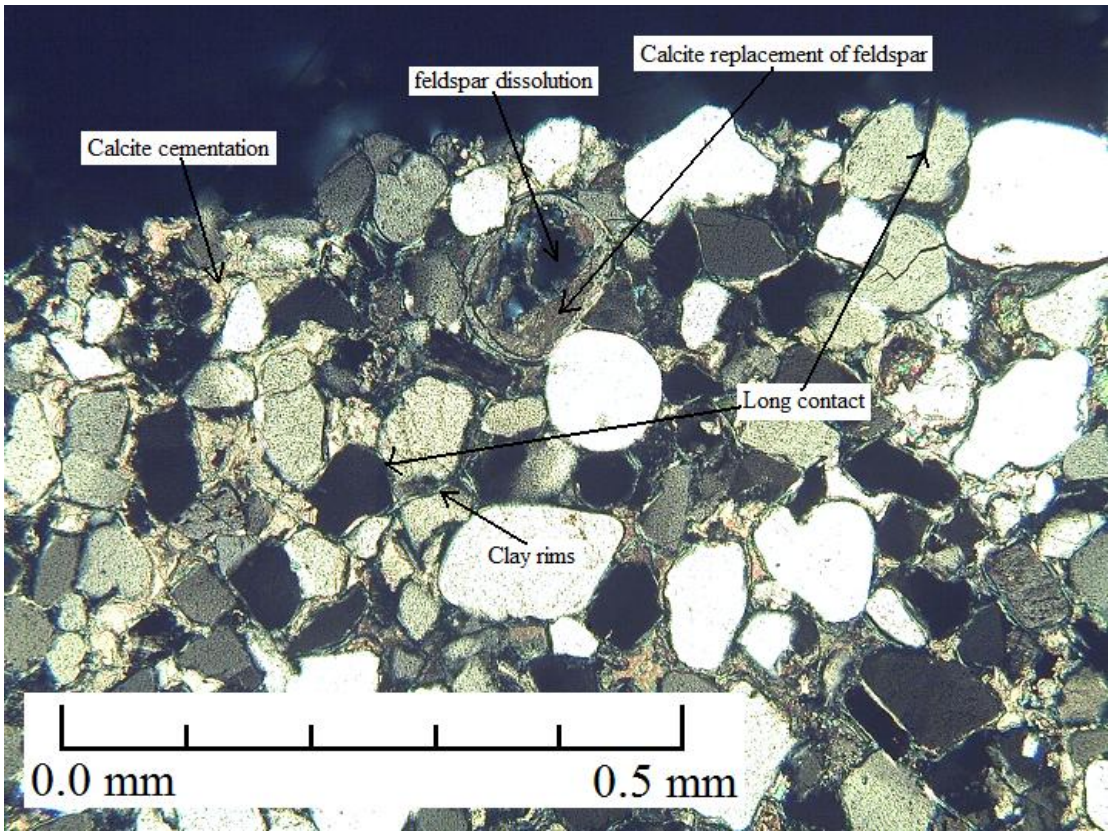

Figure 19. Photomicrograph illustrating paragenetic relationships in the Esplin Member. Clay rims must have precipitated first because they are present between compacted grains, and in calcite cemented areas. Compaction must have occurred next because there are numerous long contacts of framework grains inside calcite cemented zones. Calcite cementation must have occurred next because there are void spaces inside skeletal feldspar grains in calcite cemented areas. Sample 6/10/10.

Co-op Creek Member of the Carmel Formation

Composition, texture, and structure

The Co-op Creek Member consists of laminated shales containing small sandstone lenses with gypsum-filled fractures immediately above the contact with the Navajo Sandstone (Figure 20, 21). Above these shales, there are intrasparite/sparitic quartz grainstones (classifications of Duham, 1962 and Folk, 1974 respectively) with thin gypsum-filled fractures. At the top of the member there are mudstone/micritic limestones with quartz grains and gypsum, and claystones.

Diagenesis

The main diagenetic alterations in the Co-op Creek are: fracturing, dissolution to form vugular porosity, calcite precipitation, dolomite precipitation, gypsum precipitation and lastly dolomite precipitation and replacement of calcite by dolomite.

Interpreting the complete paragenesis of these samples was difficult. The paragenetic relationship between fracturing and dissolution could not be determined (Figure 22). Because the fractures are filled by calcite, it is clear that some calcite precipitation occurred subsequent to fracturing.

Vugular porosity suggests that dissolution of a more soluble phase, such as aragonite, high-Mg calcite or evaporites has occurred (Figure 22, 24). Calcite, dolomite and gypsum precipitation must have occurred after this dissolution because these phases precipitated in the majority of the vugs. The calcite precipitation resulted in drusy pore filling textures with the center of vugs filled by coarsely crystalline spar. Because calcite lines some of the gypsum filled vugs, the calcite probably formed prior to the gypsum. Because dolomite rhombs appear to cut some calcite pore filling textures, dolomite precipitation likely post dates calcite precipitation, at least for the pore filling calcite.

The relationship between calcite fracture filling and filling of dissolution voids could not be determined with certainty. The paragenetic relationship between gypsum and dolomite also could not be determined. In the one sample where there was gypsum and calcite precipitation in vugular porosity, there is a thin layer of precipitated calcite lining the inside of the dissolution created porosity, then gypsum fill, suggesting that calcite precipitation occurred before gypsum precipitation.

The fracturing and dissolution events may have been separated by a period of calcite precipitation, resulting in two separate phases of calcite precipitation. Another possibility is that there were two periods of dissolution (fracture, calcite, second calcite, dissolution). Figure 24 shows evidence for dissolution without any calcite precipitation, whereas Figure 22 shows evidence for calcite precipitation in dissolution porosity. This suggests that there were two periods of dissolution, or that the porosity documented in Figure 24 is not interconnected porosity. This hypothesis of two different calcite phases is substantiated by the presence of two distinct chemical phases of calcite in the quantitative electron microprobe analysis (please see following section Results - Electron Microprobe).

Following calcite precipitation, dolomite precipitated in porosity and partially replaced calcite (Figure 22, 25, 26). This is supported by the fact that there is a thin layer of micritic calcite around the detrital grains, and no such layer exists around the dolomite grains (Figure 22). The dolomite must have replaced the detrital and authigenic calcite, so it must have occurred after the calcite precipitation. The pore-filling dolomite is chemically identical to the dolomite replacing calcite, suggesting that the two dolomite types are from the same diagenetic event (see Elemental composition of carbonate cements section).

Petrophysics

The limestones present in the Co-op Creek Member range in permeability from 0.000004 to 0.454 mD at the MCJ site, while at the I-70 site, they range from 0.000044 to

0.038 mD. Porosity values range from 0.78 to 15.6% at the MCJ site, whereas at the I-70 site, porosity ranges from 1.89 to 12.3% (Table 3).

The shales/siltstones in the Co-op Creek range in permeability from 0.000116 to 0.000149 mD at the I-70 site. Porosity values range from 6.35 to 9.70% at the I-70 site (Table 5).

Figure 20. Outcrop photograph of Co-op Creek Member of the Carmel at I-70 site. Shales (green) immediately above contact with underlying Navajo Sandstone. Note thin veins of white gypsum immediately above rock hammer. Rock hammer for scale.

Figure 21. Outcrop photograph of Co-op Creek Member of the Carmel at I-70 site. Note laminated shales with sandstone lenses and intrasparite/sparatic quartz grainstone. 1.5 meter tall Jacob's Staff for scale.

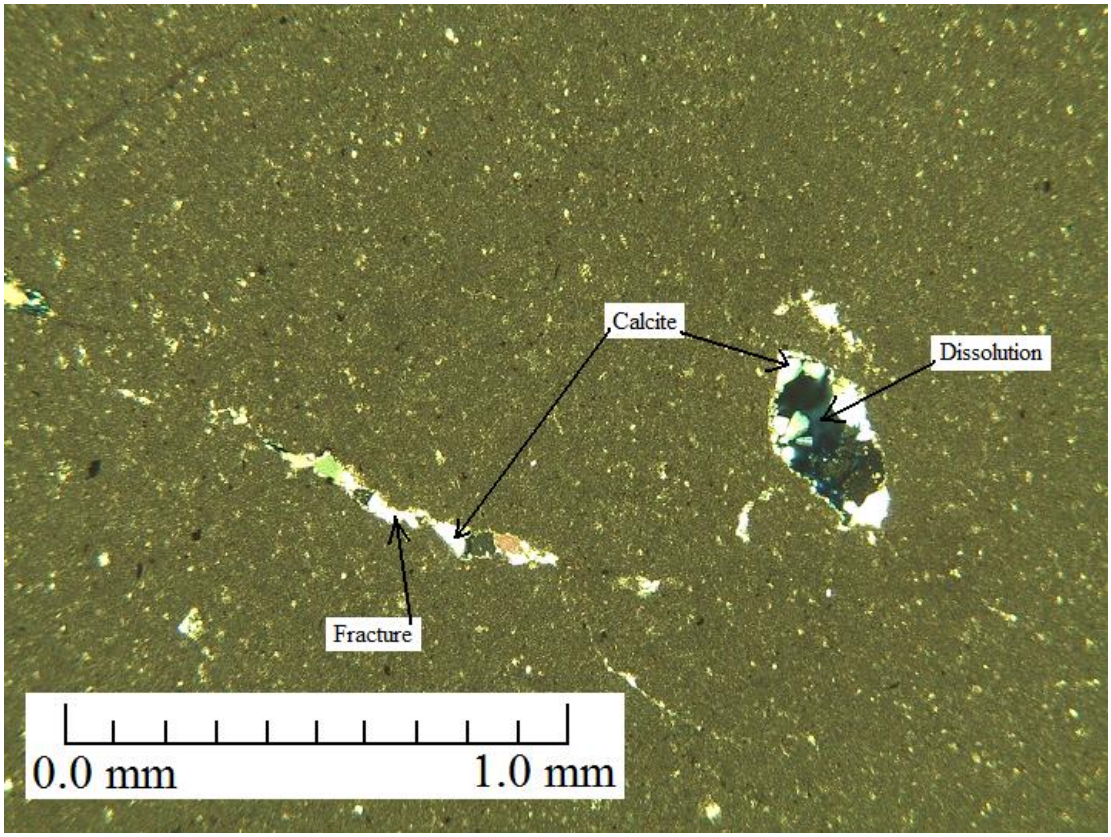

Figure 22. Photomicrograph showing calcite precipitation in fractures and inside oversized dissolution created porosity. Sample 6/10/10-17.

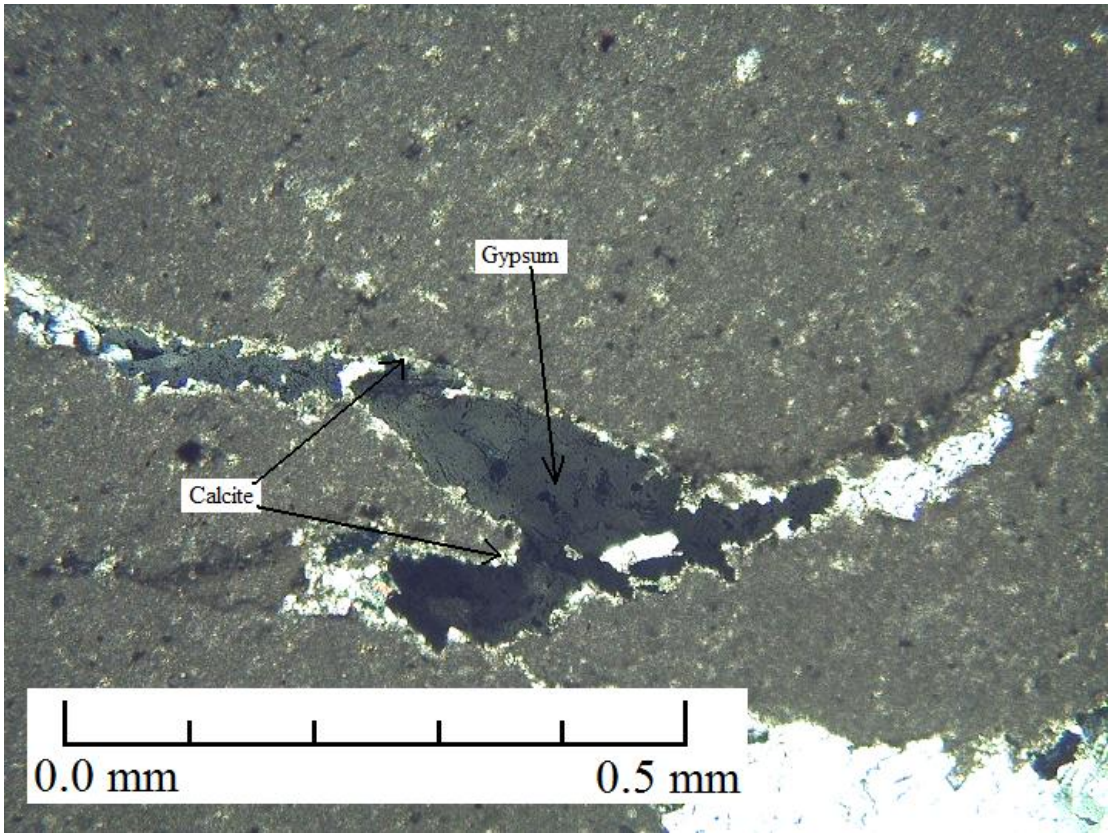

Figure 23. Photomicrograph showing a thin layer of precipitated calcite lining dissolution created vugular porosity before gypsum precipitation. Sample 6/10/10-17.

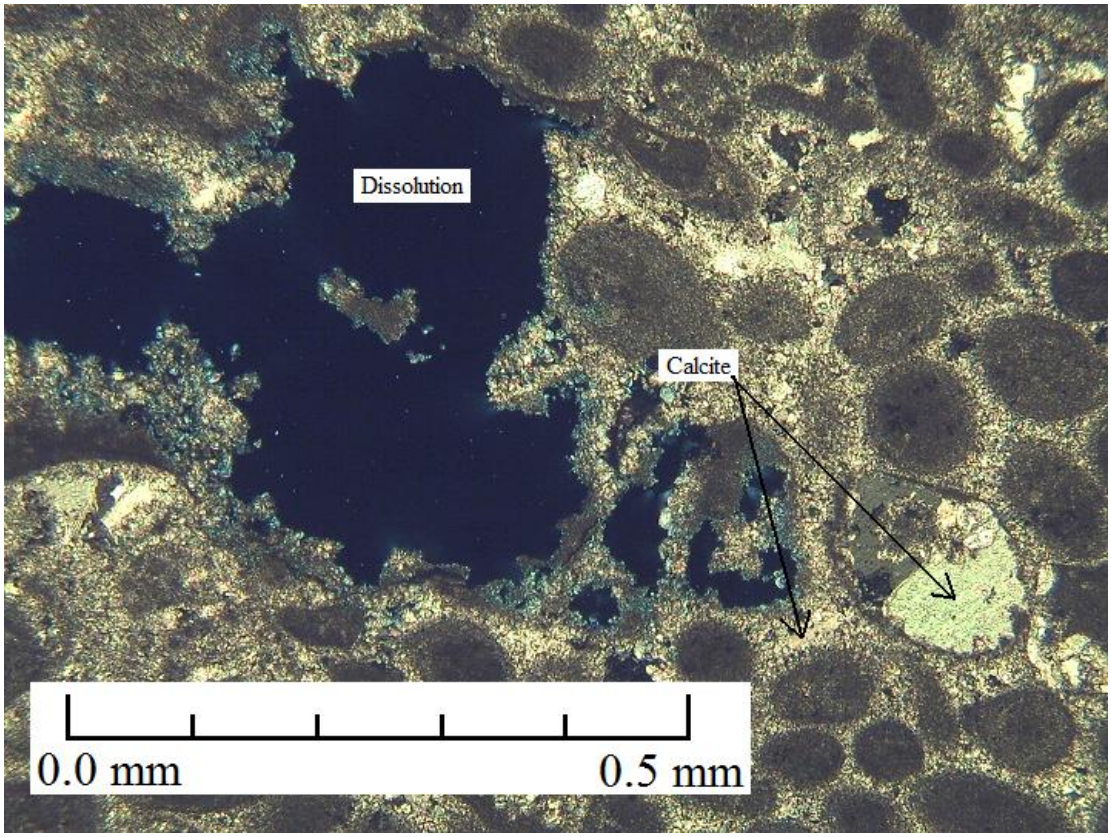

Figure 24. Photomicrograph showing calcite cementation prior to dissolution porosity. If calcite precipitation occured after, calcite would have grown inside the dissolution pores. Sample 6/10/10-18.

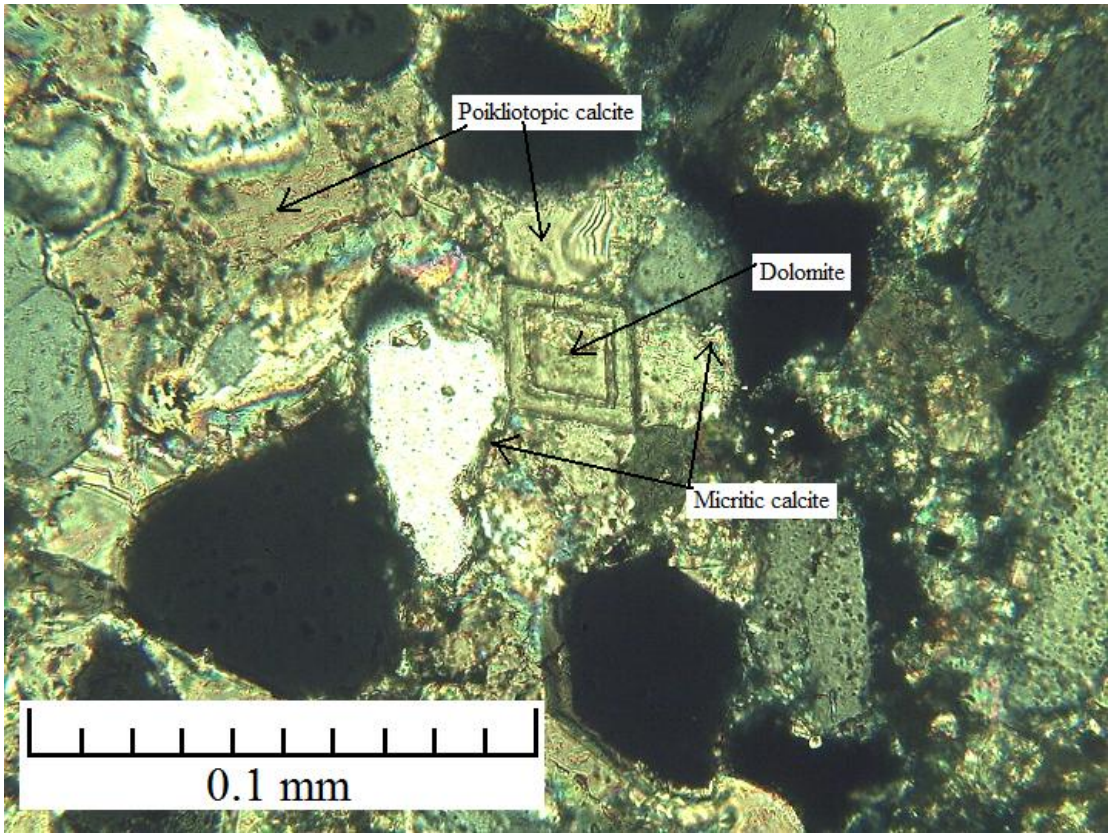

Figure 25. Photomicrograph showing dolomite that has replaced poikilotopic calcite cement. Dolomite rhombs present in calcite cemented areas are euhedral and show no sighs of transport. In addition, there is a thin layer of micritic calcite surrounding the detrital grains, and there is no such layer around the dolomite crystals. Sample 6/12/10-28.

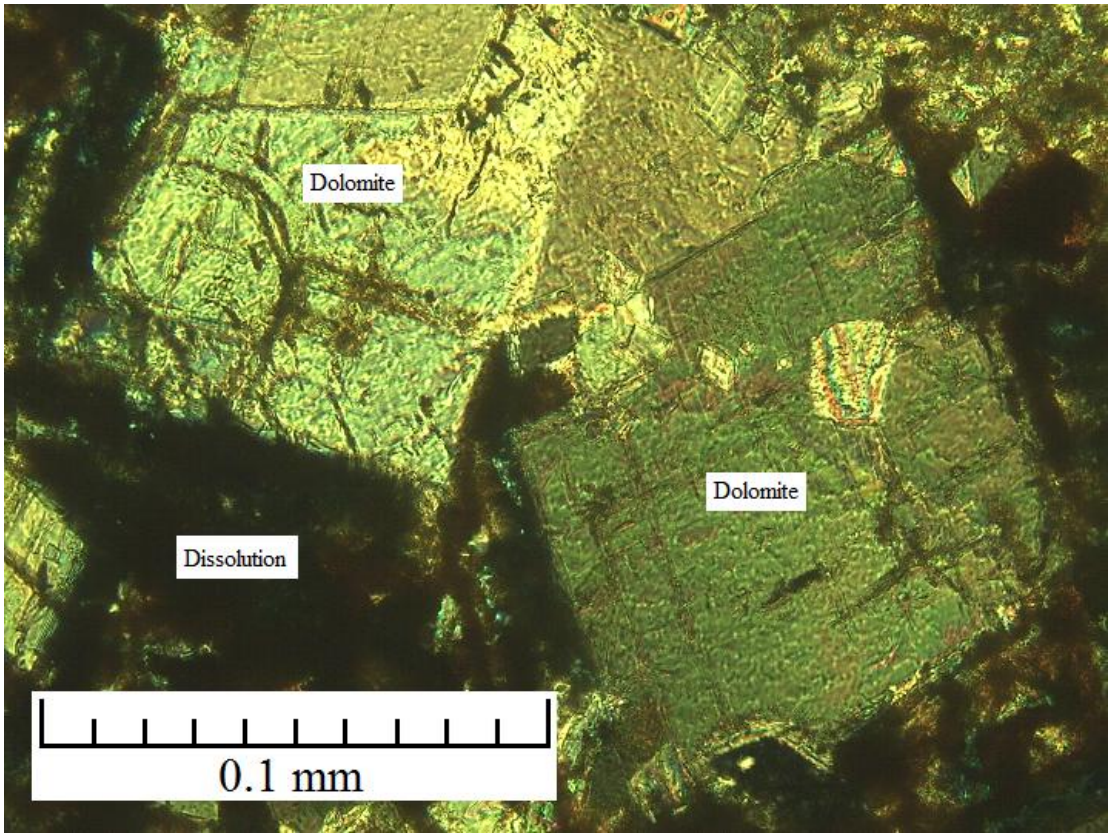

Figure 26. Photomicrograph showing evidence for calcite dissolution secondary porosity, followed by dolomite growth in porosity. Sample 6/12/10-27.

Crystal Creek Member of the Carmel Formation

Composition, texture, and structure

The Crystal Creek Member consists of mudstone/micritic limestone (classifications of Duham, 1962 and Folk, 1974 respectively) that contains large amounts of quartz grains (>40% in some samples), gypsum cement, and gypsum nodules (Figures 27 and 28). At the MCJ site, there is a unit of mixed laminated mud and then a unit of siltstone/shaley cross-bedded sandstone just below the gypsum bed instead of limestone.

Diagenesis

The principle diagenetic alterations in the Crystal Creek are precipitation of gypsum cement and replacement of dolomite by gypsum, fracturing, and precipitation of gypsum fracture fill.

The earliest diagenetic alteration may have been precipitation of poikilotopic gypsum, which locally forms nodules. Evidence for the early origin of the gypsum cement includes the uncompacted nature of the grains contained in the cement. However, an alternative explanation is that the gypsum cement formed as a replacing phase. This is suggested by rare pseudomorphs of dolomite rhombs in the cemented regions. With this scenario, dolomite precipitation must have occurred prior to gypsum cementation.

Gypsum precipitation must have predated fracturing and the fracture filling phase of gypsum cementation because there are several instances of gypsum cemented areas being cross cut by the fractures. If the poikilotopic cement occurred after the fracturing, there would a distinct textural change across the vein instead of the cement being divided across the vein (Figure 30). The gypsum fracture fill has a distinctive, bladed appearance compared to the poikilotopic gypsum.

Following this period of gypsum precipitation, there appears to have been partial replacement of gypsum by dolomite (Figure 32) and minor dolomite precipitation in porosity (Figure 31). Evidence for the replacement includes possible automorphic penetration of gypsum by dolomite. The dolomite inside the poikilotopic gypsum cemented areas is perfectly rhombic, whereas the dolomite outside the gypsum cemented areas conforms to the existing grains. The dolomite must have formed after the gypsum

cementation or else there would be imperfect dolomite rhombs conforming to the surrounding grains in the gypsum cemented areas.

Petrophysics

One sample from the Crystal Creek Member was analyzed from the I-70 site. It has a permeability of 0.105 mD and a porosity of 12.3% (Table 3).

Figure 27. Outcrop photograph of micritic limestones with gypsum filled fractures from the Crystal Creek Member at I-70 site. 1.5 meter Jacob's Staff for scale.

Figure 28. Outcrop photograph showing the contact (red line) between the underlying Crystal Creek Member, consisting of micritic limestones, and the overlying Paria River Member, consisting of bedded gypsum at the I-70 site. Rock hammer for scale.

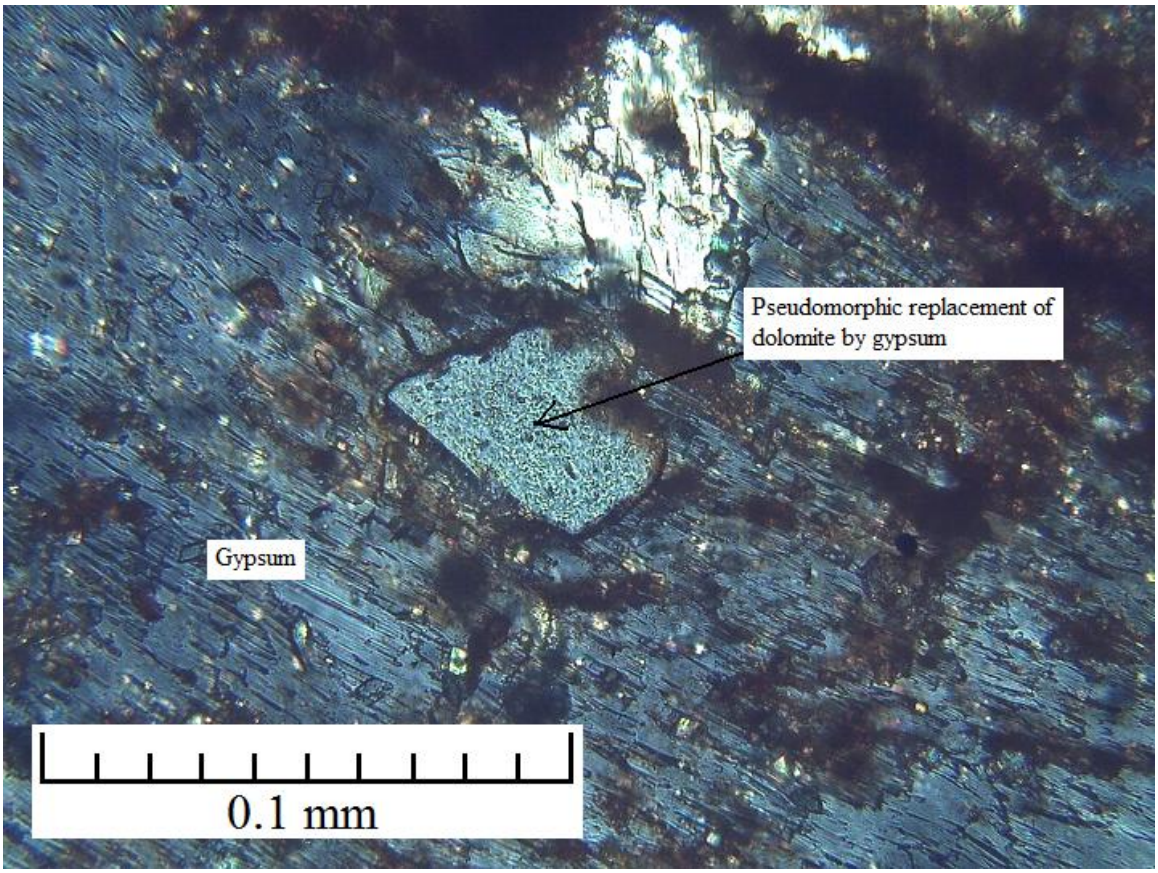

Figure 29. Photomicrograph showing pseudomorphic replacement of dolomite by gypsum. Dolomite must have precipitated prior to gypsum cementation. Sample 6/12/10-31.

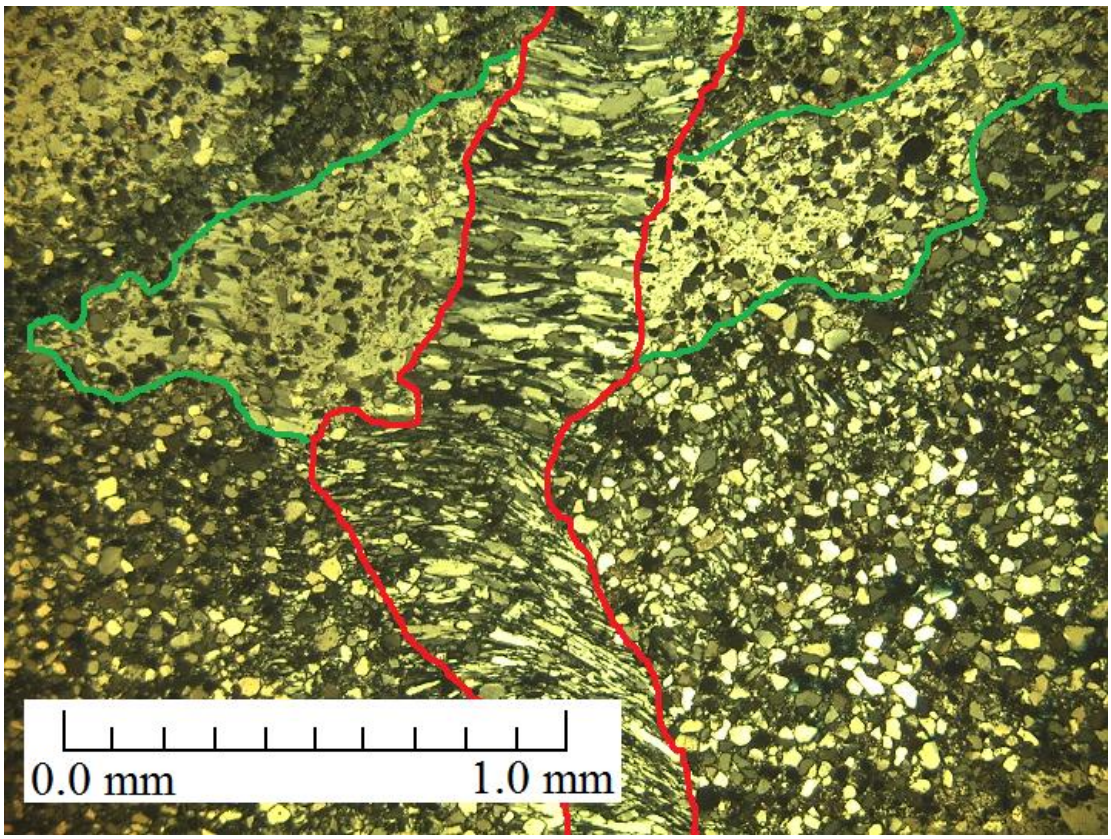

Figure 30. Photomicrograph showing evidence for poikilotopic gypsum cementation followed by fracturing, and precipitation of gypsum in fracture. Poikilotopic gypsum cement outlined in green, and cross cutting fracture outlined in red. Sample 6/12/10-32.

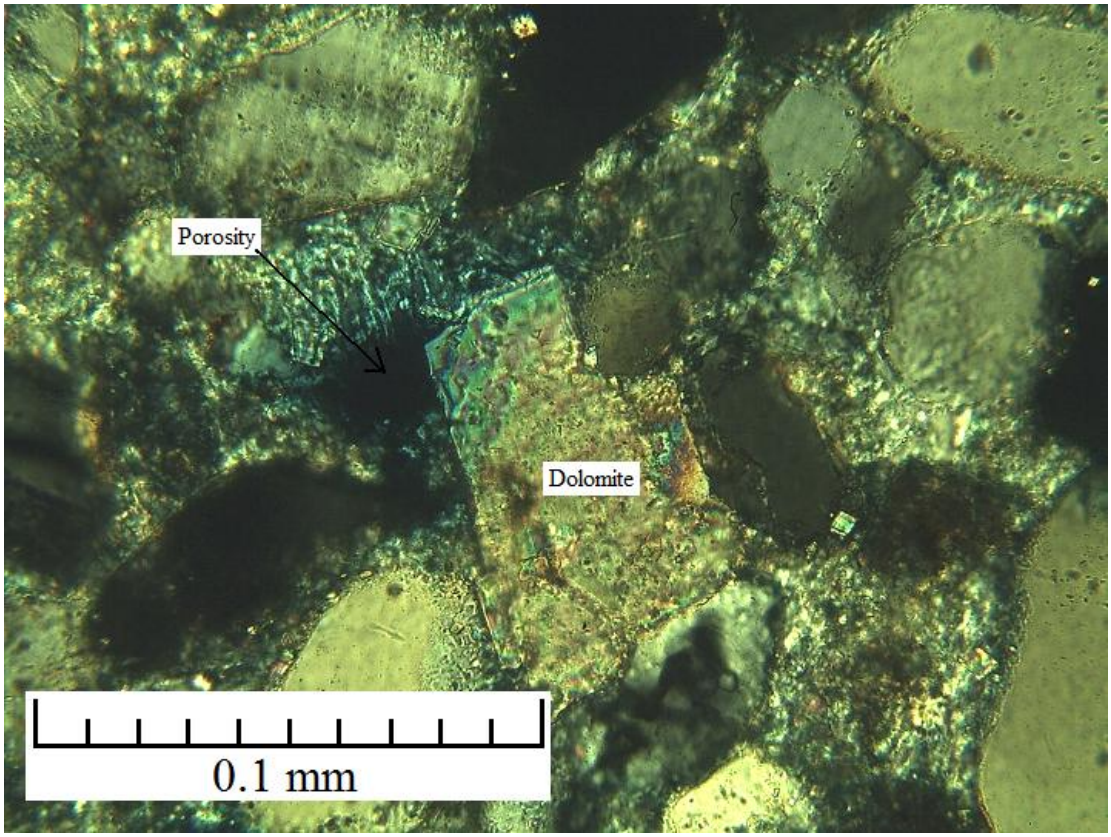

Figure 31. Photomicrograph showing pore filling dolomite. Dolomite rhomb grew in open pores conforming its shape to that of the surrounding grains. Sample 6/12/10-32.

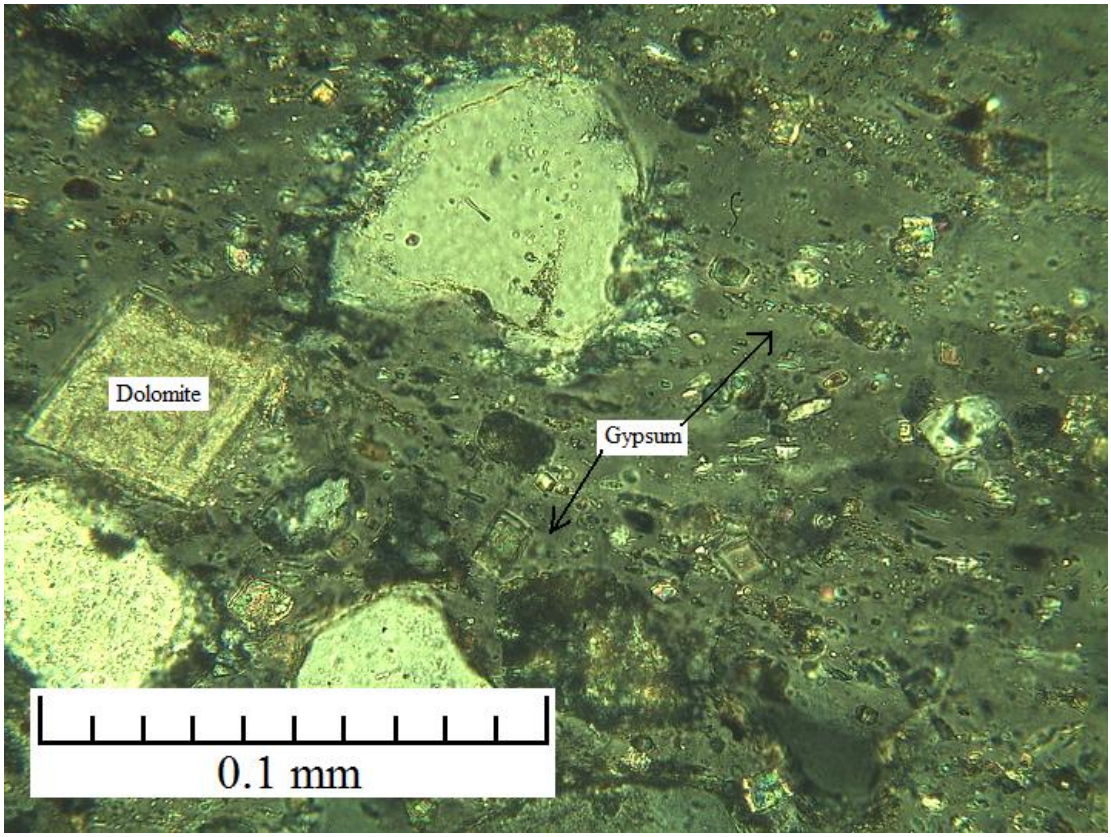

Figure 32. Photomicrograph showing relationship between gypsum precipitation and dolomite. Poikilotopic gypsum may have precipitated around dolomite rhombs. Alternatively, dolomite replaced pre-existing poikilotopic gypsum cement. Sample 6/12/10-32.

Paria River Member of the Carmel Formation

Composition, texture, and structure

The Paria River Member contains three main lithologies. The base of the unit is a thick (~2.5 meters) bed of gypsum, with minor amounts of disseminated sparite calcite crystals. Above this are thinly bedded heavily altered dolostones. The remainder of the unit consists of mudstones/micritic limestones (classifications of Duham, 1962 and Folk, 1974 respectively).

Diagenesis

The thinly bedded limestones have undergone diagenetic alterations very similar to those of the Co-op Creek Member. The main diagenetic alterations are fracturing, dissolution to form vugular porosity, calcite precipitation, and dolomite precipitation and replacement of calcite.

As for the Co-op Creek Member, determining the complete paragenetic sequence was not possible with the limited data available. In the Paria River Member, there is an ambiguous relationship between fracturing and dissolution. None of the fractures cut through any dissolution voids, so the ordering of the two events cannot be determined. In any case, there is calcite in both the fractures (Figure 34) and dissolution voids (Figure 35), so some calcite precipitation must have postdated both of these events. The calcite precipitated as a micrite cement, and also in a drusy texture in the open pores (Figure 35).

After calcite precipitation, dolomite precipitated in open pores and as overgrowths on preexisting dolomite (Figure 36). The dolomite is clearly not detrital, because many of the dolomite rhombs have grown conforming to the preexisting grains. In addition, most of the dolomite rhombs are euhedral and would not have survived transport without suffering some damage. Dolomite precipitation could have occurred after calcite precipitation because the dolomite appears to have enveloped nearby calcite crystals as it precipitated.

Two stages of dolomite precipitation resulted in zoned rhombs consisting of an inner core and an outer rim (Figure 36). There is a distinct chemical difference between the cores (an inner portion that has higher magnesium content and an outer portion that has higher manganese content: see Elemental composition of carbonate cements section)

of the dolomite rhombs, suggesting that there were indeed two different diagenetic events.

Petrophysics

The Crystal Creek member ranges in permeability from 0.000008 to 0.000993 mD at the I-70 site. In terms of porosity, values range from 1.70 to 8.14% at the I-70 site from MICP (Table 5).

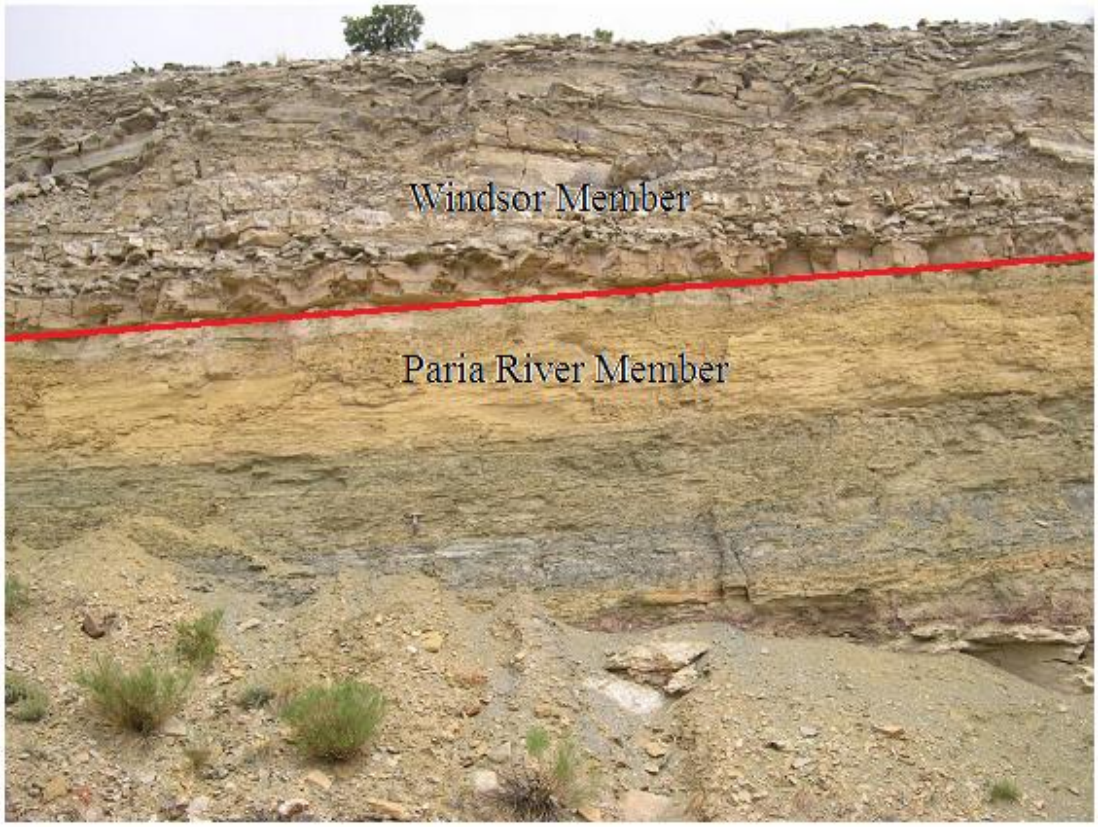

Figure 33. Outcrop photograph showing the contact between the Paria River Member and the Windsor Member at I-70 site represented by a red line. Micritic limestones and shales in the Paria River Member, are overlain by micritic limestones in the Windsor Member. Bush at top of outcrop 5 feet tall.

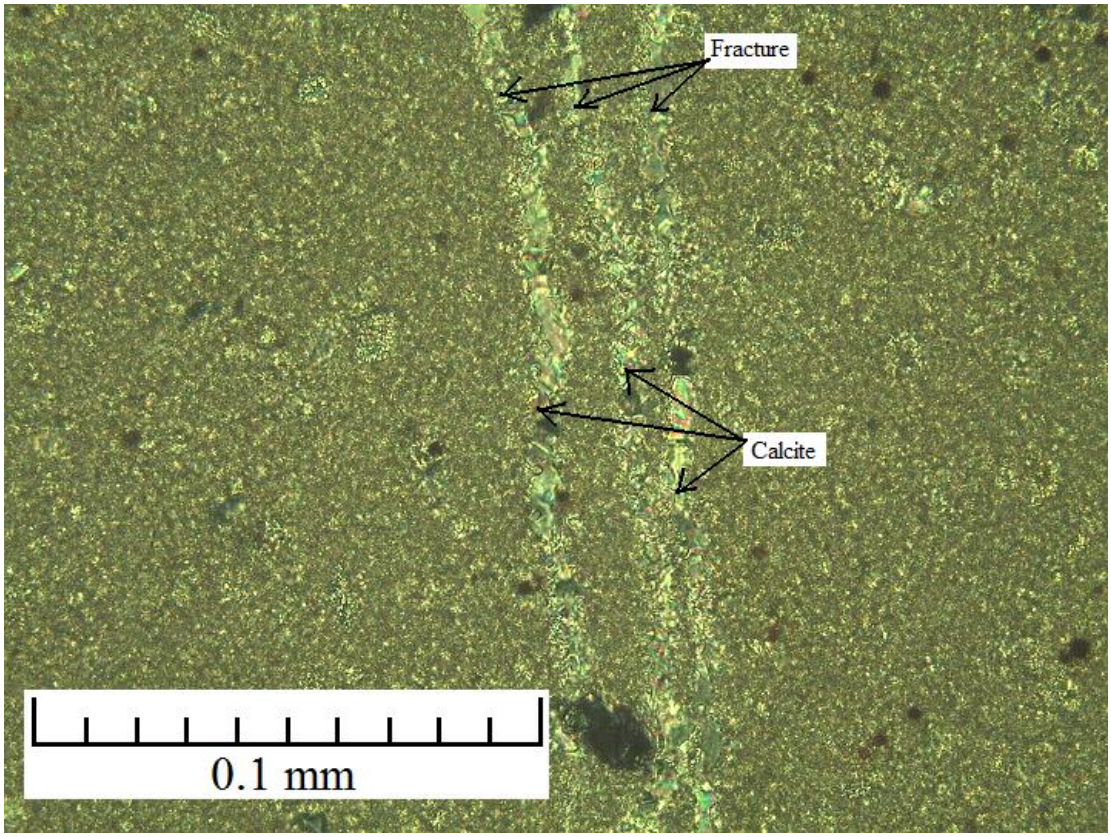

Figure 34. Photomicrograph showing fracture filled by calcite cement. Sample 6/12/10-38.

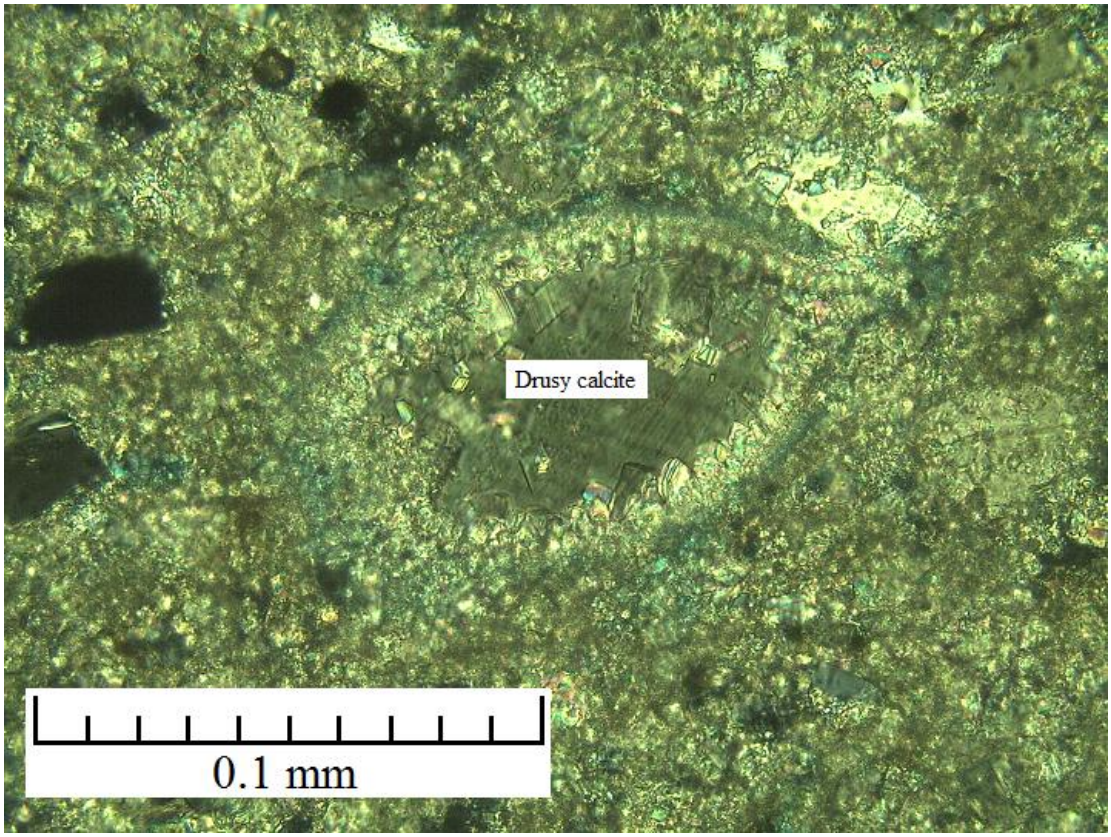

Figure 35. Photomicrograph showing drusy calcite cement that precipitated in a dissolution void. Sample 6/12/10-34.

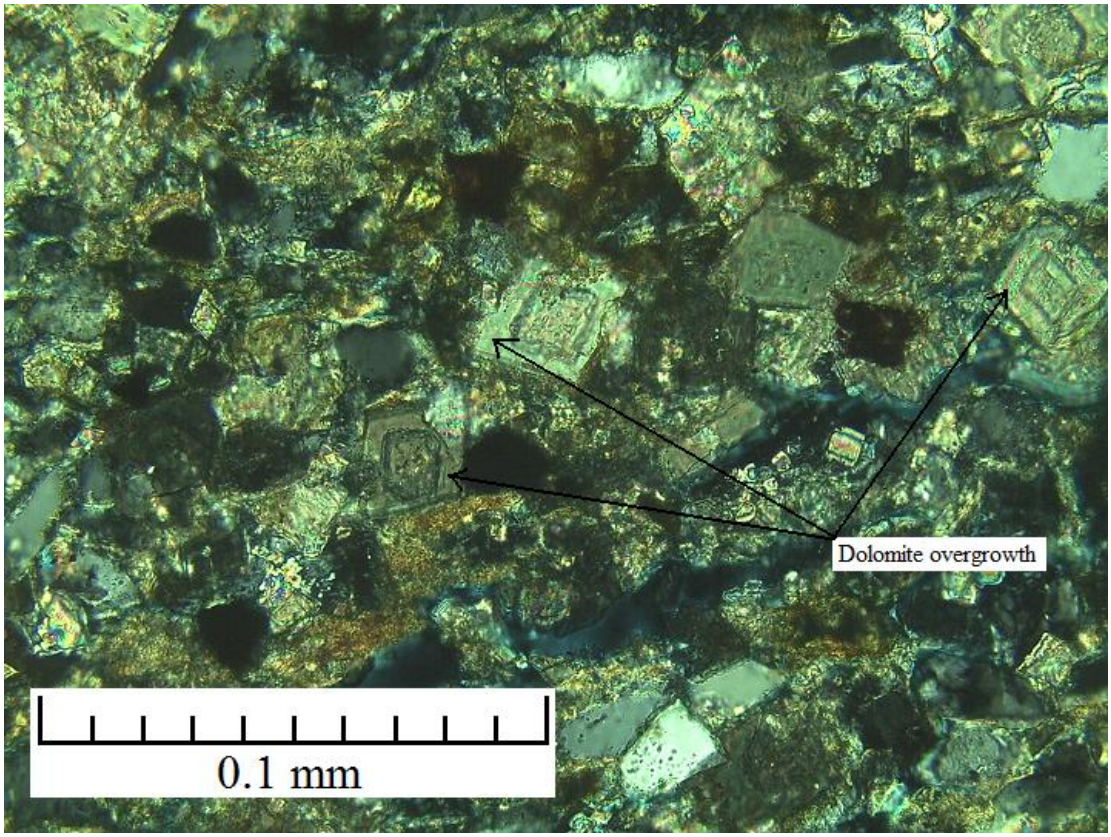

Figure 36. Photomicrograph showing dolomite overgrowths within the Paria River Member growing around preexisting dolomite. Sample 6/12/10-36.

Combined diagenesis

Figure 37 combines all the diagenesis from the Navajo Sandstone, the Temple Cap Formation, and the Carmel Formation. It is likely that some of the diagenetic alterations are actually the same alteration affecting several members/formations. For example, calcite cementation is present in every member/formation of the units examined except for the Crystal Creek Member, so it is possible that they originated from the same precipitating fluid and at the same time.

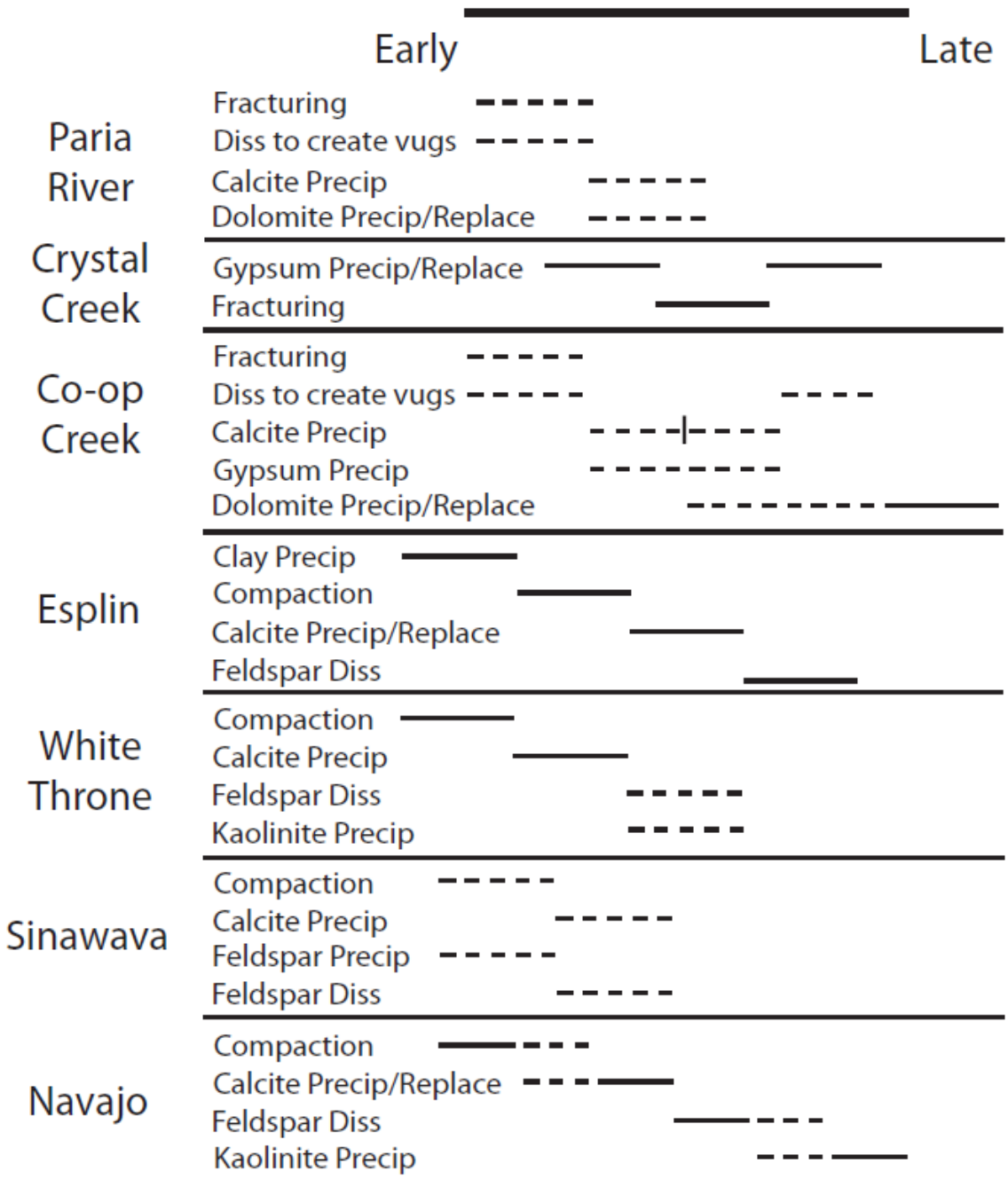

Figure 37. Diagram showing the ordering of diagenetic events in the Navajo Sandstone, Temple Cap Formation, and lower 3 members of the Carmel Formation. Solid lines indicate certainty in timing, whereas dashed lines indicate uncertainty in timing.

Burial history

Attempting to tie the diagenetic events (Figure 37) to the burial history of the Carmel Formation (Figure 38) would have been possible if the temperature of

precipitation of the cements were available. Unfortunately, a fluid inclusion study was not a part of this thesis. However, one can make generalized assumptions about the paragenesis and how it relates to the burial history. Compaction would have occurred during burial portion of the curve, from deposition of the sediments to ~75 Ma. Dissolution may have occurred during uplift, when meteoric water was introduced. However, because there are intermittent periods of dissolution and cementation, the timing of this is unclear. Feldspar dissolution and kaolinite precipitation are often associated with the introduction of meteoric water (e.g. Mansurbeg et al. 2006), so these diagenetic events may have occurred during the uplift portion of the curve, starting at ~40 Ma.

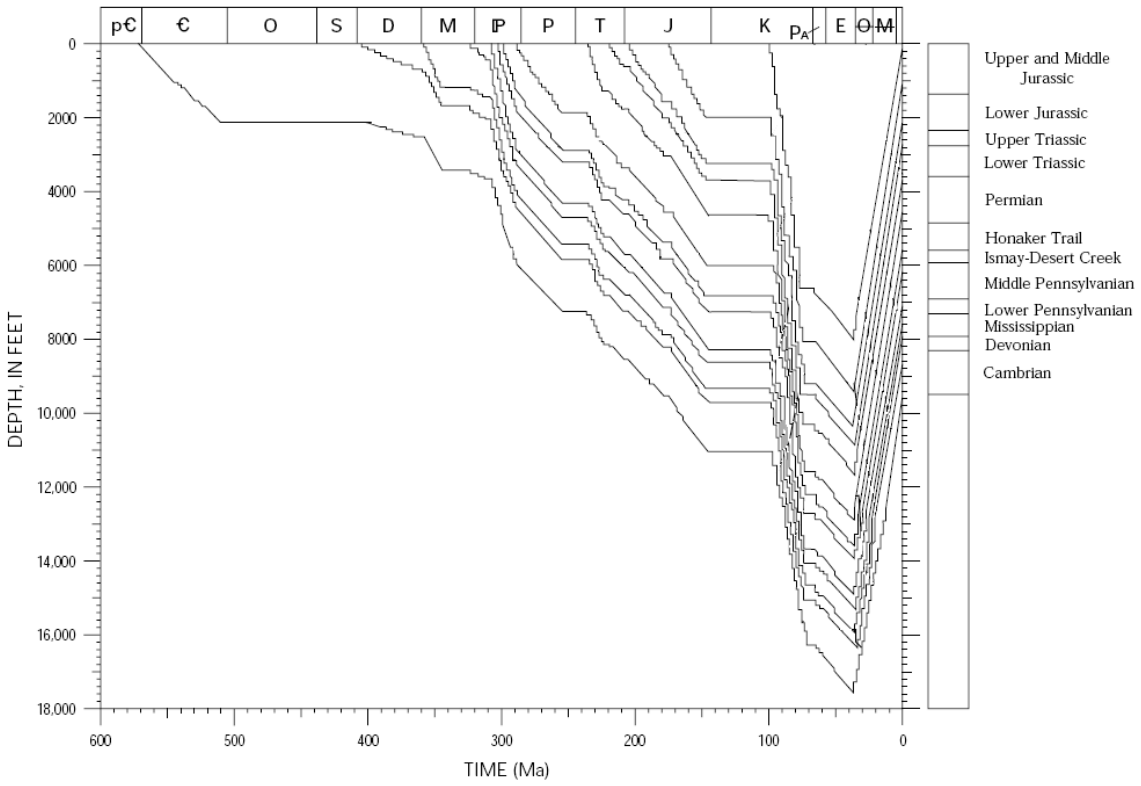

Figure 38. Burial history curve of sedimentary units near Green River, Utah. Modified from Nuccio et al., 2000.

Stable isotopes

Stable isotope compositions of the calcite and gypsum veins can provide constraints on possible environments of precipitation. $\delta^{13}C$ and $\delta^{18}O$ values from the calcite veins are shown in Table 2, while $\delta^{34}S$ values from the gypsum veins are shown in Table 3.

Carbon and oxygen isotopes from calcite

Table 2. $\delta^{18}O$ and $\delta^{13}C$ from calcite mineralized fractures at I-70 site.

Sample	$\delta^{13}C$	$\delta^{18}O$
F2B	-4.31	12.99
F2B (Duplicate)	-4.26	12.72
F2C	-4.00	14.89
F2C (Duplicate)	-3.21	15.81
F3B	-4.31	12.88
F3B (Duplicate)	-4.55	12.89

Calcite veins

Calcite is isotopically fractionated when it precipitates from water as a function of temperature. The fractionation factor is

$$1000 \ln \alpha_{\text{calcite-water}} = (2.78 \text{ X } 10^6 / T^2) - 2.89 \text{ (O'Neil, 1969)}$$

with T in Kelvin. With only the isotopic composition of the calcite and the appropriate fractionation factor, it is not possible to determine both the temperature and fluid composition uniquely. However, one can calculate possible water composition as a function of temperature (Figure 39).

If the precipitating fluid was the Carmel-Twin Creek Seaway seawater, there would have to have been temperatures between 125-150°C, which is highly unlikely at surface or near surface conditions. This is assuming that the $\delta^{18}O$ of the Carmel-Twin

Creek Seaway was approximately the same isotopic composition of modern oceans, which is likely given that during the Jurassic, there were not extensive polar ice caps or other features that would greatly alter the composition of the oceans (Sharp, 2007).

A second possibility is that the calcite is from interaction with meteoric water. Although stable isotope data from Gordon Creek was unobtainable, data for meteoric water composition was available from the Aneth Oil Field in San Juan County, Utah (southeast corner of the state). $\delta^{18}O$ values of samples from the San Juan River, composite snow samples from the Abajo Mountains, and samples from the Navajo Sandstone range from -17 to -12‰ (Spangler et al., 1996). The calcite from I-70 could have formed from meteoric water with these values at surface/near surface temperatures between 25-50°C (Figure 39).

A third possibility is that the calcite formed from ~0 SMOW waters at a higher temperature (>150°C) at depth (Figure 39). This would mean that real fractures (ones not associated with weathering processes) could be mineralized with calcite at depth, which would reduce the risk associated with CO_2 escaping through open fractures.

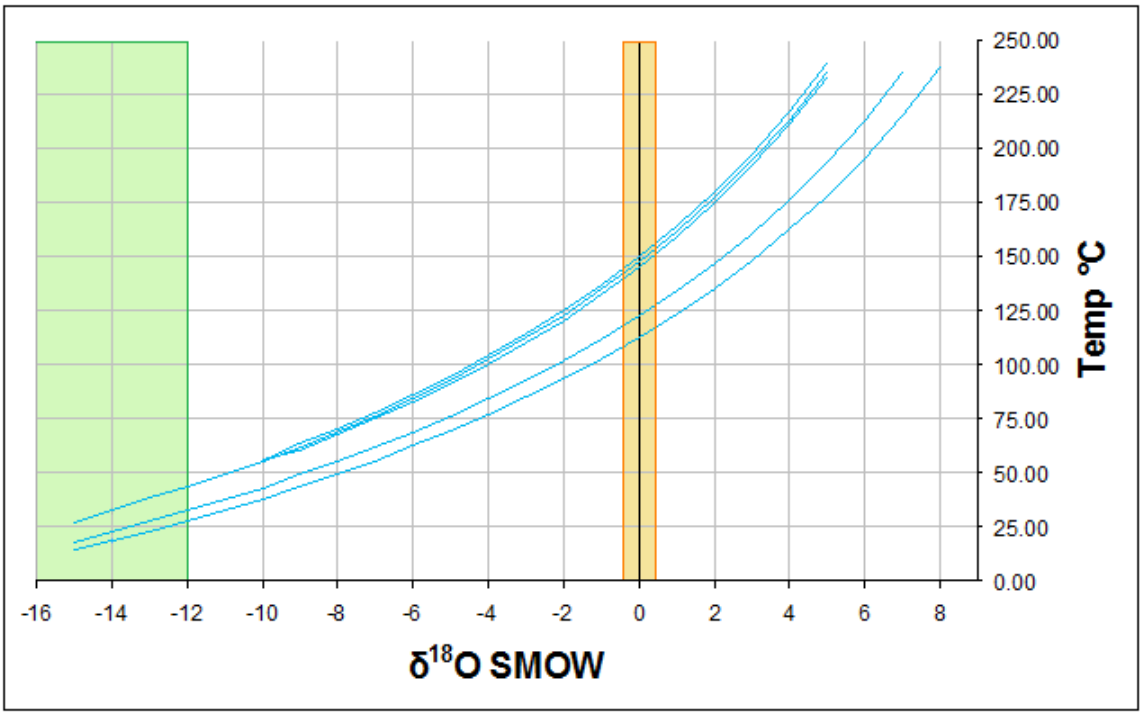

Figure 39. Graph relating possible temperature of precipitation to possible $\delta^{18}O$ of the precipitating water for calcite vein samples. The low temperature, meteoric water possibility is outlined in green. Possible Carmel-Twin Creek values are outlined in orange.

Sulfur isotopes from gypsum

Table 3. $\delta^{34}S$values obtained from gypsum veins within the Carmel.

Sample	$\delta^{34}S$
7/10/10-F1	-11.33
7/10/10-F1 (Duplicate)	-11.54
7/10/10-F4A	12.13
7/10/10-F4A (Duplicate)	11.82
7/10/10-F4B	12.14
7/10/10-F4B (Duplicate)	12.22
7/10/10-F5A	12.58
7/10/10-F5A (Duplicate)	13.25
7/10/10-F5B	12.59
7/10/10-F5B (Duplicate)	12.34
7/10/10-F6	13.16
7/10/10-F6 (Duplicate)	13.22

Gypsum veins

The sulfur isotopic compositions obtained from the gypsum veins in the Co-op Creek and Crystal Creek Members, as well as the bedded gypsum are not significantly different from one another (Table 3). It is likely that they incorporated the same sulfur source.

The $\delta^{34}S$ of the evaporites can be used as a proxy for seawater $\delta^{34}S$ because there is little to no fractionation when sulfates go into and out of solution (Sharp, 2007). Figure 40 shows the variations of $\delta^{34}S$ through geologic time, with the values determined in this study in a red box; the Carmel gypsum values are lighter than average values for other evaporites deposited during the Jurassic.

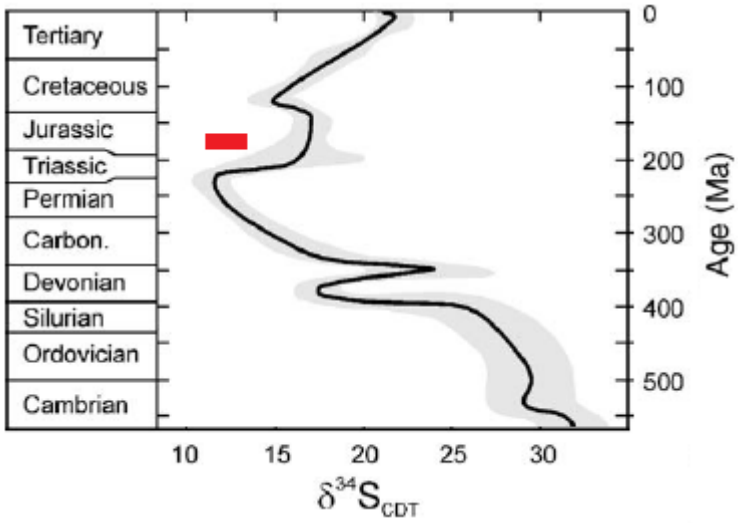

Figure 40. Changes in $\delta^{34}S$ of marine evaporites through geologic time. Data obtained from Carmel Formation bedded gypsum and gypsum veins are plotted in red; these values are 4-5‰ lighter than those deposited during the Jurassic. Modified from Newton and Bottrell, 2007.

The slightly lighter sulfur values might be explained by underlying Permo-Triassic gypsum being dissolved and then reprecipitated stratigraphically higher. Triassic sulfate has values within the same range as those in the Carmel, so it is possible that

gypsum dissolved into pore water, and this fluid was the source for the Carmel Formation gypsum. The dissolution enhanced porosity in the Carmel could have been occupied by this source gypsum. This is not a very convincing explanation, because it does not explain how bedded gypsum would form if this was the dominate source for the gypsum.

The sulfur values are all grouped around 12‰, with the notable exception of sample 7/10/10-F1, with a value of -11.4‰; a difference of 23‰ (Table 2). All of the gypsum samples were obtained from mineralized fractures and beds from the I-70 site. Having a difference of 23‰ from samples that precipitated in similar depositional environment is difficult to explain. One might think that it is a poor data point, but each sample was run twice, so the value is correct. It could also be explained by some fractionating process, such as oxidation, during diagenesis, but because the samples were spaced stratigraphically close together, this is unlikely.

The gypsum veins could have formed close to the surface or from subhorizontal compressional forces. Given that σ_1 would be oriented parallel to the long axis of the fracture and σ_3 would be oriented with the short axis of the fracture, the fractures could not have formed from pressures associated with burial. They might have formed from compressional tectonic forces, possibly associated with the formation of the San Rafael Swell, or near the surface because σ_3 should be subvertical near the surface.

Field permeametry

Field permeametry was only successful for two grids from the Navajo Sandstone, with Grid 1 being 8.5 meters below the Carmel/Navajo contact and Grid 2 being just below the Carmel/Navajo contact (Table 4). The rock permeability at every other grid

location was too low for the instrument to measure. This inability to gather data is actually a good thing in terms of the Carmel Formation acting as a seal, because it means that even without quantitative data, the Carmel Formation is relatively impermeable.

The Navajo Sandstone has an average permeability of 0.88 D (880 mD) for the two grids. There is no discernable spatial variation in the values. All data from the field permeability testing is shown in Table 4.

Table 4. Flow measurements, tank pressure, pressure gauge measurements on instrument, and calculated flow in m^2 and D.

		Flow (mm)	Tank P(psi)	P Gauge	k(m^2)	k(D)
Grid 1	A1	83	10	1.6	1.15E-12	1.15
	C1	87	10	1.2	1.22E-12	1.22
	E1	90	10	1	5.69E-14	0.06
	G1	91	10	0.8	1.29E-12	1.29
	I1	86	10	1.2	1.2E-12	1.20
	K1	77	10	2.4	1.04E-12	1.04
	A3	85	10	1.6	1.18E-12	1.18
	C3	90	10	1	5.69E-14	0.06
	E3	95	10	1.4	1.36E-12	1.36
	G3	90	10	0.8	1.27E-12	1.27
	I3	86	10	1.4	1.2E-12	1.20
	K3	86	10	1.5	1.2E-12	1.20
	A5	81	10	1.8	1.11E-12	1.11
	C5	90	10	1	5.69E-14	0.06
	E5	85	10	1.4	1.18E-12	1.18
	G5	89	10	1	5.61E-14	0.06
	I5	90	10	0.8	1.27E-12	1.27
	K5	91	10	0.8	1.29E-12	1.29
	A7	85	10	1.6	1.18E-12	1.18
	C7	92	10	0.7	1.31E-12	1.31
	E7	84	10	1.7	1.17E-12	1.17
	G7	91	10	0.8	1.29E-12	1.29
	I7	92	10	0.6	1.31E-12	1.31
	K7	76	10	2.5	1.02E-12	1.02
Grid 2	A1	88	10	1	3.96E-13	0.40
	A3	93	10	0.6	1.32E-12	1.32
	A5	90	10	1	5.69E-14	0.06
	A7	90	10	1	5.69E-14	0.06

		Flow (mm)	Tank P(psi)	P Gauge	k(m^2)	k(D)
Grid 2	C1	94	10	0.5	1.34E-12	1.34
	C3	88	10	1	5.53E-14	0.06
	C5	95	10	0.5	1.36E-12	1.36
	C7	92	10	0.6	1.31E-12	1.31
	E1	90	10	1	5.69E-14	0.06
	E3	75	10	3	1.01E-12	1.01
	E5	90	10	1	5.69E-14	0.06
	E7	90	10	1	5.69E-14	0.06
	G1	93	10	0.4	1.32E-12	1.32
	G3	92	10	0.6	1.31E-12	1.31
	G5	92	10	0.6	1.31E-12	1.31
	G7	90	10	1	5.69E-14	0.06
	I1	94	10	0.6	1.34E-12	1.34
	I3	80	10	2	1.09E-12	1.09
	I5	90	10	1	5.69E-14	0.06
	I7	83	10	2	1.15E-12	1.15

For a large number of samples from the Navajo (13 out of 44), there were sampling points that measured 2 orders of magnitude lower than values considered "normal" (between 1 and 1.4 D; Solum et al., 2010); this could be because of heterogeneities in calcite cementation, grain size variations, or sorting variations. If these are not taken into account, then the average permeability for both grids increases (1.21 D for Grid 1 and 1.25 D for Grid 2).

Mercury injection capillary pressure (MICP)

MICP testing was performed on 13 samples from the Carmel Formation, and porosity/permeability were calculated. They were chosen to represent the range of lithologies present in the Carmel Formation, as well as the different types of diagenetic alterations. Permeability ranges from 0.000004 to 0.454 mD, with an average of 0.0537 mD. Porosity ranges from 0.78 to 15.6%, with an average of 6.33%. All the data from the MICP testing is shown in Table 5, while the pressure data and curves are shown in Appendix A.

Table 5. Porosity, permeability, and density values obtained from MICP testing performed by Poro-Technology.

Sample	Air Porosity (%)	MICP Porosity (%)	Air Perm. (mD)	MICP Perm. (mD)	Bulk Den. (g/cc)	Grain Den. (g/cc)
6/10/10-12	13	12.4	0.072	0.095	2.384	2.723
6/10/10-13	16	15.6	0.222	0.454	2.11	2.5
6/10/10-14	4.5	4.87	0.039	0.00421	2.519	2.648
6/10/10-15	2.7	2.92	0.004	0.000131	2.588	2.666
6/10/10-16	--	4.35	--	0.000463	2.561	2.677
6/10/10/17	--	0.78	--	0.000004	2.676	2.684
6/10/10-18	6.1	4.84	0.001	0.000071	2.48	2.606
6/10/10-21	2.5	2.34	0.001	0.000054	2.579	2.64
6/12/10-27	11.5	10.2	0.011	0.038	2.417	2.69
6/12/10-29	2.3	1.89	0.001	0.000044	2.577	2.627
6/12/10-31FG	12.6	12.3	0.279	0.105	2.32	2.644
6/12/10-34	9.5	8.14	0.001	0.000993	2.439	2.655
6/12/10-38	2.5	1.70	0.001	0.000008	2.565	2.608

Sample outliers

Sample 6/10/10-13 and 6/12/10-31FG values (permeability of 0.454 mD and porosity of 22.2% and permeability of 0.105 mD and porosity of 12.3%) respectively) are higher than values obtained from other mudstone/micritic limestones. This could be a result of thin beds with increased quartz content and gypsum present in the samples,

which are evident in thin sections. This shows the possibility for large heterogeneities in terms of porosity and permeability.

Tight rock analysis (TRA)

TerraTek's TRA testing is proprietary, but it is a gas absorption test to measure porosity and permeability from shales. Permeability ranges from 0.000116 to 0.000267 mD, with an average of 0.000153 mD. Porosity ranges from 3.95 to 13.47%, with an average of 8.42%. All data from the TRA testing is shown in Table 6.

Table 6. Density, porosity, and permeability values obtained from TRA testing performed by TerraTek.

Sample ID	Bulk Density (g/cm^3)	Grain Density (g/cm^3)	Gas Filled Porosity (% of BV)	Pressure-Decay Perm. (mD)
6/10/10-1	2.443	2.673	8.61	0.000117
6/10/10-11	2.314	2.675	13.47	0.000118
6/11/10-22	2.412	2.511	3.95	0.000267
6/12/10-26	2.408	2.667	9.70	0.000149
6/12/10-30	2.496	2.665	6.35	0.000116

The siltstones and shales present in the Carmel Formation are more permeable than the limestones; it is mostly likely because of the sandstone lenses and sand sized grains present in these units. Data obtained from TRA testing did not produce nearly as good of an R^2 value between porosity and permeability because of a much larger range of porosity values (Figure 47).

Elemental composition of carbonate cements

Quantitative analysis of the composition of the calcite and dolomite cements, as well as the calcite fracture fill, to was used better determine the number of diagenetic phases, as well as their origin. A record of the electron microprobe data is shown on Table 7.

Table 7. Quantitative data (mole percent) from the mineral scans of calcite and dolomite.

Calcite (mole percent)							
	SiO2	MgCO3	CaCO3	MnCO3	FeCO3	SrCO3	BaCO3
Calcite Vein 1	0	20.83606	58.17203	0.818762	20.17315	0	0
Calcite Vein 2	0	0.981711	96.86195	0.237614	1.903579	0	0.015142
Calcite Vein 3	0	0.819298	96.98574	0.275314	1.919651	0	0
Calcite Vein 4	0	0.49056	97.64199	0.280138	1.570676	0.016635	0
Calcite Vein 5	0	0.658468	97.1331	0.213569	1.890754	0.073597	0.030507
Calcite Vein 6	0	1.508248	96.44556	0.350486	1.535358	0.084227	0.076118
Calcite Vein 7	0	0.811056	97.2548	0.290878	1.627947	0	0.015324
Calcite Vein 8	0	0.640529	98.50757	0.217494	0.634411	0	0
Calcite Vein 9	0	1.054985	98.04155	0.177123	0.720522	0.005821	0
Calcite Vein 10	0	1.076501	97.68119	0.23698	0.94995	0.055375	0
Calcite Vein 11	0	1.23881	97.57119	0.392434	0.737043	0	0.060525
Calcite Vein 12	0	0.530535	98.57827	0.18874	0.674491	0.027964	0
Calcite Vein 13	0	0.727251	98.14874	0.226402	0.820113	0.077499	0
Calcite Vein 14	0	0.600727	98.29629	0.161367	0.814969	0.111452	0.015197
Calcite Vein 15	0	0.379648	98.69339	0.201597	0.665352	0	0.06001
Calcite Vein 16	0.077051	0.764066	98.10853	0.366005	0.651323	0.033021	0
Calcite Vein 17	0	0.921291	97.98122	0.337602	0.729696	0	0.030191
Calcite Vein 18	0.001679	0.705665	97.99183	0.358268	0.864697	0.077865	0
Calcite Vein 19	0	0.747387	98.00456	0.410326	0.731228	0	0.106503
Calcite Vein 20	0.026962	0.766147	97.99024	0.492368	0.724285	0	0
Calcite Vein 21	0	0.803758	98.03212	0.450978	0.642712	0.055341	0.015092
Calcite Vein 22	0	0.820078	98.20555	0.311568	0.540468	0	0.122336
6-10-10-15-1	0	1.634163	98.05544	0.096094	0.16883	0.045471	0
6-10-10-15-2	0.004992	1.803237	97.9357	0.050732	0.172534	0.032802	0
6-10-10-15-3	0.041674	1.945707	97.70462	0.043766	0.234185	0	0.030048
6-10-10-15-4	0	1.595994	98.12514	0.046536	0.132275	0.05503	0.045021
6-10-10-15-5	1.228887	1.844401	96.65071	0.066826	0.209174	0	0
6-10-10-15-6	0	1.618573	98.08282	0.088531	0.210071	0	0
6-10-10-15-7	0.033391	1.650052	97.94463	0.087667	0.173117	0.005808	0.105331
6-10-10-15-8	0.960237	1.934276	96.79934	0.066474	0.229021	0.010651	0
6-10-10-15-9	3.53604	2.071963	93.8498	0.097979	0.378552	0.050552	0.015111
6-10-10-15-10	0	1.757577	97.96477	0.086831	0.190826	0	0
6-12-10-29-01	0	0.640803	96.72865	1.959242	0.56302	0.046046	0.062239

	SiO2	MgCO3	CaCO3	MnCO3	FeCO3	SrCO3	BaCO3
6-12-10-29-02	0.001709	0.527265	97.54144	1.405194	0.524395	0	0
6-12-10-29-03	0	0.523552	97.93856	0.216982	1.32091	0	0
6-12-10-29-04	0	0.216483	99.0309	0.145876	0.535178	0.041122	0.030439
6-12-10-29-05	0	1.018667	97.89035	1.055536	0.035449	0	0
6-12-10-29-06	0	1.081955	98.77937	0.018371	0	0	0.120305
6-12-10-29-07	0	0.882981	98.87366	0.140916	0.091829	0.010612	0
6-12-10-29-08	0	1.048799	98.63775	0.151085	0.065526	0.036734	0.060105
6-12-10-29-09	0.004994	1.143986	98.70029	0.077543	0.040369	0.032817	0
6-12-10-29-010	0	1.039547	98.69232	0.11531	0.090249	0.062577	0
6-12-10-29-011	0.01987	1.162592	98.51142	0.084143	0.130157	0.047044	0.044772
6-12-10-29-012	0.014874	1.051995	98.59478	0.05319	0.240475	0	0.044687
6-12-10-29-013	0.006692	1.321701	98.22246	0.056673	0.362319	0	0.030155
6-12-10-29-014	0	1.293994	98.08647	0.145044	0.315906	0.022391	0.136194
6-12-10-29-015	0	1.189149	98.26558	0.053044	0.326643	0.076451	0.089128
6-12-10-29-016	0.020159	1.377303	97.46016	0.939007	0.199475	0.003896	0
6-12-10-29-017	0	0.900919	98.02089	1.078186	0	0	0
6-12-10-29-018	0	0.992965	98.38341	0.27928	0.020681	0.025812	0.297851
6-12-10-29-019	0.006619	1.164203	98.60745	0.117713	0.085785	0.018228	0
6-12-10-29-020	0	2.324723	97.46538	0.139029	0.0604	0.01047	0
6-12-10-29-021	0	2.324215	95.97292	0.038378	1.664483	0	0
6-12-10-29-022	0	0.925004	98.81842	0.115844	0.096246	0.04449	0
6-12-10-29-023	0	0.86814	98.54173	0.300784	0.256164	0.033182	0
6-12-10-29-024	0	0.771182	98.5724	0.410848	0.181552	0.033438	0.030575
6-12-10-29-025	0	0.814947	98.6625	0.389153	0.081334	0.036949	0.015114
6-12-10-29-026	0.011826	1.420329	97.8796	0.286153	0.391313	0.010775	0
6-12-10-29-027	0.02163	0.910251	98.46911	0.266327	0.2727	0	0.059983
6-12-10-29-028	0	0.510186	98.75022	0.272724	0.16918	0.115351	0.182343
6-12-10-29-029	0	1.438405	96.73354	0.758231	0.902071	0	0.167757
6-12-10-29-030	0	1.284694	97.36338	0.329674	1.00353	0.018726	0
6-12-10-29-031	0	1.665107	97.43946	0.309194	0.575562	0.010681	0
6-12-10-29-032	0.008419	1.651627	97.83541	0.272382	0.178823	0.007811	0.045528
6-12-10-29-033	0	0.869442	98.61877	0	0.138525	0	0.373258
6-12-10-29-034	0	0.782884	98.81106	0.163718	0.120163	0.060505	0.061673
6-12-10-29-035	0.005119	0.958954	98.53302	0.302037	0.196911	0.003958	0
6-12-10-29-036	0	0.680183	98.45068	0.869135	0	0	0
6-12-10-29-037	0	4.460611	95.09083	0.282194	0.166365	0	0
6-12-10-29-038	0	2.423543	96.30141	1.214337	0	0.014775	0.045934
6-12-10-29-039	0	1.015695	98.28076	0.436733	0.046656	0.082346	0.137806
6-12-10-29-040	0.021608	3.057513	96.17551	0.701037	0	0.044332	0
6-12-10-29-041	0.001676	2.295788	96.9265	0.75081	0.025225	0	0
6-12-10-29-042	0	2.168192	97.3893	0.390037	0	0.007684	0.044792
6-12-10-29-043	0	9.619689	89.44276	0.53687	0.355969	0.044714	0
6-12-10-29-044	0	0.759218	99.04799	0.038185	0.055855	0.098758	0
6-12-10-29-045	0.011595	1.046966	98.52466	0.077159	0.189767	0.053785	0.096067
6-12-10-29-046	0.003412	1.144344	97.46882	1.217951	0.165476	0	0
6-12-10-29-047	0	1.019603	98.5722	0.2785	0.085244	0	0.044456

	SiO2	MgCO3	CaCO3	MnCO3	FeCO3	SrCO3	BaCO3
6-12-10-34-1	5.200104	2.264637	91.18037	0.241697	1.113188	0	0
6-12-10-34-2	15.29408	1.669656	82.48939	0.069311	0.403898	0.015817	0.05785
6-12-10-34-3	0.777007	1.47031	97.17941	0.188627	0.357082	0	0.027561
6-12-10-34-4	1.1731	3.905407	94.14969	0.162526	0.598629	0.010643	0
6-12-10-34-5	0.358083	2.395732	96.63273	0.056055	0.513725	0.015744	0.027931
6-12-10-34-8	2.198615	1.956948	95.2989	0.072603	0.468065	0.004873	0
6-12-10-34-9	29.22518	1.039247	69.19989	0.080201	0.386377	0.069106	0
6-12-10-34-10	10.32211	2.156804	86.25343	0.114387	1.108239	0.045029	0
6-12-10-36-02a	0.421947	1.323399	97.97473	0	0.234286	0	0.045635
6-12-10-36-04a	2.814512	1.225697	95.41839	0	0.463086	0.078316	0
6-12-10-36-06a	0.243692	1.975278	97.54955	0	0.19812	0.033362	0
Dolomite (mole percent)							
	SiO2	MgCO3	CaCO3	MnCO3	FeCO3	SrCO3	BaCO3
6-12-10-27-1	0.41296	41.62585	55.71792	0.450051	1.746177	0.020782	0.026258
6-12-10-27-2	0.020562	34.80297	55.51577	1.235064	8.399949	0.025678	0
6-12-10-27-3	0.721963	42.37221	56.10968	0.275546	0.507851	0	0.012749
6-12-10-27-4	0.235503	32.5413	55.82826	1.208933	10.08242	0	0.103585
6-12-10-27-5	0.203951	43.5827	55.37023	0.222837	0.456965	0.035206	0.128117
6-12-10-27-6	0.457064	32.64971	55.88282	1.221992	9.782881	0.00554	0
6-12-10-27-7	2.772716	41.508	54.93149	0.333989	0.41924	0.034564	0
6-12-10-27-8	0.041033	34.21398	55.62951	1.170878	8.916064	0.015556	0.012987
6-12-10-27-9	0.131414	42.54647	56.49139	0.305086	0.495155	0.030478	0
6-12-10-27-10	0	29.60895	58.88095	1.106534	10.40357	0	0
6-12-10-27-11	0.082184	42.69824	56.69239	0.316498	0.194501	0.016184	0
6-12-10-27-12	0.087836	34.32892	56.23771	1.111795	8.116888	0.103709	0.013142
6-12-10-27-12a	0	32.44218	56.96258	1.099413	9.428839	0.066987	0
6-12-10-27-13	0.566153	41.67393	56.08548	0.40541	1.248734	0.020286	0
6-12-10-27-14	0.093815	33.18919	55.90509	0.98173	9.830176	0	0
6-12-10-27-15	0.779207	41.79255	56.06547	0.453702	0.909072	0	0
6-12-10-27-16	0	36.20247	55.30248	0.985119	7.445206	0.050467	0.014263
6-12-10-27-16A	0.104602	33.09296	55.77726	1.308408	9.553117	0.022394	0.141256
6-12-10-32-1	0.752057	48.13289	50.80284	0.299504	0	0	0.012708
6-12-10-32-2	9.885063	41.44431	47.70597	0.148457	0.760386	0	0.05581
6-12-10-32-3	0.183881	48.33757	51.27803	0.172746	0	0.027774	0
6-12-10-32-4	0.372712	49.14736	50.34156	0.044349	0.094016	0	0
6-12-10-32-5	0.259603	46.91113	52.55458	0.260677	0	0	0.01401
6-12-10-32-6	0.190672	46.69273	52.37173	0.157546	0.395369	0	0.191956
6-12-10-32-7	1.491331	45.93426	51.84197	0.228451	0.432978	0.07101	0
6-12-10-32-8	0.04398	45.35607	53.67156	0.175596	0.702702	0.05009	0
6-12-10-32-9	0.231811	45.88867	53.42135	0.239064	0.213625	0.005486	0
6-12-10-32-10	0.276103	47.16043	52.22517	0.125605	0.038261	0.061291	0.11314
6-12-10-32-11	0.600119	27.58615	54.01449	0.524005	17.19375	0	0.081479
6-12-10-34-6	8.768588	35.6513	54.55597	0.082875	0.878362	0	0.06291
6-12-10-34-7	0.619938	43.69304	55.17154	0.089257	0.298083	0	0.128146
6-12-10-36-01	0.01545	42.56061	57.06155	0.044488	0.259678	0.058227	0
6-12-10-36-02	0.06751	45.49248	54.35764	0	0	0	0.08237

	SiO2	MgCO3	CaCO3	MnCO3	FeCO3	SrCO3	BaCO3
6-12-10-36-03	0.051296	43.0437	55.97793	0.106635	0.716214	0.062189	0.042029
6-12-10-36-04	0.375149	45.03463	53.08543	0.635446	0.869342	0	0
6-12-10-36-05	0.152433	44.01594	54.86735	0.084762	0.865232	0.014284	0
6-12-10-36-06	0.033316	48.14702	51.52724	0.092344	0.200083	0	0
6-12-10-36-07	0.105153	43.08597	56.38042	0.060662	0.28036	0.046832	0.040608
6-12-10-36-08	0.209162	48.28704	50.61839	0.393365	0.284222	0.139111	0.068704
6-12-10-36-09	0.031776	43.5573	55.54143	0.009419	0.700165	0.074618	0.085295
6-12-10-36-010	0.031526	49.56692	49.88157	0.025429	0.366568	0.060931	0.067064
6-12-10-36-011	0.130748	41.60892	57.25889	0.131035	0.703384	0.149093	0.017932
6-12-10-36-012	0.633098	47.85282	51.16459	0.068004	0.281491	0	0

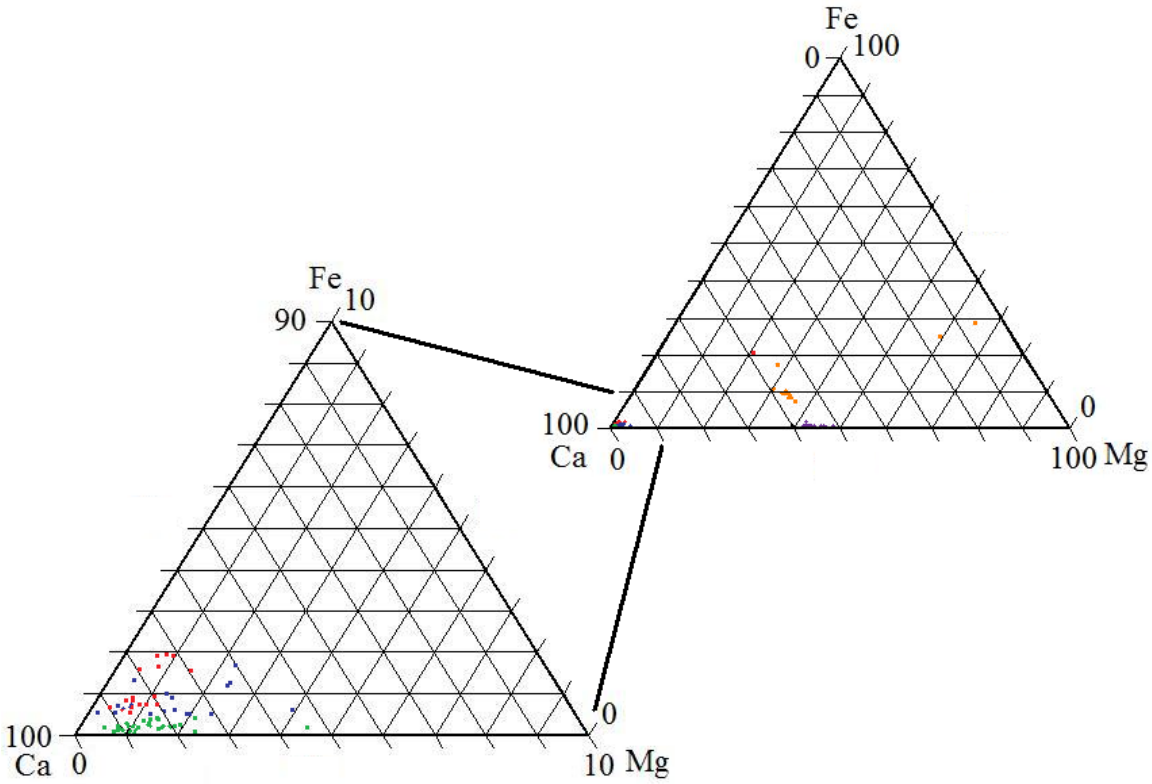

Figure 41. Ternary diagram showing composition of carbonate in mole percent normalized to calcium, magnesium, and iron values. Calcite vein values are in red, calcite phase #1 in blue, calcite phase #2 in green, dolomite cores in purple, and dolomite overgrowths in orange. The calcite corner of the ternary diagram is expanded to see individual points.

Calcite

Within the Co-op Creek Member, there are two compositionally distinct calcite cementing phases. Calcite phase #1 is relatively enriched in iron and manganese (average

of 0.5 ± 0.3 mole percent and average of 1.0 ± 0.3 mole percent respectively), whereas calcite phase #2 is not (average of 0.1 ± 0.3 mole percent and average of 0.1 ± 0.3 mole percent, respectively; Figure 42).

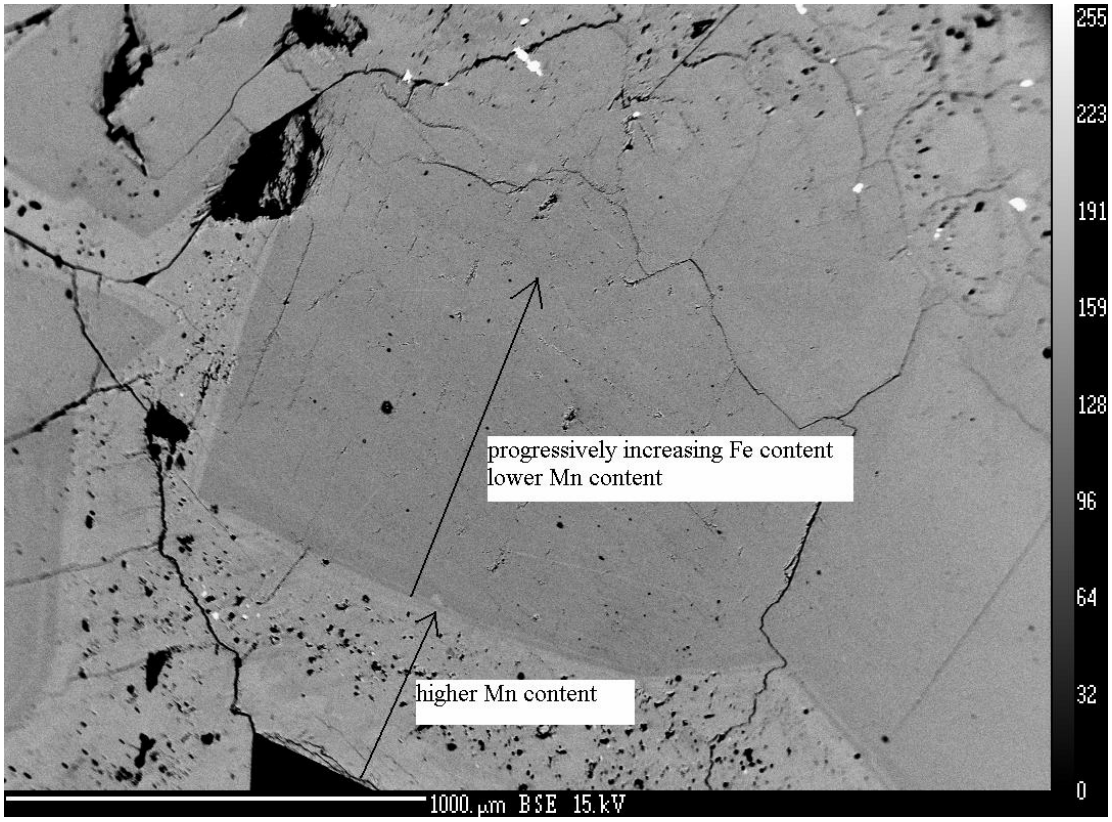

Figure 42. Backscattered electron image showing two phases of calcite within the Co-op Creek Member, and their respective chemical characteristics. From 6/12/10-29.

The elemental composition of the calcite veins is different than the calcite that fills intergranular pores. The vein fill becomes relatively depleted in iron from the outside to the inside of the vein (changes from 1.9 ± 0.3 Fe mole percent to 0.5 ± 0.3 Fe mole percent). Also, despite the presence of large crystals of barite intermixed with the calcite, there is almost no trace of barium in the calcite (<0.01 mole percent). Manganese, magnesium, and strontium are relatively consistent across the vein analyzed.

Dolomite

Dolomite crystals in the Co-op Creek Member show compositional zoning. Each crystal has two distinct parts: an inner portion that has a higher magnesium content (average of 42.2 ± 0.3 mole percent compared to an average of 38.7 ± 0.3 mole percent), and an outer portion that has a higher manganese (average of 1.1 ± 0.3 mole percent compared to an average of 0.3 ± 0.3 mole percent) and iron content (average of 9.2 ± 0.3 mole percent compared to 0.7 ± 0.3 mole percent) (Figure 43). These dolomites must be diagenetic because of the perfect euhedral nature, and because they only occur within dissolution porosity (Figure 44).

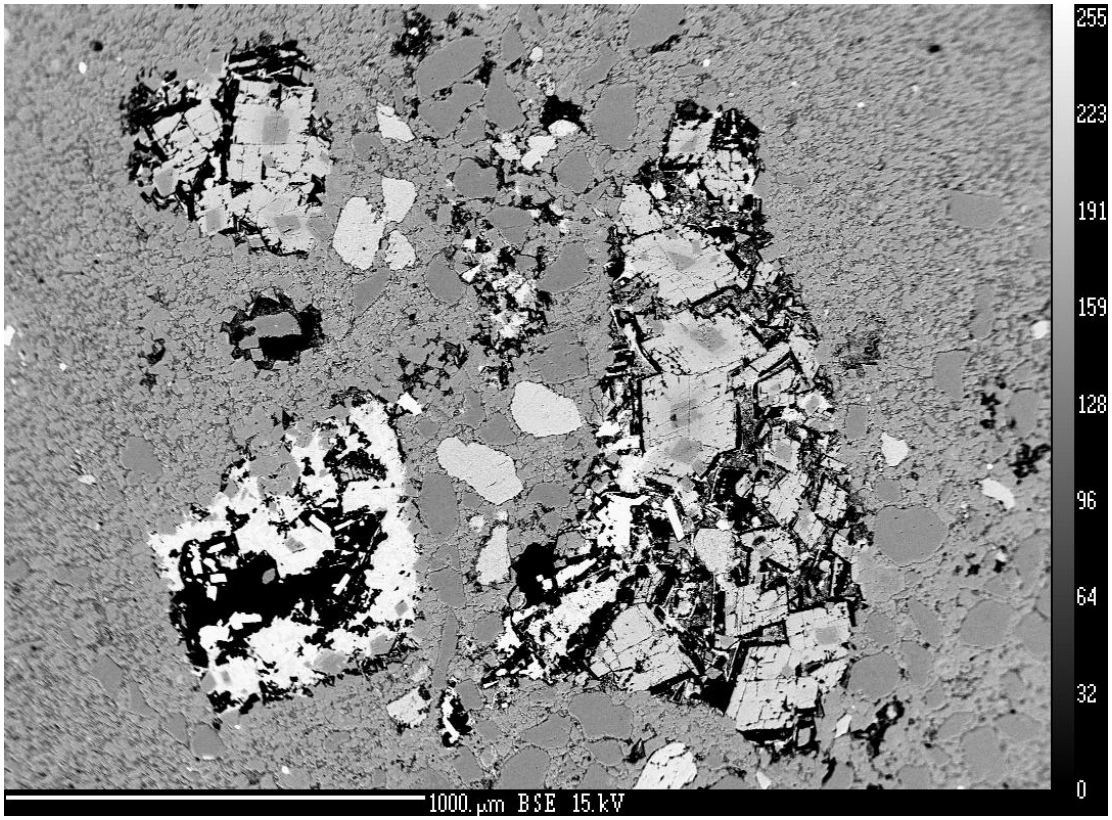

Figure 43. Backscattered electron image showing the chemical zonation of the dolomites within the Co-op Creek. Notice the distinct difference between the inner and outer portions, as well as the euhedral nature of the dolomites. Also note that the dolomites are only growing in the dissolution created porosity. From 6/12/10-27.

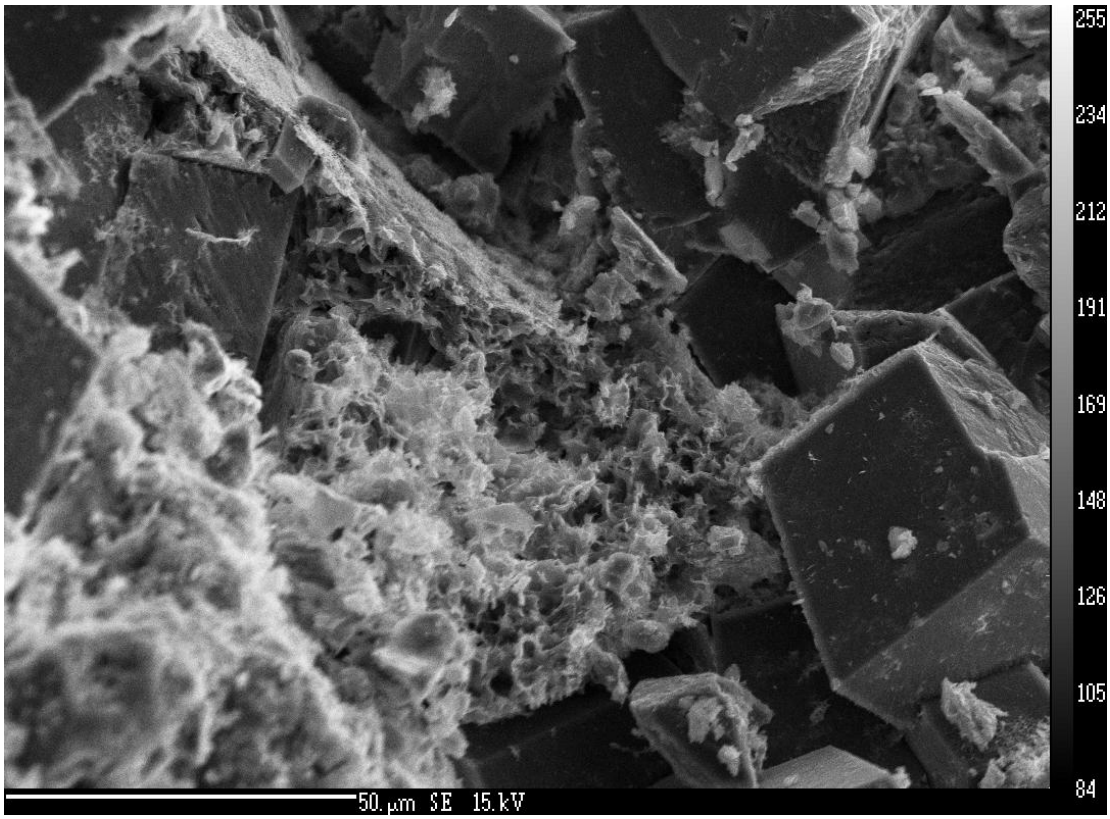

Figure 44. Secondary electron image of authigenic dolomite rhombs within open pores. From 6/12/10-27.

Dolomite in the Crystal Creek Member does not exhibit any kind of chemical zonation or overgrowth texture. Chemically, it most closely resembles the dolomite cores within the Co-op Creek Member, although the Crystal Creek Member dolomites have a higher magnesium content (average of 40.4 ± 0.3 mole percent in the Crystal Creek Member compared to an average of 37.5 ± 0.3 mole percent in the Co-op Creek Member). The dolomites in the Crystal Creek Member are also not as euhedral as the dolomites in the other members (Figure 44), and they grew in between grains as cement, and not in dissolution voids (Figure 45).

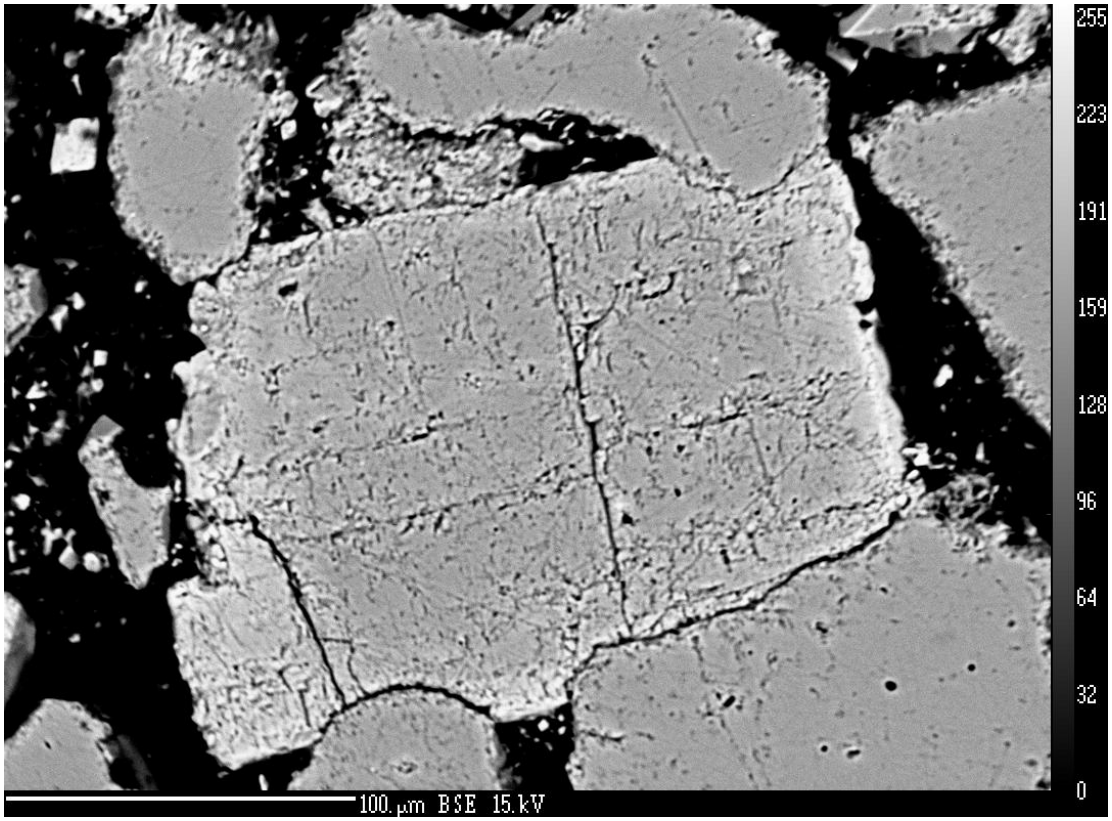

Figure 45. Backscattered electron image showing subhedral pore filling Crystal Creek dolomite. From 6/12/10-32.

In the Paria River Member, the dolomite cores have a higher magnesium content than the overgrowths (average of 47.4 ± 0.3 mole percent in the cores compared with an average of 43.0 ± 0.3 mole percent in the overgrowths). This could represent two separate precipitating fluids, one precipitating out the core, and the other precipitating the overgrowths on the dolomites.

Chapter 4: Discussion

The chapter is grouped into the following sections: 1) an evaluation of the sealing behavior of the various lithologies present in the Carmel Formation, including a discussion of their petrophysical characteristics and diagenetic alterations influencing porosity and permeability, 2) a discussion of the sealing capabilities of the lithologies in terms of CO_2 column heights, and 3) a discussion of possible seal bypass systems in the Carmel Formation.

Sealing behavior of the Carmel Formation lithologies

Traditionally in petroleum geology, shales and evaporites are viewed as sealing lithologies. Shale's small average grain size results in low permeability and the crystalline nature of evaporites also result in very low permeability. Both of these lithologies are present within the Carmel Formation. Furthermore, the ductile nature of shale reduces the likelihood of fracture development at depth.

Micritic limestones, which are also present in abundance in the Carmel Formation, are not considered traditional seals in petroleum geology because of their brittle nature. However, because the micritic limestones in the Carmel Formation have such low permeability, these should be seriously considered when evaluating the sealing behavior of the Carmel.

Petrophysical characteristics

Overall, the MICP and TRA data demonstrates that the Carmel has low permeability and porosity lithologies. This is a key characteristic if a rock unit is to inhibit the flow of fluids in the subsurface. Quantitative examination of the permeability of the different Carmel Formation lithologies reveals differences between the carbonate and clastic lithologies. The carbonates present in the Carmel have a wider range of permeability (0.000004 to 0.454 mD, average of 0.0537 mD, median of 0.0005 mD) and porosity values (0.78 to 15.6%, average of 6.33%, median of 4.84%). The clastic shales and siltstones have a more constrained range of permeability (0.000116 to 0.000267 mD, average of 0.000153 mD, median of 0.000118) and porosity values (3.95 to 13.47%, average of 8.416%, median of 8.61%).

The lower porosity values (less than 5%) obtained from 300-point counts did not correlate with data from the MICP and TRA's analysis (R^2 value of 0.1923) (Figure 46). In particular, many samples in which the point count derived porosity was 1% or less had considerably higher measured porosity values. This discrepancy is likely due to the difficulty of detecting microporosity in standard thin section analysis. For the higher porosity samples, the relationship is much stronger.

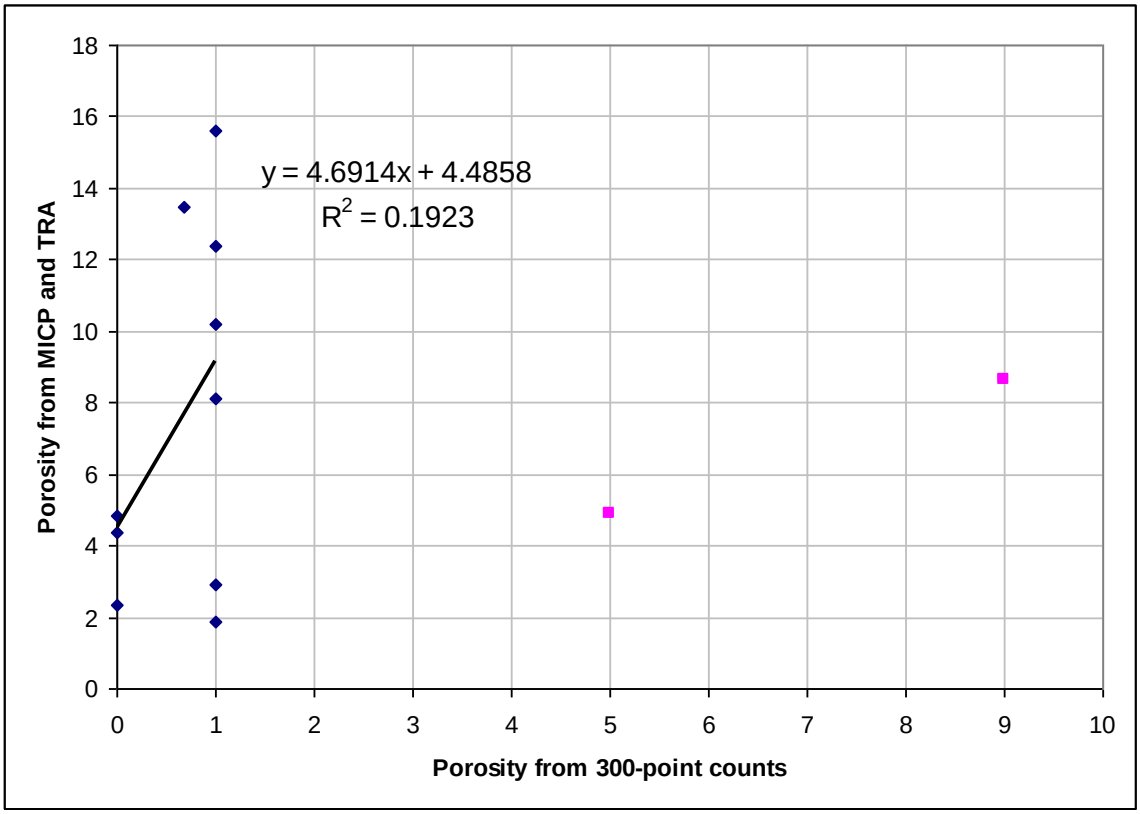

Figure 46. Scatterplot of porosity values obtained from 300-point counts and MICP/TRA values. Higher value porosity values from 300-point count method correlated more strongly with porosity derived from MICP/TRA testing compared to lower porosity values.

The siltstones and shales in the Carmel Formation are more permeable than the limestones. The sandstone lenses in the shales have a much larger average grain size, and are not as well cemented as the limestones. Data obtained from TRA testing of these samples did not produce as strong a correlation between porosity and permeability because of a much larger range of porosity values compared to the relatively consistent permeability values (Figure 47).

Combining the MICP data and the TRA data resulted in a moderately positive correlation between porosity and permeability (R^2 value of 0.58, Figure 48). This is to be

expected because different analytical methods were used and different lithologies were examined (limestone, shale).

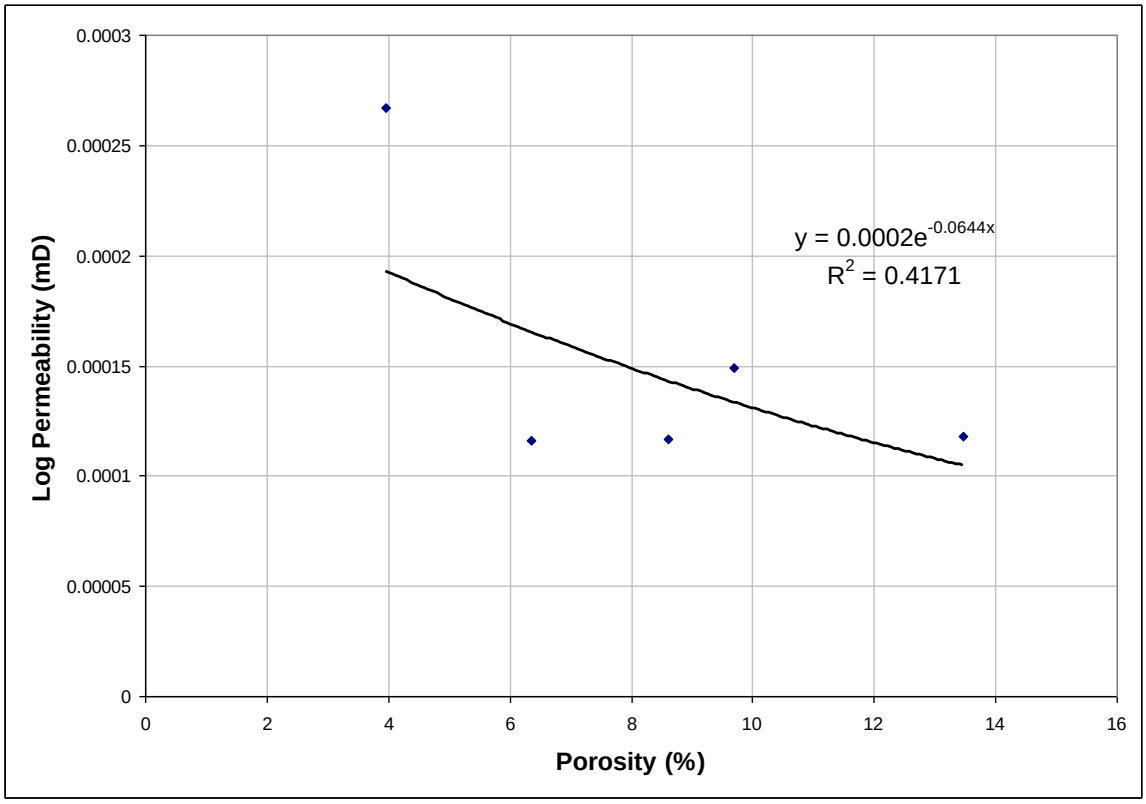

Figure 47. Scatterplot of permeability (log scale) versus porosity from data obtained through TRA. R^2 value of 0.4171.

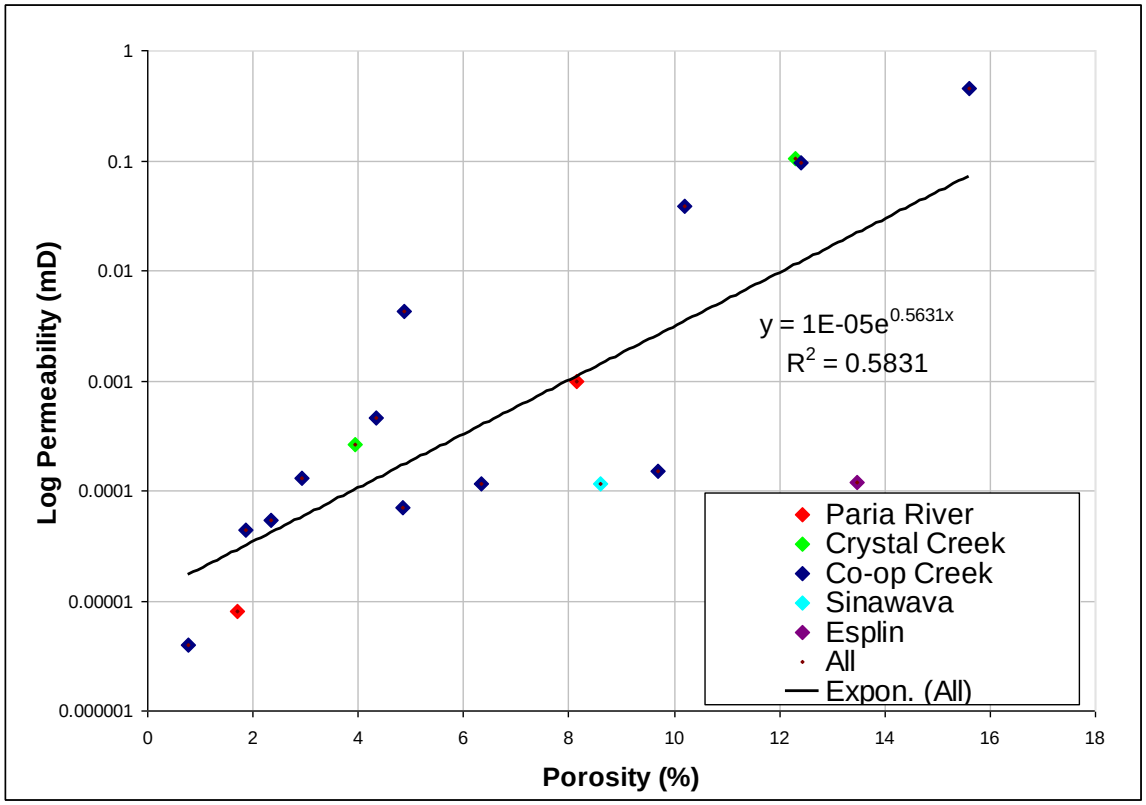

Figure 48. Scatterplot of permeability (log scale) versus porosity from both MICP and TRA data. R^2 value of 0.5831.

Influence of diagenesis on porosity and permeability

Porosity and permeability in the Carmel Formation were reduced by compaction and precipitation of authigenic minerals. Precipitated cements include calcite and gypsum, usually poikilotopic. There has also been clay precipitation and feldspar alteration to kaolinite in the feldspar bearing sandstone lenses, as well as in the Navajo Sandstone. This is extremely important in evaluating how the Carmel Formation will behave as a seal, because even small amounts of cements in the pore throats can greatly reduce permeability.

In the clastic Carmel Formation samples, we can see significant amounts of authigenic minerals (up to 10%) filling in porosity. In addition, some clastic samples

from the Carmel Formation have up to 7% secondary porosity. From the underlying Temple Cap Formation, samples contain up to 25% authigenic minerals, and up to 14% secondary porosity. In the Navajo Sandstone, samples have up to 10% authigenic minerals, and up to 15% secondary porosity.

Porosity loss due to compaction

Porosity loss because of compaction can be quantified by approximating the depositional porosity of each lithology, and subtracting the remaining porosity plus the percent of the sample taken up by precipitated cements.

Original porosity in sandstones is usually between 40-55% in high energy sands, like eolian deposited sands (North, 1985). Average porosity in the Navajo Sandstone and White Throne Member of the Temple Cap Formation after diagenesis is 22%. Average intergranular volume (9% cement + 22% porosity) is 31%, so between 9-24% of original porosity was lost due to compaction.

Original porosity in limestones ranges from 35-75% (North, 1985); this large spread in porosity is primarily controlled by the amount of primary micrite. Average porosity after diagenesis in the Carmel Formation's limestones is 6-69% (MICP testing). Unfortunately, quantifying the amount of porosity loss due to compaction is not applicable with carbonates because the 300-point count was only used with the clastic samples.

In shales, the original porosity is approximately 50-85% (North, 1985). Compaction affects shales most dramatically because shales contain phyllosilicates which are chaotically oriented during deposition, but when compacted, they realign parallel with

each other, resulting in greatly reduced porosity. Average porosity after diagenesis in the Carmel Formation's shales is 9% (TRA testing). Average intergranular volume (12% cement + 9% porosity) is 21%, so 29-64% of original porosity was lost due to compaction.

In siltstones, the primary porosity is approximately 30-52% (North, 1985). Average porosity in the siltstones present in the Temple Cap and Carmel Formations is approximately 7% (TRA testing). Average intergranular volume (11% cement + 7% porosity) is 18%, so between 12-34% of the original porosity was lost due to compaction.

Anisotropy in permeability

In most sedimentary rocks, vertical permeability is usually considerably less than horizontal permeability; this is particularly the case for shales (Clennell et al., 1999). Although a comparison of vertical and horizontal permeabilities was not performed for this thesis, SEM images of the siltstones in the Carmel Formation both parallel to bedding (Figure 49) and perpendicular to bedding (Figure 50) show distinct textural differences. In the parallel-to-bedding images, platy clay sheets are evident; images oriented perpendicular to bedding show clay sheets bent around quartz grains. Permeability parallel to the clay sheets should be much higher than perpendicular to the sheets.

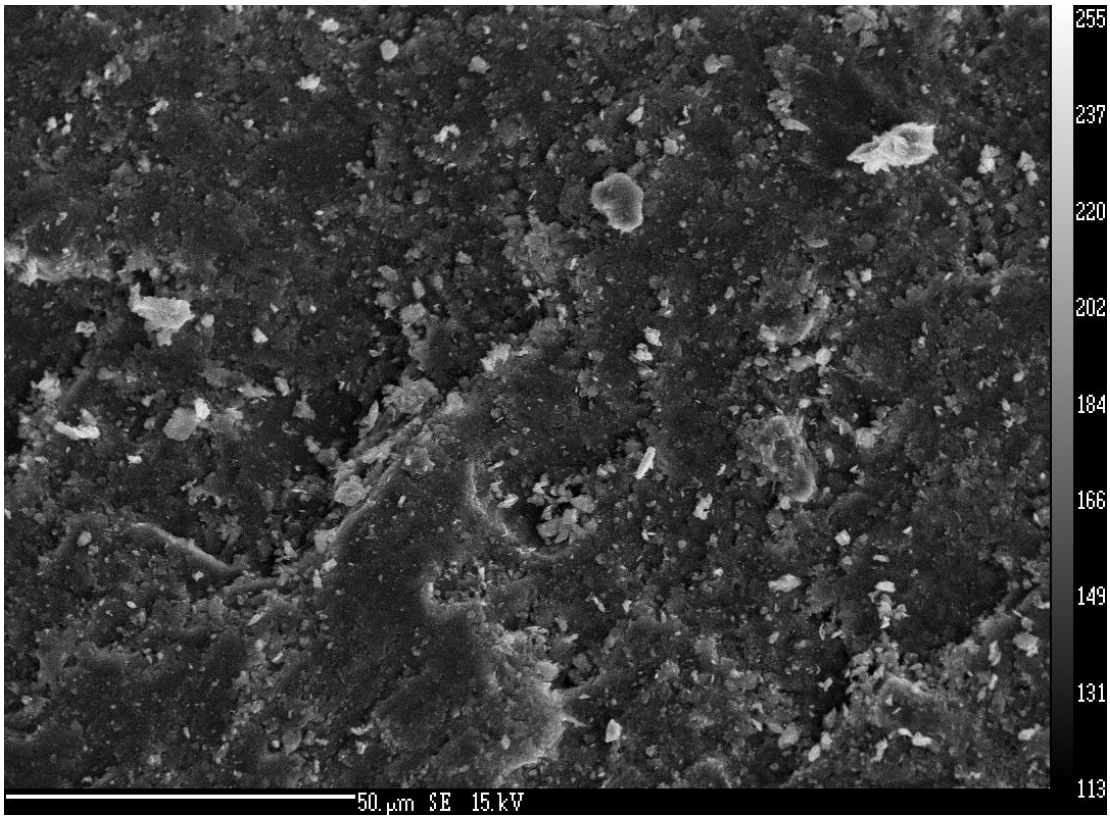

Figure 49. Secondary electron image of siltstone oriented parallel to bedding. Sample 6/12/10-25.

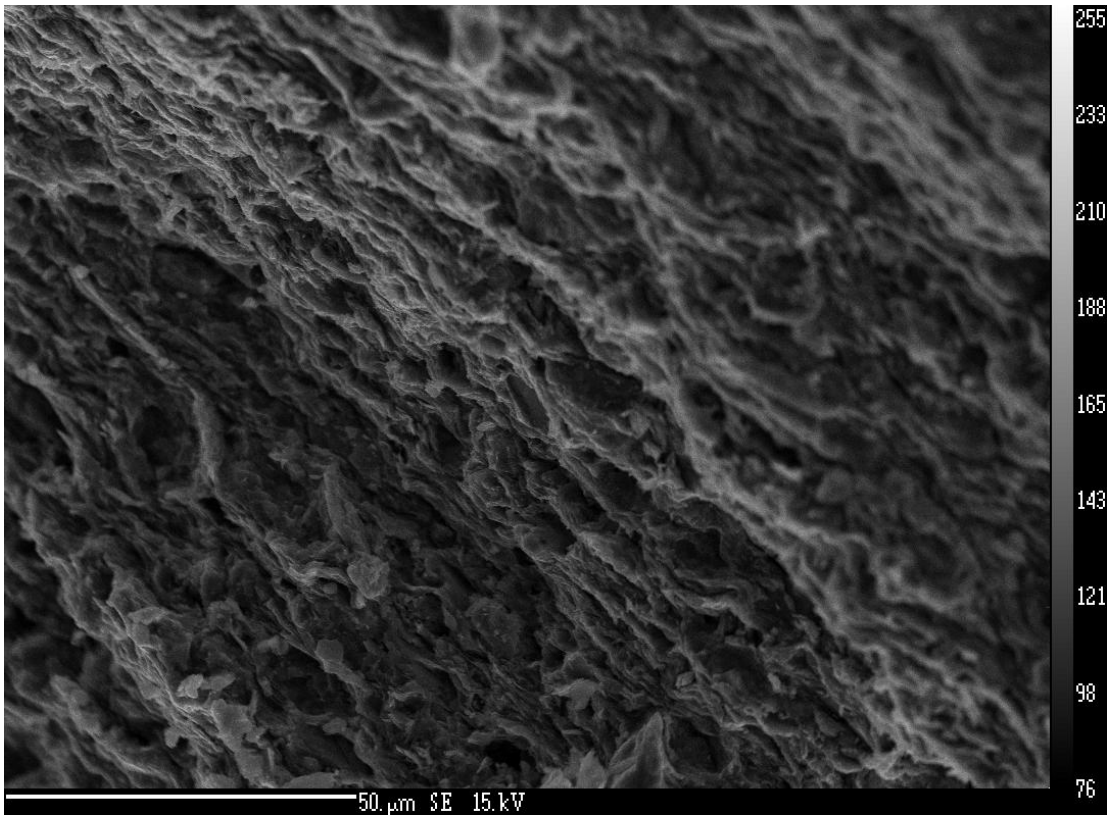

Figure 50. Secondary electron image of siltstone oriented perpendicular to bedding. Permeability parallel to clay layers should be higher than flow across clay layers. Sample 6/12/10-25.

Vertical changes in the Carmel Formation

Permeability and sealing capacity in the Carmel Formation changes vertically as a function of vertical changes in lithology (Figures 51, 52). Unfortunately, because of the low number of MICP samples, there is not a lot of coverage for sealing capacity in some sections of the Carmel. For these Figures 51 and 52, the individual circles represents permeability data points from MICP or TRA measurements, or calculated CO_2 column heights.

At the Gordon Creek field, the Carmel Formation will not act as a single continuous barrier, but rather as a number of vertically separated seals sandwiched between more permeable sections. If CO_2 did start to leak through the lower seals in the

Carmel, it would most likely be trapped by the overlying seals. For example, the Paria River Member can sequester a higher column of CO_2, so if CO_2 leaked through the underlying Co-op Creek Member, it would be trapped by the overlying formation.

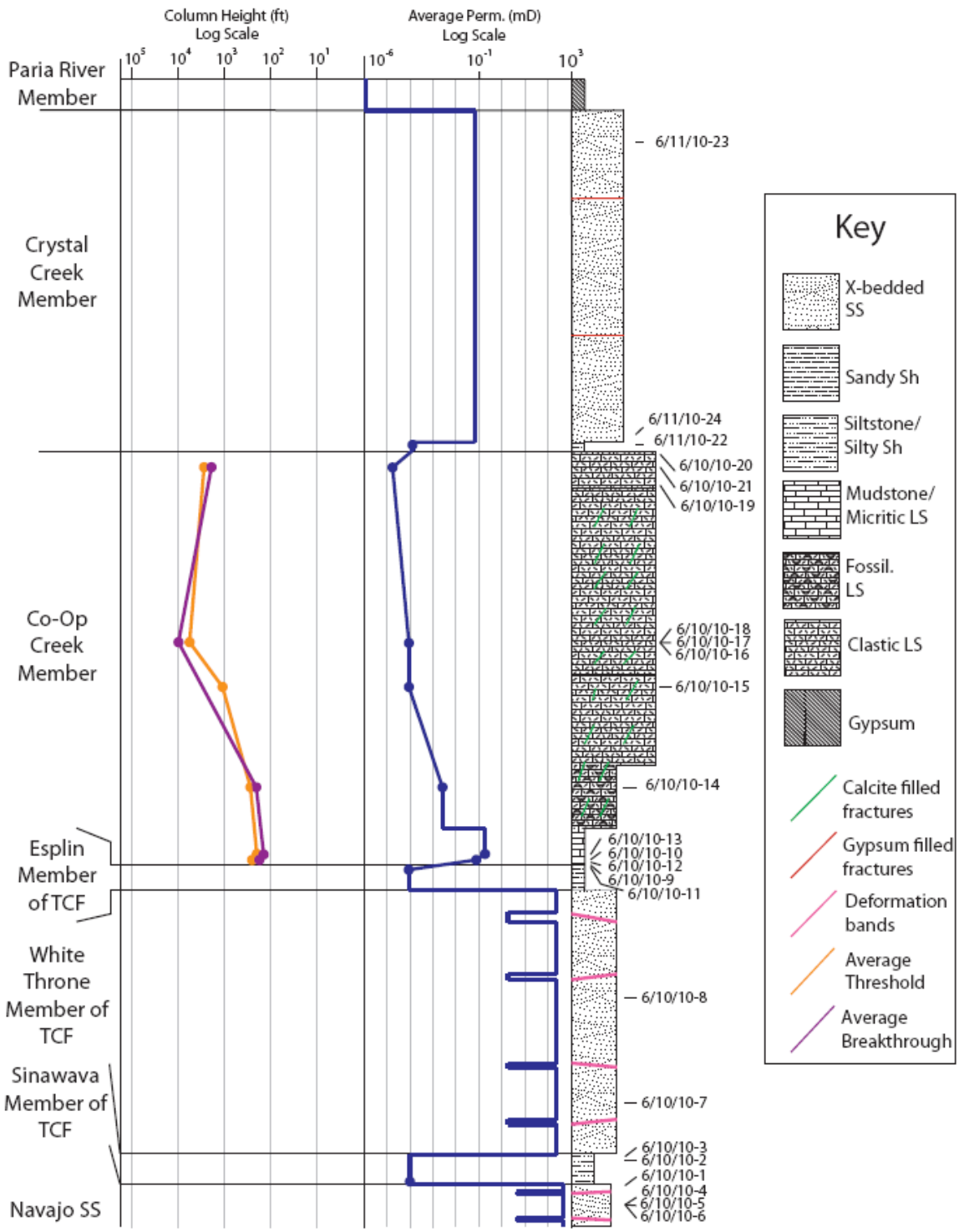

Figure 51. Simplified stratigraphic section of MCJ site showing lithologic variations within the members, permeability, and threshold/breakthrough pressure sealing capacity. For some of the members there are very few data points, which makes it impossible to see heterogeneities within the same lithologies. In addition, there was not any data recovered from the gypsum bed at the base of the Paria River Member.

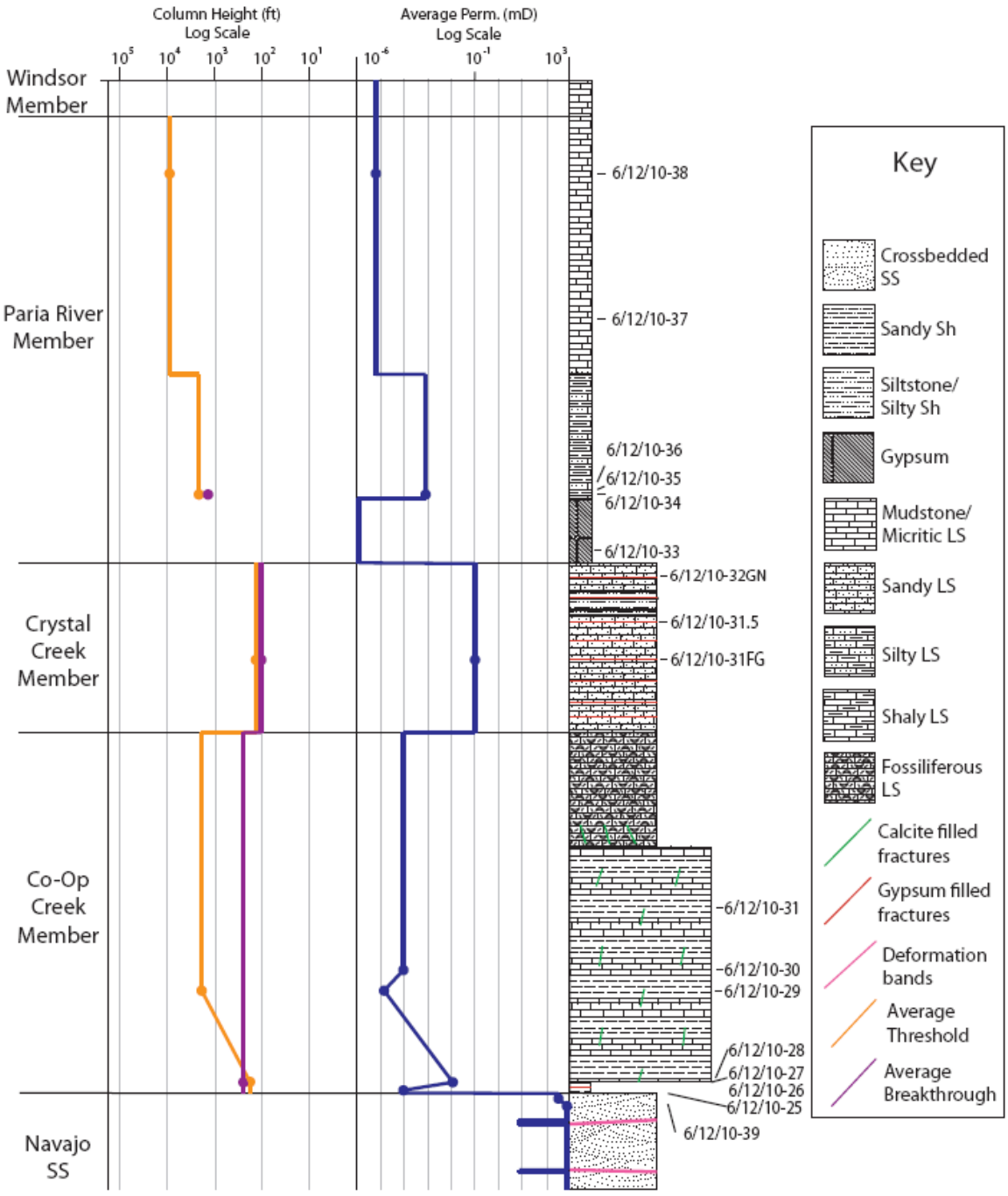

Figure 52. Simplified stratigraphic section of I-70 site showing lithologic variations within the members, permeability, and threshold/breakthrough pressure sealing capacity. For some of the members there are very few data points, which makes it impossible to see heterogeneities within the same lithologies. In addition, there was not any data recovered from the gypsum bed at the base of the Paria River Member.

Potential CO_2 storage capacity

Equations

Using the capillary pressure curves of samples from MICP, it is possible to calculate the amount of CO_2 that could be sequestered without any leakage through the seal. To begin this calculation, we must convert the MICP data into a water/CO_2 system using equations from Daniel and Kaldi (2009).

$$P_{c\ b/CO2} = Pa/m * ((\sigma_{b/CO2} * cos\theta_{b/CO2}) / (\sigma_{a/m} * cos\theta_{a/m}))$$

$\sigma_{b/CO2}$ = 21 to 27 dynes/cm
$cos\theta_{b/CO2}$ = 0°
$\sigma_{a/m}$ = 480 dynes/cm
$cos\theta_{a/m}$ = 130°

P_{bCO2} is the capillary pressure in the brine-CO_2 system, $P_{a/m}$ is the capillary pressure in the air-mercury system, σ_{bCO2} and $\sigma_{a/m}$ are the IFTs (interfacial tension) of the brine-CO_2 and air-mercury systems, respectively, and θ_{bCO2} and $\theta_{a/m}$ are the contact angles of the brine-CO_2-solid and air-mercury-solid systems, respectively (Daniel and Kaldi, 2009). P_{bCO2} and $P_{a/m}$ curves were provided by Poro-Technology along with their MICP measurements. In addition, there are two values for interfacial tension used in example calculations (21 and 27 dynes per centimeter: Daniel and Kaldi, 2009 and Daniel, 2006).

The IFT decreases as CO_2 pressure increases until the CO_2 gas-liquid boundary is reached (Espinoza and Santamarina, 2010). This means that as long as the CO_2 does not change phases, the ability of the seal to remain effective will not alter, at least in terms of the IFT.

After we obtain the capillary pressure value in the brine-CO_2 system, it must be converted into height above free water level. One can do this by rewriting the equation for capillary pressure to solve for height.

$$h = P_{c\ b/CO2} / ((\rho_b - \rho_{CO2}) * 0.433)$$

ρ_{CO2} = 0.75 g/cm^3
ρ_b = 1.006 g/cm^3

$P_{c\ b/CO2}$ is the capillary pressure reservoir for the brine-CO_2 system in psi, h is the height above free water level in feet, ρ_b is the subsurface brine density in g/cm^3, and ρ_{CO2} is the subsurface CO_2 density in g/cm^3.

<u>CO_2 column height methods</u>

Breakthrough pressure is defined as the point of maximum curvature when pore aperture diameters are plotted against mercury saturation (Schowalter, 1979; Heath, 2010). Another way to examine sealing ability is by addressing displacement pressure by assigning it a set value of wetting phase saturation (90%) (Dewhurst et al., 2002, person communication Jason Heath). This study uses both methods to provide a range of reasonable CO_2 column heights.

Breakthrough pressure calculations

After choosing the points of maximum curvature for each sample's pore aperture versus mercury saturation graph, the corresponding capillary pressure value at that data

point was selected. These were converted into CO_2 column heights in Figure 53. Four of the curves were not suitable due to erratic pore aperture versus mercury saturation curves.

Samples from the Co-op Creek Member could effectively sequester between 194-20,603 feet of CO_2, the one sample from the Crystal Creek Member could effectively sequester between 92-118 feet of CO_2, and the one sample from the Paria River Member could effectively sequester between 1,558-2,003 feet of CO_2 (Figure 53). The range of IFT values represents the standard deviation for each sample.

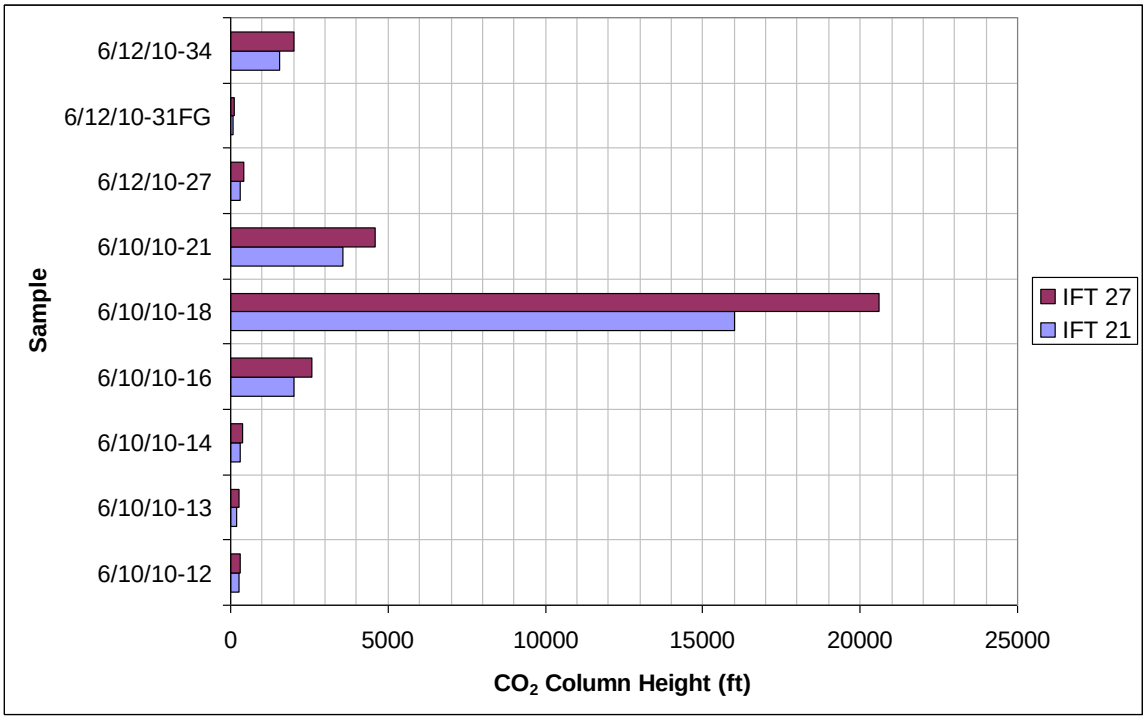

Figure 53. CO_2 column heights based on breakthrough pressure with range of IFT values between 21 and 27 dynes/cm.

Displacement pressure calculations

Another way of plotting sealing capabilities is to use displacement pressure instead of breakthrough pressure. To do this, the whole capillary pressure curves are examined to observe the point at which the wetting phase saturation passes 90%. The

standard deviation of each sample is represented by the range of interfacial tension values.

Using this method, the Co-op Creek Member should be able to seal ~251-12,504 feet of CO_2 (Figure 54). The reason for this large spread is the difference in lithologies present in the Co-op Creek Limestone and their associated permeability values. Many of the carbonates in this member contain significant amounts of clastic material, which increases the average grain size and thus permeability. The single sample from the Crystal Creek would be able to support a column of ~151-211 feet of CO_2 (Figure 55). The two samples from the Paria River would be able to seal between ~2,724-11,499 feet of CO_2 (Figure 56).

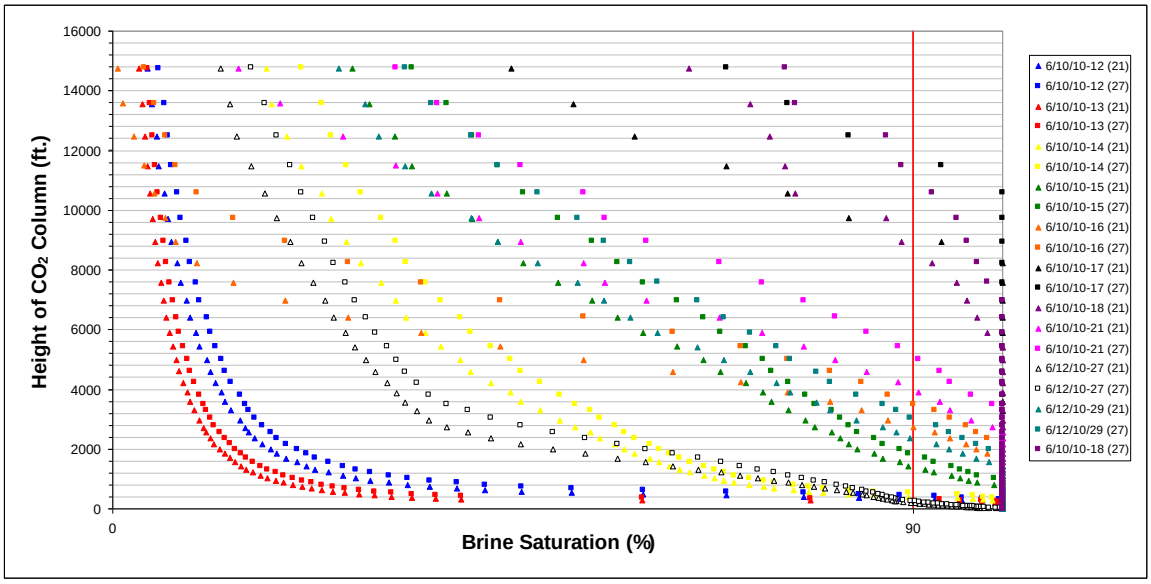

Figure 54. Graph showing height of CO_2 column versus brine saturation from Co-op Creek Member samples. Breakthrough pressures ranging from ~26-11,499 feet of CO_2.

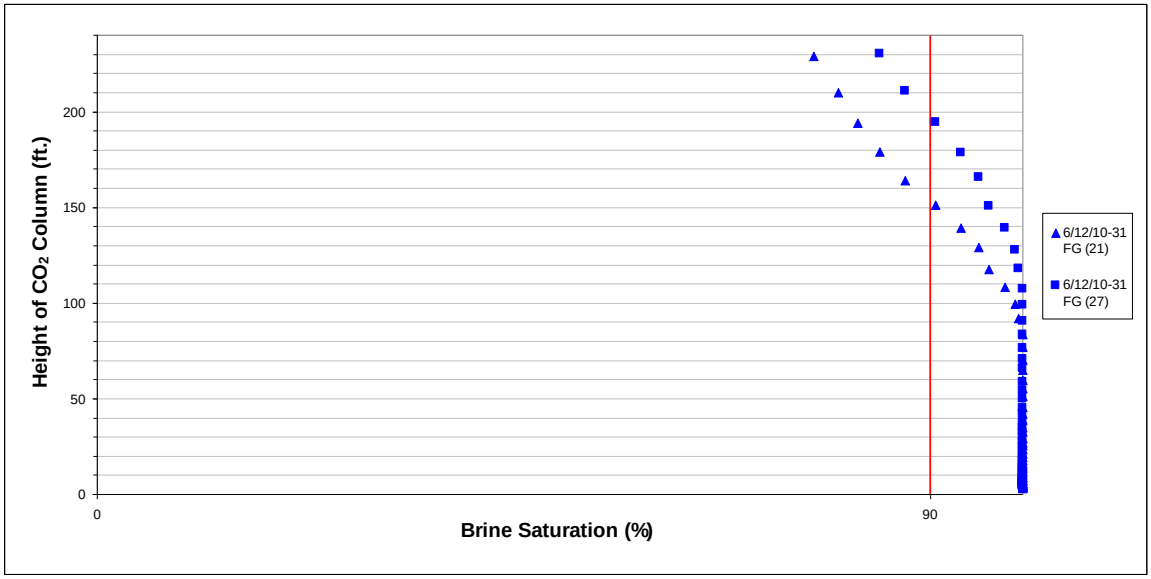

Figure 55. Graph showing height of CO_2 column versus brine saturation from Crystal Creek. Breakthrough pressures ranging from ~84-118 feet of CO_2.

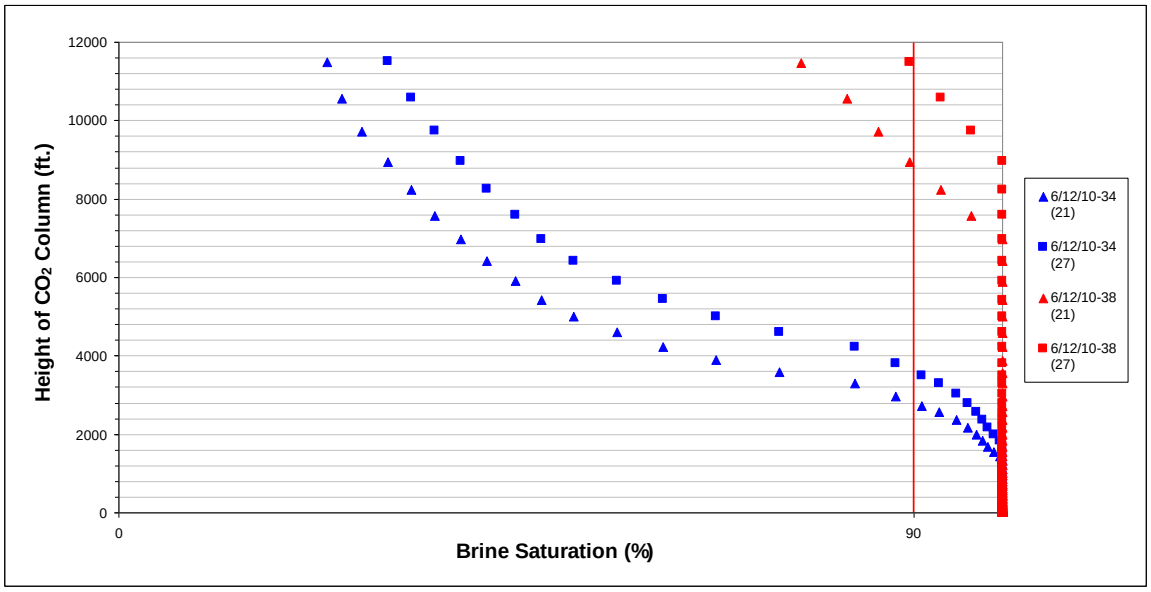

Figure 56. Graph showing height of CO_2 column versus brine saturation from Paria River. Breakthrough pressures ranging from ~1,318-9,731 feet of CO_2.

Because the Navajo is only 150-300 feet thick at Gordon Creek (McPherson and Grigg, 2010), either the Co-op Creek or the Paria River Members by themselves would be able to sequester an entire Navajo Sandstone reservoir filled with CO_2. Thus, the limestones in the Carmel Formation should safely contain the amount of CO_2 propsed for

this project, as long as there are no seal bypasses, such as fractures, non-sealing faults, or major changes in petrophysical characteristics in the subsurface lithologies.

There is a weak correlation between permeability and CO_2 column height. The correlation using CO_2 column heights derived from threshold pressure plots has an R^2 value of 0.63, and using CO_2 column heights derived from breakthrough pressure plots has an R^2 value of 0.65 (Figure 57). Capillary pressure decay is not related to permeability in any way because they are independent physical processes and characteristics, so these weak correlations are not unexpected.

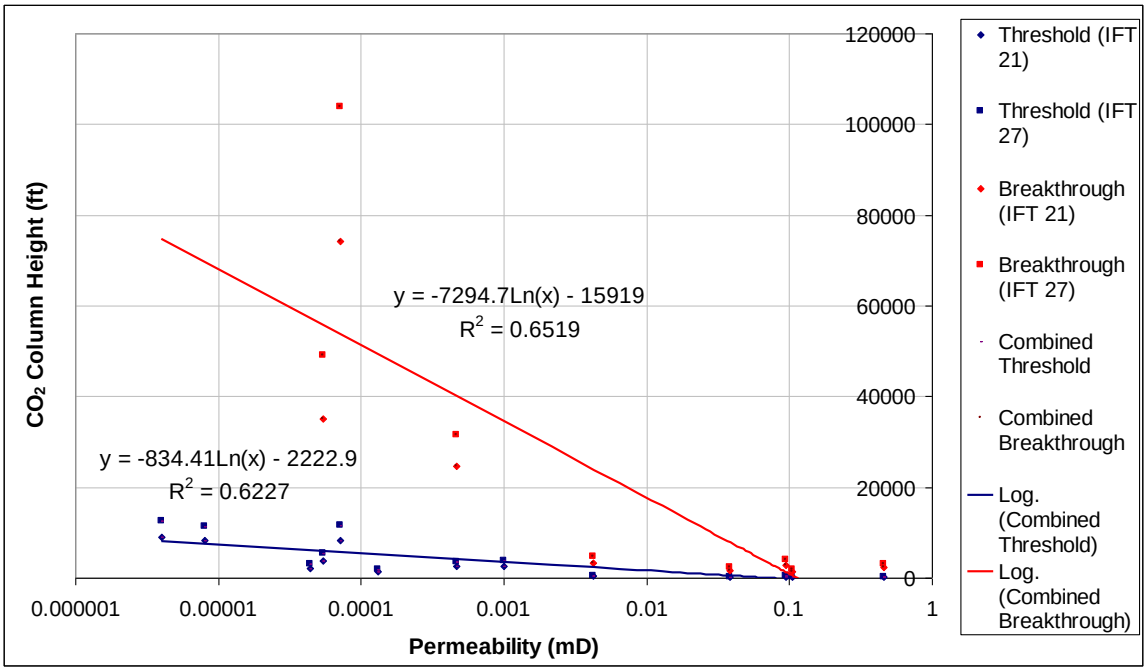

Figure 57. Graph showing permeability from MICP testing versus CO_2 column height. CO_2 column heights derived from threshold pressure are in blue with an R^2 value of 0.6227, whereas CO_2 column heights derived from breakthrough pressure are in red with an R^2 value of 0.6519.

Storage capacity compared to sealing capacity

Si-Yong Lee at the University of Utah has been working on Monte Carlo simulations to evaluate the storage capacity within the Navajo Sandstone at the Gordon

Creek field. Based on his modeling, storage estimates range from 4.75-50.32 million tons of CO_2 (P_{10} and P_{90} estimates respectively with efficiency factor of 0.0051 (P_{10} estimate)). Because the project is going to inject 3 million tons over 4 years, from a storage capacity point of view, Gordon Creek should be able to effectively store the planned amount of CO_2, even if the reality is closer to the P_{10} estimates.

Seal bypass possibilities

As noted previously, the Carmel contains an abundance of low permeability lithologies, which should provide an excellent barrier to the upward migration of CO_2 from the reservoir. However, in addition to the main lithologies present, one must consider the possibility that seal bypass systems (Cartwright, 2007) exist within the unit. For example, leaking faults or open fracture networks present in the Carmel could be pathways for sequestered CO_2 to escape.

The Carmel Formation is that it is heavily fractured in outcrop, and thus fracture bypass systems are possible. The fractured nature of the Carmel could allow CO_2 to bypass the less permeable limestones through open fractures. The shales and siltstones, which contain high clay content, would likely not retain open fractures. Rather, these lithologies are more likely to deform ductily, preventing CO_2 from escaping. This contrast in the characteristics of the lithologies present in the Carmel is actually advantageous when considering it as a sealing unit. If there were open fractures at depth, then the shales and siltstones should effectively sequester CO_2, and if fractures are absent or mineralized, the limestones could sequester an even larger column of CO_2.

During the field portion of this study, fractures were examined at the I-70 site. Calcite veins cut across the more resistant beds of limestone, but die out in the shales. This illustrates the variable ductile/brittle response to fracturing in the seals. The heavily fractured areas did not contain mineralized fractures, so they might related to outcrop weathering.

There is, however, the distinct possibility that the calcite is from interaction with meteoric water or with hot SMOW waters, reducing the possibility that the fractures are all sealed at depth. Although stable isotope data from Gordon Creek was not available, data for meteoric water composition is available from the Aneth Oil Field in San Juan County, Utah (southeast corner of the state). $\delta^{18}O$ values of samples from the San Juan River, composite snow samples from the Abajo Mountains, and samples from the Navajo Sandstone range from -17 to -12‰ (Spangler et al., 1996). The calcite from I-70 could have formed from meteoric water with these values at surface temperatures (Figure 38). It might have also formed at depth from SMOW waters. This situation would also result in the subsurface fractures being mineralized with calcite.

Chapter 5: Conclusions

1) Diagenetic alterations in the Carmel Formation have been primarily porosity/permeability reducing, with calcite and gypsum cementation being the largest source of reduction. In the Co-op Creek Limestone Member, there has been some dissolution, but this is far less than the reduction caused by precipitation. Dolomite precipitation has been an additional, although not significant, source of porosity/permeability reduction in the Carmel Formation in the three lower members.

2) Mineralized fractures that are present in outcrop at the two sampling locations might be mineralized with calcite at depth, reducing the possibility of fractures being a major conduit for CO_2 to escape. The calcite mineralization is compatible with hot ~0 SMOW waters (veins present at depth), or meteoric water (not present at depth). This study could not constrain the temperature of formation of the calcite, so environment of formation could not be determined. Also, examining the fractures in outcrop reveals that the mineralized fractures are mainly present in the limestone beds — where they transition it siltstones/shales, the fractures disappear in all but a few cases.

3) Based upon the low permeability, the Carmel should be able to effectively seal the 4 million tons of CO_2 for this project. From CO_2 height calculations, layers within the Carmel could effectively sequester a maximum of 20,603 feet (breakthrough pressure) 12,504 feet (threshold pressure) of CO_2. Because the Navajo is only 150-300 feet at the Gordon Creek site, the available porosity in the Navajo could be filled to capacity with CO_2, and the Carmel would be able to effectively sequester it.

Suggestions for future work

Prior to the Phase III injection project, additional work should be done to assess the quality of the Carmel Formation seal. In particular, conventional core should be obtained from the Carmel Formation at Gordon Creek. The vast majority of the work done in this thesis was from outcrop analogs, but because of the regional variation of the Carmel Formation, the actual section at Gordon Creek needs to be examined in detail, including additional petrophysical analyses.

Although not a focus of this study, low permeability deformation bands within the Navajo have the potential to compartmentalize portions of the reservoir; this could result in localized elevated reservoir pressures and CO_2 saturation. Further work should be done to assess the potential impact of these structures on the injectivity of the reservoir and seal integrity.

It would be beneficial to compare the calcite in the veins and the cementing calcite phases in terms of their stable isotopic composition. A compositional analysis was done using an electron microprobe, which compared the calcite cements, the calcite in replaced fossils, and calcite veins. However, because it was difficult to extract only the calcite cement for a stable isotopic study, the true composition is still undetermined.

Finally, because of the two possibilities of the source for the calcite veins within the Carmel Formation (meteoric origin or basinal water origin), it would be useful to do a fluid inclusion study to determine the temperature of formation. This would help constrain the origin of the cements.

REFERENCES

Alfè D., M. J. Gillan, G. D. Price, 2003, Thermodynamics from first principles: temperature and composition of the Earth's core, Mineralogical Magazine, v. 67, no. 1, p. 113-123.

Bannister, K. M., P. Spencer, and M. Wilsom, 1998, Sedimentation, stratigraphy, and paleoenvironments of the lower members of the Carmel Formation (Middle Jurassic, southwestern Utah): Rocky Mountain Section, Geological Society of America Abstracts With Programs, v. 30, no. 6, p. 201-204.

Beitler, B., W. T. Parry, M. A. Chan, 2005, Fingerprints of fluid flow: Chemical diagenetic history of the Jurassic Navajo Sandstone, southern Utah, U.S.A.: Journal of Sedimentary Research, v. 75, no.4, p. 547-561.

Blakey, R. C., K. G. Havholm, L. S. Jones, 1996, Stratigraphic analysis of eolian interactions with marine and fluvial deposits, Middle Jurassic Page Sandstone and Carmel Formation, Colorado Plateau, U.S.A.: Journal of Sedimentary Research, v. 66, no. 2, p. 324-342.

Cartwright, J., M. Huuse, A. Aplin, 2007, Seal bypass systems: AAPG Bulletin, v. 91, no. 8, p.1141-1166.

Clennell, M. B., D. N. Dewhurst, K. M. Brown, G. K. Westbrook, 1999, Permeability anisotropy of consolidated clays: Geological Society of London Special Publications, v. 158, p. 79-96.

Daniel, R. F., 2006, Carbon dioxide seal capacity study, Wunger Ridge, Bowen-Surat Basin, southern Queensland: Appendix 10.6.5 of report no.RPT05-0225, CO2CRC Report No: RPT05-0039.

Daniel, R. F., and J. G. Kaldi, 2009, Evaluating seal capacity of cap rocks and intraformational barriers for CO_2 containment, in M. Grobe, J. C. Pashin, and R. L. Dodge, eds., Carbon dioxide sequestration in geological media—State of the science: AAPG Studies in Geology 59, p. 335 – 345.

De Gibert, J. M., and A. A. Ekdale, 1999, Trace fossil assemblages reflecting stressed environments in the Middle Jurassic Carmel seaway of central Utah: Journal of Paleontology, v. 73, no. 4, p. 711-720.

Dewhurst, D. N., R. M. Jones, M. D. Raven, 2002, Microstructural and petrophysical characterization of Muderong Shale: application to top seal risking: Petroleum Geoscience, v. 8, p. 371-383.

Dickinson, W. R., 1970, Interpreting detrital modes of greywacke and arkose: Journal of Sedimentary Research, v. 40, no. 2, p. 695-707.

Dunham, R. J., 1962, Classification of carbonate rocks according to depositional texture. In: Ham, W. E. (ed.), Classification of carbonate rocks: American Association of Petroleum Geologists Memoir, p. 108-121.

Espinoza, D. N., J. C. Santamarina, 2010, Water-CO_2-mineral systems: Interfacial tension, contact angle, and diffusion – Implications to CO_2 geological storage: Water Resource Research, v. 46, W07537.

Esser R., R. Levey, B. McPherson, W. O'Dowd, J. Litynski, S. Plasynski, 2010, Preparing for a carbon constrained world; overview of the United States regional carbon sequestration partnerships programme and its Southwest Regional Partnership: Petroleum Geology Conference series, 7, 1189-1195.

Folk, R. L., 1974, Petrology of sedimentary rocks, Austin, Texas, Hemphill Publishing.

Folk, R. L., 1959, Practical petrographic classification of limestones: American Association of Petroleum Geologists Bulletin, v. 43, p. 1-38.

Freeman, W. E., 1976, Regional stratigraphy and depositional environments of the Glen Canyon Group and Carmel Formation (San Rafael Group): Rocky Mountain Association of Geologists-1976 symposium, p. 247-259.

Graham, D. J., N. G. Midgley, 2000, Graphical representation of particle shape using triangular diagrams: an Excel spreadsheet method: Earth Surface Processes and Landforms, v. 25, p. 1473-1477.

Heath, J., 2010, PhD Dissertation, Multi-scale petrography and fluid dynamics of caprocks associated with geologic CO_2 storage, New Mexico Institute of Mining and Technology, Hydrology, Socorro, New Mexico, 410 p.

Huntoon J. E., P. L. Hansley, N. D. Naeser, 1999, The search for a source rock for the giant tar sand triangle accumulations, southeastern Utah: AAPG Bulletin, v. 83, p. 467-495.

Jones, L. S., R.C. Blakey, 1993, Erosional remnants and adjacent unconformities along an eolian-marine boundary of the Page Sandstone and Carmel Formation, Middle Jurassic, south-central Utah: Journal of Sedimentary Petrology, v. 63, no. 5, p. 852-859.

Kowallis, B. J., E. H. Christiansen, A. L. Deino, C. Zhang, B. H. Everett, 2001, The record of Middle Jurassic volcanism in the Carmel and Temple Cap Formations of southwestern Utah: Geological Society of America Bulletin, no. 113, p. 373-387.

Mansurbeg, H., M. A. K. El-ghali, S. Morad, P. Plink-Björklund, 2006, The impact of meteoric water on the diagenetic alterations in deep-water, marine siliciclastic turbidites: Journal of Geochemical Exploration, v. 89, p. 254-258.

McPherson, B. J., R. Grigg, 2010, Gordon Creek Site Proposal: Southwest Regional Partnership on Carbon Sequestration Project Management Plan.

Mozley, P. S., 2003, Chapter: 2 Sandstones and Conglomerates: The elements of Sedimentary Petrography (unpublished manuscript), p. 1-22.

Newton R., S. Bottrell, 2007, Stable isotopes of carbon and sulphur as indicators of environmental change: past and present: Journal of Geological Society, v. 164, p. 691-708.

North, F. K., 1985, Petroleum Geology,Winchester, Mass., Allen & Unwin Inc., 607 p.

Nuccio, V. F., S. M. Condon, 2000, Burial and thermal history of the Paradox Basin, Utah and Colorado, and petroleum potential of the middle Pennsylvanian Paradox Formation, USGS Bulletin, p. 1-47.

O'Neil, J. R., 1969, Oxygen isotope fractionation in divalent metal carbonates: Journal of Chemical Physics, v. 51, p. 5547-5558.

Parry, W. T., 2009, Diagenetic characteristics of the Jurassic Navajo Sandstone in the Covenant oil field, central Utah thrust belt: AAPG Bulletin, v. 93, no. 8, p. 1039-1061.

Parry, W. T., C. B. Forster, J. P. Evans, B. B. Bowen, M. A. Chan, 2007, Geochemistry of CO_2 sequestration in the Jurassic Navajo Sandstone, Colorado Plateau, Utah: Environmental Geosciences, v. 14, no. 2, p. 91-109.

Peterson, F., and G. N. Pipiringos, 1979, Stratigraphic relationships of the Navajo Sandstone to Middle Jurassic formations in parts of southern Utah and northern Arizona: U.S. Geological Survey Professional Paper 1035-B, 43.

Richards, H. G., 1958, Cyclic deposition in the Jurassic Carmel Formation of eastern Utah: Journal of Sedimentary Petrology, v. 28, no. 1, p 40-45.

Sharp, Z. 2007, Principles of Stable Isotope Geochemistry, 1st Edition, Upper Saddle River, New Jersey, Pearson Prentice Hall.

Solum, J. G., J. P. Brandenburg, S. J. Naruk, O. V. Kostenko, S. J. Wilkins, and R. A. Schultz, 2010, Characterization of deformation bands associated with normal and reverse stress states in the Navajo Sandstone, Utah, AAPG Bulletin, v. 94, no. 9, p. 1453-1475.

Spangler, L. E., D. L. Naftz, and Z. E. Peterman, 1996, Hydrology, chemical quality, and characterization of salinity in the Navajo Aquifer in and near the Greater Aneth Oil Field, San Juan County, Utah: U.S. Geological Survey Water-Resources Investigations Report 96-4155, p. 71.

Sprinkle, D., H. Doelling, and P. Kuehne, 2010, Carmel and Temple Cap Formation measurements (unpublished data).

Uygur, K., M. D. Picard, 1980, Reservoir characteristics of Jurassic Navajo Sandstone, southern Utah: Henry Mountains Symposium, no. 8, p. 277-286.

Wilson, J. E., 2004, Characteristics of faults in nonwelded ignimbrites from the Pajarito Plateau and implications for fluid flow, New Mexico Institute of Mining and Technology, PhD dissertation, Appendix C, p. 164.

APPENDIX A – MICP

Page

6/10/10-12 Data

Int Pres psia	Pore Dia microns	Inc Int mL/gm	Cum Int mL/gm	Cum Int %PV(bc)	Cum Int %BV	Inc Int %PV(ac)	Cum Int %PV(ac)	Pore Rad microns	W.P. Sat %PV(ac)	Lev "J" Funct.
5.190	41.097	0.000	0.000	0.028	0.000	0.000	0.000	20.548	100.000	0.002
5.490	38.867	0.000	0.000	0.028	0.000	0.000	0.000	19.434	100.000	0.002
5.840	36.520	0.000	0.000	0.076	0.000	0.000	0.000	18.260	100.000	0.002
6.240	34.184	0.000	0.000	0.095	0.000	0.000	0.000	17.092	100.000	0.002
6.490	32.865	0.000	0.000	0.123	0.026	0.000	0.000	16.432	100.000	0.003
6.740	31.646	0.000	0.000	0.123	0.026	0.000	0.000	15.823	100.000	0.003
7.040	30.301	0.000	0.000	0.132	0.026	0.000	0.000	15.151	100.000	0.003
7.340	29.066	0.000	0.000	0.132	0.026	0.000	0.000	14.533	100.000	0.003
7.590	28.108	0.000	0.000	0.142	0.026	0.000	0.000	14.054	100.000	0.003
7.840	27.202	0.000	0.000	0.142	0.026	0.000	0.000	13.601	100.000	0.003
8.190	26.043	0.000	0.000	0.161	0.026	0.000	0.000	13.021	100.000	0.003
8.540	24.973	0.000	0.000	0.180	0.026	0.000	0.000	12.487	100.000	0.003
9.080	23.492	0.000	0.000	0.180	0.026	0.000	0.000	11.746	100.000	0.004
9.610	22.196	0.000	0.000	0.180	0.026	0.000	0.000	11.098	100.000	0.004
10.440	20.430	0.000	0.000	0.208	0.026	0.000	0.000	10.215	100.000	0.004
11.350	18.797	0.000	0.000	0.227	0.026	0.000	0.000	9.399	100.000	0.004
12.340	17.292	0.000	0.000	0.274	0.026	0.000	0.000	8.646	100.000	0.005
13.410	15.912	0.000	0.000	0.274	0.026	0.000	0.000	7.956	100.000	0.005
14.570	14.638	0.000	0.000	0.293	0.026	0.000	0.000	7.319	100.000	0.006
15.840	13.469	0.000	0.000	0.331	0.052	0.000	0.000	6.734	100.000	0.006
17.210	12.392	0.000	0.000	0.378	0.052	0.000	0.000	6.196	100.000	0.007
18.710	11.400	0.000	0.000	0.416	0.052	0.000	0.000	5.700	100.000	0.007
20.330	10.492	0.000	0.000	0.444	0.052	0.000	0.000	5.246	100.000	0.008
22.100	9.653	0.000	0.000	0.482	0.052	0.000	0.000	4.826	100.000	0.009
24.020	8.881	0.000	0.000	0.520	0.077	0.000	0.000	4.441	100.000	0.009
26.110	8.171	0.000	0.000	0.567	0.077	0.000	0.000	4.086	100.000	0.010
28.980	7.362	0.000	0.000	0.605	0.077	0.000	0.000	3.681	100.000	0.011
31.760	6.717	0.000	0.000	0.690	0.077	0.000	0.000	3.359	100.000	0.013
34.780	6.134	0.000	0.000	0.747	0.103	0.000	0.000	3.067	100.000	0.014
38.080	5.602	0.000	0.000	0.822	0.103	0.000	0.000	2.801	100.000	0.015
41.580	5.131	0.000	0.000	0.888	0.103	0.000	0.000	2.565	100.000	0.016
43.780	4.872	0.000	0.000	0.888	0.103	0.000	0.000	2.436	100.000	0.017
48.150	4.430	0.000	0.000	0.894	0.103	0.000	0.000	2.215	100.000	0.019
52.730	4.046	0.000	0.000	0.894	0.103	0.000	0.000	2.023	100.000	0.021
56.230	3.794	0.000	0.001	0.946	0.129	0.000	0.000	1.897	100.000	0.022
62.410	3.418	0.000	0.001	0.998	0.129	0.000	0.000	1.709	100.000	0.025
70.470	3.027	0.000	0.001	1.059	0.129	0.000	0.000	1.514	100.000	0.028
75.990	2.807	0.000	0.001	1.080	0.129	0.000	0.000	1.404	100.000	0.030
81.400	2.621	0.000	0.001	1.117	0.155	0.000	0.000	1.310	100.000	0.032
89.350	2.388	0.000	0.001	1.133	0.155	0.000	0.000	1.194	100.000	0.035
98.720	2.161	0.000	0.001	1.170	0.155	0.000	0.000	1.080	100.000	0.039

Int Pres psia	Pore Dia microns	Inc Int mL/gm	Cum Int mL/gm	Cum Int %PV(bc)	Cum Int %BV	Inc Int %PV(ac)	Cum Int %PV(ac)	Pore Rad microns	W.P. Sat %PV(ac)	Lev "J" Funct.
107.260	1.989	0.000	0.001	1.247	0.155	0.000	0.000	0.994	100.000	0.042
114.160	1.869	0.000	0.001	1.329	0.180	0.000	0.000	0.934	100.000	0.045
125.350	1.702	0.000	0.001	1.380	0.180	0.000	0.000	0.851	100.000	0.050
135.330	1.576	0.000	0.001	1.418	0.180	0.000	0.000	0.788	100.000	0.053
149.210	1.430	0.000	0.001	1.456	0.180	0.000	0.000	0.715	100.000	0.059
160.900	1.326	0.000	0.001	1.485	0.180	0.000	0.000	0.663	100.000	0.064
175.130	1.218	0.000	0.001	1.490	0.180	0.000	0.000	0.609	100.000	0.069
189.330	1.127	0.000	0.001	1.767	0.232	0.000	0.000	0.563	100.000	0.075
205.470	1.038	0.000	0.001	1.767	0.232	0.000	0.000	0.519	100.000	0.081
224.960	0.948	0.000	0.001	1.782	0.232	0.000	0.000	0.474	100.000	0.089
245.440	0.869	0.000	0.001	1.814	0.232	0.000	0.000	0.435	100.000	0.097
266.230	0.801	0.000	0.001	2.107	0.258	0.000	0.000	0.401	100.000	0.105
289.470	0.737	0.000	0.001	2.109	0.258	0.000	0.000	0.368	100.000	0.114
313.410	0.681	0.000	0.001	2.186	0.283	0.000	0.000	0.340	100.000	0.124
340.950	0.626	0.000	0.001	2.438	0.309	0.000	0.000	0.313	100.000	0.135
373.820	0.571	0.000	0.001	2.754	0.335	0.000	0.000	0.285	100.000	0.148
406.050	0.525	0.000	0.002	3.009	0.386	0.414	0.414	0.263	99.586	0.160
440.620	0.484	0.001	0.002	4.856	0.618	1.863	2.277	0.242	97.723	0.174
481.630	0.443	0.001	0.004	7.171	0.901	2.277	4.555	0.221	95.445	0.190
523.340	0.408	0.002	0.005	11.623	1.288	3.106	7.660	0.204	92.340	0.207
566.550	0.377	0.002	0.007	13.972	1.777	3.934	11.594	0.188	88.406	0.224
615.690	0.347	0.002	0.009	18.377	2.343	4.555	16.149	0.173	83.851	0.243
668.510	0.319	0.003	0.012	24.462	3.116	6.211	22.360	0.160	77.640	0.264
726.830	0.294	0.004	0.016	32.926	4.198	8.696	31.056	0.147	68.944	0.287
790.660	0.270	0.005	0.021	36.836	5.356	9.317	40.373	0.135	59.627	0.312
859.600	0.248	0.004	0.025	50.224	6.361	8.075	48.447	0.124	51.553	0.340
933.660	0.229	0.003	0.027	55.619	7.056	5.590	54.037	0.114	45.963	0.369
1014.120	0.210	0.002	0.029	59.683	7.571	4.141	58.178	0.105	41.822	0.401
1105.000	0.193	0.002	0.031	62.752	7.957	3.106	61.284	0.097	38.716	0.436
1200.150	0.178	0.002	0.032	65.779	8.344	3.106	64.389	0.089	35.611	0.474
1302.990	0.164	0.001	0.034	68.145	8.653	2.484	66.874	0.082	33.126	0.515
1415.970	0.151	0.001	0.035	70.180	8.910	2.070	68.944	0.075	31.056	0.559
1541.140	0.138	0.001	0.036	72.211	9.168	2.070	71.014	0.069	28.986	0.609
1673.610	0.128	0.001	0.036	73.884	9.374	1.656	72.671	0.064	27.329	0.661
1817.810	0.117	0.001	0.037	75.274	9.554	1.449	74.120	0.059	25.880	0.718
1977.520	0.108	0.001	0.038	76.946	9.760	1.656	75.776	0.054	24.224	0.781
2149.680	0.099	0.001	0.039	78.296	9.940	1.449	77.226	0.050	22.774	0.849
2333.980	0.091	0.001	0.039	79.326	10.069	1.035	78.261	0.046	21.739	0.922
2535.970	0.084	0.001	0.040	80.389	10.198	1.035	79.296	0.042	20.704	1.002
2757.900	0.077	0.001	0.040	81.690	10.352	1.242	80.538	0.039	19.462	1.089
2996.800	0.071	0.001	0.041	82.696	10.481	1.035	81.573	0.036	18.427	1.184
3254.670	0.066	0.000	0.041	83.393	10.558	0.621	82.195	0.033	17.805	1.286
3540.460	0.060	0.001	0.042	84.376	10.687	1.035	83.230	0.030	16.770	1.398
3845.860	0.056	0.000	0.042	85.087	10.790	0.828	84.058	0.028	15.942	1.519

Int Pres psia	Pore Dia microns	Inc Int mL/gm	Cum Int mL/gm	Cum Int %PV(bc)	Cum Int %BV	Inc Int %PV(ac)	Cum Int %PV(ac)	Pore Rad microns	W.P. Sat %PV(ac)	Lev "J" Funct.
4180.380	0.051	0.000	0.042	85.777	10.867	0.621	84.679	0.026	15.321	1.651
4426.160	0.048	0.000	0.042	86.122	10.919	0.414	85.093	0.024	14.907	1.748
4824.120	0.044	0.000	0.043	86.775	10.996	0.621	85.714	0.022	14.286	1.905
5365.740	0.040	0.001	0.043	87.779	11.125	1.035	86.749	0.020	13.251	2.119
5832.790	0.037	0.000	0.044	88.453	11.202	0.621	87.371	0.018	12.629	2.304
6329.550	0.034	0.000	0.044	88.857	11.254	0.414	87.785	0.017	12.215	2.500
6882.800	0.031	0.000	0.044	89.484	11.331	0.621	88.406	0.016	11.594	2.719
7486.810	0.029	0.000	0.044	90.131	11.408	0.621	89.027	0.014	10.973	2.957
8124.230	0.026	0.000	0.045	90.449	11.460	0.414	89.441	0.013	10.559	3.209
8838.940	0.024	0.000	0.045	91.234	11.563	0.828	90.269	0.012	9.731	3.491
9599.700	0.022	0.000	0.045	91.546	11.614	0.414	90.683	0.011	9.317	3.792
10446.940	0.020	0.000	0.045	92.071	11.691	0.621	91.304	0.010	8.696	4.126
11349.890	0.019	0.000	0.046	92.474	11.743	0.414	91.718	0.009	8.282	4.483
12333.330	0.017	0.000	0.046	93.049	11.820	0.621	92.340	0.009	7.660	4.871
13402.040	0.016	0.000	0.046	93.388	11.872	0.414	92.754	0.008	7.246	5.293
14561.980	0.015	0.000	0.046	93.919	11.949	0.621	93.375	0.007	6.625	5.752
15827.320	0.014	0.000	0.047	94.135	12.000	0.414	93.789	0.007	6.211	6.251
17203.000	0.012	0.000	0.047	94.513	12.052	0.414	94.203	0.006	5.797	6.795
18696.740	0.011	0.000	0.047	95.062	12.129	0.621	94.824	0.006	5.176	7.385
20324.570	0.011	0.000	0.047	95.312	12.155	0.207	95.031	0.005	4.969	8.028
22091.450	0.010	0.000	0.048	95.885	12.232	0.621	95.652	0.005	4.348	8.726
24013.230	0.009	0.000	0.048	96.275	12.284	0.414	96.066	0.004	3.934	9.485
26099.220	0.008	0.000	0.048	96.673	12.335	0.414	96.480	0.004	3.520	10.309
28367.170	0.008	0.000	0.048	96.866	12.361	0.207	96.687	0.004	3.313	11.204
30829.000	0.007	0.000	0.048	96.957	12.412	0.414	97.101	0.003	2.899	12.177
33506.050	0.006	0.000	0.048	97.308	12.464	0.414	97.516	0.003	2.484	13.234
36413.220	0.006	0.000	0.049	97.841	12.490	0.207	97.723	0.003	2.277	14.382
39574.090	0.005	0.000	0.049	98.074	12.515	0.207	97.930	0.003	2.070	15.631
43007.170	0.005	0.000	0.049	98.465	12.567	0.414	98.344	0.003	1.656	16.987
46741.050	0.005	0.000	0.049	98.875	12.618	0.414	98.758	0.002	1.242	18.461
50796.410	0.004	0.000	0.049	99.277	12.670	0.414	99.172	0.002	0.828	20.063
55205.280	0.004	0.000	0.050	99.876	12.747	0.621	99.793	0.002	0.207	21.805
59986.060	0.004	0.000	0.050	100.000	12.773	0.207	100.000	0.002	0.000	23.693

6/10/10-12 Pore aperture vs. mercury saturation

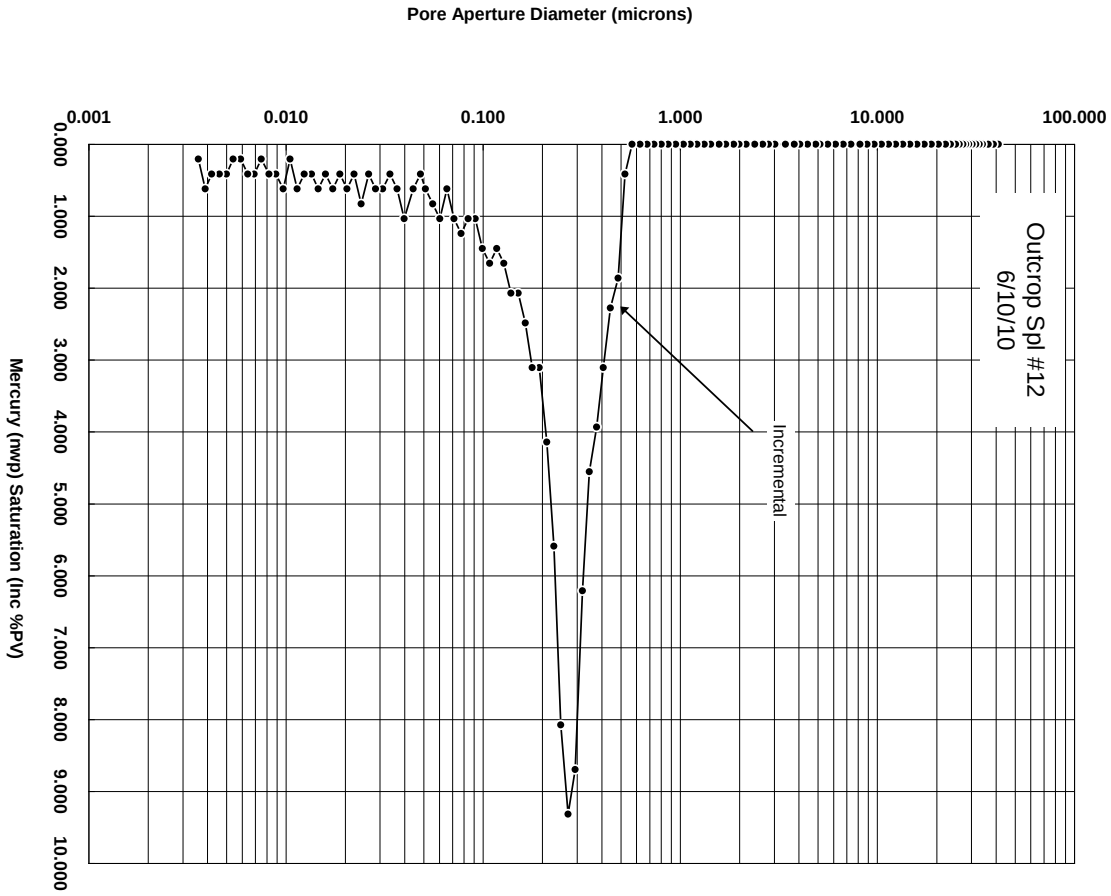

6/10/10-13 Data

Int Pres psia	Pore Dia microns	Inc Int mL/gm	Cum Int mL/gm	Cum Int %PV(bc)	Cum Int %BV	Inc Int %PV(ac)	Cum Int %PV(ac)	Pore Rad microns	W.P. Sat %PV(ac)	Lev "J" Funct.
5.190	41.097	0.000	0.000	0.000	0.000	0.000	0.000	20.548	100.000	0.004
5.490	38.867	0.000	0.000	0.000	0.000	0.000	0.000	19.434	100.000	0.004
5.840	36.520	0.000	0.000	0.000	0.000	0.000	0.000	18.260	100.000	0.004
6.240	34.184	0.000	0.000	0.000	0.000	0.000	0.000	17.092	100.000	0.005
6.490	32.865	0.000	0.000	0.000	0.000	0.000	0.000	16.432	100.000	0.005
6.740	31.646	0.000	0.000	0.000	0.000	0.000	0.000	15.823	100.000	0.005
7.040	30.301	0.000	0.000	0.000	0.000	0.000	0.000	15.151	100.000	0.005
7.340	29.066	0.000	0.000	0.149	0.023	0.000	0.000	14.533	100.000	0.006
7.590	28.108	0.000	0.000	0.149	0.023	0.000	0.000	14.054	100.000	0.006
7.840	27.202	0.000	0.000	0.149	0.023	0.000	0.000	13.601	100.000	0.006
8.190	26.043	0.000	0.000	0.149	0.023	0.000	0.000	13.021	100.000	0.006
8.540	24.973	0.000	0.000	0.149	0.023	0.000	0.000	12.487	100.000	0.007
9.080	23.492	0.000	0.000	0.149	0.023	0.000	0.000	11.746	100.000	0.007
9.610	22.196	0.000	0.000	0.149	0.023	0.000	0.000	11.098	100.000	0.007
10.440	20.430	0.000	0.000	0.149	0.023	0.000	0.000	10.215	100.000	0.008
11.350	18.797	0.000	0.000	0.149	0.023	0.000	0.000	9.399	100.000	0.009
12.340	17.292	0.000	0.000	0.149	0.023	0.000	0.000	8.646	100.000	0.009
13.410	15.912	0.000	0.000	0.149	0.023	0.000	0.000	7.956	100.000	0.010
14.570	14.638	0.000	0.000	0.149	0.023	0.000	0.000	7.319	100.000	0.011
15.840	13.469	0.000	0.000	0.149	0.023	0.000	0.000	6.734	100.000	0.012
17.210	12.392	0.000	0.000	0.149	0.023	0.000	0.000	6.196	100.000	0.013
18.710	11.400	0.000	0.000	0.149	0.023	0.000	0.000	5.700	100.000	0.014
20.330	10.492	0.000	0.000	0.298	0.047	0.000	0.000	5.246	100.000	0.016
22.100	9.653	0.000	0.000	0.298	0.047	0.000	0.000	4.826	100.000	0.017
24.020	8.881	0.000	0.000	0.298	0.047	0.000	0.000	4.441	100.000	0.018
26.110	8.171	0.000	0.000	0.298	0.047	0.000	0.000	4.086	100.000	0.020
28.980	7.362	0.000	0.000	0.298	0.047	0.000	0.000	3.681	100.000	0.022
31.760	6.717	0.000	0.000	0.298	0.047	0.000	0.000	3.359	100.000	0.024
34.780	6.134	0.000	0.000	0.298	0.047	0.000	0.000	3.067	100.000	0.027
38.080	5.602	0.000	0.000	0.298	0.047	0.000	0.000	2.801	100.000	0.029
41.580	5.131	0.000	0.000	0.298	0.047	0.000	0.000	2.565	100.000	0.032
43.800	4.871	0.000	0.000	0.298	0.047	0.000	0.000	2.435	100.000	0.034
48.160	4.430	0.000	0.000	0.298	0.047	0.000	0.000	2.215	100.000	0.037
52.740	4.045	0.000	0.000	0.298	0.047	0.000	0.000	2.023	100.000	0.041
56.240	3.793	0.000	0.000	0.149	0.023	0.000	0.000	1.896	100.000	0.043
62.420	3.417	0.000	0.000	0.149	0.023	0.000	0.000	1.709	100.000	0.048
70.490	3.026	0.000	0.000	0.149	0.023	0.000	0.000	1.513	100.000	0.054
76.290	2.796	0.000	0.000	0.298	0.047	0.000	0.000	1.398	100.000	0.059
81.690	2.611	0.000	0.000	0.298	0.047	0.000	0.000	1.306	100.000	0.063

Int Pres psia	Pore Dia microns	Inc Int mL/gm	Cum Int mL/gm	Cum Int %PV(bc)	Cum Int %BV	Inc Int %PV(ac)	Cum Int %PV(ac)	Pore Rad microns	W.P. Sat %PV(ac)	Lev "J" Funct.
89.640	2.380	0.000	0.000	0.298	0.047	0.000	0.000	1.190	100.000	0.069
99.020	2.154	0.000	0.000	0.298	0.047	0.000	0.000	1.077	100.000	0.076
107.550	1.983	0.000	0.000	0.298	0.047	0.000	0.000	0.992	100.000	0.083
114.460	1.864	0.000	0.000	0.298	0.047	0.000	0.000	0.932	100.000	0.088
125.660	1.698	0.000	0.000	0.298	0.047	0.000	0.000	0.849	100.000	0.097
135.640	1.573	0.000	0.000	0.298	0.047	0.000	0.000	0.786	100.000	0.104
149.520	1.427	0.000	0.000	0.298	0.047	0.000	0.000	0.713	100.000	0.115
161.840	1.318	0.000	0.000	0.446	0.070	0.000	0.000	0.659	100.000	0.125
177.100	1.205	0.000	0.000	0.595	0.094	0.000	0.000	0.602	100.000	0.136
191.300	1.115	0.000	0.000	0.595	0.094	0.000	0.000	0.558	100.000	0.147
207.440	1.028	0.000	0.000	0.595	0.094	0.000	0.000	0.514	100.000	0.160
226.940	0.940	0.000	0.000	0.595	0.094	0.000	0.000	0.470	100.000	0.175
247.420	0.862	0.000	0.000	0.595	0.094	0.000	0.000	0.431	100.000	0.190
268.300	0.795	0.000	0.001	0.744	0.117	0.000	0.000	0.398	100.000	0.207
291.570	0.732	0.000	0.001	1.042	0.164	0.300	0.300	0.366	99.700	0.224
315.500	0.676	0.000	0.001	1.637	0.258	0.600	0.900	0.338	99.100	0.243
343.010	0.622	0.001	0.002	3.125	0.492	1.499	2.399	0.311	97.601	0.264
375.830	0.568	0.002	0.004	5.506	0.867	2.399	4.798	0.284	95.202	0.289
408.010	0.523	0.002	0.005	7.738	1.219	2.249	7.046	0.261	92.954	0.314
442.270	0.482	0.010	0.015	22.173	3.492	14.543	21.589	0.241	78.411	0.340
482.890	0.442	0.013	0.028	40.923	6.444	18.891	40.480	0.221	59.520	0.372
524.200	0.407	0.014	0.041	61.161	9.632	20.390	60.870	0.203	39.130	0.404
567.390	0.376	0.002	0.043	63.988	10.077	2.849	63.718	0.188	36.282	0.437
616.550	0.346	0.002	0.045	66.667	10.499	2.699	66.417	0.173	33.583	0.475
669.410	0.319	0.002	0.046	68.899	10.850	2.249	68.666	0.159	31.334	0.515
727.830	0.293	0.001	0.048	70.833	11.155	1.949	70.615	0.147	29.385	0.560
791.690	0.270	0.001	0.049	72.470	11.413	1.649	72.264	0.135	27.736	0.609
861.190	0.248	0.001	0.050	74.107	11.670	1.649	73.913	0.124	26.087	0.663
934.940	0.228	0.001	0.051	75.446	11.881	1.349	75.262	0.114	24.738	0.720
1015.430	0.210	0.001	0.052	76.637	12.069	1.199	76.462	0.105	23.538	0.782
1106.340	0.193	0.001	0.052	77.827	12.256	1.199	77.661	0.096	22.339	0.852
1201.510	0.178	0.001	0.053	78.869	12.420	1.049	78.711	0.089	21.289	0.925
1304.370	0.164	0.001	0.054	79.911	12.584	1.049	79.760	0.082	20.240	1.004
1417.360	0.151	0.001	0.054	80.952	12.748	1.049	80.810	0.075	19.190	1.091
1542.540	0.138	0.001	0.055	81.845	12.889	0.900	81.709	0.069	18.291	1.187
1675.020	0.127	0.001	0.056	82.738	13.030	0.900	82.609	0.064	17.391	1.289
1819.230	0.117	0.001	0.056	83.482	13.147	0.750	83.358	0.059	16.642	1.400
1978.940	0.108	0.001	0.057	84.375	13.287	0.900	84.258	0.054	15.742	1.523
2151.110	0.099	0.001	0.057	85.119	13.404	0.750	85.007	0.050	14.993	1.656
2335.410	0.091	0.000	0.058	85.714	13.498	0.600	85.607	0.046	14.393	1.798
2537.410	0.084	0.000	0.058	86.310	13.592	0.600	86.207	0.042	13.793	1.953

Int Pres psia	Pore Dia microns	Inc Int mL/gm	Cum Int mL/gm	Cum Int %PV(bc)	Cum Int %BV	Inc Int %PV(ac)	Cum Int %PV(ac)	Pore Rad microns	W.P. Sat %PV(ac)	Lev "J" Funct.
2759.350	0.077	0.000	0.058	86.905	13.686	0.600	86.807	0.039	13.193	2.124
2998.240	0.071	0.000	0.059	87.500	13.779	0.600	87.406	0.036	12.594	2.308
3256.110	0.066	0.000	0.059	88.095	13.873	0.600	88.006	0.033	11.994	2.507
3541.910	0.060	0.000	0.060	88.690	13.967	0.600	88.606	0.030	11.394	2.727
3847.310	0.055	0.000	0.060	89.137	14.037	0.450	89.055	0.028	10.945	2.962
4181.830	0.051	0.000	0.060	89.583	14.108	0.450	89.505	0.026	10.495	3.219
4427.610	0.048	0.000	0.060	89.881	14.154	0.300	89.805	0.024	10.195	3.408
4825.570	0.044	0.000	0.061	90.327	14.225	0.450	90.255	0.022	9.745	3.715
5367.190	0.040	0.000	0.061	90.923	14.318	0.600	90.855	0.020	9.145	4.132
5834.250	0.037	0.000	0.061	91.369	14.389	0.450	91.304	0.018	8.696	4.491
6331.000	0.034	0.000	0.062	91.667	14.436	0.300	91.604	0.017	8.396	4.874
6884.250	0.031	0.000	0.062	92.113	14.506	0.450	92.054	0.016	7.946	5.300
7488.270	0.029	0.000	0.062	92.560	14.576	0.450	92.504	0.014	7.496	5.765
8125.690	0.026	0.000	0.062	92.857	14.623	0.300	92.804	0.013	7.196	6.255
8840.400	0.024	0.000	0.063	93.304	14.693	0.450	93.253	0.012	6.747	6.805
9601.160	0.022	0.000	0.063	93.601	14.740	0.300	93.553	0.011	6.447	7.391
10448.390	0.020	0.000	0.063	94.048	14.811	0.450	94.003	0.010	5.997	8.043
11351.340	0.019	0.000	0.063	94.345	14.857	0.300	94.303	0.009	5.697	8.738
12334.790	0.017	0.000	0.064	94.643	14.904	0.300	94.603	0.009	5.397	9.495
13403.500	0.016	0.000	0.064	94.940	14.951	0.300	94.903	0.008	5.097	10.318
14563.440	0.015	0.000	0.064	95.238	14.998	0.300	95.202	0.007	4.798	11.211
15828.780	0.014	0.000	0.064	95.536	15.045	0.300	95.502	0.007	4.498	12.185
17204.450	0.012	0.000	0.064	95.833	15.092	0.300	95.802	0.006	4.198	13.244
18698.200	0.011	0.000	0.065	96.131	15.139	0.300	96.102	0.006	3.898	14.394
20326.020	0.011	0.000	0.065	96.429	15.186	0.300	96.402	0.005	3.598	15.647
22092.900	0.010	0.000	0.065	96.726	15.232	0.300	96.702	0.005	3.298	17.007
24014.680	0.009	0.000	0.065	97.024	15.279	0.300	97.001	0.004	2.999	18.487
26100.680	0.008	0.000	0.065	97.321	15.326	0.300	97.301	0.004	2.699	20.093
28368.620	0.008	0.000	0.066	97.619	15.373	0.300	97.601	0.004	2.399	21.838
30830.440	0.007	0.000	0.066	97.917	15.420	0.300	97.901	0.003	2.099	23.734
33507.500	0.006	0.000	0.066	98.214	15.467	0.300	98.201	0.003	1.799	25.794
36414.670	0.006	0.000	0.066	98.661	15.537	0.450	98.651	0.003	1.349	28.032
39575.540	0.005	0.000	0.066	98.810	15.560	0.150	98.801	0.003	1.199	30.466
43008.610	0.005	0.000	0.067	99.107	15.607	0.300	99.100	0.003	0.900	33.108
46742.500	0.005	0.000	0.067	99.554	15.678	0.450	99.550	0.002	0.450	35.983
50797.860	0.004	0.000	0.067	99.851	15.725	0.300	99.850	0.002	0.150	39.105
55206.720	0.004	0.000	0.067	100.000	15.748	0.150	100.000	0.002	0.000	42.499
59987.510	0.004	0.000	0.067	100.000	15.748	0.000	100.000	0.002	0.000	46.179

6/10/10-13 Pore aperture vs. mercury saturation

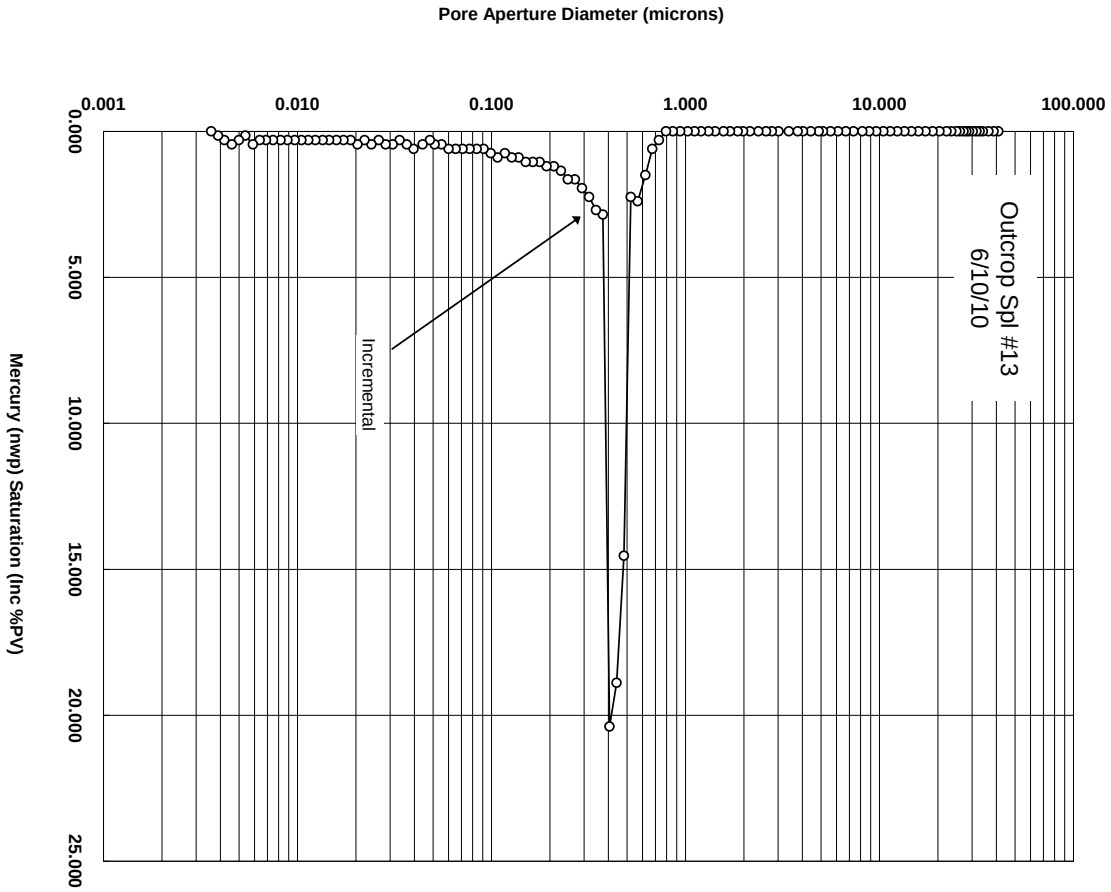

6/10/10-14 Data

Int Pres psia	Pore Dia microns	Inc Int mL/gm	Cum Int mL/gm	Cum Int %PV(bc)	Cum Int %BV	Inc Int %PV(ac)	Cum Int %PV(ac)	Pore Rad microns	W.P. Sat %PV(ac)	Lev "J" Funct.
5.190	41.088	0.000	0.000	0.035	0.000	0.000	0.000	20.544	100.000	0.001
5.490	38.847	0.000	0.000	0.070	0.000	0.000	0.000	19.424	100.000	0.001
5.840	36.533	0.000	0.000	0.070	0.000	0.000	0.000	18.267	100.000	0.001
6.240	34.184	0.000	0.000	0.116	0.000	0.000	0.000	17.092	100.000	0.001
6.490	32.867	0.000	0.000	0.151	0.000	0.000	0.000	16.434	100.000	0.001
6.740	31.648	0.000	0.000	0.151	0.000	0.000	0.000	15.824	100.000	0.001
7.040	30.301	0.000	0.000	0.186	0.000	0.000	0.000	15.151	100.000	0.001
7.340	29.063	0.000	0.000	0.198	0.000	0.000	0.000	14.531	100.000	0.001
7.590	28.106	0.000	0.000	0.233	0.000	0.000	0.000	14.053	100.000	0.001
7.840	27.214	0.000	0.000	0.233	0.000	0.000	0.000	13.607	100.000	0.001
8.190	26.044	0.000	0.000	0.267	0.027	0.000	0.000	13.022	100.000	0.001
8.540	24.982	0.000	0.000	0.314	0.027	0.000	0.000	12.491	100.000	0.001
9.080	23.491	0.000	0.000	0.326	0.027	0.000	0.000	11.745	100.000	0.001
9.610	22.191	0.000	0.000	0.372	0.027	0.000	0.000	11.096	100.000	0.001
10.440	20.428	0.000	0.000	0.407	0.027	0.000	0.000	10.214	100.000	0.001
11.350	18.795	0.000	0.000	0.430	0.027	0.000	0.000	9.398	100.000	0.002
12.340	17.293	0.000	0.000	0.500	0.027	0.000	0.000	8.646	100.000	0.002
13.410	15.910	0.000	0.000	0.558	0.027	0.000	0.000	7.955	100.000	0.002
14.570	14.639	0.000	0.000	0.593	0.027	0.000	0.000	7.320	100.000	0.002
15.840	13.470	0.000	0.000	0.651	0.027	0.000	0.000	6.735	100.000	0.002
17.220	12.392	0.000	0.000	0.721	0.027	0.000	0.000	6.196	100.000	0.002
18.710	11.402	0.000	0.000	0.802	0.054	0.000	0.000	5.701	100.000	0.002
20.330	10.493	0.000	0.000	0.872	0.054	0.000	0.000	5.246	100.000	0.003
22.100	9.653	0.000	0.000	0.965	0.054	0.000	0.000	4.826	100.000	0.003
24.020	8.882	0.000	0.000	1.081	0.054	0.000	0.000	4.441	100.000	0.003
26.110	8.172	0.000	0.000	1.197	0.054	0.000	0.000	4.086	100.000	0.003
28.980	7.362	0.000	0.000	1.337	0.082	0.000	0.000	3.681	100.000	0.004
31.750	6.718	0.000	0.000	1.581	0.082	0.000	0.000	3.359	100.000	0.004
34.780	6.134	0.000	0.000	1.709	0.082	0.000	0.000	3.067	100.000	0.005
38.080	5.602	0.000	0.000	1.906	0.109	0.000	0.000	2.801	100.000	0.005
41.580	5.131	0.000	0.000	2.104	0.109	0.000	0.000	2.565	100.000	0.006
43.310	4.926	0.000	0.000	2.129	0.109	0.000	0.000	2.463	100.000	0.006
48.020	4.442	0.000	0.000	2.129	0.109	0.000	0.000	2.221	100.000	0.006
52.390	4.072	0.000	0.000	2.144	0.109	0.000	0.000	2.036	100.000	0.007
56.680	3.764	0.000	0.000	2.144	0.109	0.000	0.000	1.882	100.000	0.008
62.570	3.409	0.000	0.000	2.160	0.109	0.000	0.000	1.705	100.000	0.008
69.050	3.090	0.000	0.000	2.164	0.109	0.000	0.000	1.545	100.000	0.009
74.290	2.872	0.000	0.000	2.225	0.109	0.000	0.000	1.436	100.000	0.010
80.740	2.642	0.000	0.001	2.391	0.136	0.000	0.000	1.321	100.000	0.011

Int Pres psia	Pore Dia microns	Inc Int mL/gm	Cum Int mL/gm	Cum Int %PV(bc)	Cum Int %BV	Inc Int %PV(ac)	Cum Int %PV(ac)	Pore Rad microns	W.P. Sat %PV(ac)	Lev "J" Funct.
89.970	2.371	0.000	0.001	2.432	0.136	0.000	0.000	1.186	100.000	0.012
97.180	2.195	0.000	0.001	2.573	0.136	0.000	0.000	1.098	100.000	0.013
105.470	2.023	0.000	0.001	2.573	0.136	0.000	0.000	1.011	100.000	0.014
115.170	1.852	0.000	0.001	2.577	0.136	0.000	0.000	0.926	100.000	0.015
124.700	1.711	0.000	0.001	2.615	0.136	0.000	0.000	0.855	100.000	0.017
136.320	1.565	0.000	0.001	2.790	0.136	0.000	0.000	0.782	100.000	0.018
149.030	1.431	0.000	0.001	2.955	0.163	0.000	0.000	0.716	100.000	0.020
160.210	1.332	0.000	0.001	2.994	0.163	0.000	0.000	0.666	100.000	0.021
174.740	1.221	0.000	0.001	2.999	0.163	0.000	0.000	0.610	100.000	0.023
189.760	1.124	0.000	0.001	3.100	0.163	0.000	0.000	0.562	100.000	0.025
205.790	1.037	0.000	0.001	3.385	0.190	0.000	0.000	0.518	100.000	0.027
224.470	0.950	0.000	0.001	3.408	0.190	0.000	0.000	0.475	100.000	0.030
243.580	0.876	0.000	0.001	3.816	0.190	0.000	0.000	0.438	100.000	0.032
265.280	0.804	0.000	0.001	3.934	0.218	0.000	0.000	0.402	100.000	0.035
288.290	0.740	0.000	0.001	4.238	0.218	0.000	0.000	0.370	100.000	0.038
313.500	0.681	0.000	0.001	4.640	0.245	0.000	0.000	0.340	100.000	0.042
341.480	0.625	0.000	0.001	5.074	0.272	0.000	0.000	0.312	100.000	0.045
372.050	0.573	0.000	0.001	5.493	0.299	0.000	0.000	0.287	100.000	0.049
407.200	0.524	0.000	0.001	6.312	0.326	0.000	0.000	0.262	100.000	0.054
440.360	0.484	0.000	0.001	6.781	0.354	0.000	0.000	0.242	100.000	0.058
479.990	0.444	0.000	0.002	7.967	0.408	1.117	1.117	0.222	98.883	0.064
521.260	0.409	0.000	0.002	8.823	0.462	1.117	2.235	0.205	97.765	0.069
565.130	0.378	0.000	0.002	9.658	0.517	1.117	3.352	0.189	96.648	0.075
615.430	0.347	0.000	0.002	11.377	0.599	1.676	5.028	0.173	94.972	0.082
670.010	0.318	0.001	0.003	16.803	0.871	5.587	10.615	0.159	89.385	0.089
726.850	0.294	0.001	0.004	20.093	1.061	3.911	14.525	0.147	85.475	0.096
790.680	0.270	0.001	0.004	22.632	1.197	2.793	17.318	0.135	82.682	0.105
859.600	0.248	0.001	0.005	25.493	1.333	2.793	20.112	0.124	79.888	0.114
934.850	0.228	0.000	0.005	27.171	1.415	1.676	21.788	0.114	78.212	0.124
1015.570	0.210	0.000	0.006	28.819	1.496	1.676	23.464	0.105	76.536	0.135
1105.100	0.193	0.000	0.006	30.488	1.605	2.235	25.698	0.097	74.302	0.147
1197.030	0.178	0.000	0.006	31.740	1.659	1.117	26.816	0.089	73.184	0.159
1304.220	0.164	0.000	0.006	33.218	1.741	1.676	28.492	0.082	71.508	0.173
1415.520	0.151	0.000	0.007	34.595	1.823	1.676	30.168	0.075	69.832	0.188
1539.350	0.139	0.000	0.007	35.729	1.877	1.117	31.285	0.069	68.715	0.204
1672.890	0.128	0.000	0.007	36.831	1.932	1.117	32.402	0.064	67.598	0.222
1816.810	0.117	0.000	0.007	37.974	1.986	1.117	33.520	0.059	66.480	0.241
1974.840	0.108	0.000	0.008	39.230	2.068	1.676	35.196	0.054	64.804	0.262
2148.300	0.099	0.000	0.008	40.461	2.122	1.117	36.313	0.050	63.687	0.285
2334.700	0.091	0.000	0.008	41.493	2.176	1.117	37.430	0.046	62.570	0.310
2537.050	0.084	0.000	0.008	42.688	2.231	1.117	38.547	0.042	61.453	0.337

Int Pres psia	Pore Dia microns	Inc Int mL/gm	Cum Int mL/gm	Cum Int %PV(bc)	Cum Int %BV	Inc Int %PV(ac)	Cum Int %PV(ac)	Pore Rad microns	W.P. Sat %PV(ac)	Lev "J" Funct.
2755.460	0.077	0.000	0.008	43.715	2.285	1.117	39.665	0.039	60.335	0.366
2997.190	0.071	0.000	0.009	45.057	2.367	1.676	41.341	0.036	58.659	0.398
3254.990	0.066	0.000	0.009	46.296	2.421	1.117	42.458	0.033	57.542	0.432
3539.410	0.060	0.000	0.009	47.538	2.476	1.117	43.575	0.030	56.425	0.470
3843.070	0.056	0.000	0.009	48.795	2.557	1.676	45.251	0.028	54.749	0.510
4172.660	0.051	0.000	0.010	50.045	2.612	1.117	46.369	0.026	53.631	0.554
4431.610	0.048	0.000	0.010	51.295	2.693	1.676	48.045	0.024	51.955	0.588
4833.320	0.044	0.000	0.010	52.926	2.775	1.676	49.721	0.022	50.279	0.641
5364.260	0.040	0.000	0.011	55.034	2.884	2.235	51.955	0.020	48.045	0.712
5829.850	0.037	0.000	0.011	56.998	2.993	2.235	54.190	0.018	45.810	0.773
6334.510	0.034	0.000	0.011	58.358	3.047	1.117	55.307	0.017	44.693	0.840
6880.980	0.031	0.000	0.012	60.144	3.156	2.235	57.542	0.016	42.458	0.913
7487.240	0.029	0.000	0.012	62.123	3.265	2.235	59.777	0.014	40.223	0.993
8126.010	0.026	0.000	0.012	63.506	3.319	1.117	60.894	0.013	39.106	1.078
8838.130	0.024	0.000	0.013	65.523	3.428	2.235	63.128	0.012	36.872	1.173
9609.000	0.022	0.000	0.013	67.187	3.509	1.676	64.804	0.011	35.196	1.275
10441.990	0.020	0.000	0.013	68.875	3.618	2.235	67.039	0.010	32.961	1.385
11343.140	0.019	0.000	0.014	70.126	3.673	1.117	68.156	0.009	31.844	1.505
12333.900	0.017	0.000	0.014	71.908	3.754	1.676	69.832	0.009	30.168	1.636
13409.190	0.016	0.000	0.014	73.857	3.863	2.235	72.067	0.008	27.933	1.779
14567.870	0.015	0.000	0.015	75.380	3.945	1.676	73.743	0.007	26.257	1.933
15825.170	0.014	0.000	0.015	77.126	4.026	1.676	75.419	0.007	24.581	2.100
17206.150	0.012	0.000	0.015	77.863	4.081	1.117	76.536	0.006	23.464	2.283
18705.810	0.011	0.000	0.015	80.036	4.190	2.235	78.771	0.006	21.229	2.482
20320.860	0.011	0.000	0.016	81.407	4.271	1.676	80.447	0.005	19.553	2.696
22090.460	0.010	0.000	0.016	82.914	4.353	1.676	82.123	0.005	17.877	2.931
24012.830	0.009	0.000	0.016	83.907	4.380	0.559	82.682	0.004	17.318	3.186
26097.810	0.008	0.000	0.017	85.683	4.489	2.235	84.916	0.004	15.084	3.463
28367.860	0.008	0.000	0.017	87.556	4.598	2.235	87.151	0.004	12.849	3.764
30827.240	0.007	0.000	0.017	88.605	4.652	1.117	88.268	0.003	11.732	4.090
33506.980	0.006	0.000	0.017	90.001	4.706	1.117	89.385	0.003	10.615	4.446
36412.960	0.006	0.000	0.018	90.890	4.761	1.117	90.503	0.003	9.497	4.831
39574.220	0.005	0.000	0.018	92.998	4.870	2.235	92.737	0.003	7.263	5.251
43008.570	0.005	0.000	0.018	94.368	4.951	1.676	94.413	0.003	5.587	5.706
46740.300	0.005	0.000	0.018	95.602	5.006	1.117	95.531	0.002	4.469	6.201
50798.380	0.004	0.000	0.019	97.861	5.114	2.235	97.765	0.002	2.235	6.740
55201.560	0.004	0.000	0.019	98.313	5.142	0.559	98.324	0.002	1.676	7.324
59986.620	0.004	0.000	0.019	100.000	5.223	1.676	100.000	0.002	0.000	7.959

6/10/10-14 Pore aperture vs. mercury saturation

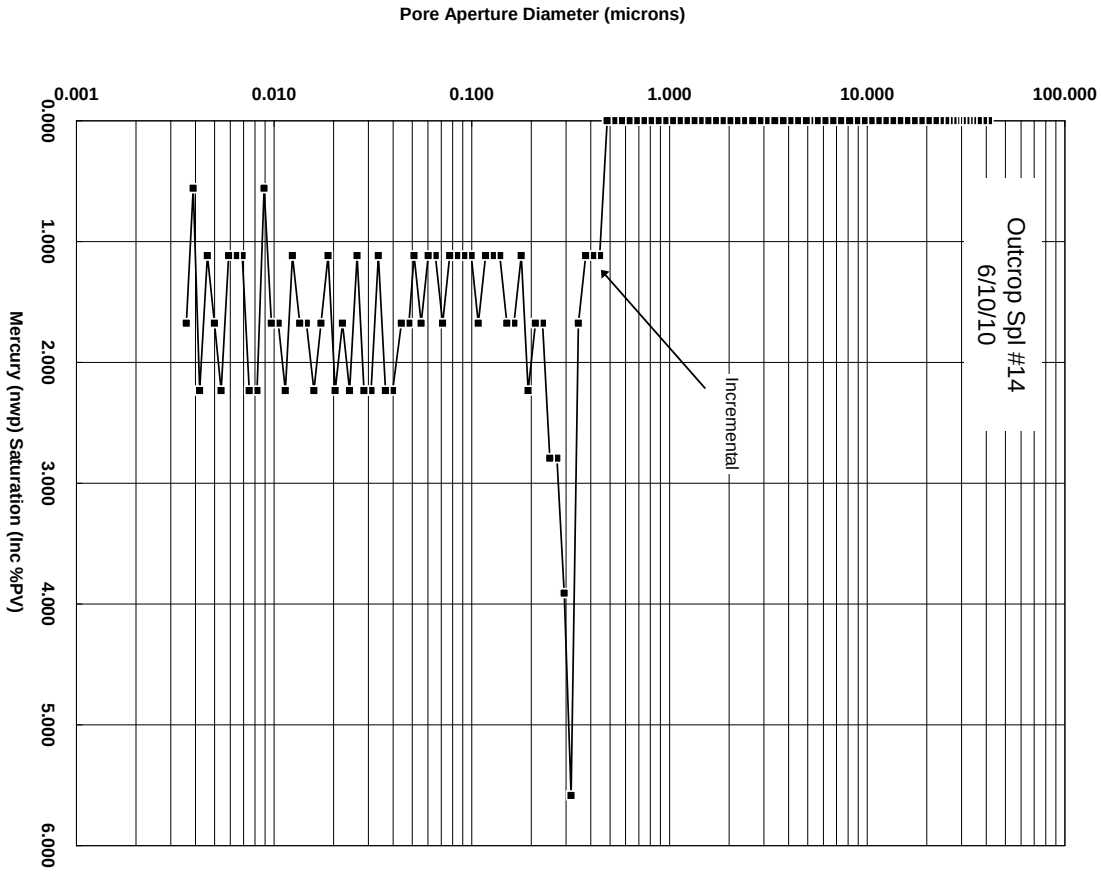

6/10/10-15 Data

Int Pres psia	Pore Dia microns	Inc Int mL/gm	Cum Int mL/gm	Cum Int %PV(bc)	Cum Int %BV	Inc Int %PV(ac)	Cum Int %PV(ac)	Pore Rad microns	W.P. Sat %PV(ac)	Lev "J" Funct.
5.190	41.088	0.000	0.000	0.072	0.000	0.000	0.000	20.544	100.000	0.000
5.490	38.847	0.000	0.000	0.119	0.000	0.000	0.000	19.424	100.000	0.000
5.840	36.533	0.000	0.000	0.143	0.000	0.000	0.000	18.267	100.000	0.000
6.240	34.184	0.000	0.000	0.191	0.000	0.000	0.000	17.092	100.000	0.000
6.490	32.867	0.000	0.000	0.262	0.000	0.000	0.000	16.434	100.000	0.000
6.740	31.648	0.000	0.000	0.262	0.000	0.000	0.000	15.824	100.000	0.000
7.040	30.301	0.000	0.000	0.310	0.000	0.000	0.000	15.151	100.000	0.000
7.340	29.063	0.000	0.000	0.358	0.000	0.000	0.000	14.531	100.000	0.000
7.590	28.106	0.000	0.000	0.381	0.000	0.000	0.000	14.053	100.000	0.000
7.840	27.214	0.000	0.000	0.405	0.000	0.000	0.000	13.607	100.000	0.000
8.190	26.044	0.000	0.000	0.477	0.028	0.000	0.000	13.022	100.000	0.000
8.540	24.982	0.000	0.000	0.500	0.028	0.000	0.000	12.491	100.000	0.000
9.080	23.491	0.000	0.000	0.548	0.028	0.000	0.000	11.745	100.000	0.000
9.610	22.191	0.000	0.000	0.643	0.028	0.000	0.000	11.096	100.000	0.000
10.440	20.428	0.000	0.000	0.691	0.028	0.000	0.000	10.214	100.000	0.000
11.350	18.795	0.000	0.000	0.739	0.028	0.000	0.000	9.398	100.000	0.000
12.340	17.293	0.000	0.000	0.834	0.028	0.000	0.000	8.646	100.000	0.000
13.410	15.910	0.000	0.000	0.953	0.028	0.000	0.000	7.955	100.000	0.000
14.570	14.639	0.000	0.000	1.025	0.028	0.000	0.000	7.320	100.000	0.000
15.840	13.470	0.000	0.000	1.144	0.028	0.000	0.000	6.735	100.000	0.000
17.220	12.392	0.000	0.000	1.239	0.028	0.000	0.000	6.196	100.000	0.001
18.710	11.402	0.000	0.000	1.358	0.056	0.000	0.000	5.701	100.000	0.001
20.330	10.493	0.000	0.000	1.454	0.056	0.000	0.000	5.246	100.000	0.001
22.100	9.653	0.000	0.000	1.644	0.056	0.000	0.000	4.826	100.000	0.001
24.020	8.882	0.000	0.000	1.811	0.056	0.000	0.000	4.441	100.000	0.001
26.110	8.172	0.000	0.000	2.002	0.056	0.000	0.000	4.086	100.000	0.001
28.980	7.362	0.000	0.000	2.288	0.084	0.000	0.000	3.681	100.000	0.001
31.750	6.718	0.000	0.000	2.598	0.084	0.000	0.000	3.359	100.000	0.001
34.780	6.134	0.000	0.000	2.812	0.084	0.000	0.000	3.067	100.000	0.001
38.080	5.602	0.000	0.000	3.122	0.112	0.000	0.000	2.801	100.000	0.001
41.580	5.131	0.000	0.000	3.455	0.112	0.000	0.000	2.565	100.000	0.001
43.310	4.925	0.000	0.000	3.477	0.112	0.000	0.000	2.463	100.000	0.001
48.030	4.442	0.000	0.000	3.551	0.112	0.000	0.000	2.221	100.000	0.001
52.390	4.072	0.000	0.000	3.621	0.112	0.000	0.000	2.036	100.000	0.002
57.340	3.720	0.000	0.000	3.621	0.112	0.000	0.000	1.860	100.000	0.002
62.580	3.409	0.000	0.000	3.621	0.112	0.000	0.000	1.704	100.000	0.002
69.050	3.089	0.000	0.000	3.621	0.112	0.000	0.000	1.545	100.000	0.002
74.300	2.871	0.000	0.000	3.621	0.112	0.000	0.000	1.436	100.000	0.002
80.750	2.642	0.000	0.000	3.799	0.112	0.000	0.000	1.321	100.000	0.002

Int Pres psia	Pore Dia microns	Inc Int mL/gm	Cum Int mL/gm	Cum Int %PV(bc)	Cum Int %BV	Inc Int %PV(ac)	Cum Int %PV(ac)	Pore Rad microns	W.P. Sat %PV(ac)	Lev "J" Funct.
89.980	2.371	0.000	0.001	3.915	0.140	0.000	0.000	1.185	100.000	0.003
97.190	2.195	0.000	0.001	4.171	0.140	0.000	0.000	1.097	100.000	0.003
105.480	2.022	0.000	0.001	4.171	0.140	0.000	0.000	1.011	100.000	0.003
115.180	1.852	0.000	0.001	4.210	0.140	0.000	0.000	0.926	100.000	0.003
124.710	1.711	0.000	0.001	4.210	0.140	0.000	0.000	0.855	100.000	0.004
136.340	1.565	0.000	0.001	4.210	0.140	0.000	0.000	0.782	100.000	0.004
149.050	1.431	0.000	0.001	4.210	0.140	0.000	0.000	0.716	100.000	0.005
160.230	1.331	0.000	0.001	4.210	0.140	0.000	0.000	0.666	100.000	0.005
174.760	1.221	0.000	0.001	4.226	0.140	0.000	0.000	0.610	100.000	0.005
189.780	1.124	0.000	0.001	4.226	0.140	0.000	0.000	0.562	100.000	0.006
205.810	1.037	0.000	0.001	4.226	0.140	0.000	0.000	0.518	100.000	0.006
224.490	0.950	0.000	0.001	4.487	0.140	0.000	0.000	0.475	100.000	0.007
243.610	0.876	0.000	0.001	4.678	0.140	0.000	0.000	0.438	100.000	0.007
265.310	0.804	0.000	0.001	4.937	0.169	0.000	0.000	0.402	100.000	0.008
288.320	0.740	0.000	0.001	5.041	0.169	0.000	0.000	0.370	100.000	0.009
313.610	0.680	0.000	0.001	5.197	0.169	0.000	0.000	0.340	100.000	0.009
341.520	0.625	0.000	0.001	5.657	0.197	0.000	0.000	0.312	100.000	0.010
372.090	0.573	0.000	0.001	5.979	0.197	0.000	0.000	0.287	100.000	0.011
407.260	0.524	0.000	0.001	6.678	0.225	0.000	0.000	0.262	100.000	0.012
440.420	0.484	0.000	0.001	6.785	0.225	0.000	0.000	0.242	100.000	0.013
480.070	0.444	0.000	0.001	7.213	0.225	0.000	0.000	0.222	100.000	0.015
521.350	0.409	0.000	0.001	7.617	0.253	0.000	0.000	0.205	100.000	0.016
565.230	0.377	0.000	0.001	7.663	0.253	0.000	0.000	0.189	100.000	0.017
615.560	0.347	0.000	0.001	8.158	0.281	0.000	0.000	0.173	100.000	0.019
670.240	0.318	0.000	0.001	8.522	0.281	0.000	0.000	0.159	100.000	0.020
727.140	0.293	0.000	0.001	8.987	0.309	0.000	0.000	0.147	100.000	0.022
791.020	0.270	0.000	0.001	9.347	0.309	0.000	0.000	0.135	100.000	0.024
859.980	0.248	0.000	0.001	9.720	0.309	0.000	0.000	0.124	100.000	0.026
935.260	0.228	0.000	0.001	10.184	0.337	0.000	0.000	0.114	100.000	0.028
1016.010	0.210	0.000	0.001	10.420	0.337	0.000	0.000	0.105	100.000	0.031
1105.560	0.193	0.000	0.001	11.035	0.365	0.000	0.000	0.097	100.000	0.033
1197.510	0.178	0.000	0.001	11.478	0.365	0.000	0.000	0.089	100.000	0.036
1304.720	0.164	0.000	0.001	12.238	0.393	0.962	0.962	0.082	99.038	0.039
1416.040	0.151	0.000	0.002	13.223	0.449	1.923	2.885	0.075	97.115	0.043
1539.880	0.139	0.000	0.002	14.318	0.477	0.962	3.846	0.069	96.154	0.047
1673.430	0.128	0.000	0.002	15.312	0.506	0.962	4.808	0.064	95.192	0.051
1817.370	0.117	0.000	0.002	16.223	0.534	0.962	5.769	0.059	94.231	0.055
1975.400	0.108	0.000	0.002	17.469	0.590	1.923	7.692	0.054	92.308	0.060
2148.830	0.099	0.000	0.002	18.778	0.618	0.962	8.654	0.050	91.346	0.065
2335.280	0.091	0.000	0.002	20.247	0.674	1.923	10.577	0.046	89.423	0.071
2537.650	0.084	0.000	0.003	21.366	0.702	0.962	11.538	0.042	88.462	0.077

Int Pres psia	Pore Dia microns	Inc Int mL/gm	Cum Int mL/gm	Cum Int %PV(bc)	Cum Int %BV	Inc Int %PV(ac)	Cum Int %PV(ac)	Pore Rad microns	W.P. Sat %PV(ac)	Lev "J" Funct.
2756.060	0.077	0.000	0.003	22.678	0.758	1.923	13.462	0.039	86.538	0.083
2997.800	0.071	0.000	0.003	23.945	0.786	0.962	14.423	0.036	85.577	0.091
3255.610	0.066	0.000	0.003	25.368	0.843	1.923	16.346	0.033	83.654	0.098
3540.050	0.060	0.000	0.003	26.489	0.871	0.962	17.308	0.030	82.692	0.107
3843.720	0.056	0.000	0.003	27.501	0.899	0.962	18.269	0.028	81.731	0.116
4173.320	0.051	0.000	0.003	28.466	0.927	0.962	19.231	0.026	80.769	0.126
4432.290	0.048	0.000	0.004	29.443	0.983	1.923	21.154	0.024	78.846	0.134
4834.020	0.044	0.000	0.004	30.768	1.011	0.962	22.115	0.022	77.885	0.146
5364.980	0.040	0.000	0.004	32.405	1.067	1.923	24.038	0.020	75.962	0.162
5830.590	0.037	0.000	0.004	33.740	1.123	1.923	25.962	0.018	74.038	0.176
6335.270	0.034	0.000	0.004	35.239	1.151	0.962	26.923	0.017	73.077	0.191
6881.750	0.031	0.000	0.004	36.966	1.208	1.923	28.846	0.016	71.154	0.208
7488.020	0.029	0.000	0.005	39.449	1.292	2.885	31.731	0.014	68.269	0.226
8126.800	0.026	0.000	0.005	41.180	1.348	1.923	33.654	0.013	66.346	0.246
8838.940	0.024	0.000	0.005	43.780	1.432	2.885	36.538	0.012	63.462	0.267
9609.810	0.022	0.000	0.006	46.687	1.545	3.846	40.385	0.011	59.615	0.290
10442.810	0.020	0.000	0.006	49.489	1.629	2.885	43.269	0.010	56.731	0.316
11343.960	0.019	0.000	0.006	52.095	1.713	2.885	46.154	0.009	53.846	0.343
12334.730	0.017	0.000	0.007	55.174	1.826	3.846	50.000	0.009	50.000	0.373
13410.010	0.016	0.000	0.007	58.677	1.938	3.846	53.846	0.008	46.154	0.405
14568.700	0.015	0.000	0.007	61.461	2.022	2.885	56.731	0.007	43.269	0.440
15826.010	0.014	0.000	0.008	63.824	2.106	2.885	59.615	0.007	40.385	0.478
17206.970	0.012	0.000	0.008	66.572	2.191	2.885	62.500	0.006	37.500	0.520
18706.650	0.011	0.000	0.008	69.642	2.303	3.846	66.346	0.006	33.654	0.565
20321.700	0.011	0.000	0.008	71.871	2.359	1.923	68.269	0.005	31.731	0.614
22091.310	0.010	0.000	0.009	74.054	2.443	2.885	71.154	0.005	28.846	0.668
24013.680	0.009	0.000	0.009	76.130	2.500	1.923	73.077	0.004	26.923	0.726
26098.680	0.008	0.000	0.009	78.388	2.584	2.885	75.962	0.004	24.038	0.789
28368.730	0.008	0.000	0.010	81.278	2.668	2.885	78.846	0.004	21.154	0.857
30828.110	0.007	0.000	0.010	83.029	2.752	2.885	81.731	0.003	18.269	0.932
33507.860	0.006	0.000	0.010	85.095	2.808	1.923	83.654	0.003	16.346	1.013
36413.840	0.006	0.000	0.010	87.404	2.893	2.885	86.538	0.003	13.462	1.101
39575.110	0.005	0.000	0.011	89.782	2.949	1.923	88.462	0.003	11.538	1.196
43009.470	0.005	0.000	0.011	91.923	3.033	2.885	91.346	0.003	8.654	1.300
46741.210	0.005	0.000	0.011	93.464	3.089	1.923	93.269	0.002	6.731	1.413
50799.300	0.004	0.000	0.011	96.436	3.174	2.885	96.154	0.002	3.846	1.535
55202.470	0.004	0.000	0.012	98.260	3.230	1.923	98.077	0.002	1.923	1.668
59987.550	0.004	0.000	0.012	100.000	3.286	1.923	100.000	0.002	0.000	1.813

6/10/10-15 Pore aperture vs. mercury saturation

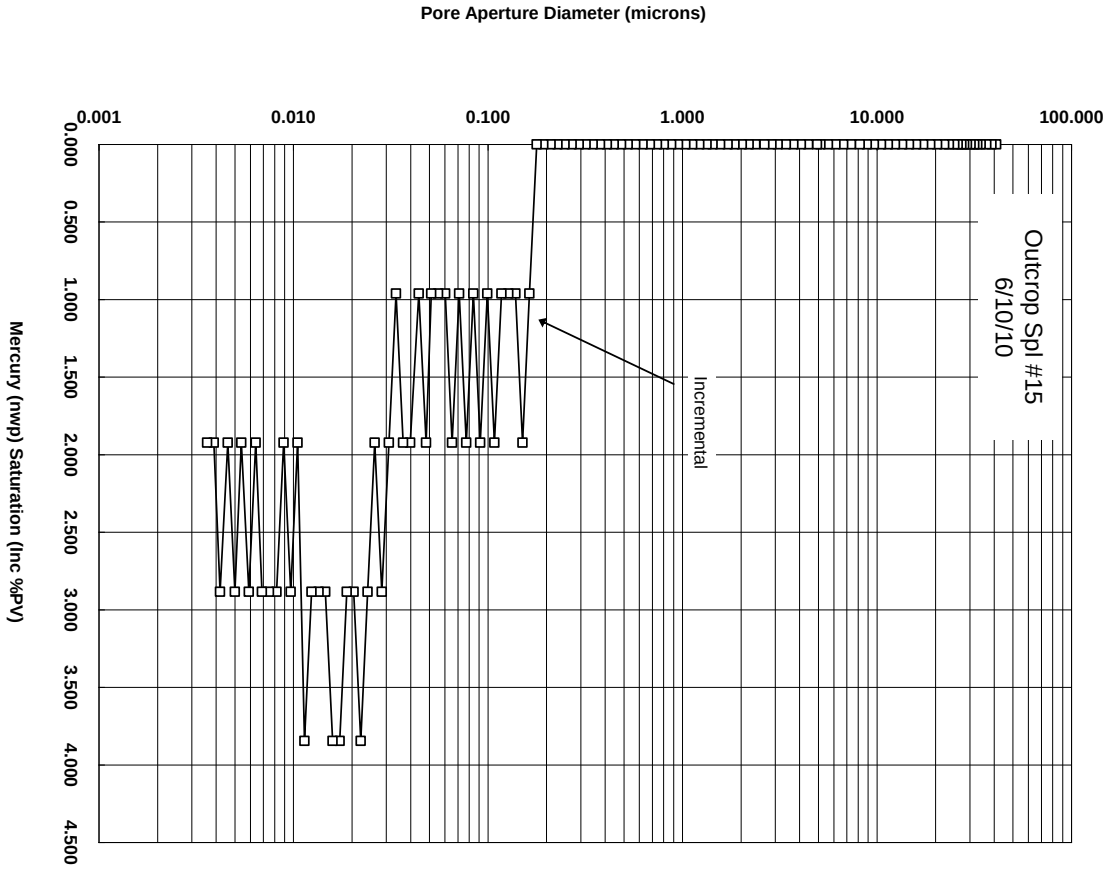

6/10/10-16 Data

Int Pres psia	Pore Dia microns	Inc Int mL/gm	Cum Int mL/gm	Cum Int %PV(bc)	Cum Int %BV	Inc Int %PV(ac)	Cum Int %PV(ac)	Pore Rad microns	W.P. Sat %PV(ac)	Lev "J" Funct.
5.190	41.088	0.000	0.000	0.077	0.000	0.000	0.000	20.544	100.000	0.000
5.490	38.847	0.000	0.000	0.193	0.000	0.000	0.000	19.424	100.000	0.000
5.840	36.533	0.000	0.000	0.231	0.000	0.000	0.000	18.267	100.000	0.000
6.240	34.184	0.000	0.000	0.424	0.026	0.000	0.000	17.092	100.000	0.000
6.490	32.867	0.000	0.000	0.540	0.026	0.000	0.000	16.434	100.000	0.000
6.740	31.648	0.000	0.000	0.540	0.026	0.000	0.000	15.824	100.000	0.000
7.040	30.301	0.000	0.000	0.617	0.026	0.000	0.000	15.151	100.000	0.000
7.340	29.063	0.000	0.000	0.694	0.026	0.000	0.000	14.531	100.000	0.000
7.590	28.106	0.000	0.000	0.732	0.026	0.000	0.000	14.053	100.000	0.000
7.840	27.214	0.000	0.000	0.809	0.051	0.000	0.000	13.607	100.000	0.000
8.190	26.044	0.000	0.000	0.925	0.051	0.000	0.000	13.022	100.000	0.000
8.540	24.982	0.000	0.000	1.002	0.051	0.000	0.000	12.491	100.000	0.000
9.080	23.491	0.000	0.000	1.118	0.051	0.000	0.000	11.745	100.000	0.000
9.610	22.191	0.000	0.000	1.156	0.051	0.000	0.000	11.096	100.000	0.000
10.440	20.428	0.000	0.000	1.349	0.077	0.000	0.000	10.214	100.000	0.000
11.350	18.795	0.000	0.000	1.503	0.077	0.000	0.000	9.398	100.000	0.001
12.340	17.293	0.000	0.000	1.657	0.077	0.000	0.000	8.646	100.000	0.001
13.410	15.910	0.000	0.000	1.773	0.102	0.000	0.000	7.955	100.000	0.001
14.570	14.639	0.000	0.000	1.888	0.102	0.000	0.000	7.320	100.000	0.001
15.840	13.470	0.000	0.000	2.004	0.102	0.000	0.000	6.735	100.000	0.001
17.220	12.392	0.000	0.000	2.158	0.102	0.000	0.000	6.196	100.000	0.001
18.710	11.402	0.000	0.001	2.274	0.128	0.000	0.000	5.701	100.000	0.001
20.330	10.493	0.000	0.001	2.428	0.128	0.000	0.000	5.246	100.000	0.001
22.100	9.653	0.000	0.001	2.582	0.128	0.000	0.000	4.826	100.000	0.001
24.020	8.882	0.000	0.001	2.698	0.128	0.000	0.000	4.441	100.000	0.001
26.110	8.172	0.000	0.001	2.852	0.154	0.000	0.000	4.086	100.000	0.001
28.980	7.362	0.000	0.001	3.083	0.154	0.000	0.000	3.681	100.000	0.001
31.750	6.718	0.000	0.001	3.314	0.179	0.000	0.000	3.359	100.000	0.001
34.780	6.134	0.000	0.001	3.430	0.179	0.000	0.000	3.067	100.000	0.002
38.080	5.602	0.000	0.001	3.545	0.179	0.000	0.000	2.801	100.000	0.002
41.580	5.131	0.000	0.001	3.700	0.179	0.000	0.000	2.565	100.000	0.002
43.860	4.864	0.000	0.001	3.714	0.179	0.000	0.000	2.432	100.000	0.002
47.770	4.465	0.000	0.001	3.714	0.179	0.000	0.000	2.233	100.000	0.002
52.470	4.065	0.000	0.001	3.902	0.205	0.000	0.000	2.033	100.000	0.002
56.880	3.750	0.000	0.001	4.004	0.205	0.000	0.000	1.875	100.000	0.003
62.250	3.427	0.000	0.001	4.166	0.205	0.000	0.000	1.713	100.000	0.003
68.370	3.120	0.000	0.001	4.323	0.230	0.000	0.000	1.560	100.000	0.003
77.280	2.761	0.000	0.001	4.625	0.230	0.000	0.000	1.380	100.000	0.004
81.710	2.611	0.000	0.001	4.625	0.230	0.000	0.000	1.305	100.000	0.004

Int Pres psia	Pore Dia microns	Inc Int mL/gm	Cum Int mL/gm	Cum Int %PV(bc)	Cum Int %BV	Inc Int %PV(ac)	Cum Int %PV(ac)	Pore Rad microns	W.P. Sat %PV(ac)	Lev "J" Funct.
89.000	2.397	0.000	0.001	4.630	0.230	0.000	0.000	1.198	100.000	0.004
97.080	2.197	0.000	0.001	4.650	0.230	0.000	0.000	1.099	100.000	0.005
107.290	1.988	0.000	0.001	4.716	0.230	0.000	0.000	0.994	100.000	0.005
115.940	1.840	0.000	0.001	4.943	0.256	0.000	0.000	0.920	100.000	0.005
126.630	1.685	0.000	0.001	4.943	0.256	0.000	0.000	0.842	100.000	0.006
137.200	1.555	0.000	0.001	5.000	0.256	0.000	0.000	0.777	100.000	0.006
148.080	1.441	0.000	0.001	5.107	0.256	0.000	0.000	0.720	100.000	0.007
162.650	1.312	0.000	0.001	5.353	0.282	0.000	0.000	0.656	100.000	0.008
175.630	1.215	0.000	0.001	5.518	0.282	0.000	0.000	0.607	100.000	0.008
189.850	1.124	0.000	0.001	5.537	0.282	0.000	0.000	0.562	100.000	0.009
206.230	1.034	0.000	0.001	5.734	0.307	0.000	0.000	0.517	100.000	0.010
225.860	0.945	0.000	0.001	5.945	0.307	0.000	0.000	0.472	100.000	0.011
245.300	0.870	0.000	0.001	5.965	0.307	0.000	0.000	0.435	100.000	0.011
264.730	0.806	0.000	0.001	5.997	0.307	0.000	0.000	0.403	100.000	0.012
289.820	0.736	0.000	0.001	6.047	0.307	0.000	0.000	0.368	100.000	0.013
314.680	0.678	0.000	0.001	6.047	0.307	0.000	0.000	0.339	100.000	0.015
342.250	0.623	0.000	0.001	6.264	0.333	0.000	0.000	0.312	100.000	0.016
370.820	0.575	0.000	0.001	6.478	0.333	0.000	0.000	0.288	100.000	0.017
405.530	0.526	0.000	0.001	6.700	0.333	0.000	0.000	0.263	100.000	0.019
440.690	0.484	0.000	0.001	6.929	0.359	0.000	0.000	0.242	100.000	0.021
478.370	0.446	0.000	0.002	7.341	0.384	0.000	0.000	0.223	100.000	0.022
518.950	0.411	0.000	0.002	7.401	0.384	0.000	0.000	0.206	100.000	0.024
565.950	0.377	0.000	0.002	7.445	0.384	0.000	0.000	0.188	100.000	0.026
615.360	0.347	0.000	0.002	7.913	0.410	0.000	0.000	0.173	100.000	0.029
667.760	0.320	0.000	0.002	8.296	0.435	0.000	0.000	0.160	100.000	0.031
727.530	0.293	0.000	0.002	8.745	0.461	0.000	0.000	0.147	100.000	0.034
790.010	0.270	0.000	0.002	8.812	0.461	0.000	0.000	0.135	100.000	0.037
860.770	0.248	0.000	0.002	9.240	0.487	0.000	0.000	0.124	100.000	0.040
932.880	0.229	0.000	0.002	9.677	0.487	0.000	0.000	0.114	100.000	0.043
1014.850	0.210	0.000	0.002	10.110	0.512	0.000	0.000	0.105	100.000	0.047
1104.500	0.193	0.000	0.002	10.185	0.512	0.000	0.000	0.097	100.000	0.051
1200.730	0.178	0.000	0.002	10.686	0.538	0.000	0.000	0.089	100.000	0.056
1303.090	0.164	0.000	0.002	11.172	0.563	0.000	0.000	0.082	100.000	0.061
1415.120	0.151	0.000	0.002	11.552	0.589	0.000	0.000	0.075	100.000	0.066
1539.870	0.139	0.000	0.002	11.870	0.615	0.000	0.000	0.069	100.000	0.072
1673.390	0.128	0.000	0.003	12.333	0.640	0.000	0.000	0.064	100.000	0.078
1816.820	0.117	0.000	0.003	12.800	0.666	0.000	0.000	0.059	100.000	0.085
1976.700	0.108	0.000	0.003	13.153	0.666	0.000	0.000	0.054	100.000	0.092
2149.450	0.099	0.000	0.003	13.959	0.717	0.000	0.000	0.050	100.000	0.100
2335.620	0.091	0.000	0.003	14.331	0.743	0.000	0.000	0.046	100.000	0.109
2537.100	0.084	0.000	0.003	15.078	0.768	0.000	0.000	0.042	100.000	0.118

Int Pres psia	Pore Dia microns	Inc Int mL/gm	Cum Int mL/gm	Cum Int %PV(bc)	Cum Int %BV	Inc Int %PV(ac)	Cum Int %PV(ac)	Pore Rad microns	W.P. Sat %PV(ac)	Lev "J" Funct.
2757.540	0.077	0.000	0.003	15.707	0.794	0.000	0.000	0.039	100.000	0.128
2996.130	0.071	0.000	0.003	16.749	0.871	1.765	1.765	0.036	98.235	0.139
3257.450	0.066	0.000	0.004	17.775	0.922	1.176	2.941	0.033	97.059	0.152
3537.540	0.060	0.000	0.004	18.325	0.973	1.176	4.118	0.030	95.882	0.165
3847.830	0.055	0.000	0.004	19.844	1.050	1.765	5.882	0.028	94.118	0.179
4184.710	0.051	0.000	0.004	21.963	1.127	1.765	7.647	0.026	92.353	0.195
4432.250	0.048	0.000	0.005	23.100	1.229	2.353	10.000	0.024	90.000	0.206
4836.630	0.044	0.001	0.005	26.750	1.357	2.941	12.941	0.022	87.059	0.225
5363.170	0.040	0.001	0.006	29.462	1.485	2.941	15.882	0.020	84.118	0.250
5828.840	0.037	0.001	0.006	32.203	1.639	3.529	19.412	0.018	80.588	0.271
6337.260	0.034	0.001	0.007	36.600	1.844	4.706	24.118	0.017	75.882	0.295
6885.840	0.031	0.001	0.008	40.987	2.074	5.294	29.412	0.016	70.588	0.321
7487.870	0.029	0.001	0.009	49.467	2.407	7.647	37.059	0.014	62.941	0.349
8136.990	0.026	0.002	0.011	55.720	2.843	10.000	47.059	0.013	52.941	0.379
8844.730	0.024	0.002	0.013	68.872	3.253	9.412	56.471	0.012	43.529	0.412
9596.830	0.022	0.002	0.014	71.396	3.637	8.824	65.294	0.011	34.706	0.447
10447.100	0.020	0.001	0.016	78.413	3.995	8.235	73.529	0.010	26.471	0.486
11354.520	0.019	0.001	0.017	86.627	4.303	7.059	80.588	0.009	19.412	0.529
12338.780	0.017	0.001	0.018	90.098	4.559	5.882	86.471	0.009	13.529	0.574
13398.600	0.016	0.001	0.019	91.087	4.738	4.118	90.588	0.008	9.412	0.624
14572.490	0.015	0.000	0.019	94.368	4.840	2.353	92.941	0.007	7.059	0.678
15840.840	0.014	0.000	0.019	95.308	4.892	1.176	94.118	0.007	5.882	0.737
17215.510	0.012	0.000	0.019	96.085	4.943	1.176	95.294	0.006	4.706	0.801
18710.070	0.011	0.000	0.020	97.260	4.994	1.176	96.471	0.006	3.529	0.871
20322.740	0.011	0.000	0.020	97.476	5.045	1.176	97.647	0.005	2.353	0.946
22099.470	0.010	0.000	0.020	98.971	5.096	1.176	98.824	0.005	1.176	1.029
24017.430	0.009	0.000	0.020	99.329	5.122	0.588	99.412	0.004	0.588	1.118
26103.240	0.008	0.000	0.020	99.921	5.148	0.588	100.000	0.004	0.000	1.215
28367.440	0.008	0.000	0.020	99.929	5.148	0.000	100.000	0.004	0.000	1.321
30830.580	0.007	0.000	0.020	100.000	5.148	0.000	100.000	0.003	0.000	1.435
33506.220	0.006	0.000	0.020	100.000	5.148	0.000	100.000	0.003	0.000	1.560
36413.560	0.006	0.000	0.020	100.000	5.148	0.000	100.000	0.003	0.000	1.695
39575.570	0.005	0.000	0.020	100.000	5.148	0.000	100.000	0.003	0.000	1.842
43010.550	0.005	0.000	0.020	100.000	5.148	0.000	100.000	0.003	0.000	2.002
46742.650	0.005	0.000	0.020	100.000	5.148	0.000	100.000	0.002	0.000	2.176
50797.540	0.004	0.000	0.020	100.000	5.148	0.000	100.000	0.002	0.000	2.365
55205.160	0.004	0.000	0.020	100.000	5.148	0.000	100.000	0.002	0.000	2.570
59989.260	0.004	0.000	0.020	100.000	5.148	0.000	100.000	0.002	0.000	2.793

6/10/10-16 Pore aperture vs. mercury saturation

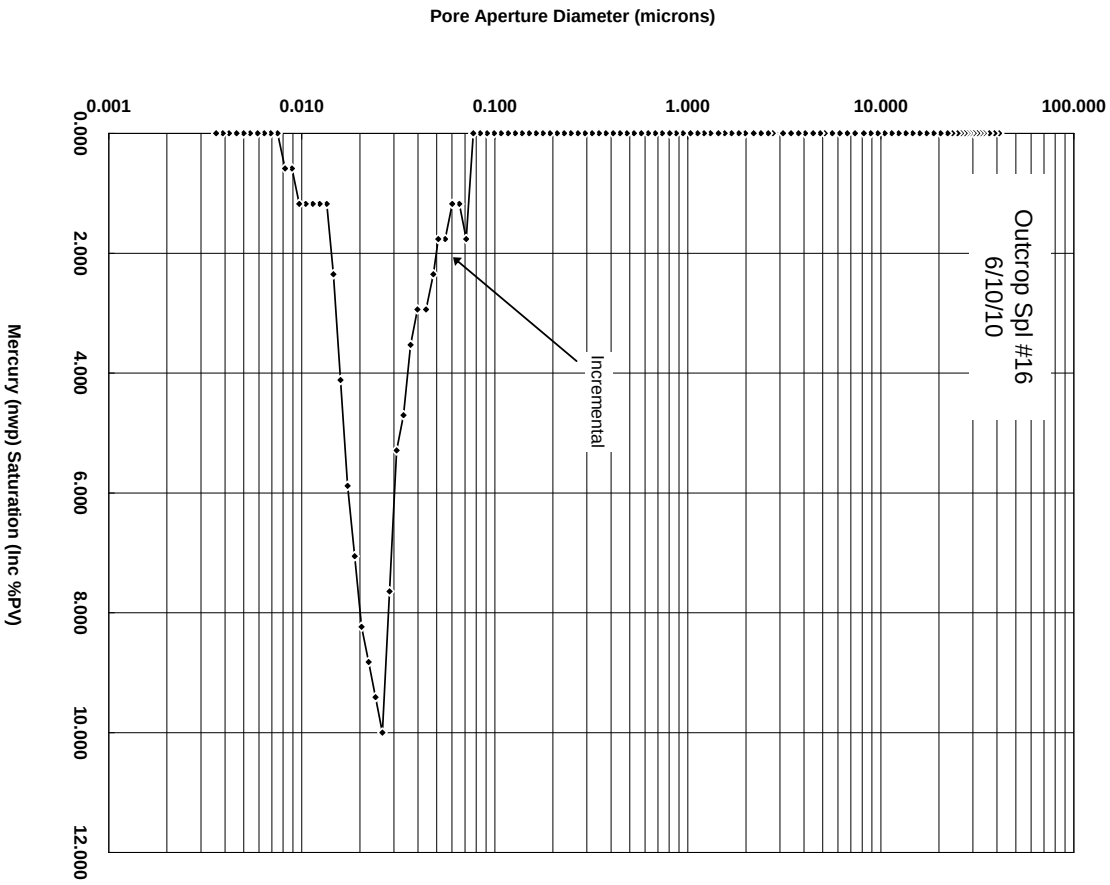

6/10/10-17 Data

Int Pres psia	Pore Dia microns	Inc Int mL/gm	Cum Int mL/gm	Cum Int %PV(bc)	Cum Int %BV	Inc Int %PV(ac)	Cum Int %PV(ac)	Pore Rad microns	W.P. Sat %PV(ac)	Lev "J" Funct.
5.190	41.087	0.000	0.000	0.197	0.000	0.000	0.000	20.544	100.000	0.000
5.490	38.858	0.000	0.000	0.525	0.000	0.000	0.000	19.429	100.000	0.000
5.840	36.521	0.000	0.000	0.853	0.000	0.000	0.000	18.261	100.000	0.000
6.240	34.189	0.000	0.000	1.575	0.027	0.000	0.000	17.095	100.000	0.000
6.490	32.873	0.000	0.000	1.838	0.027	0.000	0.000	16.437	100.000	0.000
6.740	31.641	0.000	0.000	2.363	0.027	0.000	0.000	15.820	100.000	0.000
7.040	30.300	0.000	0.000	2.691	0.027	0.000	0.000	15.150	100.000	0.000
7.340	29.063	0.000	0.000	2.888	0.054	0.000	0.000	14.532	100.000	0.000
7.590	28.094	0.000	0.000	3.216	0.054	0.000	0.000	14.047	100.000	0.000
7.840	27.211	0.000	0.000	3.282	0.054	0.000	0.000	13.606	100.000	0.000
8.190	26.042	0.000	0.000	3.741	0.054	0.000	0.000	13.021	100.000	0.000
8.540	24.979	0.000	0.000	4.069	0.054	0.000	0.000	12.489	100.000	0.000
9.080	23.494	0.000	0.000	4.266	0.054	0.000	0.000	11.747	100.000	0.000
9.610	22.195	0.000	0.000	5.054	0.080	0.000	0.000	11.097	100.000	0.000
10.440	20.428	0.000	0.000	5.579	0.080	0.000	0.000	10.214	100.000	0.000
11.350	18.796	0.000	0.000	5.973	0.080	0.000	0.000	9.398	100.000	0.000
12.340	17.292	0.000	0.000	6.432	0.107	0.000	0.000	8.646	100.000	0.000
13.410	15.909	0.000	0.000	6.892	0.107	0.000	0.000	7.955	100.000	0.000
14.570	14.639	0.000	0.000	7.417	0.107	0.000	0.000	7.319	100.000	0.000
15.840	13.470	0.000	0.001	8.401	0.134	0.000	0.000	6.735	100.000	0.000
17.210	12.393	0.000	0.001	8.927	0.134	0.000	0.000	6.196	100.000	0.000
18.710	11.402	0.000	0.001	10.371	0.161	0.000	0.000	5.701	100.000	0.000
20.330	10.491	0.000	0.001	10.896	0.161	0.000	0.000	5.246	100.000	0.000
22.100	9.653	0.000	0.001	11.355	0.161	0.000	0.000	4.826	100.000	0.000
24.020	8.882	0.000	0.001	11.946	0.187	0.000	0.000	4.441	100.000	0.000
26.100	8.172	0.000	0.001	12.340	0.187	0.000	0.000	4.086	100.000	0.000
28.980	7.362	0.000	0.001	12.996	0.187	0.000	0.000	3.681	100.000	0.000
31.750	6.718	0.000	0.001	13.521	0.187	0.000	0.000	3.359	100.000	0.000
34.780	6.134	0.000	0.001	14.440	0.214	0.000	0.000	3.067	100.000	0.000
38.080	5.603	0.000	0.001	14.899	0.214	0.000	0.000	2.801	100.000	0.000
41.580	5.131	0.000	0.001	15.424	0.214	0.000	0.000	2.565	100.000	0.000
43.070	4.954	0.000	0.001	15.518	0.214	0.000	0.000	2.477	100.000	0.000
46.830	4.555	0.000	0.001	15.847	0.241	0.000	0.000	2.277	100.000	0.000
51.940	4.108	0.000	0.001	15.904	0.241	0.000	0.000	2.054	100.000	0.001
56.130	3.800	0.000	0.001	16.416	0.241	0.000	0.000	1.900	100.000	0.001
65.290	3.267	0.000	0.001	17.459	0.268	0.000	0.000	1.634	100.000	0.001
69.200	3.083	0.000	0.001	17.833	0.268	0.000	0.000	1.541	100.000	0.001
74.930	2.847	0.000	0.001	17.972	0.268	0.000	0.000	1.424	100.000	0.001
81.990	2.602	0.000	0.001	18.460	0.268	0.000	0.000	1.301	100.000	0.001

Int Pres psia	Pore Dia microns	Inc Int mL/gm	Cum Int mL/gm	Cum Int %PV(bc)	Cum Int %BV	Inc Int %PV(ac)	Cum Int %PV(ac)	Pore Rad microns	W.P. Sat %PV(ac)	Lev "J" Funct.
92.040	2.318	0.000	0.001	19.450	0.294	0.000	0.000	1.159	100.000	0.001
96.950	2.200	0.000	0.001	19.535	0.294	0.000	0.000	1.100	100.000	0.001
106.300	2.007	0.000	0.001	20.135	0.294	0.000	0.000	1.003	100.000	0.001
114.640	1.861	0.000	0.001	20.305	0.294	0.000	0.000	0.930	100.000	0.001
125.580	1.699	0.000	0.001	20.330	0.294	0.000	0.000	0.849	100.000	0.001
136.290	1.565	0.000	0.001	20.330	0.294	0.000	0.000	0.783	100.000	0.001
148.460	1.437	0.000	0.001	20.867	0.294	0.000	0.000	0.718	100.000	0.002
161.430	1.321	0.000	0.001	21.385	0.321	0.000	0.000	0.661	100.000	0.002
174.850	1.220	0.000	0.001	21.736	0.321	0.000	0.000	0.610	100.000	0.002
190.280	1.121	0.000	0.001	22.561	0.321	0.000	0.000	0.561	100.000	0.002
206.610	1.033	0.000	0.001	22.658	0.321	0.000	0.000	0.516	100.000	0.002
225.470	0.946	0.000	0.001	22.781	0.321	0.000	0.000	0.473	100.000	0.002
243.420	0.876	0.000	0.001	23.450	0.348	0.000	0.000	0.438	100.000	0.002
265.710	0.803	0.000	0.001	23.670	0.348	0.000	0.000	0.401	100.000	0.003
288.800	0.739	0.000	0.001	24.176	0.348	0.000	0.000	0.369	100.000	0.003
314.730	0.678	0.000	0.001	24.826	0.375	0.000	0.000	0.339	100.000	0.003
341.000	0.626	0.000	0.001	24.999	0.375	0.000	0.000	0.313	100.000	0.003
371.460	0.574	0.000	0.001	25.035	0.375	0.000	0.000	0.287	100.000	0.004
404.800	0.527	0.000	0.001	25.877	0.375	0.000	0.000	0.264	100.000	0.004
439.330	0.486	0.000	0.002	26.605	0.401	0.000	0.000	0.243	100.000	0.004
476.180	0.448	0.000	0.002	27.377	0.401	0.000	0.000	0.224	100.000	0.005
519.540	0.411	0.000	0.002	27.391	0.401	0.000	0.000	0.205	100.000	0.005
563.750	0.378	0.000	0.002	27.767	0.401	0.000	0.000	0.189	100.000	0.006
615.110	0.347	0.000	0.002	28.519	0.428	0.000	0.000	0.173	100.000	0.006
669.110	0.319	0.000	0.002	29.349	0.428	0.000	0.000	0.159	100.000	0.007
724.770	0.294	0.000	0.002	29.728	0.428	0.000	0.000	0.147	100.000	0.007
788.570	0.271	0.000	0.002	29.728	0.428	0.000	0.000	0.135	100.000	0.008
860.910	0.248	0.000	0.002	29.880	0.428	0.000	0.000	0.124	100.000	0.009
933.480	0.229	0.000	0.002	30.674	0.455	0.000	0.000	0.114	100.000	0.010
1016.340	0.210	0.000	0.002	31.195	0.455	0.000	0.000	0.105	100.000	0.010
1102.330	0.194	0.000	0.002	31.796	0.455	0.000	0.000	0.097	100.000	0.011
1200.150	0.178	0.000	0.002	32.055	0.455	0.000	0.000	0.089	100.000	0.012
1302.060	0.164	0.000	0.002	32.089	0.482	0.000	0.000	0.082	100.000	0.013
1416.280	0.151	0.000	0.002	32.111	0.482	0.000	0.000	0.075	100.000	0.014
1537.860	0.139	0.000	0.002	32.893	0.482	0.000	0.000	0.069	100.000	0.016
1672.570	0.128	0.000	0.002	33.426	0.482	0.000	0.000	0.064	100.000	0.017
1817.270	0.117	0.000	0.002	34.258	0.508	0.000	0.000	0.059	100.000	0.019
1974.990	0.108	0.000	0.002	34.396	0.508	0.000	0.000	0.054	100.000	0.020
2147.050	0.099	0.000	0.002	34.700	0.508	0.000	0.000	0.050	100.000	0.022
2334.150	0.091	0.000	0.002	35.496	0.508	0.000	0.000	0.046	100.000	0.024
2535.400	0.084	0.000	0.002	36.294	0.535	0.000	0.000	0.042	100.000	0.026

Int Pres psia	Pore Dia microns	Inc Int mL/gm	Cum Int mL/gm	Cum Int %PV(bc)	Cum Int %BV	Inc Int %PV(ac)	Cum Int %PV(ac)	Pore Rad microns	W.P. Sat %PV(ac)	Lev "J" Funct.
2754.480	0.077	0.000	0.002	36.761	0.535	0.000	0.000	0.039	100.000	0.028
2994.500	0.071	0.000	0.002	36.934	0.535	0.000	0.000	0.036	100.000	0.031
3254.650	0.066	0.000	0.002	37.607	0.562	0.000	0.000	0.033	100.000	0.033
3536.440	0.060	0.000	0.002	38.087	0.562	0.000	0.000	0.030	100.000	0.036
3843.090	0.056	0.000	0.002	38.869	0.562	0.000	0.000	0.028	100.000	0.039
4174.010	0.051	0.000	0.002	39.137	0.562	0.000	0.000	0.026	100.000	0.043
4430.790	0.048	0.000	0.002	40.123	0.589	0.000	0.000	0.024	100.000	0.045
4834.540	0.044	0.000	0.002	41.556	0.616	0.000	0.000	0.022	100.000	0.049
5354.490	0.040	0.000	0.002	41.599	0.616	0.000	0.000	0.020	100.000	0.055
5819.610	0.037	0.000	0.002	42.798	0.616	0.000	0.000	0.018	100.000	0.059
6323.970	0.034	0.000	0.002	44.082	0.642	0.000	0.000	0.017	100.000	0.065
6873.310	0.031	0.000	0.002	44.594	0.642	0.000	0.000	0.016	100.000	0.070
7474.090	0.029	0.000	0.003	44.929	0.669	0.000	0.000	0.014	100.000	0.076
8123.400	0.026	0.000	0.003	45.079	0.669	0.000	0.000	0.013	100.000	0.083
8830.480	0.024	0.000	0.003	45.916	0.669	0.000	0.000	0.012	100.000	0.090
9596.900	0.022	0.000	0.003	46.470	0.669	0.000	0.000	0.011	100.000	0.098
10430.670	0.021	0.000	0.003	46.470	0.669	0.000	0.000	0.010	100.000	0.107
11341.080	0.019	0.000	0.003	46.552	0.669	0.000	0.000	0.009	100.000	0.116
12330.740	0.017	0.000	0.003	46.955	0.696	0.000	0.000	0.009	100.000	0.126
13401.140	0.016	0.000	0.003	47.273	0.696	0.000	0.000	0.008	100.000	0.137
14566.460	0.015	0.000	0.003	50.909	0.749	6.897	6.897	0.007	93.103	0.149
15839.180	0.014	0.000	0.003	56.364	0.830	10.345	17.241	0.007	82.759	0.162
17210.140	0.012	0.000	0.003	60.000	0.883	6.897	24.138	0.006	75.862	0.176
18708.590	0.011	0.000	0.004	63.636	0.937	6.897	31.034	0.006	68.966	0.191
20331.450	0.011	0.000	0.004	69.091	1.017	10.345	41.379	0.005	58.621	0.208
22090.990	0.010	0.000	0.004	72.727	1.070	6.897	48.276	0.005	51.724	0.226
24012.880	0.009	0.000	0.004	76.364	1.124	6.897	55.172	0.004	44.828	0.245
26101.410	0.008	0.000	0.004	80.000	1.178	6.897	62.069	0.004	37.931	0.267
28364.890	0.008	0.000	0.005	83.636	1.231	6.897	68.966	0.004	31.034	0.290
30831.850	0.007	0.000	0.005	85.455	1.258	3.448	72.414	0.003	27.586	0.315
33503.830	0.006	0.000	0.005	87.273	1.285	3.448	75.862	0.003	24.138	0.342
36414.560	0.006	0.000	0.005	89.091	1.311	3.448	79.310	0.003	20.690	0.372
39574.320	0.005	0.000	0.005	92.727	1.365	6.897	86.207	0.003	13.793	0.404
43010.230	0.005	0.000	0.005	94.545	1.392	3.448	89.655	0.003	10.345	0.440
46742.040	0.005	0.000	0.005	98.182	1.445	6.897	96.552	0.002	3.448	0.478
50796.180	0.004	0.000	0.005	98.182	1.445	0.000	96.552	0.002	3.448	0.519
55204.450	0.004	0.000	0.006	100.000	1.472	3.448	100.000	0.002	0.000	0.564
59990.070	0.004	0.000	0.006	100.000	1.472	0.000	100.000	0.002	0.000	0.613

6/10/10-17 Pore aperture vs. mercury saturation

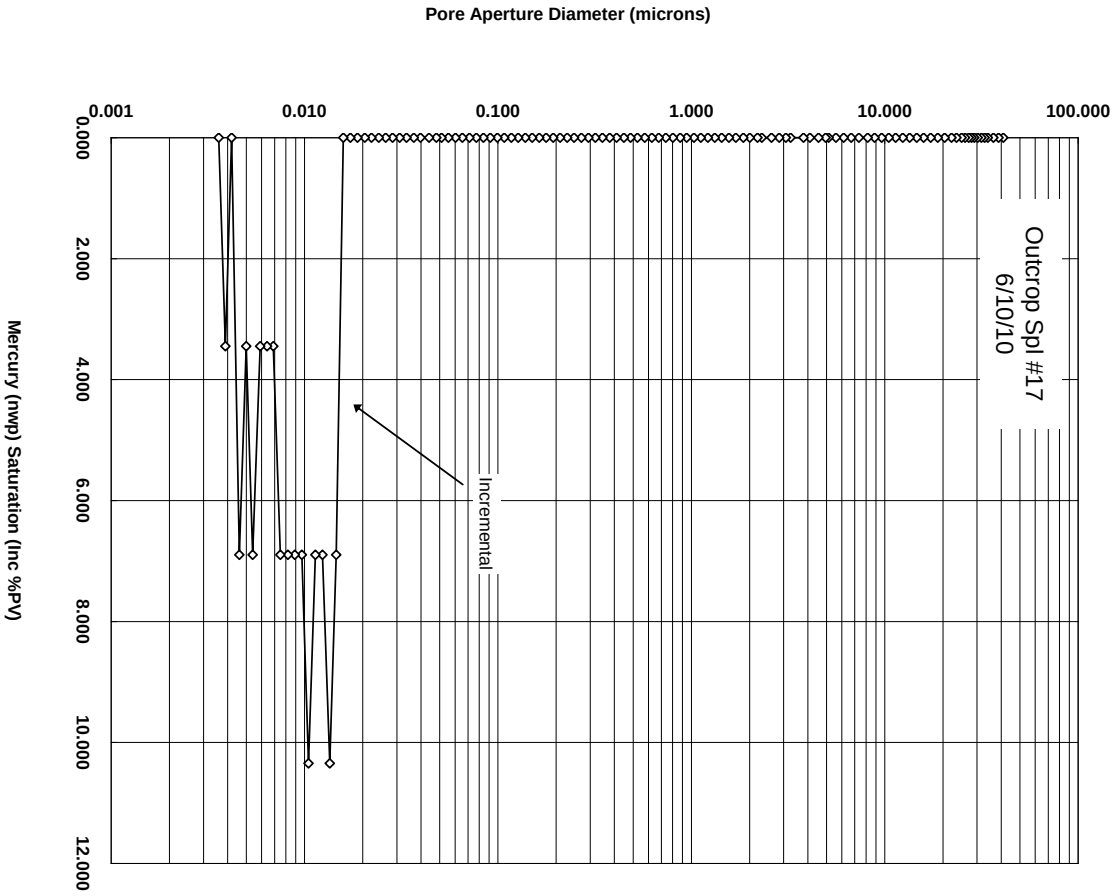

6/10/10-18 Data

Int Pres psia	Pore Dia microns	Inc Int mL/gm	Cum Int mL/gm	Cum Int %PV(bc)	Cum Int %BV	Inc Int %PV(ac)	Cum Int %PV(ac)	Pore Rad microns	W.P. Sat %PV(ac)	Lev "J" Funct.
5.190	41.097	0.000	0.000	0.216	0.000	0.000	0.000	20.548	100.000	0.000
5.490	38.867	0.000	0.000	0.444	0.027	0.000	0.000	19.434	100.000	0.000
5.840	36.520	0.000	0.000	0.719	0.055	0.000	0.000	18.260	100.000	0.000
6.240	34.184	0.000	0.000	0.935	0.055	0.000	0.000	17.092	100.000	0.000
6.490	32.865	0.000	0.000	1.079	0.055	0.000	0.000	16.432	100.000	0.000
6.740	31.646	0.000	0.000	1.187	0.082	0.000	0.000	15.823	100.000	0.000
7.040	30.301	0.000	0.000	1.343	0.082	0.000	0.000	15.151	100.000	0.000
7.340	29.066	0.000	0.000	1.474	0.082	0.000	0.000	14.533	100.000	0.000
7.590	28.108	0.000	0.000	1.582	0.110	0.000	0.000	14.054	100.000	0.000
7.840	27.202	0.000	0.000	1.678	0.110	0.000	0.000	13.601	100.000	0.000
8.190	26.043	0.000	0.000	1.786	0.110	0.000	0.000	13.021	100.000	0.000
8.540	24.973	0.000	0.000	1.906	0.110	0.000	0.000	12.487	100.000	0.000
9.080	23.492	0.000	0.001	2.074	0.137	0.000	0.000	11.746	100.000	0.000
9.610	22.196	0.000	0.001	2.206	0.137	0.000	0.000	11.098	100.000	0.000
10.440	20.430	0.000	0.001	2.601	0.165	0.000	0.000	10.215	100.000	0.000
11.350	18.797	0.000	0.001	3.548	0.220	0.000	0.000	9.399	100.000	0.000
12.340	17.292	0.000	0.001	3.788	0.247	0.000	0.000	8.646	100.000	0.000
13.410	15.912	0.000	0.001	3.992	0.247	0.000	0.000	7.956	100.000	0.000
14.570	14.638	0.000	0.001	4.303	0.275	0.000	0.000	7.319	100.000	0.000
15.840	13.469	0.000	0.001	4.519	0.275	0.000	0.000	6.734	100.000	0.000
17.210	12.392	0.000	0.001	4.759	0.302	0.000	0.000	6.196	100.000	0.000
18.710	11.400	0.000	0.001	4.939	0.302	0.000	0.000	5.700	100.000	0.000
20.330	10.492	0.000	0.001	5.286	0.330	0.000	0.000	5.246	100.000	0.000
22.100	9.653	0.000	0.001	5.478	0.330	0.000	0.000	4.826	100.000	0.000
24.020	8.881	0.000	0.001	5.670	0.357	0.000	0.000	4.441	100.000	0.000
26.110	8.171	0.000	0.001	5.898	0.357	0.000	0.000	4.086	100.000	0.000
28.980	7.362	0.000	0.002	6.545	0.412	0.000	0.000	3.681	100.000	0.001
31.760	6.717	0.000	0.002	6.809	0.412	0.000	0.000	3.359	100.000	0.001
34.780	6.134	0.000	0.002	7.121	0.440	0.000	0.000	3.067	100.000	0.001
38.080	5.602	0.000	0.002	7.408	0.467	0.000	0.000	2.801	100.000	0.001
41.580	5.131	0.000	0.002	7.636	0.467	0.000	0.000	2.565	100.000	0.001
43.170	4.942	0.000	0.002	7.667	0.467	0.000	0.000	2.471	100.000	0.001
47.480	4.493	0.000	0.002	7.855	0.495	0.000	0.000	2.247	100.000	0.001
52.130	4.092	0.000	0.002	7.855	0.495	0.000	0.000	2.046	100.000	0.001
57.150	3.733	0.000	0.002	7.937	0.495	0.000	0.000	1.866	100.000	0.001
63.940	3.336	0.000	0.002	8.099	0.495	0.000	0.000	1.668	100.000	0.001
67.800	3.146	0.000	0.002	8.122	0.495	0.000	0.000	1.573	100.000	0.001
75.020	2.844	0.000	0.002	8.122	0.495	0.000	0.000	1.422	100.000	0.001
82.500	2.586	0.000	0.002	8.265	0.522	0.000	0.000	1.293	100.000	0.001

Int Pres psia	Pore Dia microns	Inc Int mL/gm	Cum Int mL/gm	Cum Int %PV(bc)	Cum Int %BV	Inc Int %PV(ac)	Cum Int %PV(ac)	Pore Rad microns	W.P. Sat %PV(ac)	Lev "J" Funct.
89.800	2.376	0.000	0.002	8.341	0.522	0.000	0.000	1.188	100.000	0.002
98.870	2.158	0.000	0.002	8.370	0.522	0.000	0.000	1.079	100.000	0.002
106.390	2.005	0.000	0.002	8.373	0.522	0.000	0.000	1.003	100.000	0.002
116.290	1.835	0.000	0.002	8.407	0.522	0.000	0.000	0.917	100.000	0.002
124.910	1.708	0.000	0.002	8.407	0.522	0.000	0.000	0.854	100.000	0.002
137.030	1.557	0.000	0.002	8.481	0.522	0.000	0.000	0.778	100.000	0.002
148.320	1.438	0.000	0.002	8.500	0.522	0.000	0.000	0.719	100.000	0.003
160.250	1.331	0.000	0.002	8.646	0.522	0.000	0.000	0.666	100.000	0.003
175.790	1.214	0.000	0.002	8.711	0.550	0.000	0.000	0.607	100.000	0.003
190.400	1.120	0.000	0.002	8.804	0.550	0.000	0.000	0.560	100.000	0.003
208.640	1.023	0.000	0.002	9.221	0.577	0.000	0.000	0.511	100.000	0.004
225.930	0.944	0.000	0.002	9.525	0.577	0.000	0.000	0.472	100.000	0.004
245.350	0.870	0.000	0.002	9.612	0.605	0.000	0.000	0.435	100.000	0.004
265.960	0.802	0.000	0.002	9.681	0.605	0.000	0.000	0.401	100.000	0.005
289.160	0.738	0.000	0.002	10.043	0.632	0.000	0.000	0.369	100.000	0.005
315.790	0.676	0.000	0.002	10.122	0.632	0.000	0.000	0.338	100.000	0.005
341.500	0.625	0.000	0.002	10.481	0.660	0.000	0.000	0.312	100.000	0.006
370.840	0.575	0.000	0.002	10.560	0.660	0.000	0.000	0.288	100.000	0.006
404.600	0.527	0.000	0.003	10.949	0.687	0.000	0.000	0.264	100.000	0.007
439.980	0.485	0.000	0.003	10.995	0.687	0.000	0.000	0.242	100.000	0.008
479.340	0.445	0.000	0.003	11.367	0.715	0.000	0.000	0.223	100.000	0.008
519.940	0.410	0.000	0.003	11.733	0.715	0.000	0.000	0.205	100.000	0.009
566.080	0.377	0.000	0.003	11.853	0.742	0.000	0.000	0.188	100.000	0.010
613.270	0.348	0.000	0.003	12.231	0.770	0.000	0.000	0.174	100.000	0.011
667.680	0.320	0.000	0.003	12.629	0.770	0.000	0.000	0.160	100.000	0.012
727.500	0.293	0.000	0.003	13.112	0.825	0.000	0.000	0.147	100.000	0.013
789.700	0.270	0.000	0.003	13.521	0.825	0.000	0.000	0.135	100.000	0.014
857.750	0.249	0.000	0.003	13.949	0.852	0.000	0.000	0.124	100.000	0.015
933.280	0.229	0.000	0.003	14.295	0.880	0.000	0.000	0.114	100.000	0.016
1015.650	0.210	0.000	0.003	14.374	0.880	0.000	0.000	0.105	100.000	0.018
1103.660	0.193	0.000	0.003	14.410	0.880	0.000	0.000	0.097	100.000	0.019
1199.000	0.178	0.000	0.003	14.486	0.907	0.000	0.000	0.089	100.000	0.021
1302.440	0.164	0.000	0.003	14.692	0.907	0.000	0.000	0.082	100.000	0.023
1416.300	0.151	0.000	0.003	14.800	0.907	0.000	0.000	0.075	100.000	0.024
1538.090	0.139	0.000	0.003	14.849	0.907	0.000	0.000	0.069	100.000	0.027
1671.490	0.128	0.000	0.003	15.151	0.935	0.000	0.000	0.064	100.000	0.029
1817.940	0.117	0.000	0.003	15.259	0.935	0.000	0.000	0.059	100.000	0.031
1977.550	0.108	0.000	0.004	15.600	0.962	0.000	0.000	0.054	100.000	0.034
2147.760	0.099	0.000	0.004	15.719	0.962	0.000	0.000	0.050	100.000	0.037
2334.790	0.091	0.000	0.004	16.027	0.990	0.000	0.000	0.046	100.000	0.040
2536.200	0.084	0.000	0.004	16.175	0.990	0.000	0.000	0.042	100.000	0.044

Int Pres psia	Pore Dia microns	Inc Int mL/gm	Cum Int mL/gm	Cum Int %PV(bc)	Cum Int %BV	Inc Int %PV(ac)	Cum Int %PV(ac)	Pore Rad microns	W.P. Sat %PV(ac)	Lev "J" Funct.
2757.560	0.077	0.000	0.004	16.501	1.017	0.000	0.000	0.039	100.000	0.048
2995.360	0.071	0.000	0.004	16.561	1.017	0.000	0.000	0.036	100.000	0.052
3253.060	0.066	0.000	0.004	16.960	1.045	0.000	0.000	0.033	100.000	0.056
3540.950	0.060	0.000	0.004	17.342	1.072	0.000	0.000	0.030	100.000	0.061
3843.650	0.056	0.000	0.004	17.537	1.100	0.000	0.000	0.028	100.000	0.066
4176.950	0.051	0.000	0.004	17.858	1.100	0.000	0.000	0.026	100.000	0.072
4429.560	0.048	0.000	0.004	18.225	1.127	0.000	0.000	0.024	100.000	0.077
4836.610	0.044	0.000	0.004	18.668	1.155	0.000	0.000	0.022	100.000	0.084
5361.230	0.040	0.000	0.004	19.141	1.182	0.000	0.000	0.020	100.000	0.093
5819.200	0.037	0.000	0.004	19.514	1.210	0.000	0.000	0.018	100.000	0.101
6336.000	0.034	0.000	0.005	20.040	1.237	0.000	0.000	0.017	100.000	0.110
6878.270	0.031	0.000	0.005	20.293	1.265	0.000	0.000	0.016	100.000	0.119
7482.780	0.029	0.000	0.005	20.829	1.292	0.000	0.000	0.014	100.000	0.129
8122.890	0.026	0.000	0.005	21.353	1.320	0.000	0.000	0.013	100.000	0.140
8831.890	0.024	0.000	0.005	21.756	1.347	0.000	0.000	0.012	100.000	0.153
9611.680	0.022	0.000	0.005	23.032	1.430	1.705	1.705	0.011	98.295	0.166
10445.140	0.020	0.000	0.005	23.939	1.485	1.136	2.841	0.010	97.159	0.181
11347.180	0.019	0.000	0.006	24.628	1.540	1.136	3.977	0.009	96.023	0.196
12332.050	0.017	0.000	0.006	25.604	1.595	1.136	5.114	0.009	94.886	0.213
13409.400	0.016	0.001	0.006	27.893	1.732	2.841	7.955	0.008	92.045	0.232
14574.720	0.015	0.001	0.007	30.696	1.897	3.409	11.364	0.007	88.636	0.252
15835.820	0.014	0.000	0.007	32.068	1.980	1.705	13.068	0.007	86.932	0.274
17213.550	0.012	0.002	0.009	39.869	2.475	10.227	23.295	0.006	76.705	0.298
18700.090	0.011	0.000	0.009	40.854	2.530	1.136	24.432	0.006	75.568	0.323
20322.120	0.011	0.000	0.010	42.240	2.612	1.705	26.136	0.005	73.864	0.351
22091.170	0.010	0.000	0.010	44.069	2.722	2.273	28.409	0.005	71.591	0.382
24014.370	0.009	0.001	0.011	49.065	3.052	6.818	35.227	0.004	64.773	0.415
26097.660	0.008	0.000	0.011	50.501	3.134	1.705	36.932	0.004	63.068	0.451
28366.730	0.008	0.000	0.012	51.488	3.189	1.136	38.068	0.004	61.932	0.490
30829.710	0.007	0.000	0.012	52.614	3.272	1.705	39.773	0.003	60.227	0.533
33505.460	0.006	0.001	0.012	54.753	3.382	2.273	42.045	0.003	57.955	0.579
36413.160	0.006	0.000	0.013	55.683	3.464	1.705	43.750	0.003	56.250	0.629
39574.430	0.005	0.007	0.020	86.839	5.389	39.773	83.523	0.003	16.477	0.684
43008.310	0.005	0.001	0.020	89.127	5.526	2.841	86.364	0.003	13.636	0.743
46741.020	0.005	0.001	0.021	93.641	5.801	5.682	92.045	0.002	7.955	0.808
50798.140	0.004	0.001	0.022	96.620	5.994	3.977	96.023	0.002	3.977	0.878
55202.090	0.004	0.000	0.022	96.714	5.994	0.000	96.023	0.002	3.977	0.954
59991.900	0.004	0.001	0.023	100.000	6.186	3.977	100.000	0.002	0.000	1.037

6/10/10-18 Pore aperture vs. mercury saturation

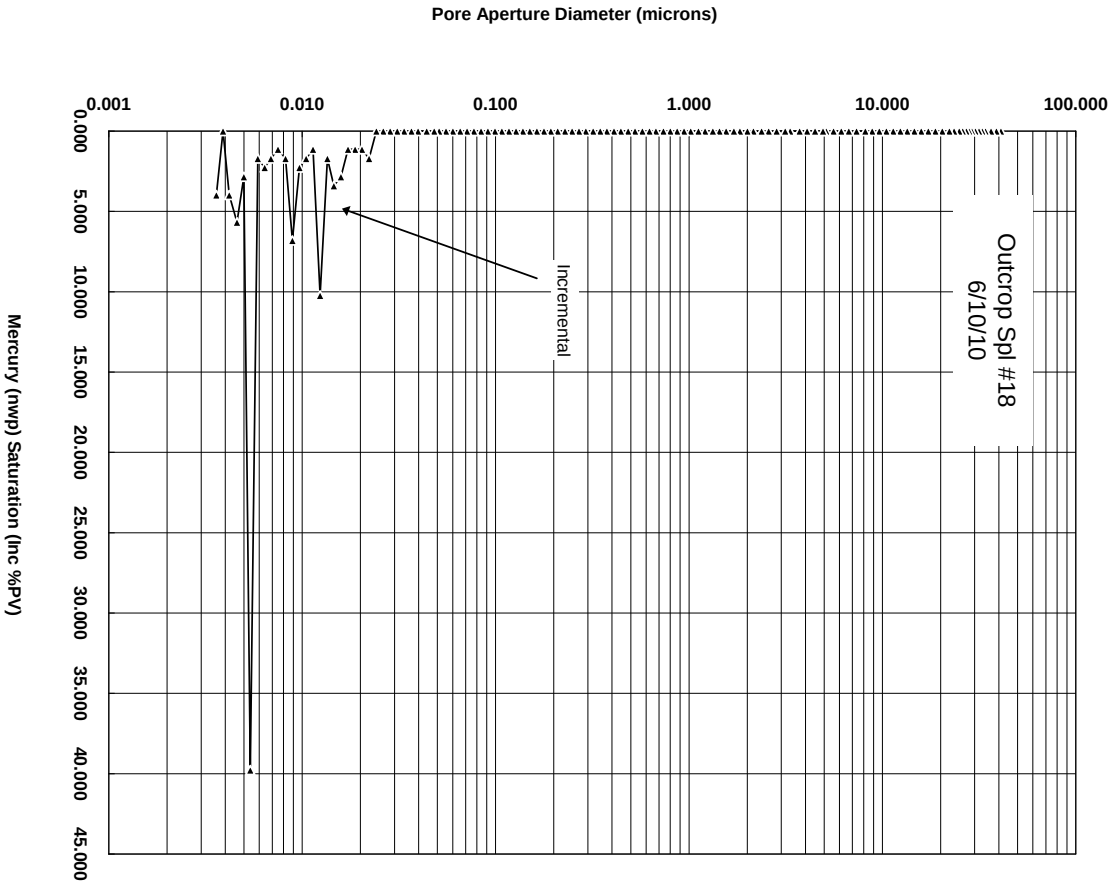

6/10/10-21 Data

Int Pres psia	Pore Dia microns	Inc Int mL/gm	Cum Int mL/gm	Cum Int %PV(bc)	Cum Int %BV	Inc Int %PV(ac)	Cum Int %PV(ac)	Pore Rad microns	W.P. Sat %PV(ac)	Lev "J" Funct.
5.190	41.088	0.000	0.000	0.195	0.000	0.000	0.000	20.544	100.000	0.000
5.490	38.847	0.000	0.000	0.403	0.000	0.000	0.000	19.424	100.000	0.000
5.840	36.533	0.000	0.000	0.623	0.028	0.000	0.000	18.267	100.000	0.000
6.240	34.184	0.000	0.000	0.855	0.028	0.000	0.000	17.092	100.000	0.000
6.490	32.867	0.000	0.000	0.977	0.028	0.000	0.000	16.434	100.000	0.000
6.740	31.648	0.000	0.000	1.111	0.028	0.000	0.000	15.824	100.000	0.000
7.040	30.301	0.000	0.000	1.270	0.028	0.000	0.000	15.151	100.000	0.000
7.340	29.063	0.000	0.000	1.404	0.055	0.000	0.000	14.531	100.000	0.000
7.590	28.106	0.000	0.000	1.502	0.055	0.000	0.000	14.053	100.000	0.000
7.840	27.214	0.000	0.000	1.599	0.055	0.000	0.000	13.607	100.000	0.000
8.190	26.044	0.000	0.000	1.734	0.055	0.000	0.000	13.022	100.000	0.000
8.540	24.982	0.000	0.000	1.819	0.055	0.000	0.000	12.491	100.000	0.000
9.080	23.491	0.000	0.000	2.027	0.055	0.000	0.000	11.745	100.000	0.000
9.610	22.191	0.000	0.000	2.173	0.055	0.000	0.000	11.096	100.000	0.000
10.440	20.428	0.000	0.000	2.356	0.083	0.000	0.000	10.214	100.000	0.000
11.350	18.795	0.000	0.000	2.564	0.083	0.000	0.000	9.398	100.000	0.000
12.340	17.293	0.000	0.000	2.747	0.083	0.000	0.000	8.646	100.000	0.000
13.410	15.910	0.000	0.000	2.905	0.083	0.000	0.000	7.955	100.000	0.000
14.570	14.639	0.000	0.000	3.064	0.083	0.000	0.000	7.320	100.000	0.000
15.840	13.470	0.000	0.000	3.235	0.110	0.000	0.000	6.735	100.000	0.000
17.220	12.392	0.000	0.000	3.394	0.110	0.000	0.000	6.196	100.000	0.000
18.710	11.402	0.000	0.000	3.528	0.110	0.000	0.000	5.701	100.000	0.000
20.330	10.493	0.000	0.000	3.711	0.110	0.000	0.000	5.246	100.000	0.000
22.100	9.653	0.000	0.000	3.845	0.110	0.000	0.000	4.826	100.000	0.000
24.020	8.882	0.000	0.000	4.016	0.110	0.000	0.000	4.441	100.000	0.001
26.110	8.172	0.000	0.001	4.175	0.138	0.000	0.000	4.086	100.000	0.001
28.980	7.362	0.000	0.001	4.407	0.138	0.000	0.000	3.681	100.000	0.001
31.750	6.718	0.000	0.001	4.615	0.138	0.000	0.000	3.359	100.000	0.001
34.780	6.134	0.000	0.001	4.785	0.138	0.000	0.000	3.067	100.000	0.001
38.080	5.602	0.000	0.001	4.993	0.138	0.000	0.000	2.801	100.000	0.001
41.580	5.131	0.000	0.001	5.225	0.165	0.000	0.000	2.565	100.000	0.001
43.770	4.873	0.000	0.001	5.308	0.165	0.000	0.000	2.437	100.000	0.001
47.690	4.473	0.000	0.001	5.339	0.165	0.000	0.000	2.237	100.000	0.001
52.390	4.072	0.000	0.001	5.407	0.165	0.000	0.000	2.036	100.000	0.001
56.800	3.756	0.000	0.001	5.448	0.165	0.000	0.000	1.878	100.000	0.001
62.170	3.431	0.000	0.001	5.448	0.165	0.000	0.000	1.716	100.000	0.001
68.290	3.124	0.000	0.001	5.448	0.165	0.000	0.000	1.562	100.000	0.001
77.190	2.764	0.000	0.001	5.641	0.165	0.000	0.000	1.382	100.000	0.002
81.630	2.613	0.000	0.001	5.641	0.165	0.000	0.000	1.307	100.000	0.002

Int Pres psia	Pore Dia microns	Inc Int mL/gm	Cum Int mL/gm	Cum Int %PV(bc)	Cum Int %BV	Inc Int %PV(ac)	Cum Int %PV(ac)	Pore Rad microns	W.P. Sat %PV(ac)	Lev "J" Funct.
88.920	2.399	0.000	0.001	5.641	0.165	0.000	0.000	1.200	100.000	0.002
97.000	2.199	0.000	0.001	5.641	0.165	0.000	0.000	1.100	100.000	0.002
107.210	1.990	0.000	0.001	5.641	0.165	0.000	0.000	0.995	100.000	0.002
115.850	1.841	0.000	0.001	5.641	0.165	0.000	0.000	0.921	100.000	0.003
126.540	1.686	0.000	0.001	5.641	0.165	0.000	0.000	0.843	100.000	0.003
137.110	1.556	0.000	0.001	5.842	0.165	0.000	0.000	0.778	100.000	0.003
147.990	1.442	0.000	0.001	5.877	0.165	0.000	0.000	0.721	100.000	0.003
162.570	1.312	0.000	0.001	5.891	0.165	0.000	0.000	0.656	100.000	0.004
175.540	1.215	0.000	0.001	5.901	0.165	0.000	0.000	0.608	100.000	0.004
189.760	1.124	0.000	0.001	5.907	0.165	0.000	0.000	0.562	100.000	0.004
206.140	1.035	0.000	0.001	6.084	0.193	0.000	0.000	0.517	100.000	0.004
225.770	0.945	0.000	0.001	6.125	0.193	0.000	0.000	0.472	100.000	0.005
245.210	0.870	0.000	0.001	6.254	0.193	0.000	0.000	0.435	100.000	0.005
264.640	0.806	0.000	0.001	6.291	0.193	0.000	0.000	0.403	100.000	0.006
289.730	0.736	0.000	0.001	6.330	0.193	0.000	0.000	0.368	100.000	0.006
314.590	0.678	0.000	0.001	6.330	0.193	0.000	0.000	0.339	100.000	0.007
342.160	0.624	0.000	0.001	6.330	0.193	0.000	0.000	0.312	100.000	0.007
370.730	0.575	0.000	0.001	6.357	0.193	0.000	0.000	0.288	100.000	0.008
405.440	0.526	0.000	0.001	6.483	0.193	0.000	0.000	0.263	100.000	0.009
440.600	0.484	0.000	0.001	6.529	0.193	0.000	0.000	0.242	100.000	0.010
478.280	0.446	0.000	0.001	6.677	0.193	0.000	0.000	0.223	100.000	0.010
518.850	0.411	0.000	0.001	6.742	0.193	0.000	0.000	0.206	100.000	0.011
565.860	0.377	0.000	0.001	6.775	0.193	0.000	0.000	0.189	100.000	0.012
615.270	0.347	0.000	0.001	6.776	0.193	0.000	0.000	0.173	100.000	0.013
667.670	0.320	0.000	0.001	6.914	0.220	0.000	0.000	0.160	100.000	0.014
727.430	0.293	0.000	0.001	7.074	0.220	0.000	0.000	0.147	100.000	0.016
789.920	0.270	0.000	0.001	7.209	0.220	0.000	0.000	0.135	100.000	0.017
860.670	0.248	0.000	0.001	7.209	0.220	0.000	0.000	0.124	100.000	0.019
932.780	0.229	0.000	0.001	7.416	0.220	0.000	0.000	0.114	100.000	0.020
1014.750	0.210	0.000	0.001	7.629	0.220	0.000	0.000	0.105	100.000	0.022
1104.400	0.193	0.000	0.001	7.905	0.248	0.000	0.000	0.097	100.000	0.024
1200.620	0.178	0.000	0.001	8.196	0.248	0.000	0.000	0.089	100.000	0.026
1302.980	0.164	0.000	0.001	8.530	0.248	0.000	0.000	0.082	100.000	0.028
1415.000	0.151	0.000	0.001	9.079	0.275	0.000	0.000	0.075	100.000	0.031
1539.740	0.139	0.000	0.001	9.820	0.303	0.000	0.000	0.069	100.000	0.033
1673.250	0.128	0.000	0.001	10.271	0.303	0.000	0.000	0.064	100.000	0.036
1816.670	0.117	0.000	0.001	10.839	0.330	0.000	0.000	0.059	100.000	0.039
1976.540	0.108	0.000	0.001	11.576	0.358	0.000	0.000	0.054	100.000	0.043
2149.280	0.099	0.000	0.001	12.398	0.358	0.000	0.000	0.050	100.000	0.047
2335.430	0.091	0.000	0.001	13.335	0.385	0.000	0.000	0.046	100.000	0.051
2536.900	0.084	0.000	0.002	14.224	0.413	0.000	0.000	0.042	100.000	0.055

Int Pres psia	Pore Dia microns	Inc Int mL/gm	Cum Int mL/gm	Cum Int %PV(bc)	Cum Int %BV	Inc Int %PV(ac)	Cum Int %PV(ac)	Pore Rad microns	W.P. Sat %PV(ac)	Lev "J" Funct.
2757.330	0.077	0.000	0.002	15.119	0.440	0.000	0.000	0.039	100.000	0.060
2995.900	0.071	0.000	0.002	15.989	0.468	0.000	0.000	0.036	100.000	0.065
3257.200	0.066	0.000	0.002	17.293	0.523	0.000	0.000	0.033	100.000	0.071
3537.280	0.060	0.000	0.002	18.141	0.550	0.000	0.000	0.030	100.000	0.077
3847.550	0.055	0.000	0.002	19.498	0.578	0.000	0.000	0.028	100.000	0.083
4184.410	0.051	0.000	0.002	21.222	0.633	0.000	0.000	0.026	100.000	0.091
4431.930	0.048	0.000	0.002	22.105	0.660	1.176	1.176	0.024	98.824	0.096
4836.280	0.044	0.000	0.003	24.750	0.715	2.353	3.529	0.022	96.471	0.105
5362.810	0.040	0.000	0.003	26.129	0.770	2.353	5.882	0.020	94.118	0.116
5828.460	0.037	0.000	0.003	27.449	0.798	1.176	7.059	0.018	92.941	0.126
6336.870	0.034	0.000	0.003	29.160	0.853	2.353	9.412	0.017	90.588	0.137
6885.430	0.031	0.000	0.003	30.766	0.908	2.353	11.765	0.016	88.235	0.149
7487.450	0.029	0.000	0.004	33.559	0.990	3.529	15.294	0.014	84.706	0.162
8136.540	0.026	0.000	0.004	35.932	1.073	3.529	18.824	0.013	81.176	0.176
8844.240	0.024	0.000	0.004	41.309	1.155	3.529	22.353	0.012	77.647	0.192
9596.330	0.022	0.000	0.005	42.112	1.265	4.706	27.059	0.011	72.941	0.208
10446.570	0.020	0.000	0.005	45.341	1.375	4.706	31.765	0.010	68.235	0.226
11353.910	0.019	0.001	0.006	51.463	1.568	8.235	40.000	0.009	60.000	0.246
12338.110	0.017	0.000	0.006	55.384	1.678	4.706	44.706	0.009	55.294	0.267
13397.910	0.016	0.000	0.006	56.904	1.733	2.353	47.059	0.008	52.941	0.290
14571.700	0.015	0.001	0.007	63.050	1.898	7.059	54.118	0.007	45.882	0.316
15839.990	0.014	0.000	0.007	66.461	2.008	4.706	58.824	0.007	41.176	0.343
17214.600	0.012	0.000	0.008	69.898	2.118	4.706	63.529	0.006	36.471	0.373
18709.040	0.011	0.000	0.008	76.523	2.228	4.706	68.235	0.006	31.765	0.406
20321.690	0.011	0.001	0.009	77.837	2.366	5.882	74.118	0.005	25.882	0.441
22098.310	0.010	0.001	0.009	84.051	2.531	7.059	81.176	0.005	18.824	0.479
24016.220	0.009	0.000	0.010	86.790	2.641	4.706	85.882	0.004	14.118	0.521
26101.980	0.008	0.000	0.010	90.252	2.723	3.529	89.412	0.004	10.588	0.566
28366.150	0.008	0.000	0.010	91.666	2.778	2.353	91.765	0.004	8.235	0.615
30829.250	0.007	0.000	0.010	92.863	2.806	1.176	92.941	0.003	7.059	0.668
33504.870	0.006	0.000	0.010	94.972	2.861	2.353	95.294	0.003	4.706	0.726
36412.190	0.006	0.000	0.011	95.738	2.888	1.176	96.471	0.003	3.529	0.789
39574.180	0.005	0.000	0.011	96.862	2.916	1.176	97.647	0.003	2.353	0.858
43009.150	0.005	0.000	0.011	98.036	2.943	1.176	98.824	0.003	1.176	0.932
46741.230	0.005	0.000	0.011	98.862	2.971	1.176	100.000	0.002	0.000	1.013
50796.090	0.004	0.000	0.011	99.559	2.971	0.000	100.000	0.002	0.000	1.101
55203.710	0.004	0.000	0.011	99.990	2.971	0.000	100.000	0.002	0.000	1.197
59987.800	0.004	0.000	0.011	100.000	2.971	0.000	100.000	0.002	0.000	1.300

6/10/10-21 Pore aperture vs. mercury saturation

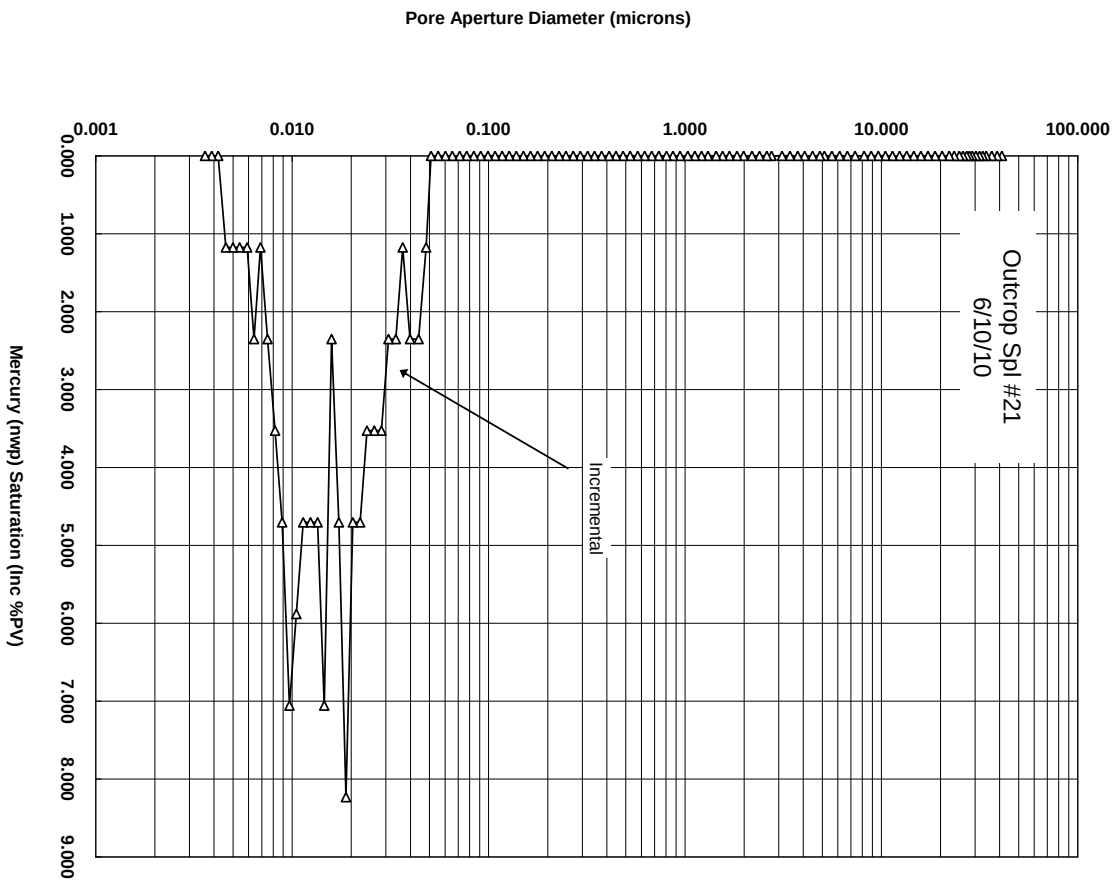

6/12/10-27 Data

Int Pres psia	Pore Dia microns	Inc Int mL/gm	Cum Int mL/gm	Cum Int %PV(bc)	Cum Int %BV	Inc Int %PV(ac)	Cum Int %PV(ac)	Pore Rad microns	W.P. Sat %PV(ac)	Lev "J" Funct.
5.190	41.087	0.000	0.000	0.021	0.000	0.000	0.000	20.544	100.000	0.001
5.490	38.858	0.000	0.000	0.035	0.000	0.000	0.000	19.429	100.000	0.002
5.840	36.521	0.000	0.000	0.057	0.000	0.000	0.000	18.261	100.000	0.002
6.240	34.189	0.000	0.000	0.078	0.000	0.000	0.000	17.095	100.000	0.002
6.490	32.873	0.000	0.000	0.085	0.000	0.000	0.000	16.437	100.000	0.002
6.740	31.641	0.000	0.000	0.099	0.000	0.000	0.000	15.820	100.000	0.002
7.040	30.300	0.000	0.000	0.113	0.000	0.000	0.000	15.150	100.000	0.002
7.340	29.063	0.000	0.000	0.134	0.026	0.000	0.000	14.532	100.000	0.002
7.590	28.094	0.000	0.000	0.141	0.026	0.000	0.000	14.047	100.000	0.002
7.840	27.211	0.000	0.000	0.148	0.026	0.000	0.000	13.606	100.000	0.002
8.190	26.042	0.000	0.000	0.169	0.026	0.000	0.000	13.021	100.000	0.002
8.540	24.979	0.000	0.000	0.184	0.026	0.000	0.000	12.489	100.000	0.002
9.080	23.494	0.000	0.000	0.198	0.026	0.000	0.000	11.747	100.000	0.003
9.610	22.195	0.000	0.000	0.219	0.026	0.000	0.000	11.097	100.000	0.003
10.440	20.428	0.000	0.000	0.226	0.026	0.000	0.000	10.214	100.000	0.003
11.350	18.796	0.000	0.000	0.254	0.026	0.000	0.000	9.398	100.000	0.003
12.340	17.292	0.000	0.000	0.275	0.026	0.000	0.000	8.646	100.000	0.003
13.410	15.909	0.000	0.000	0.304	0.026	0.000	0.000	7.955	100.000	0.004
14.570	14.639	0.000	0.000	0.325	0.026	0.000	0.000	7.319	100.000	0.004
15.840	13.470	0.000	0.000	0.353	0.026	0.000	0.000	6.735	100.000	0.004
17.210	12.393	0.000	0.000	0.374	0.026	0.000	0.000	6.196	100.000	0.005
18.710	11.402	0.000	0.000	0.416	0.053	0.000	0.000	5.701	100.000	0.005
20.330	10.491	0.000	0.000	0.445	0.053	0.000	0.000	5.246	100.000	0.006
22.100	9.653	0.000	0.000	0.473	0.053	0.000	0.000	4.826	100.000	0.006
24.020	8.882	0.000	0.000	0.501	0.053	0.000	0.000	4.441	100.000	0.007
26.100	8.172	0.000	0.000	0.536	0.053	0.000	0.000	4.086	100.000	0.007
28.980	7.362	0.000	0.000	0.600	0.053	0.000	0.000	3.681	100.000	0.008
31.750	6.718	0.000	0.000	0.649	0.079	0.000	0.000	3.359	100.000	0.009
34.780	6.134	0.000	0.000	0.720	0.079	0.000	0.000	3.067	100.000	0.010
38.080	5.603	0.000	0.000	0.776	0.079	0.000	0.000	2.801	100.000	0.010
41.580	5.131	0.000	0.000	0.854	0.079	0.000	0.000	2.565	100.000	0.011
43.020	4.959	0.000	0.000	1.104	0.105	0.259	0.259	2.480	99.741	0.012
46.850	4.553	0.000	0.001	1.606	0.158	0.518	0.777	2.277	99.223	0.013
51.940	4.107	0.000	0.001	2.387	0.237	0.777	1.554	2.054	98.446	0.014
56.150	3.799	0.000	0.001	2.890	0.290	0.518	2.073	1.899	97.927	0.015
65.280	3.268	0.000	0.001	3.250	0.342	0.518	2.591	1.634	97.409	0.018
69.180	3.084	0.000	0.001	3.553	0.369	0.259	2.850	1.542	97.150	0.019
74.910	2.848	0.000	0.001	3.646	0.369	0.000	2.850	1.424	97.150	0.021
82.140	2.597	0.000	0.002	3.887	0.395	0.259	3.109	1.299	96.891	0.023

Int Pres psia	Pore Dia microns	Inc Int mL/gm	Cum Int mL/gm	Cum Int %PV(bc)	Cum Int %BV	Inc Int %PV(ac)	Cum Int %PV(ac)	Pore Rad microns	W.P. Sat %PV(ac)	Lev "J" Funct.
92.020	2.318	0.000	0.002	4.133	0.421	0.259	3.368	1.159	96.632	0.025
96.920	2.201	0.000	0.002	4.388	0.448	0.259	3.627	1.100	96.373	0.027
106.270	2.007	0.000	0.002	4.655	0.474	0.259	3.886	1.004	96.114	0.029
114.610	1.861	0.000	0.002	4.910	0.500	0.259	4.145	0.931	95.855	0.032
125.540	1.699	0.000	0.002	5.183	0.527	0.259	4.404	0.850	95.596	0.035
136.240	1.566	0.000	0.002	5.562	0.579	0.518	4.922	0.783	95.078	0.038
148.400	1.438	0.000	0.002	5.961	0.606	0.259	5.181	0.719	94.819	0.041
161.370	1.322	0.000	0.003	6.429	0.658	0.518	5.699	0.661	94.301	0.044
174.930	1.220	0.000	0.003	6.894	0.711	0.518	6.218	0.610	93.782	0.048
190.200	1.122	0.000	0.003	7.431	0.763	0.518	6.736	0.561	93.264	0.052
206.520	1.033	0.000	0.003	7.950	0.816	0.518	7.254	0.516	92.746	0.057
225.360	0.947	0.000	0.003	8.461	0.869	0.518	7.772	0.473	92.228	0.062
243.310	0.877	0.000	0.004	8.989	0.921	0.518	8.290	0.438	91.710	0.067
265.590	0.803	0.000	0.004	9.493	0.974	0.518	8.808	0.402	91.192	0.073
288.660	0.739	0.000	0.004	9.981	1.027	0.518	9.326	0.370	90.674	0.080
314.310	0.679	0.000	0.004	10.616	1.079	0.518	9.845	0.339	90.155	0.087
340.850	0.626	0.000	0.004	11.144	1.132	0.518	10.363	0.313	89.637	0.094
371.290	0.575	0.000	0.005	11.756	1.211	0.777	11.140	0.287	88.860	0.102
404.620	0.527	0.000	0.005	12.504	1.290	0.777	11.917	0.264	88.083	0.111
439.140	0.486	0.000	0.005	12.865	1.316	0.259	12.176	0.243	87.824	0.121
475.990	0.448	0.000	0.005	13.213	1.343	0.259	12.435	0.224	87.565	0.131
519.330	0.411	0.000	0.005	13.694	1.395	0.518	12.953	0.205	87.047	0.143
563.530	0.379	0.000	0.006	14.047	1.448	0.518	13.472	0.189	86.528	0.155
614.890	0.347	0.000	0.006	14.671	1.501	0.518	13.990	0.173	86.010	0.169
668.880	0.319	0.000	0.006	15.279	1.553	0.518	14.508	0.159	85.492	0.184
724.520	0.294	0.000	0.006	15.820	1.632	0.777	15.285	0.147	84.715	0.200
788.310	0.271	0.000	0.006	16.564	1.685	0.518	15.803	0.135	84.197	0.217
860.630	0.248	0.000	0.007	17.376	1.790	1.036	16.839	0.124	83.161	0.237
933.190	0.229	0.000	0.007	18.342	1.869	0.777	17.617	0.114	82.383	0.257
1016.020	0.210	0.000	0.008	19.371	1.974	1.036	18.653	0.105	81.347	0.280
1101.990	0.194	0.000	0.008	20.518	2.106	1.295	19.948	0.097	80.052	0.304
1199.790	0.178	0.001	0.009	21.768	2.238	1.295	21.244	0.089	78.756	0.330
1301.980	0.164	0.001	0.009	23.127	2.369	1.295	22.539	0.082	77.461	0.359
1415.850	0.151	0.001	0.010	24.573	2.527	1.554	24.093	0.075	75.907	0.390
1537.410	0.139	0.001	0.010	26.219	2.685	1.554	25.648	0.069	74.352	0.423
1672.070	0.128	0.001	0.011	27.997	2.870	1.813	27.461	0.064	72.539	0.461
1816.740	0.117	0.001	0.012	29.991	3.080	2.073	29.534	0.059	70.466	0.500
1974.410	0.108	0.001	0.013	32.158	3.291	2.073	31.606	0.054	68.394	0.544
2146.420	0.099	0.001	0.014	34.639	3.554	2.591	34.197	0.050	65.803	0.591
2333.460	0.091	0.001	0.015	37.389	3.844	2.850	37.047	0.046	62.953	0.643
2534.640	0.084	0.001	0.016	40.480	4.160	3.109	40.155	0.042	59.845	0.698

Int Pres psia	Pore Dia microns	Inc Int mL/gm	Cum Int mL/gm	Cum Int %PV(bc)	Cum Int %BV	Inc Int %PV(ac)	Cum Int %PV(ac)	Pore Rad microns	W.P. Sat %PV(ac)	Lev "J" Funct.
2753.660	0.078	0.001	0.017	43.768	4.476	3.109	43.264	0.039	56.736	0.758
2993.900	0.071	0.001	0.018	47.259	4.844	3.627	46.891	0.036	53.109	0.825
3253.680	0.066	0.001	0.020	50.840	5.213	3.627	50.518	0.033	49.482	0.896
3535.390	0.060	0.001	0.021	54.499	5.581	3.627	54.145	0.030	45.855	0.974
3841.970	0.056	0.001	0.023	57.887	5.923	3.368	57.513	0.028	42.487	1.058
4172.830	0.051	0.001	0.024	60.436	6.187	2.591	60.104	0.026	39.896	1.149
4429.570	0.048	0.001	0.024	62.777	6.424	2.332	62.435	0.024	37.565	1.220
4833.280	0.044	0.001	0.025	64.749	6.634	2.073	64.508	0.022	35.492	1.331
5353.200	0.040	0.001	0.026	66.047	6.766	1.295	65.803	0.020	34.197	1.474
5818.300	0.037	0.001	0.026	67.273	6.898	1.295	67.098	0.018	32.902	1.603
6322.640	0.034	0.000	0.027	68.340	7.003	1.036	68.135	0.017	31.865	1.741
6871.960	0.031	0.000	0.027	69.475	7.108	1.036	69.171	0.016	30.829	1.893
7472.710	0.029	0.000	0.028	70.608	7.240	1.295	70.466	0.014	29.534	2.058
8122.000	0.026	0.000	0.028	71.697	7.345	1.036	71.503	0.013	28.497	2.237
8829.060	0.024	0.000	0.028	72.838	7.477	1.295	72.798	0.012	27.202	2.432
9595.460	0.022	0.000	0.029	73.924	7.582	1.036	73.834	0.011	26.166	2.643
10429.210	0.021	0.001	0.029	75.160	7.714	1.295	75.130	0.010	24.870	2.873
11339.580	0.019	0.001	0.030	76.363	7.819	1.036	76.166	0.009	23.834	3.123
12329.220	0.017	0.001	0.030	77.695	7.951	1.295	77.461	0.009	22.539	3.396
13399.600	0.016	0.001	0.031	78.945	8.082	1.295	78.756	0.008	21.244	3.691
14564.900	0.015	0.001	0.031	80.254	8.214	1.295	80.052	0.007	19.948	4.012
15837.600	0.014	0.001	0.032	81.767	8.372	1.554	81.606	0.007	18.394	4.362
17208.540	0.012	0.001	0.032	83.006	8.503	1.295	82.902	0.006	17.098	4.740
18706.980	0.011	0.001	0.033	84.394	8.661	1.554	84.456	0.006	15.544	5.152
20329.840	0.011	0.001	0.034	86.054	8.819	1.554	86.010	0.005	13.990	5.599
22089.360	0.010	0.000	0.034	86.810	8.898	0.777	86.788	0.005	13.212	6.084
24011.240	0.009	0.000	0.034	87.907	9.004	1.036	87.824	0.004	12.176	6.613
26099.760	0.008	0.001	0.035	89.433	9.162	1.554	89.378	0.004	10.622	7.189
28363.230	0.008	0.000	0.035	90.234	9.241	0.777	90.155	0.004	9.845	7.812
30830.170	0.007	0.001	0.036	91.412	9.372	1.295	91.451	0.003	8.549	8.492
33502.130	0.006	0.000	0.036	92.382	9.478	1.036	92.487	0.003	7.513	9.227
36412.850	0.006	0.000	0.036	93.473	9.583	1.036	93.523	0.003	6.477	10.029
39572.580	0.005	0.000	0.037	94.507	9.688	1.036	94.560	0.003	5.440	10.899
43008.460	0.005	0.001	0.037	95.730	9.820	1.295	95.855	0.003	4.145	11.846
46740.280	0.005	0.001	0.038	97.199	9.951	1.295	97.150	0.002	2.850	12.874
50794.390	0.004	0.000	0.038	97.975	10.030	0.777	97.927	0.002	2.073	13.990
55202.640	0.004	0.000	0.039	98.902	10.136	1.036	98.964	0.002	1.036	15.204
59988.240	0.004	0.000	0.039	100.000	10.241	1.036	100.000	0.002	0.000	16.522

6/12/10-27 Pore aperture vs. mercury saturation

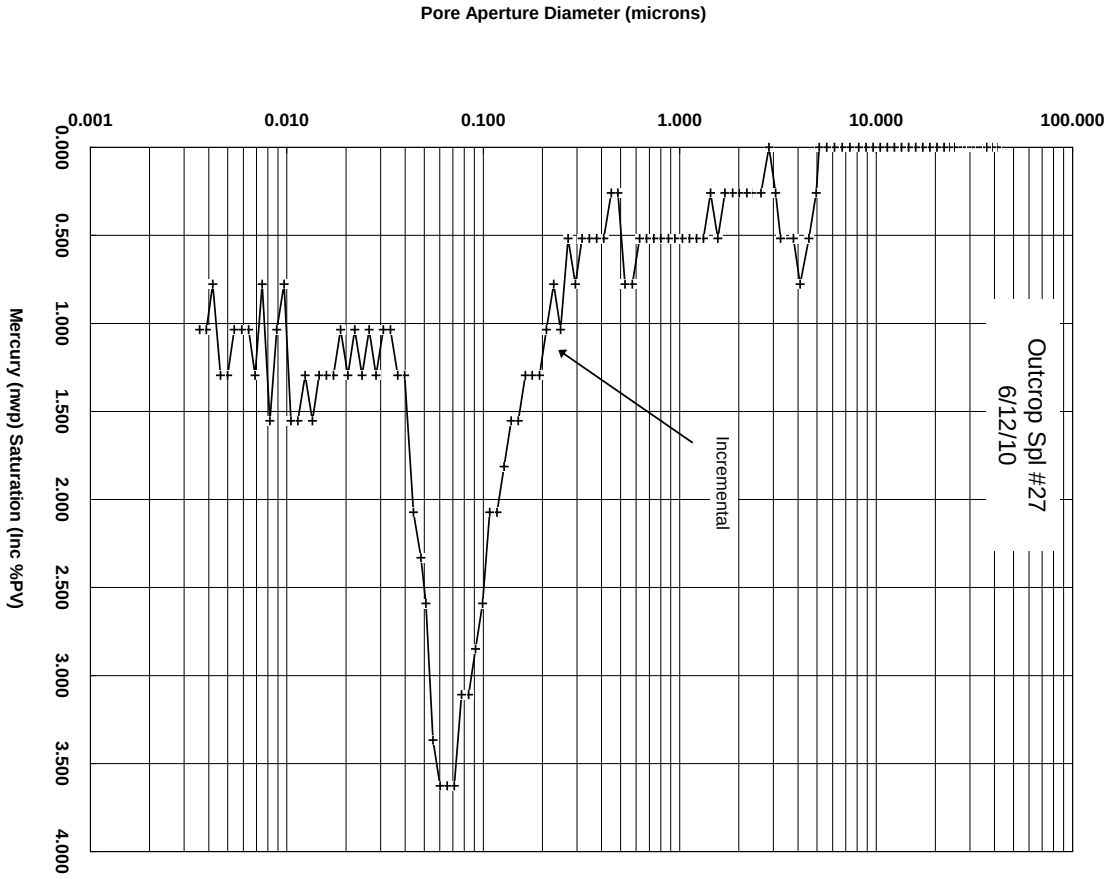

6/12/10-29 Data

Int Pres psia	Pore Dia microns	Inc Int mL/gm	Cum Int mL/gm	Cum Int %PV(bc)	Cum Int %BV	Inc Int %PV(ac)	Cum Int %PV(ac)	Pore Rad microns	W.P. Sat %PV(ac)	Lev "J" Funct.
5.190	41.097	0.000	0.000	0.054	0.000	0.000	0.000	20.548	100.000	0.000
5.490	38.867	0.000	0.000	0.080	0.000	0.000	0.000	19.434	100.000	0.000
5.840	36.520	0.000	0.000	0.161	0.000	0.000	0.000	18.260	100.000	0.000
6.240	34.184	0.000	0.000	0.187	0.000	0.000	0.000	17.092	100.000	0.000
6.490	32.865	0.000	0.000	0.227	0.000	0.000	0.000	16.432	100.000	0.000
6.740	31.646	0.000	0.000	0.268	0.000	0.000	0.000	15.823	100.000	0.000
7.040	30.301	0.000	0.000	0.294	0.000	0.000	0.000	15.151	100.000	0.000
7.340	29.066	0.000	0.000	0.348	0.000	0.000	0.000	14.533	100.000	0.000
7.590	28.108	0.000	0.000	0.361	0.000	0.000	0.000	14.054	100.000	0.000
7.840	27.202	0.000	0.000	0.401	0.000	0.000	0.000	13.601	100.000	0.000
8.190	26.043	0.000	0.000	0.428	0.000	0.000	0.000	13.021	100.000	0.000
8.540	24.973	0.000	0.000	0.468	0.000	0.000	0.000	12.487	100.000	0.000
9.080	23.492	0.000	0.000	0.495	0.000	0.000	0.000	11.746	100.000	0.000
9.610	22.196	0.000	0.000	0.535	0.000	0.000	0.000	11.098	100.000	0.000
10.440	20.430	0.000	0.000	0.589	0.028	0.000	0.000	10.215	100.000	0.000
11.350	18.797	0.000	0.000	0.629	0.028	0.000	0.000	9.399	100.000	0.000
12.340	17.292	0.000	0.000	0.722	0.028	0.000	0.000	8.646	100.000	0.000
13.410	15.912	0.000	0.000	0.776	0.028	0.000	0.000	7.956	100.000	0.000
14.570	14.638	0.000	0.000	0.829	0.028	0.000	0.000	7.319	100.000	0.000
15.840	13.469	0.000	0.000	0.910	0.028	0.000	0.000	6.734	100.000	0.000
17.210	12.392	0.000	0.000	1.003	0.028	0.000	0.000	6.196	100.000	0.000
18.710	11.400	0.000	0.000	1.070	0.028	0.000	0.000	5.700	100.000	0.000
20.330	10.492	0.000	0.000	1.150	0.028	0.000	0.000	5.246	100.000	0.000
22.100	9.653	0.000	0.000	1.257	0.028	0.000	0.000	4.826	100.000	0.000
24.020	8.881	0.000	0.000	1.351	0.028	0.000	0.000	4.441	100.000	0.001
26.110	8.171	0.000	0.000	1.793	0.057	0.000	0.000	4.086	100.000	0.001
28.980	7.362	0.000	0.000	1.940	0.057	0.000	0.000	3.681	100.000	0.001
31.760	6.717	0.000	0.000	2.167	0.057	0.000	0.000	3.359	100.000	0.001
34.780	6.134	0.000	0.000	2.368	0.057	0.000	0.000	3.067	100.000	0.001
38.080	5.602	0.000	0.000	2.649	0.057	0.000	0.000	2.801	100.000	0.001
41.580	5.131	0.000	0.000	2.876	0.057	0.000	0.000	2.565	100.000	0.001
43.220	4.936	0.000	0.000	2.885	0.057	0.000	0.000	2.468	100.000	0.001
47.530	4.488	0.000	0.000	3.114	0.085	0.000	0.000	2.244	100.000	0.001
52.180	4.088	0.000	0.000	3.418	0.085	0.000	0.000	2.044	100.000	0.001
57.200	3.730	0.000	0.000	3.511	0.085	0.000	0.000	1.865	100.000	0.001
63.990	3.334	0.000	0.000	3.647	0.085	0.000	0.000	1.667	100.000	0.001
67.850	3.144	0.000	0.000	3.765	0.085	0.000	0.000	1.572	100.000	0.001
75.060	2.842	0.000	0.000	3.939	0.085	0.000	0.000	1.421	100.000	0.002
82.540	2.585	0.000	0.000	4.356	0.113	0.000	0.000	1.292	100.000	0.002

Int Pres psia	Pore Dia microns	Inc Int mL/gm	Cum Int mL/gm	Cum Int %PV(bc)	Cum Int %BV	Inc Int %PV(ac)	Cum Int %PV(ac)	Pore Rad microns	W.P. Sat %PV(ac)	Lev "J" Funct.
89.830	2.375	0.000	0.000	4.575	0.113	0.000	0.000	1.187	100.000	0.002
98.890	2.157	0.000	0.001	5.334	0.141	0.000	0.000	1.079	100.000	0.002
106.420	2.005	0.000	0.001	5.490	0.141	0.000	0.000	1.002	100.000	0.002
116.300	1.834	0.000	0.001	5.781	0.141	0.000	0.000	0.917	100.000	0.003
124.930	1.708	0.000	0.001	5.854	0.141	0.000	0.000	0.854	100.000	0.003
137.040	1.557	0.000	0.001	6.248	0.141	0.000	0.000	0.778	100.000	0.003
148.330	1.438	0.000	0.001	6.334	0.141	0.000	0.000	0.719	100.000	0.003
160.250	1.331	0.000	0.001	6.651	0.170	0.000	0.000	0.666	100.000	0.003
175.790	1.214	0.000	0.001	6.909	0.170	0.000	0.000	0.607	100.000	0.004
190.400	1.120	0.000	0.001	7.235	0.170	0.000	0.000	0.560	100.000	0.004
208.640	1.022	0.000	0.001	7.488	0.170	0.000	0.000	0.511	100.000	0.005
225.930	0.944	0.000	0.001	7.737	0.198	0.000	0.000	0.472	100.000	0.005
245.350	0.870	0.000	0.001	7.952	0.198	0.000	0.000	0.435	100.000	0.005
266.140	0.802	0.000	0.001	8.221	0.198	0.000	0.000	0.401	100.000	0.006
289.150	0.738	0.000	0.001	8.666	0.198	0.000	0.000	0.369	100.000	0.006
315.780	0.676	0.000	0.001	9.019	0.226	0.000	0.000	0.338	100.000	0.007
341.490	0.625	0.000	0.001	9.372	0.226	0.000	0.000	0.312	100.000	0.007
370.830	0.575	0.000	0.001	9.652	0.226	0.000	0.000	0.288	100.000	0.008
404.590	0.527	0.000	0.001	10.031	0.254	0.000	0.000	0.264	100.000	0.009
439.960	0.485	0.000	0.001	10.302	0.254	0.000	0.000	0.242	100.000	0.010
479.320	0.445	0.000	0.001	10.667	0.254	0.000	0.000	0.223	100.000	0.010
519.920	0.410	0.000	0.001	11.092	0.283	0.000	0.000	0.205	100.000	0.011
566.050	0.377	0.000	0.001	11.571	0.283	0.000	0.000	0.188	100.000	0.012
613.240	0.348	0.000	0.001	12.023	0.283	0.000	0.000	0.174	100.000	0.013
667.650	0.320	0.000	0.001	12.520	0.311	0.000	0.000	0.160	100.000	0.015
727.470	0.293	0.000	0.001	13.014	0.311	0.000	0.000	0.147	100.000	0.016
789.660	0.270	0.000	0.001	13.497	0.339	0.000	0.000	0.135	100.000	0.017
857.710	0.249	0.000	0.001	14.115	0.339	0.000	0.000	0.124	100.000	0.019
933.240	0.229	0.000	0.001	14.664	0.367	0.000	0.000	0.114	100.000	0.020
1015.590	0.210	0.000	0.001	15.162	0.367	0.000	0.000	0.105	100.000	0.022
1103.600	0.193	0.000	0.001	15.735	0.396	0.000	0.000	0.097	100.000	0.024
1198.930	0.178	0.000	0.001	16.349	0.396	0.000	0.000	0.089	100.000	0.026
1302.490	0.164	0.000	0.002	16.853	0.424	0.000	0.000	0.082	100.000	0.028
1416.210	0.151	0.000	0.002	17.549	0.424	0.000	0.000	0.075	100.000	0.031
1537.990	0.139	0.000	0.002	18.283	0.452	0.000	0.000	0.069	100.000	0.033
1671.380	0.128	0.000	0.002	18.961	0.452	0.000	0.000	0.064	100.000	0.036
1817.830	0.117	0.000	0.002	19.732	0.480	0.000	0.000	0.059	100.000	0.040
1977.420	0.108	0.000	0.002	20.683	0.509	0.000	0.000	0.054	100.000	0.043
2147.620	0.099	0.000	0.002	21.551	0.537	0.000	0.000	0.050	100.000	0.047
2334.640	0.091	0.000	0.002	22.449	0.537	0.000	0.000	0.046	100.000	0.051
2536.040	0.084	0.000	0.002	23.500	0.565	1.493	1.493	0.042	98.507	0.055

Int Pres psia	Pore Dia microns	Inc Int mL/gm	Cum Int mL/gm	Cum Int %PV(bc)	Cum Int %BV	Inc Int %PV(ac)	Cum Int %PV(ac)	Pore Rad microns	W.P. Sat %PV(ac)	Lev "J" Funct.
2757.380	0.077	0.000	0.002	24.520	0.593	1.493	2.985	0.039	97.015	0.060
2995.160	0.071	0.000	0.002	25.719	0.622	1.493	4.478	0.036	95.522	0.065
3252.860	0.066	0.000	0.002	26.923	0.650	1.493	5.970	0.033	94.030	0.071
3540.720	0.060	0.000	0.002	28.356	0.678	1.493	7.463	0.030	92.537	0.077
3843.400	0.056	0.000	0.003	29.691	0.735	2.985	10.448	0.028	89.552	0.084
4176.680	0.051	0.000	0.003	31.189	0.763	1.493	11.940	0.026	88.060	0.091
4429.290	0.048	0.000	0.003	32.424	0.791	1.493	13.433	0.024	86.567	0.096
4836.310	0.044	0.000	0.003	34.529	0.848	2.985	16.418	0.022	83.582	0.105
5360.900	0.040	0.000	0.003	36.507	0.904	2.985	19.403	0.020	80.597	0.117
5818.850	0.037	0.000	0.003	37.963	0.932	1.493	20.896	0.018	79.104	0.127
6335.620	0.034	0.000	0.004	40.240	0.989	2.985	23.881	0.017	76.119	0.138
6877.860	0.031	0.000	0.004	41.989	1.017	1.493	25.373	0.016	74.627	0.150
7482.340	0.029	0.000	0.004	44.281	1.074	2.985	28.358	0.014	71.642	0.163
8122.440	0.026	0.000	0.004	46.198	1.130	2.985	31.343	0.013	68.657	0.177
8831.400	0.024	0.000	0.004	48.500	1.187	2.985	34.328	0.012	65.672	0.192
9611.160	0.022	0.000	0.005	51.878	1.271	4.478	38.806	0.011	61.194	0.209
10444.580	0.020	0.000	0.005	54.421	1.328	2.985	41.791	0.010	58.209	0.227
11346.590	0.019	0.000	0.005	56.844	1.384	2.985	44.776	0.009	55.224	0.247
12331.440	0.017	0.000	0.005	59.289	1.441	2.985	47.761	0.009	52.239	0.268
13408.760	0.016	0.000	0.005	62.965	1.526	4.478	52.239	0.008	47.761	0.292
14574.060	0.015	0.000	0.006	66.275	1.610	4.478	56.716	0.007	43.284	0.317
15835.150	0.014	0.000	0.006	68.387	1.667	2.985	59.701	0.007	40.299	0.345
17212.900	0.012	0.000	0.006	73.012	1.752	4.478	64.179	0.006	35.821	0.375
18699.440	0.011	0.000	0.006	74.422	1.808	2.985	67.164	0.006	32.836	0.407
20321.450	0.011	0.000	0.007	76.180	1.865	2.985	70.149	0.005	29.851	0.442
22090.500	0.010	0.000	0.007	78.027	1.893	1.493	71.642	0.005	28.358	0.481
24013.730	0.009	0.000	0.007	80.103	1.949	2.985	74.627	0.004	25.373	0.523
26097.020	0.008	0.000	0.007	81.772	2.006	2.985	77.612	0.004	22.388	0.568
28366.080	0.008	0.000	0.007	83.550	2.034	1.493	79.104	0.004	20.896	0.618
30829.030	0.007	0.000	0.007	85.379	2.091	2.985	82.090	0.003	17.910	0.671
33504.790	0.006	0.000	0.008	87.390	2.147	2.985	85.075	0.003	14.925	0.729
36412.470	0.006	0.000	0.008	89.142	2.204	2.985	88.060	0.003	11.940	0.793
39574.060	0.005	0.000	0.008	94.603	2.288	4.478	92.537	0.003	7.463	0.862
43007.960	0.005	0.000	0.008	95.476	2.345	2.985	95.522	0.003	4.478	0.936
46740.700	0.005	0.000	0.008	96.806	2.373	1.493	97.015	0.002	2.985	1.018
50797.850	0.004	0.000	0.009	97.923	2.401	1.493	98.507	0.002	1.493	1.106
55201.770	0.004	0.000	0.009	98.819	2.430	1.493	100.000	0.002	0.000	1.202
59991.610	0.004	0.000	0.009	100.000	2.430	0.000	100.000	0.002	0.000	1.306

6/12/10-29 Pore aperture vs. mercury saturation

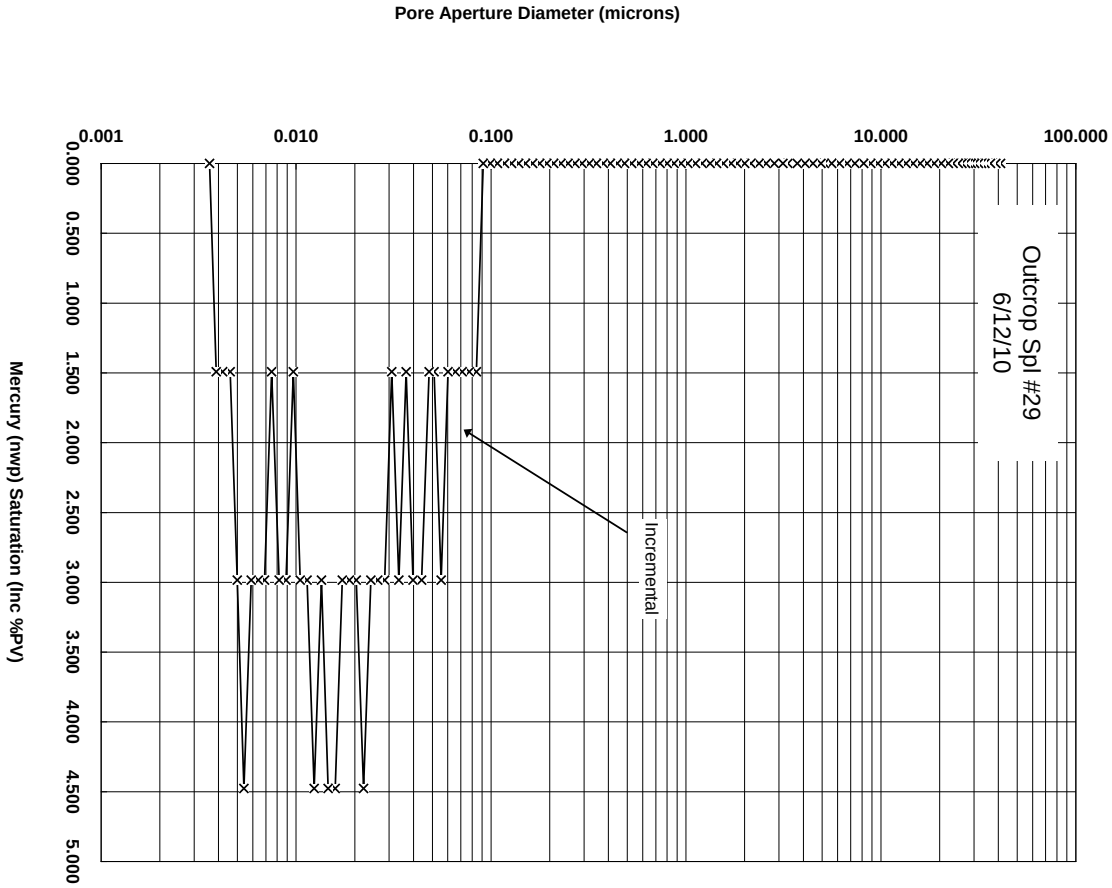

6/12/10-31FG Data

Int Pres psia	Pore Dia microns	Inc Int mL/gm	Cum Int mL/gm	Cum Int %PV(bc)	Cum Int %BV	Inc Int %PV(ac)	Cum Int %PV(ac)	Pore Rad microns	W.P. Sat %PV(ac)	Lev "J" Funct.
5.190	41.087	0.000	0.000	0.011	0.000	0.000	0.000	20.544	100.000	0.002
5.490	38.858	0.000	0.000	0.022	0.000	0.000	0.000	19.429	100.000	0.002
5.840	36.521	0.000	0.000	0.043	0.000	0.000	0.000	18.261	100.000	0.002
6.240	34.189	0.000	0.000	0.054	0.000	0.000	0.000	17.095	100.000	0.003
6.490	32.873	0.000	0.000	0.075	0.000	0.000	0.000	16.437	100.000	0.003
6.740	31.641	0.000	0.000	0.086	0.000	0.000	0.000	15.820	100.000	0.003
7.040	30.300	0.000	0.000	0.097	0.000	0.000	0.000	15.150	100.000	0.003
7.340	29.063	0.000	0.000	0.108	0.026	0.000	0.000	14.532	100.000	0.003
7.590	28.094	0.000	0.000	0.119	0.026	0.000	0.000	14.047	100.000	0.003
7.840	27.211	0.000	0.000	0.129	0.026	0.000	0.000	13.606	100.000	0.003
8.190	26.042	0.000	0.000	0.151	0.026	0.000	0.000	13.021	100.000	0.003
8.540	24.979	0.000	0.000	0.162	0.026	0.000	0.000	12.489	100.000	0.004
9.080	23.494	0.000	0.000	0.162	0.026	0.000	0.000	11.747	100.000	0.004
9.610	22.195	0.000	0.000	0.205	0.026	0.000	0.000	11.097	100.000	0.004
10.440	20.428	0.000	0.000	0.226	0.026	0.000	0.000	10.214	100.000	0.004
11.350	18.796	0.000	0.000	0.248	0.026	0.000	0.000	9.398	100.000	0.005
12.340	17.292	0.000	0.000	0.269	0.026	0.000	0.000	8.646	100.000	0.005
13.410	15.909	0.000	0.000	0.302	0.026	0.000	0.000	7.955	100.000	0.006
14.570	14.639	0.000	0.000	0.334	0.053	0.000	0.000	7.319	100.000	0.006
15.840	13.470	0.000	0.000	0.366	0.053	0.000	0.000	6.735	100.000	0.007
17.210	12.393	0.000	0.000	0.377	0.053	0.000	0.000	6.196	100.000	0.007
18.710	11.402	0.000	0.000	0.453	0.053	0.000	0.000	5.701	100.000	0.008
20.330	10.491	0.000	0.000	0.463	0.053	0.000	0.000	5.246	100.000	0.008
22.100	9.653	0.000	0.000	0.506	0.053	0.000	0.000	4.826	100.000	0.009
24.020	8.882	0.000	0.000	0.550	0.079	0.000	0.000	4.441	100.000	0.010
26.100	8.172	0.000	0.000	0.593	0.079	0.000	0.000	4.086	100.000	0.011
28.980	7.362	0.000	0.000	0.668	0.079	0.000	0.000	3.681	100.000	0.012
31.750	6.718	0.000	0.000	0.733	0.079	0.000	0.000	3.359	100.000	0.013
34.780	6.134	0.000	0.000	0.819	0.105	0.000	0.000	3.067	100.000	0.015
38.080	5.603	0.000	0.000	0.905	0.105	0.000	0.000	2.801	100.000	0.016
41.580	5.131	0.000	0.001	0.991	0.132	0.000	0.000	2.565	100.000	0.017
44.000	4.848	0.000	0.001	1.029	0.132	0.000	0.000	2.424	100.000	0.018
47.590	4.483	0.000	0.001	1.029	0.132	0.000	0.000	2.241	100.000	0.020
52.960	4.028	0.000	0.001	1.029	0.132	0.000	0.000	2.014	100.000	0.022
57.130	3.734	0.000	0.001	1.029	0.132	0.000	0.000	1.867	100.000	0.024
63.020	3.385	0.000	0.001	1.053	0.132	0.000	0.000	1.692	100.000	0.026
68.730	3.104	0.000	0.001	1.087	0.132	0.000	0.000	1.552	100.000	0.029
74.240	2.874	0.000	0.001	1.087	0.132	0.000	0.000	1.437	100.000	0.031
83.600	2.552	0.000	0.001	1.155	0.132	0.000	0.000	1.276	100.000	0.035

Int Pres psia	Pore Dia microns	Inc Int mL/gm	Cum Int mL/gm	Cum Int %PV(bc)	Cum Int %BV	Inc Int %PV(ac)	Cum Int %PV(ac)	Pore Rad microns	W.P. Sat %PV(ac)	Lev "J" Funct.
89.760	2.377	0.000	0.001	1.210	0.158	0.000	0.000	1.188	100.000	0.037
97.120	2.197	0.000	0.001	1.233	0.158	0.000	0.000	1.098	100.000	0.040
106.020	2.012	0.000	0.001	1.310	0.158	0.000	0.000	1.006	100.000	0.044
114.660	1.861	0.000	0.001	1.359	0.158	0.000	0.000	0.930	100.000	0.048
125.500	1.700	0.000	0.001	1.625	0.211	0.000	0.000	0.850	100.000	0.052
136.170	1.567	0.000	0.001	1.699	0.211	0.000	0.000	0.783	100.000	0.057
149.410	1.428	0.000	0.001	2.098	0.263	0.429	0.429	0.714	99.571	0.062
161.800	1.318	0.000	0.001	2.521	0.316	0.429	0.858	0.659	99.142	0.067
176.320	1.210	0.001	0.002	3.682	0.447	1.073	1.931	0.605	98.069	0.074
191.190	1.116	0.001	0.003	5.226	0.658	1.717	3.648	0.558	96.352	0.080
209.920	1.016	0.001	0.003	6.336	0.789	1.073	4.721	0.508	95.279	0.088
226.430	0.942	0.001	0.004	8.294	1.026	1.931	6.652	0.471	93.348	0.094
246.220	0.866	0.001	0.005	10.956	1.368	2.790	9.442	0.433	90.558	0.103
267.230	0.798	0.002	0.007	14.059	1.763	3.219	12.661	0.399	87.339	0.111
291.820	0.731	0.001	0.008	16.784	2.105	2.790	15.451	0.366	84.549	0.122
316.340	0.674	0.001	0.009	19.100	2.395	2.361	17.811	0.337	82.189	0.132
342.050	0.624	0.001	0.010	21.417	2.658	2.146	19.957	0.312	80.043	0.143
373.100	0.572	0.001	0.011	23.748	2.974	2.575	22.532	0.286	77.468	0.156
406.360	0.525	0.001	0.013	26.359	3.289	2.575	25.107	0.263	74.893	0.169
440.700	0.484	0.001	0.014	28.717	3.579	2.361	27.468	0.242	72.532	0.184
479.420	0.445	0.001	0.015	31.054	3.868	2.361	29.828	0.223	70.172	0.200
523.330	0.408	0.001	0.016	33.400	4.158	2.361	32.189	0.204	67.811	0.218
567.520	0.376	0.001	0.017	35.714	4.447	2.361	34.549	0.188	65.451	0.237
615.660	0.347	0.001	0.018	38.031	4.737	2.361	36.910	0.173	63.090	0.257
667.920	0.319	0.001	0.019	40.254	5.026	2.361	39.270	0.160	60.730	0.278
726.500	0.294	0.001	0.020	42.634	5.316	2.361	41.631	0.147	58.369	0.303
790.420	0.270	0.001	0.021	44.946	5.605	2.361	43.991	0.135	56.009	0.330
858.950	0.248	0.001	0.022	47.246	5.895	2.361	46.352	0.124	53.648	0.358
932.070	0.229	0.001	0.023	49.249	6.132	1.931	48.283	0.114	51.717	0.389
1013.500	0.211	0.001	0.024	51.557	6.421	2.361	50.644	0.105	49.356	0.423
1104.300	0.193	0.001	0.025	53.529	6.684	2.146	52.790	0.097	47.210	0.460
1198.910	0.178	0.001	0.027	55.819	6.974	2.361	55.150	0.089	44.850	0.500
1305.340	0.163	0.001	0.028	58.142	7.263	2.361	57.511	0.082	42.489	0.544
1416.200	0.151	0.001	0.029	60.094	7.500	1.931	59.442	0.075	40.558	0.590
1540.040	0.139	0.001	0.030	62.263	7.763	2.146	61.588	0.069	38.412	0.642
1671.470	0.128	0.001	0.030	63.977	7.974	1.717	63.305	0.064	36.695	0.697
1818.980	0.117	0.001	0.031	65.868	8.211	1.931	65.236	0.059	34.764	0.758
1975.620	0.108	0.001	0.032	67.767	8.447	1.931	67.167	0.054	32.833	0.824
2147.200	0.099	0.001	0.033	69.341	8.658	1.717	68.884	0.050	31.116	0.895
2334.860	0.091	0.001	0.034	70.917	8.842	1.502	70.386	0.046	29.614	0.973
2534.990	0.084	0.001	0.034	72.434	9.026	1.502	71.888	0.042	28.112	1.057

Int Pres psia	Pore Dia microns	Inc Int mL/gm	Cum Int mL/gm	Cum Int %PV(bc)	Cum Int %BV	Inc Int %PV(ac)	Cum Int %PV(ac)	Pore Rad microns	W.P. Sat %PV(ac)	Lev "J" Funct.
2756.850	0.077	0.001	0.035	73.968	9.237	1.717	73.605	0.039	26.395	1.149
2997.510	0.071	0.001	0.036	75.469	9.421	1.502	75.107	0.036	24.893	1.250
3256.340	0.066	0.001	0.036	76.651	9.553	1.073	76.180	0.033	23.820	1.358
3540.370	0.060	0.001	0.037	77.833	9.711	1.288	77.468	0.030	22.532	1.476
3847.710	0.055	0.001	0.037	78.788	9.816	0.858	78.326	0.028	21.674	1.604
4178.700	0.051	0.001	0.038	79.770	9.947	1.073	79.399	0.026	20.601	1.742
4430.050	0.048	0.000	0.038	80.411	10.026	0.644	80.043	0.024	19.957	1.847
4833.720	0.044	0.000	0.039	81.312	10.132	0.858	80.901	0.022	19.099	2.015
5358.280	0.040	0.000	0.039	82.123	10.237	0.858	81.760	0.020	18.240	2.234
5818.530	0.037	0.000	0.039	82.907	10.342	0.858	82.618	0.018	17.382	2.426
6324.410	0.034	0.001	0.040	83.923	10.474	1.073	83.691	0.017	16.309	2.637
6880.500	0.031	0.000	0.040	84.298	10.500	0.215	83.906	0.016	16.094	2.869
7479.660	0.029	0.000	0.040	85.179	10.632	1.073	84.979	0.014	15.021	3.118
8132.250	0.026	0.000	0.041	85.998	10.737	0.858	85.837	0.013	14.163	3.391
8832.040	0.024	0.000	0.041	86.779	10.816	0.644	86.481	0.012	13.519	3.682
9607.680	0.022	0.000	0.041	87.417	10.895	0.644	87.124	0.011	12.876	4.006
10438.340	0.020	0.000	0.042	88.254	11.000	0.858	87.983	0.010	12.017	4.352
11349.780	0.019	0.000	0.042	88.947	11.105	0.858	88.841	0.009	11.159	4.732
12325.740	0.017	0.000	0.043	89.674	11.184	0.644	89.485	0.009	10.515	5.139
13408.290	0.016	0.000	0.043	90.347	11.263	0.644	90.129	0.008	9.871	5.590
14565.720	0.015	0.000	0.043	90.995	11.342	0.644	90.773	0.007	9.227	6.073
15832.140	0.014	0.000	0.044	91.708	11.447	0.858	91.631	0.007	8.369	6.601
17204.290	0.012	0.000	0.044	92.318	11.526	0.644	92.275	0.006	7.725	7.173
18693.990	0.011	0.000	0.044	93.020	11.605	0.644	92.918	0.006	7.082	7.794
20319.860	0.011	0.000	0.044	93.394	11.658	0.429	93.348	0.005	6.652	8.472
22095.860	0.010	0.000	0.045	94.080	11.737	0.644	93.991	0.005	6.009	9.212
24016.150	0.009	0.000	0.045	94.663	11.816	0.644	94.635	0.004	5.365	10.013
26102.090	0.008	0.000	0.045	95.264	11.869	0.429	95.064	0.004	4.936	10.883
28366.890	0.008	0.000	0.045	95.606	11.921	0.429	95.494	0.004	4.506	11.827
30829.400	0.007	0.000	0.046	96.213	12.000	0.644	96.137	0.003	3.863	12.854
33505.190	0.006	0.000	0.046	96.994	12.105	0.858	96.996	0.003	3.004	13.969
36413.630	0.006	0.000	0.046	97.397	12.158	0.429	97.425	0.003	2.575	15.182
39574.190	0.005	0.000	0.046	97.621	12.211	0.429	97.854	0.003	2.146	16.500
43007.840	0.005	0.000	0.047	97.950	12.263	0.429	98.283	0.003	1.717	17.931
46741.360	0.005	0.000	0.047	98.373	12.316	0.429	98.712	0.002	1.288	19.488
50798.040	0.004	0.000	0.047	99.343	12.369	0.429	99.142	0.002	0.858	21.179
55202.360	0.004	0.000	0.047	99.987	12.421	0.429	99.571	0.002	0.429	23.015
59984.750	0.004	0.000	0.047	100.000	12.474	0.429	100.000	0.002	0.000	25.009

6/12/10-31FG Pore aperture vs. mercury saturation

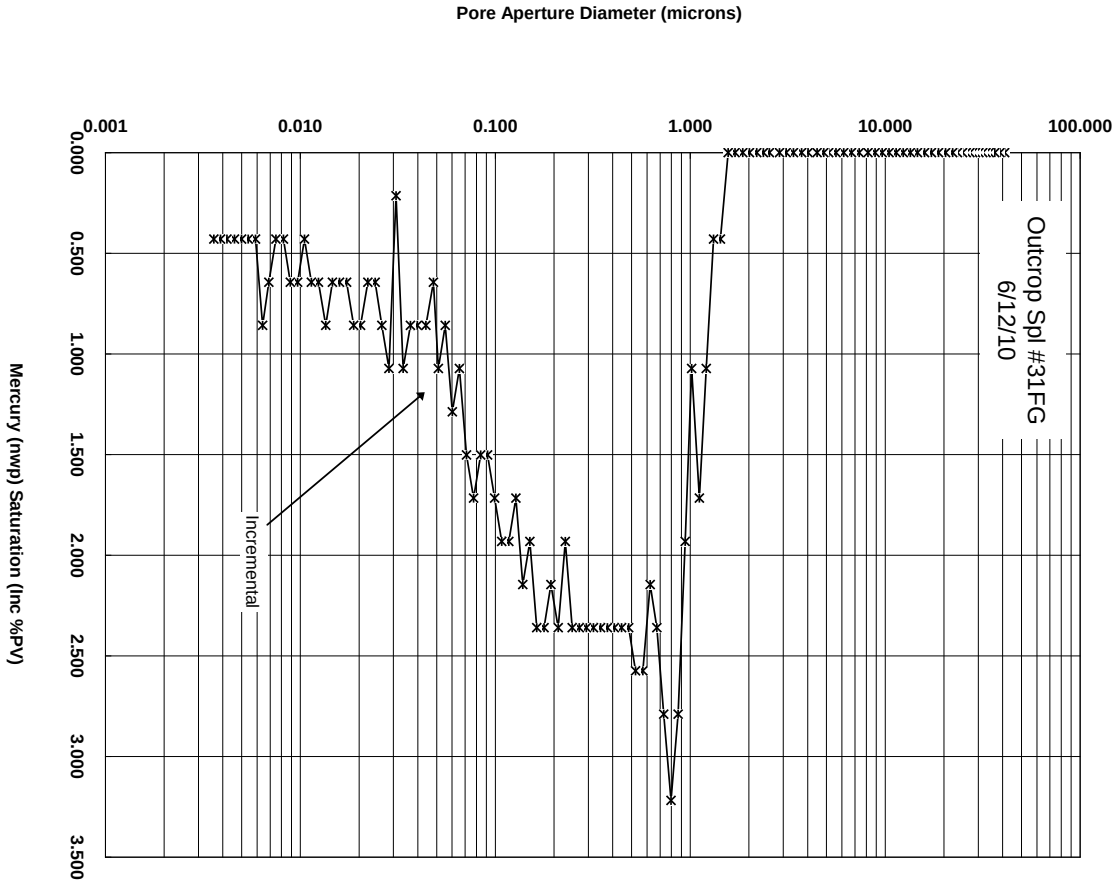

6/12/10-34 Data

Int Pres psia	Pore Dia microns	Inc Int mL/gm	Cum Int mL/gm	Cum Int %PV(bc)	Cum Int %BV	Inc Int %PV(ac)	Cum Int %PV(ac)	Pore Rad microns	W.P. Sat %PV(ac)	Lev "J" Funct.
5.190	41.083	0.000	0.000	0.019	0.000	0.000	0.000	20.541	100.000	0.000
5.490	38.852	0.000	0.000	0.028	0.000	0.000	0.000	19.426	100.000	0.000
5.840	36.524	0.000	0.000	0.056	0.000	0.000	0.000	18.262	100.000	0.000
6.240	34.180	0.000	0.000	0.075	0.000	0.000	0.000	17.090	100.000	0.000
6.490	32.872	0.000	0.000	0.084	0.000	0.000	0.000	16.436	100.000	0.000
6.740	31.642	0.000	0.000	0.112	0.000	0.000	0.000	15.821	100.000	0.000
7.040	30.297	0.000	0.000	0.121	0.000	0.000	0.000	15.149	100.000	0.000
7.340	29.065	0.000	0.000	0.140	0.000	0.000	0.000	14.533	100.000	0.000
7.590	28.104	0.000	0.000	0.158	0.027	0.000	0.000	14.052	100.000	0.000
7.840	27.208	0.000	0.000	0.168	0.027	0.000	0.000	13.604	100.000	0.000
8.190	26.045	0.000	0.000	0.186	0.027	0.000	0.000	13.022	100.000	0.000
8.540	24.982	0.000	0.000	0.196	0.027	0.000	0.000	12.491	100.000	0.000
9.080	23.495	0.000	0.000	0.224	0.027	0.000	0.000	11.748	100.000	0.000
9.610	22.199	0.000	0.000	0.252	0.027	0.000	0.000	11.100	100.000	0.000
10.440	20.429	0.000	0.000	0.289	0.027	0.000	0.000	10.215	100.000	0.001
11.350	18.795	0.000	0.000	0.317	0.027	0.000	0.000	9.398	100.000	0.001
12.340	17.294	0.000	0.000	0.345	0.027	0.000	0.000	8.647	100.000	0.001
13.410	15.911	0.000	0.000	0.382	0.027	0.000	0.000	7.956	100.000	0.001
14.570	14.639	0.000	0.000	0.429	0.027	0.000	0.000	7.320	100.000	0.001
15.840	13.470	0.000	0.000	0.466	0.053	0.000	0.000	6.735	100.000	0.001
17.210	12.393	0.000	0.000	0.522	0.053	0.000	0.000	6.196	100.000	0.001
18.710	11.403	0.000	0.000	0.568	0.053	0.000	0.000	5.702	100.000	0.001
20.330	10.492	0.000	0.000	0.634	0.053	0.000	0.000	5.246	100.000	0.001
22.100	9.652	0.000	0.000	0.699	0.053	0.000	0.000	4.826	100.000	0.001
24.020	8.881	0.000	0.000	0.764	0.053	0.000	0.000	4.441	100.000	0.001
26.100	8.172	0.000	0.000	0.848	0.080	0.000	0.000	4.086	100.000	0.001
28.980	7.362	0.000	0.000	0.950	0.080	0.000	0.000	3.681	100.000	0.001
31.750	6.718	0.000	0.000	1.062	0.080	0.000	0.000	3.359	100.000	0.002
34.780	6.134	0.000	0.000	1.174	0.107	0.000	0.000	3.067	100.000	0.002
38.080	5.603	0.000	0.000	1.304	0.107	0.000	0.000	2.801	100.000	0.002
41.580	5.131	0.000	0.001	1.444	0.133	0.000	0.000	2.565	100.000	0.002
42.690	4.997	0.000	0.001	1.464	0.133	0.000	0.000	2.499	100.000	0.002
47.270	4.512	0.000	0.001	1.474	0.133	0.000	0.000	2.256	100.000	0.002
53.450	3.991	0.000	0.001	1.478	0.133	0.000	0.000	1.996	100.000	0.003
59.330	3.595	0.000	0.001	1.485	0.133	0.000	0.000	1.798	100.000	0.003
61.770	3.453	0.000	0.001	1.491	0.133	0.000	0.000	1.727	100.000	0.003
68.910	3.096	0.000	0.001	1.491	0.133	0.000	0.000	1.548	100.000	0.003
76.220	2.799	0.000	0.001	1.496	0.133	0.000	0.000	1.399	100.000	0.004
82.540	2.584	0.000	0.001	1.499	0.133	0.000	0.000	1.292	100.000	0.004

Int Pres psia	Pore Dia microns	Inc Int mL/gm	Cum Int mL/gm	Cum Int %PV(bc)	Cum Int %BV	Inc Int %PV(ac)	Cum Int %PV(ac)	Pore Rad microns	W.P. Sat %PV(ac)	Lev "J" Funct.
89.560	2.382	0.000	0.001	1.502	0.133	0.000	0.000	1.191	100.000	0.004
97.700	2.183	0.000	0.001	1.532	0.133	0.000	0.000	1.092	100.000	0.005
106.930	1.995	0.000	0.001	1.614	0.133	0.000	0.000	0.997	100.000	0.005
114.530	1.863	0.000	0.001	1.614	0.133	0.000	0.000	0.931	100.000	0.006
126.250	1.690	0.000	0.001	1.669	0.133	0.000	0.000	0.845	100.000	0.006
135.500	1.574	0.000	0.001	1.696	0.160	0.000	0.000	0.787	100.000	0.007
148.400	1.438	0.000	0.001	1.773	0.160	0.000	0.000	0.719	100.000	0.007
160.240	1.331	0.000	0.001	1.825	0.160	0.000	0.000	0.666	100.000	0.008
175.400	1.216	0.000	0.001	1.825	0.160	0.000	0.000	0.608	100.000	0.009
190.860	1.118	0.000	0.001	1.825	0.160	0.000	0.000	0.559	100.000	0.010
206.040	1.035	0.000	0.001	1.843	0.160	0.000	0.000	0.518	100.000	0.010
225.110	0.948	0.000	0.001	1.929	0.160	0.000	0.000	0.474	100.000	0.011
244.290	0.873	0.000	0.001	2.011	0.187	0.000	0.000	0.437	100.000	0.012
265.750	0.803	0.000	0.001	2.105	0.187	0.000	0.000	0.401	100.000	0.013
288.000	0.741	0.000	0.001	2.164	0.187	0.000	0.000	0.370	100.000	0.014
313.920	0.680	0.000	0.001	2.176	0.187	0.000	0.000	0.340	100.000	0.016
341.560	0.625	0.000	0.001	2.357	0.213	0.000	0.000	0.312	100.000	0.017
371.240	0.575	0.000	0.001	2.474	0.213	0.000	0.000	0.287	100.000	0.019
403.550	0.529	0.000	0.001	2.493	0.213	0.000	0.000	0.264	100.000	0.020
437.360	0.488	0.000	0.001	2.517	0.213	0.000	0.000	0.244	100.000	0.022
477.430	0.447	0.000	0.001	2.701	0.240	0.000	0.000	0.223	100.000	0.024
520.220	0.410	0.000	0.001	2.824	0.240	0.000	0.000	0.205	100.000	0.026
566.280	0.377	0.000	0.001	2.861	0.240	0.000	0.000	0.188	100.000	0.028
615.000	0.347	0.000	0.001	3.099	0.267	0.000	0.000	0.173	100.000	0.031
667.550	0.320	0.000	0.001	3.162	0.267	0.000	0.000	0.160	100.000	0.033
728.850	0.293	0.000	0.001	3.348	0.294	0.000	0.000	0.146	100.000	0.036
791.020	0.270	0.000	0.001	3.501	0.294	0.000	0.000	0.135	100.000	0.039
858.840	0.248	0.000	0.001	3.675	0.320	0.000	0.000	0.124	100.000	0.043
933.750	0.229	0.000	0.001	3.830	0.347	0.000	0.000	0.114	100.000	0.047
1013.720	0.210	0.000	0.001	4.074	0.347	0.000	0.000	0.105	100.000	0.051
1103.450	0.193	0.000	0.001	4.182	0.374	0.000	0.000	0.097	100.000	0.055
1199.230	0.178	0.000	0.002	4.495	0.400	0.000	0.000	0.089	100.000	0.060
1304.700	0.164	0.000	0.002	4.741	0.427	0.000	0.000	0.082	100.000	0.065
1417.410	0.151	0.000	0.002	4.957	0.427	0.000	0.000	0.075	100.000	0.071
1539.060	0.139	0.000	0.002	5.180	0.454	0.000	0.000	0.069	100.000	0.077
1673.070	0.128	0.000	0.002	5.499	0.480	0.000	0.000	0.064	100.000	0.083
1818.380	0.117	0.000	0.002	5.833	0.507	0.000	0.000	0.059	100.000	0.091
1976.730	0.108	0.000	0.002	6.176	0.534	0.000	0.000	0.054	100.000	0.099
2146.630	0.099	0.000	0.002	6.562	0.560	0.000	0.000	0.050	100.000	0.107
2335.270	0.091	0.000	0.002	7.154	0.614	0.328	0.328	0.046	99.672	0.116
2537.560	0.084	0.000	0.003	7.504	0.667	0.656	0.984	0.042	99.016	0.126

Int Pres psia	Pore Dia microns	Inc Int mL/gm	Cum Int mL/gm	Cum Int %PV(bc)	Cum Int %BV	Inc Int %PV(ac)	Cum Int %PV(ac)	Pore Rad microns	W.P. Sat %PV(ac)	Lev "J" Funct.
2758.310	0.077	0.000	0.003	8.165	0.721	0.656	1.639	0.039	98.361	0.137
2997.660	0.071	0.000	0.003	8.832	0.774	0.656	2.295	0.036	97.705	0.149
3255.770	0.066	0.000	0.003	9.494	0.827	0.656	2.951	0.033	97.049	0.162
3540.020	0.060	0.000	0.003	10.533	0.907	0.984	3.934	0.030	96.066	0.176
3848.950	0.055	0.000	0.004	11.843	1.014	1.311	5.246	0.028	94.754	0.192
4183.090	0.051	0.001	0.004	13.575	1.174	1.967	7.213	0.026	92.787	0.208
4436.340	0.048	0.001	0.005	15.195	1.334	1.967	9.180	0.024	90.820	0.221
4835.660	0.044	0.001	0.006	16.780	1.574	2.951	12.131	0.022	87.869	0.241
5367.220	0.040	0.001	0.007	22.420	1.948	4.590	16.721	0.020	83.279	0.268
5832.990	0.037	0.003	0.010	26.610	2.642	8.525	25.246	0.018	74.754	0.291
6339.000	0.034	0.002	0.012	36.930	3.229	7.213	32.459	0.017	67.541	0.316
6888.380	0.031	0.002	0.014	42.354	3.709	5.902	38.361	0.016	61.639	0.343
7486.650	0.029	0.002	0.016	47.289	4.136	5.246	43.607	0.014	56.393	0.373
8137.840	0.026	0.002	0.017	51.922	4.537	4.918	48.525	0.013	51.475	0.406
8843.400	0.024	0.001	0.018	54.544	4.830	3.607	52.131	0.012	47.869	0.441
9611.620	0.022	0.001	0.019	57.997	5.070	2.951	55.082	0.011	44.918	0.479
10448.010	0.020	0.001	0.020	60.150	5.337	3.279	58.361	0.010	41.639	0.521
11354.110	0.019	0.001	0.021	63.953	5.577	2.951	61.311	0.009	38.689	0.566
12337.330	0.017	0.001	0.022	65.853	5.817	2.951	64.262	0.009	35.738	0.615
13410.390	0.016	0.001	0.023	68.492	6.031	2.623	66.885	0.008	33.115	0.668
14573.540	0.015	0.001	0.023	70.946	6.244	2.623	69.508	0.007	30.492	0.726
15839.480	0.014	0.001	0.024	73.634	6.485	2.951	72.459	0.007	27.541	0.789
17214.230	0.012	0.001	0.025	75.733	6.671	2.295	74.754	0.006	25.246	0.858
18707.820	0.011	0.001	0.026	77.235	6.805	1.639	76.393	0.006	23.607	0.932
20331.600	0.011	0.001	0.026	79.299	6.992	2.295	78.689	0.005	21.311	1.013
22097.750	0.010	0.001	0.027	81.723	7.205	2.623	81.311	0.005	18.689	1.101
24012.560	0.009	0.000	0.027	82.757	7.285	0.984	82.295	0.004	17.705	1.197
26099.760	0.008	0.000	0.028	84.012	7.392	1.311	83.607	0.004	16.393	1.301
28369.110	0.008	0.001	0.029	86.885	7.632	2.951	86.557	0.004	13.443	1.414
30829.990	0.007	0.001	0.029	88.366	7.766	1.639	88.197	0.003	11.803	1.537
33504.400	0.006	0.000	0.029	89.328	7.846	0.984	89.180	0.003	10.820	1.670
36413.210	0.006	0.001	0.030	90.916	7.979	1.639	90.820	0.003	9.180	1.815
39574.610	0.005	0.001	0.031	93.132	8.166	2.295	93.115	0.003	6.885	1.972
43007.960	0.005	0.000	0.031	94.005	8.273	1.311	94.426	0.003	5.574	2.144
46739.750	0.005	0.001	0.032	95.852	8.433	1.967	96.393	0.002	3.607	2.330
50797.820	0.004	0.001	0.032	97.278	8.566	1.639	98.033	0.002	1.967	2.532
55206.520	0.004	0.000	0.033	99.407	8.673	1.311	99.344	0.002	0.656	2.752
59984.020	0.004	0.000	0.033	100.000	8.726	0.656	100.000	0.002	0.000	2.990

6/12/10-34 Pore aperture vs. mercury saturation

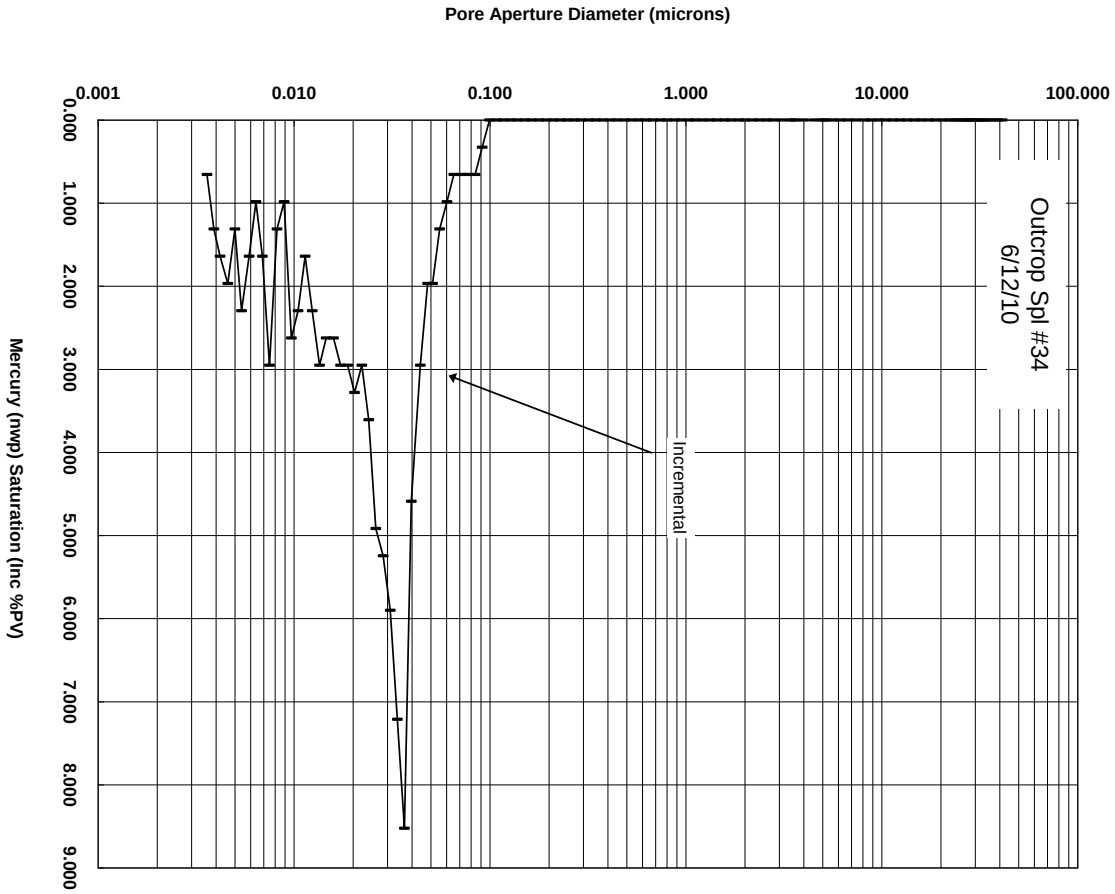

6/12/10-38 Data

Int Pres psia	Pore Dia microns	Inc Int mL/gm	Cum Int mL/gm	Cum Int %PV(bc)	Cum Int %BV	Inc Int %PV(ac)	Cum Int %PV(ac)	Pore Rad microns	W.P. Sat %PV(ac)	Lev "J" Funct.
5.190	41.087	0.000	0.000	0.231	0.000	0.000	0.000	20.544	100.000	0.000
5.490	38.858	0.000	0.000	0.463	0.000	0.000	0.000	19.429	100.000	0.000
5.840	36.521	0.000	0.000	0.709	0.029	0.000	0.000	18.261	100.000	0.000
6.240	34.189	0.000	0.000	0.969	0.029	0.000	0.000	17.095	100.000	0.000
6.490	32.873	0.000	0.000	1.142	0.029	0.000	0.000	16.437	100.000	0.000
6.740	31.641	0.000	0.000	1.302	0.029	0.000	0.000	15.820	100.000	0.000
7.040	30.300	0.000	0.000	1.461	0.029	0.000	0.000	15.150	100.000	0.000
7.340	29.063	0.000	0.000	1.620	0.029	0.000	0.000	14.532	100.000	0.000
7.590	28.094	0.000	0.000	1.764	0.029	0.000	0.000	14.047	100.000	0.000
7.840	27.211	0.000	0.000	1.866	0.058	0.000	0.000	13.606	100.000	0.000
8.190	26.042	0.000	0.000	2.025	0.058	0.000	0.000	13.021	100.000	0.000
8.540	24.979	0.000	0.000	2.184	0.058	0.000	0.000	12.489	100.000	0.000
9.080	23.494	0.000	0.000	2.343	0.058	0.000	0.000	11.747	100.000	0.000
9.610	22.195	0.000	0.000	2.531	0.058	0.000	0.000	11.097	100.000	0.000
10.440	20.428	0.000	0.000	2.762	0.058	0.000	0.000	10.214	100.000	0.000
11.350	18.796	0.000	0.000	2.979	0.058	0.000	0.000	9.398	100.000	0.000
12.340	17.292	0.000	0.000	3.196	0.087	0.000	0.000	8.646	100.000	0.000
13.410	15.909	0.000	0.000	3.413	0.087	0.000	0.000	7.955	100.000	0.000
14.570	14.639	0.000	0.000	3.601	0.087	0.000	0.000	7.319	100.000	0.000
15.840	13.470	0.000	0.000	3.774	0.087	0.000	0.000	6.735	100.000	0.000
17.210	12.393	0.000	0.000	3.977	0.087	0.000	0.000	6.196	100.000	0.000
18.710	11.402	0.000	0.000	4.179	0.087	0.000	0.000	5.701	100.000	0.000
20.330	10.491	0.000	0.000	4.382	0.116	0.000	0.000	5.246	100.000	0.000
22.100	9.653	0.000	0.000	4.555	0.116	0.000	0.000	4.826	100.000	0.000
24.020	8.882	0.000	0.000	4.758	0.116	0.000	0.000	4.441	100.000	0.000
26.100	8.172	0.000	0.000	4.960	0.116	0.000	0.000	4.086	100.000	0.000
28.980	7.362	0.000	0.000	5.235	0.116	0.000	0.000	3.681	100.000	0.000
31.750	6.718	0.000	0.000	5.466	0.116	0.000	0.000	3.359	100.000	0.000
34.780	6.134	0.000	0.001	5.727	0.145	0.000	0.000	3.067	100.000	0.000
38.080	5.603	0.000	0.001	6.016	0.145	0.000	0.000	2.801	100.000	0.000
41.580	5.131	0.000	0.001	6.291	0.145	0.000	0.000	2.565	100.000	0.000
43.920	4.857	0.000	0.001	6.343	0.145	0.000	0.000	2.429	100.000	0.000
47.500	4.491	0.000	0.001	6.442	0.145	0.000	0.000	2.245	100.000	0.000
52.870	4.035	0.000	0.001	6.528	0.145	0.000	0.000	2.017	100.000	0.001
57.050	3.739	0.000	0.001	6.553	0.145	0.000	0.000	1.870	100.000	0.001
62.940	3.389	0.000	0.001	6.581	0.145	0.000	0.000	1.695	100.000	0.001
68.620	3.109	0.000	0.001	6.696	0.145	0.000	0.000	1.554	100.000	0.001
74.130	2.878	0.000	0.001	6.752	0.174	0.000	0.000	1.439	100.000	0.001
83.510	2.554	0.000	0.001	6.904	0.174	0.000	0.000	1.277	100.000	0.001

Int Pres psia	Pore Dia microns	Inc Int mL/gm	Cum Int mL/gm	Cum Int %PV(bc)	Cum Int %BV	Inc Int %PV(ac)	Cum Int %PV(ac)	Pore Rad microns	W.P. Sat %PV(ac)	Lev "J" Funct.
89.670	2.379	0.000	0.001	7.023	0.174	0.000	0.000	1.190	100.000	0.001
97.030	2.199	0.000	0.001	7.065	0.174	0.000	0.000	1.099	100.000	0.001
105.920	2.014	0.000	0.001	7.155	0.174	0.000	0.000	1.007	100.000	0.001
114.570	1.862	0.000	0.001	7.439	0.174	0.000	0.000	0.931	100.000	0.001
125.410	1.701	0.000	0.001	7.574	0.174	0.000	0.000	0.851	100.000	0.001
136.070	1.568	0.000	0.001	7.596	0.174	0.000	0.000	0.784	100.000	0.001
149.320	1.429	0.000	0.001	7.613	0.174	0.000	0.000	0.714	100.000	0.001
161.720	1.319	0.000	0.001	7.858	0.174	0.000	0.000	0.660	100.000	0.002
176.250	1.210	0.000	0.001	8.105	0.202	0.000	0.000	0.605	100.000	0.002
191.140	1.116	0.000	0.001	8.339	0.202	0.000	0.000	0.558	100.000	0.002
209.880	1.016	0.000	0.001	8.342	0.202	0.000	0.000	0.508	100.000	0.002
226.420	0.942	0.000	0.001	8.620	0.202	0.000	0.000	0.471	100.000	0.002
246.240	0.866	0.000	0.001	8.867	0.202	0.000	0.000	0.433	100.000	0.002
267.290	0.798	0.000	0.001	9.146	0.231	0.000	0.000	0.399	100.000	0.003
291.910	0.731	0.000	0.001	9.420	0.231	0.000	0.000	0.365	100.000	0.003
316.470	0.674	0.000	0.001	9.667	0.231	0.000	0.000	0.337	100.000	0.003
342.200	0.623	0.000	0.001	9.909	0.231	0.000	0.000	0.312	100.000	0.003
373.200	0.572	0.000	0.001	10.261	0.231	0.000	0.000	0.286	100.000	0.004
406.580	0.525	0.000	0.001	10.566	0.260	0.000	0.000	0.262	100.000	0.004
440.950	0.484	0.000	0.001	10.702	0.260	0.000	0.000	0.242	100.000	0.004
479.700	0.445	0.000	0.001	11.016	0.260	0.000	0.000	0.222	100.000	0.005
523.640	0.407	0.000	0.001	11.211	0.260	0.000	0.000	0.204	100.000	0.005
567.860	0.376	0.000	0.001	11.406	0.260	0.000	0.000	0.188	100.000	0.006
616.030	0.346	0.000	0.001	11.684	0.289	0.000	0.000	0.173	100.000	0.006
668.320	0.319	0.000	0.001	11.737	0.289	0.000	0.000	0.160	100.000	0.007
726.930	0.294	0.000	0.001	12.044	0.289	0.000	0.000	0.147	100.000	0.007
790.870	0.270	0.000	0.001	12.255	0.289	0.000	0.000	0.135	100.000	0.008
859.430	0.248	0.000	0.001	12.589	0.289	0.000	0.000	0.124	100.000	0.009
932.580	0.229	0.000	0.001	12.938	0.318	0.000	0.000	0.114	100.000	0.009
1014.040	0.210	0.000	0.001	13.276	0.318	0.000	0.000	0.105	100.000	0.010
1104.860	0.193	0.000	0.001	13.378	0.318	0.000	0.000	0.097	100.000	0.011
1199.500	0.178	0.000	0.001	13.769	0.318	0.000	0.000	0.089	100.000	0.012
1305.950	0.163	0.000	0.001	14.284	0.347	0.000	0.000	0.082	100.000	0.013
1416.840	0.151	0.000	0.001	14.485	0.347	0.000	0.000	0.075	100.000	0.014
1540.700	0.139	0.000	0.001	14.841	0.347	0.000	0.000	0.069	100.000	0.015
1672.160	0.128	0.000	0.001	15.131	0.347	0.000	0.000	0.064	100.000	0.017
1819.680	0.117	0.000	0.001	15.371	0.376	0.000	0.000	0.059	100.000	0.018
1976.350	0.108	0.000	0.001	15.875	0.376	0.000	0.000	0.054	100.000	0.020
2147.950	0.099	0.000	0.001	16.197	0.376	0.000	0.000	0.050	100.000	0.021
2335.620	0.091	0.000	0.001	16.530	0.405	0.000	0.000	0.046	100.000	0.023
2535.770	0.084	0.000	0.001	16.919	0.405	0.000	0.000	0.042	100.000	0.025

Int Pres psia	Pore Dia microns	Inc Int mL/gm	Cum Int mL/gm	Cum Int %PV(bc)	Cum Int %BV	Inc Int %PV(ac)	Cum Int %PV(ac)	Pore Rad microns	W.P. Sat %PV(ac)	Lev "J" Funct.
2757.640	0.077	0.000	0.001	17.345	0.405	0.000	0.000	0.039	100.000	0.027
2998.320	0.071	0.000	0.002	17.801	0.434	0.000	0.000	0.036	100.000	0.030
3257.160	0.066	0.000	0.002	18.225	0.434	0.000	0.000	0.033	100.000	0.032
3541.200	0.060	0.000	0.002	18.712	0.434	0.000	0.000	0.030	100.000	0.035
3848.540	0.055	0.000	0.002	19.221	0.463	0.000	0.000	0.028	100.000	0.038
4179.540	0.051	0.000	0.002	19.751	0.463	0.000	0.000	0.026	100.000	0.042
4430.890	0.048	0.000	0.002	20.196	0.492	0.000	0.000	0.024	100.000	0.044
4834.570	0.044	0.000	0.002	20.862	0.492	0.000	0.000	0.022	100.000	0.048
5359.120	0.040	0.000	0.002	21.589	0.521	0.000	0.000	0.020	100.000	0.053
5819.380	0.037	0.000	0.002	22.106	0.521	0.000	0.000	0.018	100.000	0.058
6325.260	0.034	0.000	0.002	22.929	0.549	0.000	0.000	0.017	100.000	0.063
6881.340	0.031	0.000	0.002	23.953	0.578	0.000	0.000	0.016	100.000	0.068
7480.500	0.029	0.000	0.002	24.848	0.578	0.000	0.000	0.014	100.000	0.074
8133.080	0.026	0.000	0.002	25.958	0.607	0.000	0.000	0.013	100.000	0.081
8832.870	0.024	0.000	0.002	27.102	0.636	0.000	0.000	0.012	100.000	0.088
9608.500	0.022	0.000	0.002	28.486	0.665	0.000	0.000	0.011	100.000	0.095
10439.150	0.020	0.000	0.002	29.925	0.694	0.000	0.000	0.010	100.000	0.104
11350.290	0.019	0.000	0.003	31.794	0.723	0.000	0.000	0.009	100.000	0.113
12326.510	0.017	0.000	0.003	33.464	0.781	3.509	3.509	0.009	96.491	0.122
13409.030	0.016	0.000	0.003	36.058	0.839	3.509	7.018	0.008	92.982	0.133
14566.440	0.015	0.000	0.003	38.190	0.896	3.509	10.526	0.007	89.474	0.145
15832.830	0.014	0.000	0.003	40.716	0.954	3.509	14.035	0.007	85.965	0.157
17204.950	0.012	0.000	0.004	43.139	1.012	3.509	17.544	0.006	82.456	0.171
18694.620	0.011	0.000	0.004	45.702	1.099	5.263	22.807	0.006	77.193	0.186
20320.450	0.011	0.000	0.004	48.554	1.157	3.509	26.316	0.005	73.684	0.202
22096.400	0.010	0.000	0.004	52.559	1.243	5.263	31.579	0.005	68.421	0.220
24016.640	0.009	0.000	0.005	56.123	1.330	5.263	36.842	0.004	63.158	0.239
26102.530	0.008	0.000	0.005	60.182	1.417	5.263	42.105	0.004	57.895	0.259
28367.290	0.008	0.000	0.005	63.205	1.504	5.263	47.368	0.004	52.632	0.282
30829.750	0.007	0.000	0.006	66.899	1.591	5.263	52.632	0.003	47.368	0.306
33505.500	0.006	0.000	0.006	70.075	1.677	5.263	57.895	0.003	42.105	0.333
36413.890	0.006	0.000	0.006	74.092	1.764	5.263	63.158	0.003	36.842	0.362
39574.390	0.005	0.000	0.006	77.891	1.851	5.263	68.421	0.003	31.579	0.393
43007.970	0.005	0.000	0.007	82.699	1.966	7.018	75.439	0.003	24.561	0.427
46741.450	0.005	0.000	0.007	86.309	2.053	5.263	80.702	0.002	19.298	0.464
50798.050	0.004	0.001	0.008	92.040	2.198	8.772	89.474	0.002	10.526	0.505
55202.310	0.004	0.000	0.008	96.277	2.285	5.263	94.737	0.002	5.263	0.549
59984.650	0.004	0.000	0.008	100.000	2.371	5.263	100.000	0.002	0.000	0.596

6/12/10-38 Pore aperture vs. mercury saturation